TECHNICAL REPORT RD-TI-96-1

A DIGITAL SUPER-SERVO CONTROLLER DESIGN METHODOLOGY

Wanda M. Hughes
Technology Integration Office
Research, Development, and Engineering Center

September 1996

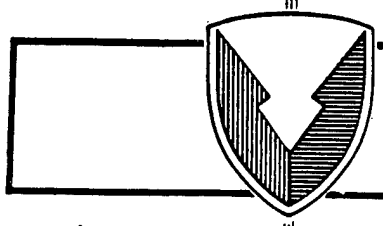

U.S. ARMY MISSILE COMMAND
Redstone Arsenal, Alabama 35898–5000

Approved for public release; distribution is unlimited.

DTIC QUALITY INSPECTED 4

19961211 062

DESTRUCTION NOTICE

FOR CLASSIFIED DOCUMENTS, FOLLOW THE PROCEDURES IN DoD 5200.22-M, INDUSTRIAL SECURITY MANUAL, SECTION II-19 OR DoD 5200.1-R, INFORMATION SECURITY PROGRAM REGULATION, CHAPTER IX. FOR UNCLASSIFIED, LIMITED DOCUMENTS, DESTROY BY ANY METHOD THAT WILL PREVENT DISCLOSURE OF CONTENTS OR RECONSTRUCTION OF THE DOCUMENT.

DISCLAIMER

THE FINDINGS IN THIS REPORT ARE NOT TO BE CONSTRUED AS AN OFFICIAL DEPARTMENT OF THE ARMY POSITION UNLESS SO DESIGNATED BY OTHER AUTHORIZED DOCUMENTS.

TRADE NAMES

USE OF TRADE NAMES OR MANUFACTURERS IN THIS REPORT DOES NOT CONSTITUTE AN OFFICIAL ENDORSEMENT OR APPROVAL OF THE USE OF SUCH COMMERCIAL HARDWARE OR SOFTWARE.

REPORT DOCUMENTATION PAGE

Form Approved
OMB No. 0704-0188

1a.REPORT SECURITY CLASSIFICATION UNCLASSIFIED	1b.RESTRICTIVE MARKINGS
2a.SECURITY CLASSIFICATION AUTHORITY	3.DISTRIBUTION/AVAILABILITY OF REPORT Approved for public release; distribution is unlimited.
2b.DECLASSIFICATION/DOWNGRADING SCHEDULE	
4.PERFORMING ORGANIZATION REPORT NUMBER(S) TR-RD-TI-96-1	5.MONITORING ORGANIZATION REPORT NUMBER(S)
6a.NAME OF PERFORMING ORGANIZATION Technology Integration Office RDEC 6b.OFFICE SYMBOL (If Applicable) AMSMI-RD-TI	7a.NAME OF MONITORING ORGANIZATION
6c.ADDRESS (City, State, and ZIP Code) Commander, U. S. Army Missile Command ATTN: AMSMI-RD-TI Redstone Arsenal, AL 35898-5254	7b.ADDRESS (City, State, and ZIP Code)
8a.NAME OF FUNDING/SPONSORING ORGANIZATION 8b.OFFICE SYMBOL (If Applicable)	9.PROCUREMENT INSTRUMENT IDENTIFICATION NUMBER
8c.ADDRESS (City, State, and ZIP Code)	10.SOURCE OF FUNDING NUMBERS PROGRAM ELEMENT NO. / PROJECT NO. / TASK NO. / WORK UNIT ACCESSION NO.

11.TITLE (Include Security Classification)
A Digital Super-Servo Controller Design Methodology

12.PERSONAL AUTHOR(S)
Wanda M. Hughes

13a.TYPE OF REPORT	13b.TIME COVERED	14.DATE OF REPORT (Year, Month, Day)	15. PAGE COUNT
Final	FROM 10/94 TO 7/96	September 1996	

16.SUPPLEMENTARY NOTATION

17. COSATI CODES			18.SUBJECT TERMS (Continue on reverse if necessary and identify by block number)
FIELD	GROUP	SUB-GROUP	Subspace Stabilization, Digital Control, Servo-Tracking, Multirate Sampling, Intersample Control, Command-Following, Disturbance Accommodation

19.ABSTRACT (Continue on reverse if necessary and identify by block number)

This report compiles, refines, and extends a general theory for developing digital servo-tracking controllers which will achieve a high-level of servo-tracking performance that is unmatched by currently available digital servo-design methods. This general theory applies to multiple-input/multiple-output linear time-invariant systems subjected to plant parameter-perturbations and complex, multi-variable, time-varying servo-commands and disturbances. Obstacles to achieve high-performance servo-tracking are identified and discussed, along with key shortcomings inherent in conventional design methods. In addition, a collection of example problems are worked in detail to illustrate the design techniques described and developed in this study. Simulation results are used to demonstrate the performance of the resulting controllers. (Continued on page ii.)

20.DISTRIBUTION/AVAILABILITY OF ABSTRACT ☒UNCLASSIFIED/UNLIMITED ☐SAME AS RPT. ☐DTIC USERS	21.ABSTRACT SECURITY CLASSIFICATION UNCLASSIFIED
22a.NAME OF RESPONSIBLE INDIVIDUAL Wanda M. Hughes	22b.TELEPHONE (Include Area Code) (205) 876-4484 22c.OFFICE SYMBOL AMSMI-RD-TI

DD Form 1473, JUN 86 *Previous editions are obsolete.*

SECURITY CLASSIFICATION OF THIS PAGE
UNCLASSIFIED

19. ABSTRACT (Cont.)

The digital servo-controller theory presented in this report is ideal in the sense that the design procedure encompasses a superset of desirable characteristics. That is, the design procedure: (1) is purely linear algebraic in nature; (2) accommodates linear time-invariant systems subjected to generalized, multi-variable, independent disturbances having complex time behavior; (3) produces a servo-controller that provides high-fidelity servo-tracking of generalized, multi-variable servo-commands having complex time-behavior; (4) is generalized to include any order of system having Multiple Control-Inputs and Multiple Plant-Outputs (MIMO) systems; (5) provides performance robustness against uncertain variations in plant parameters; (6) minimizes intersample misbehavior (ripple) to the highest degree possible utilizing a digital controller; and, (7) controls the motions of the servo state-vector to a subspace making those motions invisible in the tracking-error.

EXECUTIVE SUMMARY

The objective of this research effort is to compile, refine, and extend a general theory for developing digital servo-tracking controllers which will achieve a high-level of servo-tracking performance that is unmatched by currently available digital servo-design methods. This general theory applies to multiple-input/multiple-output linear time-invariant systems subjected to plant parameter-perturbations and complex, multi-variable, time-varying servo-commands and disturbances. Obstacles to achieving high-performance servo-tracking are identified and discussed, along with key shortcomings inherent in conventional design methods. In addition, a collection of example problems are worked in detail to illustrate the design techniques described and developed in this study. Simulation results are used to demonstrate the performance of the resulting controllers.

The digital servo-controller theory presented in this report is ideal in the sense that the design procedure encompasses a superset of desirable characteristics. That is, the design procedure: (1) is purely linear algebraic in nature; (2) accommodates linear time-invariant systems subjected to generalized, multi-variable, independent disturbances having complex time behavior; (3) produces a servo-controller that provides high-fidelity servo-tracking of generalized, multi-variable servo-commands having complex time-behavior; (4) is generalized to include any order of system having Multiple Control-Inputs and Multiple Plant-Outputs (MIMO) systems; (5) provides performance robustness against uncertain variations in plant parameters; (6) minimizes intersample misbehavior (ripple) to the highest degree possible utilizing a digital controller; and, (7) controls the motions of the servo state-vector to a subspace making those motions invisible in the tracking-error.

TABLE OF CONTENTS

TABLE OF CONTENTS (Conc)

LIST OF ILLUSTRATIONS

LIST OF ILLUSTRATIONS (Cont)

LIST OF ILLUSTRATIONS (Cont)

LIST OF ILLUSTRATIONS (Cont)

LIST OF ILLUSTRATIONS (Cont)

LIST OF ILLUSTRATIONS (Cont)

LIST OF ILLUSTRATIONS (Cont)

1. INTRODUCTION TO THE SERVO-TRACKING PROBLEM IN CONTROL ENGINEERING

This chapter provides an overview of the servo-tracking problem and discusses the difficulties encountered in designing digital controllers to achieve high-performance servo-tracking. The shortcomings of conventional servo-controllers are also discussed.

1.1. History and General Overview of the Servo-Tracking Problem

The term *servo-tracking* is used to describe a process in which one or more outputs of a system tend to follow (or track) time-variations of certain inputs to the system. The alternative term *servomechanism* originated [1], in 1934, from the words *servant* (or slave) and *mechanism*. Thus, the term *servomechanism*, implied a slave-type mechanism. Today, this term refers to an important class of feedback control systems that are widely used in industrial applications. Over the years, the word *servomechanism* has been shortened to *servo*.

Instruments and machines that were designed to perform servo-tracking appeared in the early 1880's in connection with speed regulation requirements for steam engines. Speed governors that performed set-point regulation in the face of uncertain "loads" are a specific type of servomechanism that appeared during that time. Later in the 1930's and 1940's, servomechanisms became essential components in electro-mechanical systems associated with airplane autopilots, anti-aircraft fire directors, and bomb sights, to name a few examples.

In general, an industrial servo performs the task of controlling some physical quantity $y(t)$ by comparing its actual value $y(t)$ at time t with a desired, or commanded, value $y_c(t)$ at time t and using the real-time difference (or servo-tracking error) $\varepsilon_y(t) = y_c(t) - y(t)$ to control $y(t)$ into agreement with $y_c(t)$ (i.e., control $\varepsilon_y(t) \to 0$). The basic idea of servo-tracking is illustrated in Figure 1.1. The primary control task is to achieve closed-loop stability for the (possibly unstable) system and to simultaneously, quickly achieve $y(t) \to y_c(t)$ and maintain $y(t) \approx y_c(t)$ thereafter. The servo-tracking controller design problem in control engineering is to create a controlling device and associated control algorithm that will achieve accurate servo-tracking of all expected "commands" $y_c(t)$, while simultaneously satisfying additional performance criteria that may be specified, in the face of a wide variety of uncertain disturbances and initial conditions.

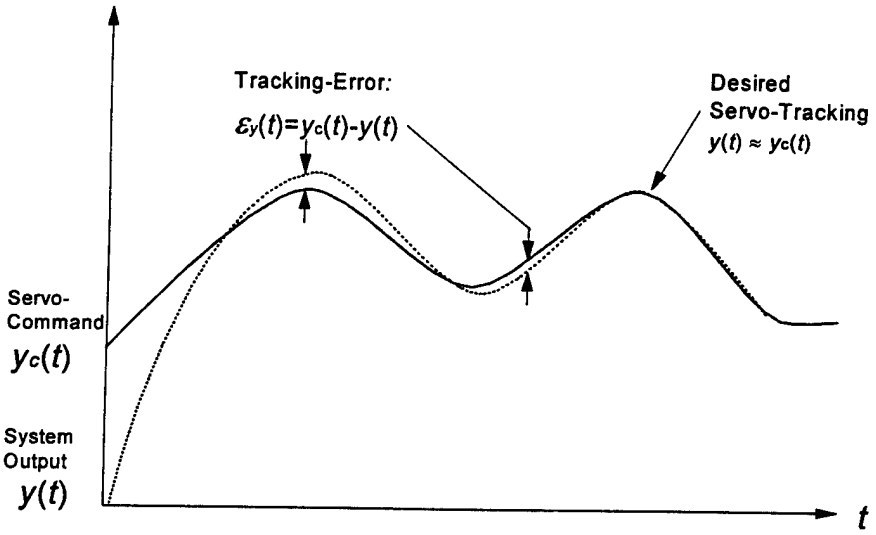

Figure 1.1 Servo-Tracking Behavior: $y(t)$ Must Quickly Become Equal-to and Thereafter Accurately Track $y_c(t)$.

The physical quantity being controlled by a servo-tracking controller may be position, velocity, chemical composition, temperature, light intensity, or any other measurable and controllable entity [2]. Also, the servo-controller may take on many forms. For instance, a person reaching to pick up a moving object can be viewed as a biological, servo-controlled system. In that case the tracking-error, continually sensed by the eyes, is the difference between the position $y_c(t)$ of the object and that of the hand $y(t)$. In fact, the pointing of the eyes themselves is another example of a biological servo-system, as are the automatic iris-adjustments within each eye.

1.2. Difficulties in Achieving High-Performance Servo-Tracking

As discussed in the previous section, in addition to achieving closed-loop stability, the purpose of a servo-controller is to reduce to zero the difference between the plant output and the command input. However, simply achieving a zero tracking-error eventually is not sufficient, in general. High-performance servo-tracking requires essentially zero tracking-error while simultaneously achieving and maintaining some minimum quality of performance for the closed-loop system. The performance specifications typically involve rise-time, settling-time, and/or overshoot of the variable $y(t)$ being controlled, or the gain and phase margins of the closed-loop system. Several difficulties can arise when attempting to achieve high-performance servo-tracking. Primarily, these difficulties can be attributed to the inherent uncertainty about the servo-commands and disturbance inputs.

1.2.1. The Nature of Uncertain Servo-Commands $y_c(t)$ in Control Problems

In industrial applications, the servo-command $y_c(t)$ is not necessarily a single scalar input and not limited to simple, stepwise-constants, ramps, or acceleration-type commands. Rather, the $y_c(t)$ may be a "vector," or set, of independent inputs and may vary with time in complex, unpredictable ways. Practical servo-commands are almost always uncertain in the sense that their time-behavior is not precisely known a priori, and is only revealed or available for measurement in an on-line, real-time fashion. A typical time-plot of such a servo-command input is shown in Figure 1.2 where it can be seen that the rate of change of the servo-command may vary unexpectedly with time. Those changes in the motion of $y_c(t)$ cannot be predicted and corrections for them must be made by the servo-controller in a real-time manner, based on measurements of the command and plant response up to that particular point-in-time.

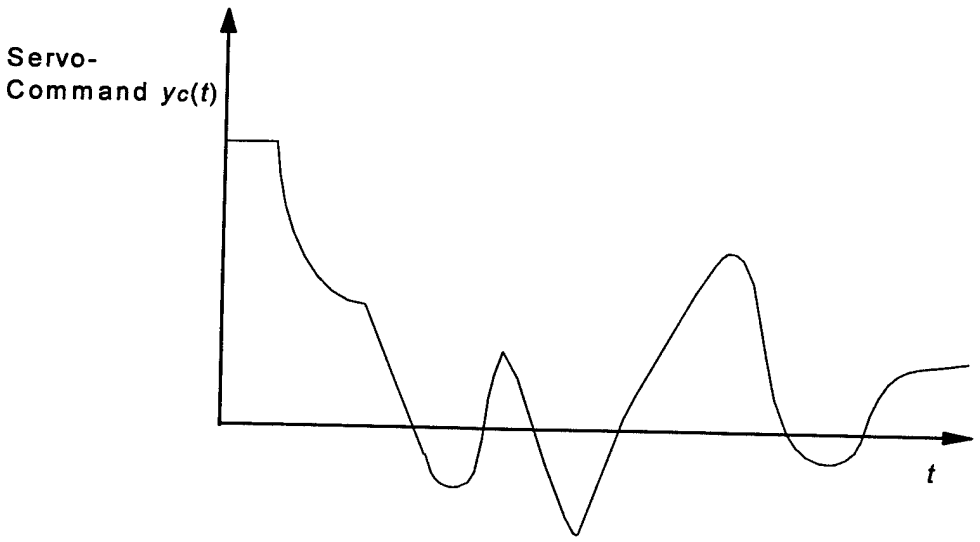

Figure 1.2 Typical Time-Plot of a Servo-Command Input $y_c(t)$.

1.2.2. The Nature of Uncertain Disturbances in Control Problems

In control engineering, disturbances are defined technically as uncontrollable inputs that affect system behavior. The uncertainty associated with disturbances is similar to that associated with servo-commands in that disturbances can vary with time in uncertain and complex ways. However, unlike servo-commands, disturbances are usually not directly measurable. Disturbances can occur both internal and external to the controlled system. External disturbances arise from effects external to the plant, such as system loads, environmental winds, temperature changes, and precipitation. Internal disturbances arise from effects associated with the physical or dynamic characteristics of the plant, such as friction, time-delays, dc biases, and uncertain parameter-perturbations.

Parameter-perturbation "disturbances" are of particular importance because they occur in many types of servo-tracking problems and arise when the values of the plant's parameters vary

in relation to their nominal or assumed values due, for instance, to fluctuations in subsystem component outputs or modeling errors. Conventional servo-controllers are tuned to the assumed nominal plant-parameter values during the design process. If those parameter values are inaccurate, or change during normal operation in some unpredictable manner, an inappropriate servo-control action may result.

1.3. Summary of Conventional Approaches to the Design of Servo-Tracking Controllers for Linear Time-Invariant Systems

The servo-tracking design problem came to the forefront in the 1930's. From that time through the late 1950's, a general theory of control was developed and is known today as *classical* control theory. That theory is still used in many control design problems, especially for linear systems with a single control-input and a single plant-output. The so-called *modern* control theory, developed since the late 1950's, is suitable for both single control-input, single plant-output systems, as well as more complicated systems such as those having multiple control-inputs and multiple plant-outputs. It has been asserted [5] that the advances achieved in space exploration during the past 35 years were possible only because of the advent of modern control theory.

1.3.1. Classical Approaches to the Design of Servo-Tracking Controllers for Linear Time-Invariant Systems

Early approaches to designing servo-tracking controllers were based on the solution of differential equations by classical means. This type of analysis can be tedious for anything other than relatively simple systems. The *Laplace transform* (transforms time functions into functions of a complex variable s [31]) was a primary tool in those early approaches.

A typical servo-control system as configured in classical control theory is illustrated in Figure 1.3, where $P(s)$ is the scalar, transfer function of the plant to be controlled, $w(t)$ is a scalar, external disturbance, and $u(t)$ is the scalar, servo-control input to the plant. The classical servo-controller design problem is to determine the transfer function $G_c(s)$ (compensator) that will achieve and maintain closed-loop stability, a zero tracking-error and, in addition, cause the closed-loop system to exhibit certain desired characteristics. Those characteristics include design specifications such as settling-time, rise-time, and percent overshoot, related to the step response of the system [3].

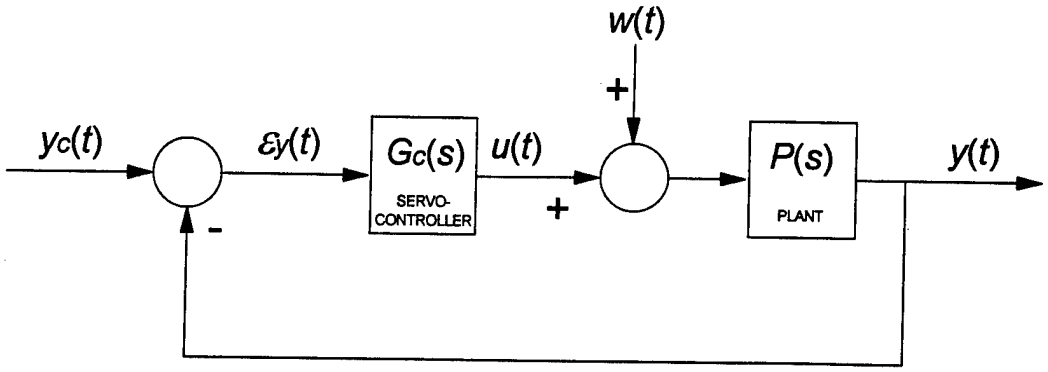

Figure 1.3 Typical Servo-Control System Considered in Classical Control Engineering.

Some examples of classical methods for designing servo-tracking controllers $G_c(s)$ are the methods of steady-state errors, the Nyquist Stability Theorem [24], the root locus method of Evans [30], and the frequency domain methods of Bode [26]. The design and analysis of servo-tracking controllers $G_c(s)$ using classical control engineering methods are described in [5]-[23].

1.3.2. Modern Approaches to the Design of Servo-Tracking Controllers for Linear Time-Invariant Systems

Modern control theory can be applied to complex, time-varying systems having multiple control-inputs and/or multiple plant-outputs, as well as simpler single input/single-output systems. The tools of modern control theory are developed primarily in the time domain. Modern control theory, sometimes referred to as *state-space* control theory, characterizes systems by a collection of n physical quantities $\{x_1, x_2, ..., x_n\}$ called *state-variables* which enable a n^{th}-order differential equation model of a system to be converted into a set of n first-order differential equations called *state-equations*. Those state-equations govern the time-evolution $x_i(t)$ of the n state-variables associated with the dynamic behavior of the plant. Those first-order equations can, in the case of linear plants, be expressed in vector-matrix notation to simplify the mathematical calculations. When a physical system has been modeled by a set of mathematical equations, the subsequent method of analysis and servo-controller design is independent of the nature of the physical system. The required servo-controller action $u(t)$ is determined by a "control-law" or "algorithm" that uses the measured, or estimated, state-variables from the plant and the measured servo-commands (and may also use estimates of the "states" of the servo-commands and the disturbances [32]-[40]).

Pole placement (the designation of closed-loop poles), observer theory ("state-estimation theory"), and optimal control methods (all based on state-space theory and linear-algebra techniques) are used extensively in the application of modern control engineering to the design and analysis of linear servo-tracking control systems. Servo-tracking design methodologies that make use of those methods are described in [20-21,32-39,42,44,47-56]

1.4. The Concept of Digital Control in the Design of Servo-Tracking Controllers for Linear Time-Invariant Systems

The increasing reliance on microprocessors in industrial servo-tracking control system implementations has made it necessary to develop controller design methods that result in servo-controller algorithms which can be realized in digital computer environments. *Digital* control is a way of computing and applying control actions that uses digital data sampling and data processing techniques to update, or determine new values for, the control $u(t)$ at sequential, discrete points in time, $t = t_o + kT$, $k = 0, 1, 2, ...$, where t_o is the initial time and the positive constant T (typically referred to as the *sample-period*) is determined in part by the digital hardware's computing speed and in part by the availability of the sampled data. Because those algorithms are realized by digital processors, the resulting servo-controller is often referred to as a "digital" servo-controller. Since the digital servo-controller is implemented on a microprocessor, digital computer, or similar type of data processing circuitry, a non-zero time-interval is required in order to format the raw measurement data and perform the computations necessary to fully execute the servo-tracking controller algorithm. Therefore, the resulting real-time digital-control decisions are generated at discrete-values in time $t = t_o + kT$, $k = 0, 1, 2, ...$, hereafter called "discrete-time" where the control "decision" made at time $t = t_o+kT$ is not updated again until the "next" value of discrete-time $t = t_o+(k+1)T$. According to the scientific definition [32] of discrete-time control, during the interval of time between successive discrete times $(t_o+kT, t_o+(k+1)T)$, $k = 0, 1, 2, ...$, the digital controller applies (possibly time-varying) control-actions to the plant in an <u>open-loop</u> manner, with no knowledge of, or reaction to, uncertain time-variations in servo-commands $y_c(t)$, disturbances $w(t)$, etc., that may occur <u>during</u> the time-interval ("intersample-interval") $t_o + kT \le t < t_o + (k+1)T$.

Discretization is the process of representing a given plant mathematical model, originally developed in the form of a set of differential equations, by an equivalent set of difference equations, assuming the discrete-time control $u(kT)$ will vary in a pre-specified manner across each sample-interval [33]. Modern day methods of designing digital servo-tracking controllers involve discretizing the continuous-time state-space model of the plant and then performing a digital controller design using the tools of modern discrete-time control theory. The vector/matrix methods of modern linear control theory lend themselves very well to computer computation. It is this characteristic that has allowed modern control theory to solve many complex servo-tracking problems that could not otherwise be solved by classical control theory. Discussions of digital servo-tracking controller design using modern control engineering techniques are found in [3,20-21,33,47,52,56,58].

1.5. Shortcomings of Contemporary Methods for Designing Servo-Tracking Controllers for Linear Time-Invariant Systems [59]

A review of contemporary servo-tracking controller design methods, for the purposes of identifying their shortcomings, was performed as a part of this research effort. The findings of that review were presented in [59]. Many of those same shortcomings were identified in two independent studies reported in two more recent papers [60,61]. These various shortcomings are discussed in this section as part of the motivation for this research effort.

1.5.1. The Restriction to Step + Ramp + Acceleration-Type Representations of Servo-Command Time-Behavior

Classical and modern servo-tracking control methods consistently rely on "step", "step+ramp," and "step+ramp+acceleration" type characterizations of the anticipated servo-command inputs. Many servo-commands are members of that class of commands. However, some types of servo-commands, such as weighted linear combinations of (known) exponentials or sinusoids, cannot be accurately characterized in this way. For example, a servo-command having the form $y_c(t) = ce^{-\alpha t}\cos(\beta t)$, where α and β are known constants and c is some unknown constant, is not accurately represented by any of the type characterizations mentioned above. Consistently classifying servo-commands by those types has resulted in a controller design guideline that characterizes servo systems as "Type 1", "Type 2", and "Type 3". The resulting overall closed-loop systems are such that Type 1 systems perform well for step-type servo-commands. Similarly, Type 2 and Type 3 systems perform well for step+ramp and step+ramp+acceleration-type servo-commands, respectively. Such systems are considered essential to achieving good servo-tracking performance. Indeed, when a servo-command belongs to the particular class of step, or ramp, or acceleration type commands, good servo-tracking performance may be obtained. However, when the time-behavior of the servo-command does not conform to this class of variations, and the controller algorithm is designed as a Type 1, 2, or 3 system, performance limitations will result. Examples of classical and modern servo-tracking controller design methods that rely on this type command characterization are found in [20,21,46-48]. Servo-tracking controller design methods which accommodate a more general class of servo-commands are discussed in [37,38,40,44].

1.5.2. Zero-Order-Hold versus Discrete-Continuous Control

Digital controllers are characterized by an alternating closed-loop/open-loop behavior; closed-loop at the discrete-times $t = t_0 + kT$ and open-loop over the intersample intervals $kT \le t < (k+1)T$; $k = 0, 1, 2, \ldots$. This mode of behavior makes the performance of digitally controlled systems more sensitive to the uncertainties (uncertain commands, disturbances, noisy measurements, etc.) associated with the servo-tracking problem. Recall from Subsection 1.4 that a digital servo-controller updates the control decisions only at the discrete times $t = t_o + kT$, $k = 0, 1, 2, \ldots$, with no knowledge of, or reaction to, "events" that may occur during the intersample interval $t_o + kT \le t < t_o + (k+1)T$. This situation has resulted in the commonly held assumption, among digital control designers, that the appropriate control input that should be applied to the plant between consecutive discrete points-in-time $(t_o + kT, t_o + (k+1)T)$ is a constant value $u(t) \equiv \text{constant} = u(kT)$ that is computed at the beginning $t = t_o + kT$ of each sample-interval [58]. This traditional choice of constant digital control-action is commonly known as "zero-order-hold" (z.o.h.) type control. A graphical representation of a typical z.o.h. type digital control-action is shown in Figure 1.4.

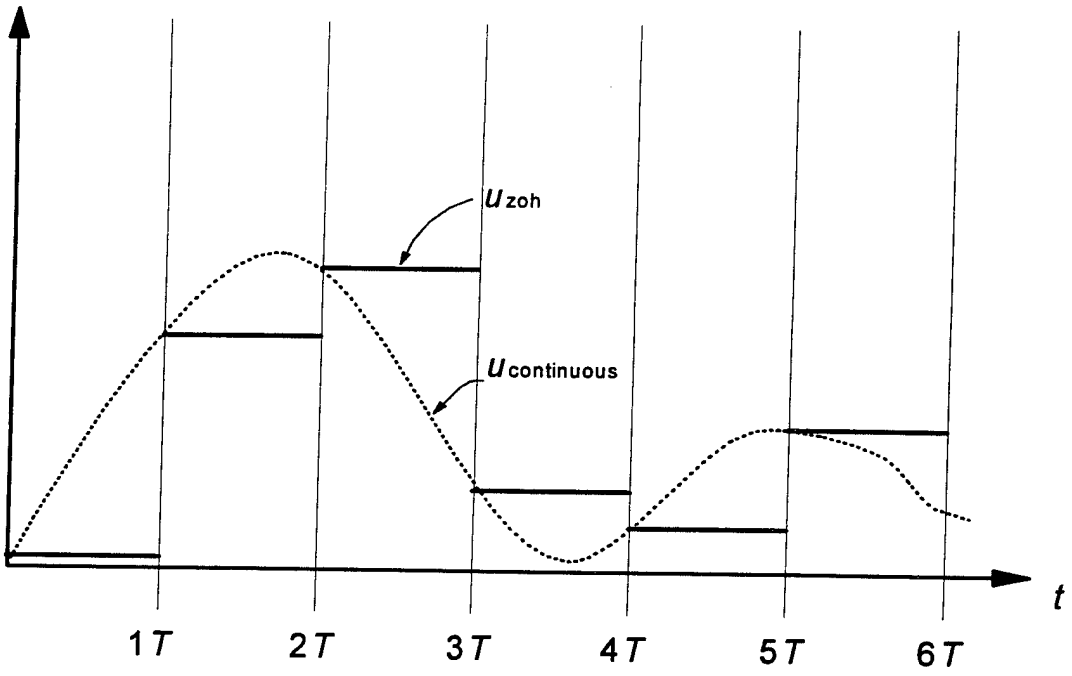

Figure 1.4 Illustration of Zero-Order-Hold (z.o.h.) Control-Action.

Digital servo-controllers that allow for the possibility of a time-varying control action across each sample-interval have been described in the literature [46,58,62-68]. The modes of time-variation (or holding actions) considered in those references are commonly referred to as *first-order*, *second-order*, and *exponential* hold. Such classical control schemes smooth out the otherwise rough stair-step waveform of a z.o.h. control-action (as shown in Figure 1.4) but can not intelligently choose smart control-variations that serve to maintain the servo-tracking error near zero between the sample times, $t_o + kT < t < t_o + (k+1)T$. In fact, those holding actions can lead to an undesirable "build-up" of the servo-tracking error during the discrete time-interval between the sample times. This build-up of servo-tracking error is known as *intersample misbehavior* and is a common obstacle to achieving high-performance servo-tracking using conventional digital control methods.

Intersample misbehavior (*ripple*) in digital servo-controlled systems can be caused by: (i) time-variations of the servo-commands; (ii) time-variations of the disturbances; and (iii) open-loop instability of the plant. Most digital control texts define ripple as the build-up of error between the sampling instants when the error at the sampling instants is zero ("deadbeat"). In Figure 1.5, a plant output $y(t)$ which, at $t = kT$, $k = 3, 4, 5, \ldots$, appears to be accurately tracking a constant servo-command $y_c(t)$ is shown. The plant output achieves deadbeat response because the tracking-error is zero at the sample times $t = kT$, $k = 3, 4, 5, \ldots$. However, in reality, $y(t)$ is drifting with respect to $y_c(t)$ and is, in fact, doing a poor job of tracking the constant servo-command. This drifting of tracking error between the discrete sample-times can be very difficult to reduce with the traditional-type intersample holding-actions described in this Section. However, a recently introduced technique for digital-control, called "discrete-continuous" control [38] leads to a more intelligent choice of intersample control-variations and thereby can reduce this mode of intersample misbehavior. The technique in [38] has been

incorporated into the new digital-servo controller design procedure developed in this report and will be described in detail in Chapter 3.

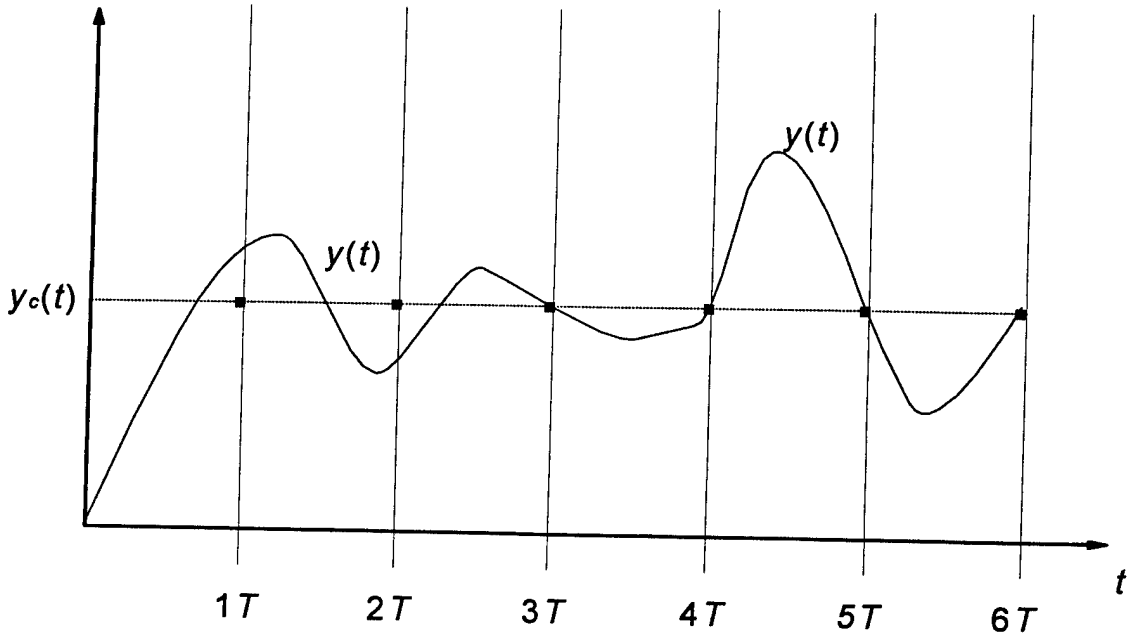

Figure 1.5 Illustration of Intersample Misbehavior of Output Response $y(t)$.

1.5.3. Failure to Exploit Available Real-Time Information

Contemporary and classical design methodologies for servo-controller algorithms are based on closed-loop stability and steady-state tracking-error considerations as $t \rightarrow \infty$ (or as $kT \rightarrow \infty$). This type of "steady-state error" design procedure does not address the important task of minimizing the instantaneous real-time tracking-error $\varepsilon_y(t)$, based on the real-time behavior of the servo-commands $y_c(t)$ [59]. Additional useful dynamic information about the disturbances and plant model is encoded in the plant output measurements $y(t)$. That information can be decoded and utilized in real-time by properly processing the plant output measurements $y(t)$. Similarly, useful information concerning the dynamic nature of the uncertain servo-commands is encoded in the real-time measurements of the servo-commands $y_c(t)$. Classical and modern servo-controller design methods, such as those described in [8,17,20,21,46,47,58], do not attempt to exploit this useful encoded information. Modern servo-controller design techniques such as those presented in [32-40] do recognize and exploit this useful real-time information.

1.5.4. Sensitivity to Parameter Perturbations

Conventional (classical and modern) servo-tracking design techniques do not incorporate explicit means for accommodating the almost certain event that at least one of the actual plant-parameter values will fail to match the value used during the design process. As discussed in Subsection 1.2.2, such parameter mismatches tend to cause an inappropriate feedback control-action to occur, which can result in loss of tracking quality and even cause a loss of closed-loop stability.

The degree to which a servo-tracking controller maintains performance specifications in the face of off-nominal values of plant parameters can be viewed as a measure of the robustness quality of that servo-tracking controller. Today's modern tracking-systems impose close-tolerance, high-performance demands on such things as settling-time, peak-errors and disturbance rejection. A tracking system whose stability is sensitive to certain parameter values will not consistently meet those demands. Therefore it is important that the closed-loop performance specifications, in addition to closed-loop stability, be maintained in the face of unmeasurable changes in plant-parameter values [59]. Servo-tracking controller design methods that achieve a degree of robustness to parameter variations are presented in [34,35,39]; however those techniques assume zero, constant, or stepwise-constant servo-commands and do not include complex, time-varying commands as discussed in Subsection 1.5.1. The servo-design methodology developed in this report will achieve robustness to plant parameter-variations and can be applied to systems that must track high-order, time-varying, servo-commands.

1.5.5. Systematic Design Procedures

Many of the servo-tracking controller theories and design procedures published in the professional journals are burdened by complexity. Classical design methods were often graphical and difficult to utilize when higher-order, multiple-input, multiple-output (MIMO) systems were considered. On the other hand, some modern design methods, such as pole-placement and observer theory, rely primarily on state-space and linear algebra techniques to reduce the complexity of the design somewhat. In fact, single and multiple control-input/plant-output time-invariant (and also time-varying) systems are handled with ease by the same methodology in modern control, whereas classical control methods are primarily suitable only for time-invariant systems (of the single control-input, single plant-output type). In addition the vector/matrix mathematical representations of modern control allow for relatively easy implementation of the servo-controller algorithm on a digital processor. Methods that utilize a simple algebraic pole-placement and observer theory approach to designing servo-tracking controllers are detailed in [37,38,40].

1.6. Goals of This Research Effort

The primary goal of this research effort is to develop a new, linear-algebraic procedure for designing high-performance digital servo-tracking controllers for linear, time-invariant MIMO systems. Digital servo-controllers designed by this procedure should be capable of reducing the effects of the shortcomings discussed in Section 1.5. A design methodology for partially achieving this goal for continuous-time (analog) controllers was presented in [35]. However, a general MIMO *digital* servo-control theory for linear plants, which overcomes the shortcomings identified in this Chapter and in [59-61], has apparently not been published in the literature. To accomplish the primary goal of this research

effort, several existing servo-controller results will be modified and incorporated into the new digital servo-controller design procedure. Those existing results are: (i) a linear-algebraic continuous-time servo-control method [37,70], which will be adapted to discrete-time; (ii) a recently developed discrete-continuous control result [38] that accommodates intersample ripple; and (iii) a linear adaptive control technique [34] that accommodates parameter-perturbations. The servo-controller design procedure presented in this report incorporates several additional features that enable the resulting digital servo-controllers to achieve a level of servo-tracking performance that is not obtainable by contemporary methods. A collection of worked examples, with simulations results, will be presented to illustrate the design procedure and level of servo-tracking performance that can be obtained by the new digital servo-tracking controller design method developed here.

2. THEORY AND DESIGN PROCEDURE FOR A NEW DIGITAL SERVO-TRACKING CONTROLLER FOR LINEAR DYNAMICAL SYSTEMS

2.1. Overview of Chapter 2

This research effort is concerned with the development of a new digital control design methodology, based on linear-algebraic methods, for the MIMO servo-tracking problem with an n^{th}-order linear plant and uncertain servo-commands and disturbances. As mentioned in Chapter 1, a linear-algebra type analog (continuous-time) control design methodology for high-performance servo-tracking in continuous-time was presented in [37,70]. In this Chapter a digital servo-tracking control design methodology is developed which parallels the continuous-time methodology in [37,70], with several improvements. That methodology subdivides the servo-tracking problem into intermediate subproblems that can be solved by simple linear-algebra techniques. This technique is unique in that no linear-algebra-based digital servo-tracking design-methodology currently exists that achieves a high-level of servo-tracking performance while overcoming the obstacles inherent in conventional servo-tracking design methods (as detailed in Chapter 1).

2.2. Mathematical Model of a Generic MIMO Linear Dynamical Plant

The specific class of plants considered in this research is the set of finite-dimensional, real-valued, MIMO, time-invariant linear dynamical plants. This class of plants can be represented by a linear-differential state-equation and an output equation of the general form

$$\begin{aligned} \dot{x}(t) &= Ax(t) + Bu(t) + Fw(t) \\ y(t) &= Cx(t) \end{aligned} \quad , \tag{2.1}$$

where

$x(t)$ = n-dimensional plant state-vector,

$u(t)$ = r-dimensional plant control input-vector,

$w(t)$ = p-dimensional vector representing the (assumed independent) multi-dimensional external disturbances,

$y(t)$ = m-dimensional plant output-vector,

A = n x n real-valued matrix (assumed known and constant for now, but will be considered subject to uncertain perturbations ΔA in Section 3.2),

B = n x r real-valued, constant, known matrix,

C = m x n real-valued, constant, known matrix (assumed to have maximal rank m), and

F = n x p real-valued, constant, known matrix.

A block diagram representation of the class of plants in (2.1) is shown in Figure 2.1.

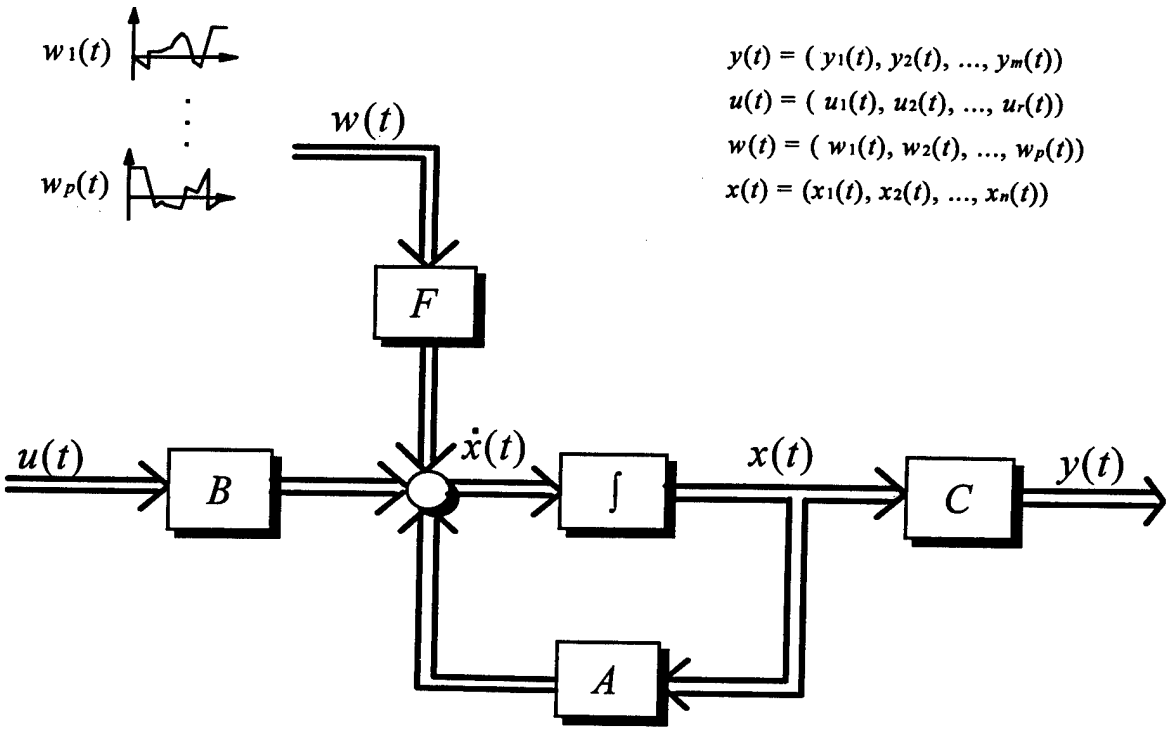

Figure 2.1 Block Diagram Model of the Class of Continuous-Time Plants Considered in This Study.

In order to design an effective servo-tracking controller for the class of plants in (2.1), it is generally necessary that the control input $u(t)$ be able to "steer" or control the plant state $x(t)$, without restriction, throughout state-space. For this reason, it is assumed that the plant in (2.1) is completely controllable, in the sense of Kalman. That is, for any pair of states (x_o, x_T) there exists a control action $u(t)$, $t_0 \le t \le T < \infty$, which can control the plant state $x(t)$ from the state x_o, at the initial time t_o, to the state $x(T) = x_T$ at some finite time $T > t_o$.

2.3. Information Aspects of the Servo-Tracking Problem

The typical MIMO servo-tracking control problem consists of the design of a controller that will make each of the plant outputs $y_i(t)$ quickly coincide with and thereafter accurately track any admissible servo-command $y_{ci}(t)$, $i = 0, 1, 2, ..., m$, in the face of arbitrary plant initial-conditions $x(t_o)$ and uncertain, unmeasurable plant disturbances $w(t)$ of a specified class. To accomplish this feat, the servo-tracking controller processes real-time information, as provided to it, in a two-input/one-output data-processing operation (algorithm) as shown in Figure 2.2. Here, the real-time inputs to the algorithm are the m-dimensional vector of plant-output measurements $y = (y_1, y_2, \cdots, y_m)$ and the m-dimensional vector of (assumed independent) servo-command measurements $y_c = (y_{c1}, y_{c2}, \cdots, y_{cm})$. In general, the

set of output measurements $y(t)$ does not necessarily comprise the set of measurements to be servo-controlled. However, in this report, to avoid unnecessary complexity, it is assumed that the set of output measurements $y(t)$ do in fact comprise the set of measurements we desire to control. The real-time output of the algorithm is the r-dimensional vector of servo-tracking control signals $u=(u_1,u_2,\cdots,u_r)$ which drive the various control actuators (final control elements) that alter the plant-state motion $x(t)$. The quality of tracking performance achieved by a servo-tracking controller is directly related to how well the controller extracts and processes the useful information encoded into $y_c(t)$ and $y(t)$ to produce the control actuation signal $u(t)$.

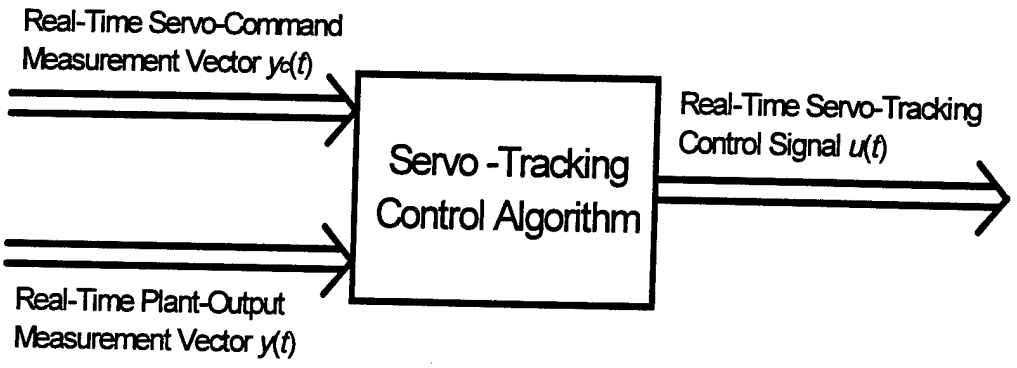

Figure 2.2 Typical Servo-Tracking Controller Viewed as a Two-Input/One-Output Algorithm.

Throughout this study it will be assumed, for simplicity, that the control actuators are "ideal" in the sense that they exactly replicate the associated control signal $u_i(t)$ with no time-lag, ringing, overshoot, and other imperfections often associated with specific actuator hardware. This assumption enables us to focus attention on the scientific issue of maximizing servo-tracking performance, with respect to the servo-tracking algorithm design, without involving the various imperfections of application-specific actuator hardware. Of course, in real applications, an appropriate dynamic model of the actuator imperfections would be incorporated with the plant model to allow the control algorithm design to account for those actuator imperfections.

As stated in Chapter 1, the main tasks of the servo-tracking controller are to achieve closed-loop stability for the (possibly unstable) plant and to quickly achieve and maintain accurate servo-tracking $y_i(t) \approx y_{ci}(t)$. The performance of a servo-tracking controller is usually characterized in terms of the time-variations in the tracking-error vector $\varepsilon_y(t)$ defined as the instantaneous difference between the desired response (= the vector servo-command $y_c(t)$) and the actual response (= the vector plant output $y(t)$), which was written (in Section 1.1) as

$$\varepsilon_y(t) = y_c(t) - y(t). \tag{2.2}$$

Thus, the task of the servo-tracking controller is to regulate the tracking-error in (2.2) to zero, within a specified settling-time, and thereafter keep $\varepsilon_y(t)$ sufficiently close to zero in the face of any admissible (anticipated) behavior of $y_c(t)$ and/or $w(t)$.

2.4. Assumptions Concerning the Availability of Measurements of the Plant Output $y(t)$ and the Servo-Command $y_c(t)$

The digital servo-controller design procedure developed in this study assumes that only real-time discrete-time measurements of the plant-output vector $y(t)$ and servo-command vector $y_c(t)$ are available as inputs to the servo-controller. Those discrete-time measurements are obtained from a discrete-time sensor that periodically samples the vectors $y(t)$ and $y_c(t)$ and then communicates those values to the digital servo-controller. The analog-to-digital converter (the sample/hold device) associated with that discrete-time sensor has a value of "hold time" T that can be chosen by the designer. Therefore, it is assumed that the inputs to the control algorithm are the discrete-time data for the plant-output vector $y(kT)$ and the servo-command vector $y_c(kT)$ and the output of the servo-control algorithm is the control vector $u(kT)$.

2.5. Representation of Uncertainty in the Servo-Tracking Problem

Some examples of the sources of uncertainty that can arise in practical servo-tracking control systems are uncertain loading effects on the plant, dc bias effects, modeling errors, uncertain variations in servo-commands, sensor noise, etc. The time-domain behavior of such uncertain "inputs" can be classified into two broad categories: 1) noise-type behavior; and 2) waveform-structured behavior.

Noise-type inputs are characterized by random, erratic time-behavior exhibiting relatively high-frequency components. The uncertain time-behavior of such inputs is best described by "long-term average" statistical properties such as mean, covariance, power spectral density, etc., based on the input's averaged behavior over a relatively long time-interval. Examples of such noise-type inputs are fluid turbulence, radio static, and sensor noise.

A large class of industrial control problems involve uncertain inputs which do not behave like noise-type inputs. In particular, they are not random and erratic in time, but rather their time-behavior has some degree of regularity or "structure," at least over short windows-of-time $\{\Delta t_i\}_1^N$. This type of time-behavior is referred to as waveform-structured behavior [40]. A typical time-plot of a generic uncertain input $s(t)$ having waveform structure is shown in Figure 2.3. Inputs of this type can be considered analytical over each interval Δt_i with uncertain "jumps" in the value, derivatives, etc., of $s(t)$, occurring only at the edges of the time-intervals Δt_i. Some examples of waveform-structured uncertain inputs are dynamic loading effects, dc bias effects, and uncertain servo-commands.

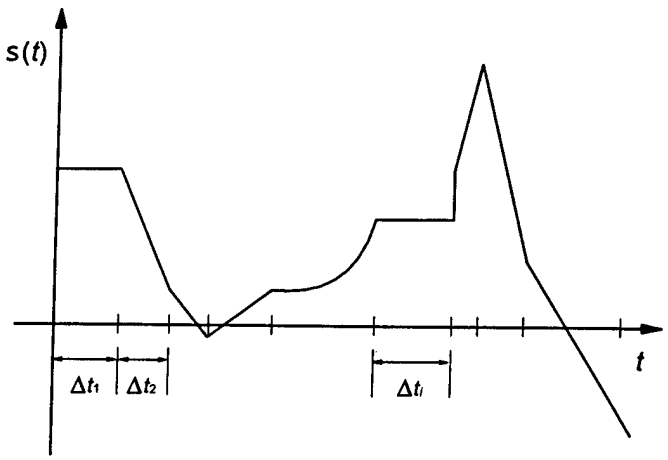

Figure 2.3 Time-Plot of an Uncertain Input $\mathsf{s}(t)$ Having Waveform Structure.

2.5.1. A Linear Waveform Model and Linear State Model for an Uncertain Waveform-Structured Input $\mathsf{s}(t)$

The class of practical uncertain inputs (i.e., disturbances, servo-commands) addressed in this research are assumed to have waveform structure in the sense just defined and the uncertain time-behavior of those inputs is assumed to be modeled in the "linear waveform model" [40] format

$$\mathsf{s}(t) = c_1 f_1(t) + c_2 f_2(t) + \cdots + c_q f_q(t), \tag{2.3}$$

where the set of functions $\{f_i(t)\}_1^q$ (hereafter called the "basis set" [40] for $\mathsf{s}(t)$) are chosen by the designer to mirror the collection of independent waveform patterns that can be exhibited by $\mathsf{s}(t)$ over short time-windows Δt_i. The weighting coefficients c_i, $i = 1, 2, \ldots, q$, in (2.3) are completely unknown, uncontrollable, and unpredictable "stepwise-constants" that may "jump"in value at the edges of the time-windows Δt_i as shown in Figure 2.4. In some cases, $\mathsf{s}(t)$ is not directly measurable and must be estimated from the plant output $y(t)$. In those cases, the servo-tracking controller will be unable to estimate $\mathsf{s}(t)$ and adapt to rapidly changing c_i values, if the time-interval Δt_i between successive jumps in the c_i is too small Therefore it is necessary to assume that the jumping of the c_i's in (2.3) occur only occasionally such that, on average, the minimum spacing Δt_{min} between successive jumps is somewhat larger than the digital servo-controller sampling-period T. More generally (2.3) may be used to represent an m-vector $\mathsf{s}(t)$ of uncertain inputs of the form

$$\mathsf{s}(t) = \begin{pmatrix} \mathsf{s}_1(t) \\ \mathsf{s}_2(t) \\ \cdot \\ \cdot \\ \cdot \\ \mathsf{s}_m(t) \end{pmatrix}, \tag{2.4}$$

where each scalar input $\mathsf{s}_i(t)$, $i = 1, 2, \ldots, \mathsf{m}$, has an associated linear waveform-model of the form (2.3).

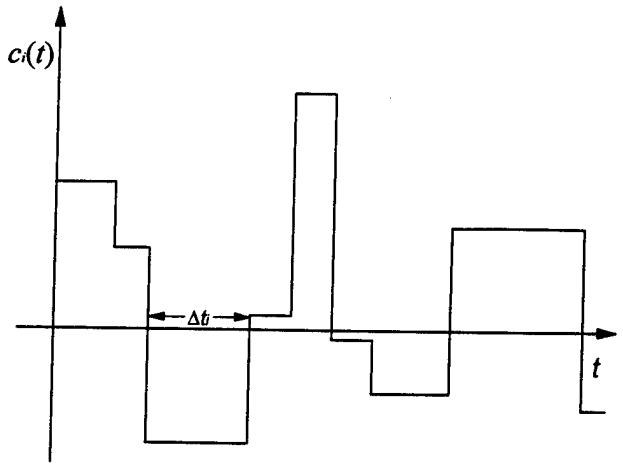

Figure 2.4 Uncertain Stepwise-Constant Time-Behavior of the $c_i(t)$'s in (2.3).

The first step in accessing the useful information embedded in an uncertain, waveform-structured input $s_i(t)$ is to identify an appropriate set of basis functions $\{f_i(t)\}_1^q$ that can model the time-behavior of $s_i(t)$ across each of the intervals $\{\Delta t_i\}$. Those basis functions can be determined by analyzing historical data or dynamic characteristics of the process that creates the input $s_i(t)$ or through visual observation or computer analysis of $s_i(t)$ recordings. For mathematical convenience, it is further assumed that each $f_i(t)$ satisfies some linear homogeneous differential equation $\mathcal{D}_i$ with constant coefficients (this constant coefficient assumption can be relaxed to known, time-varying coefficients, as shown in [40]). The assumption that each $f_i(t)$ satisfies some linear differential equation is rather commonly satisfied in realistic, practical problems. The governing differential equation $\mathcal{D}_i$ may differ in order and/or coefficient values for each $f_i(t)$. Those differential equations for each $f_i(t)$ can be combined to form a single linear homogeneous differential equation $\mathcal{D}$ which can be written as (assuming $m = 1$; i.e., $s_i = s$)

$$\frac{d^{\rho}s(t)}{dt^{\rho}} + \alpha_{\rho}\frac{d^{\rho-1}s(t)}{dt^{\rho-1}} + \alpha_{\rho-1}\frac{d^{\rho-2}s(t)}{dt^{\rho-2}} + \cdots + \alpha_2\frac{ds(t)}{dt} + \alpha_1 s(t) = 0, \tag{2.5}$$

where the α_i, $i = 1, 2, \ldots, \rho$, are known (knowable) constants that depend only on the known basis functions $f_i(t)$; i.e., the α_i do not depend on the "values" of the totally unknown c_i's in (2.3).

In order to mathematically account for the uncertain jumping of the weighting coefficients c_i at the edges of the time-windows Δt_i, an impulsive-type forcing function $\omega(t)$ can be added to the right-side of the differential equation model (2.5). This forcing function $\omega(t)$ consists of impulses, doublets, etc. with completely unknown intensities and unknown arrival-times. With the addition of such a symbolic forcing term $\omega(t)$, (2.5) becomes

$$\frac{d^{\rho}s(t)}{dt^{\rho}} + \alpha_{\rho}\frac{d^{\rho-1}s(t)}{dt^{\rho-1}} + \alpha_{\rho-1}\frac{d^{\rho-2}s(t)}{dt^{\rho-2}} + \cdots + \alpha_2\frac{ds(t)}{dt} + \alpha_1 s(t) = \omega(t). \tag{2.6}$$

The uncertain, stepwise-constant behavior of the c_i's in (2.3) can now be imagined as the result of the action of $\omega(t)$ on the solutions $\mathsf{s}(t)$ of (2.6).

To utilize (2.6) in developing a control algorithm, it is convenient to express the uncertain input model (2.6) in a state-variable format. For this purpose, write $\mathsf{s}(t)$ in the form

$$\mathsf{s}(t) = l\,q(t) \quad , \tag{2.7}$$

where

$$l = (1, 0, \cdots, 0)$$
$$q = (q_1, q_2, \cdots, q_\rho)^{\prime}$$

and where the q_i are referred to as "state-variables" for the uncertain input $\mathsf{s}(t)$. The vector $q(t)$ is called a state vector for the uncertain input because at each t it embodies the "current" information needed to predict the behavior of $\mathsf{s}(t)$ over the time-interval Δt_i. One of the many possible choices for the q_i's in (2.7) is the phase variable choice. That is, $q_i(t) = \dfrac{d\mathsf{s}^{(i-1)}(t)}{dt^{(i-1)}}$, $i = 1, 2, \ldots, \rho$. Selecting the q_i's in that way and using (2.7) allows (2.6) to be rewritten equivalently as the following set of first-order, coupled linear differential equations, having uncertain Dirac impulse sequences $\kappa_i(t)$ as inputs (the latter inputs represent the equivalent effect of the impulsive forcing term $\omega(t)$ in (2.6))

$$\begin{aligned}
&\dot{q}_1(t) = q_2(t) + \kappa_1(t); \quad && q_1(t) = \mathsf{s}(t) \\
&\dot{q}_2(t) = q_3(t) + \kappa_2(t); \quad && q_2(t) = \dot{\mathsf{s}}(t) \\
&\quad\vdots \\
&\dot{q}_\rho(t) = -\alpha_1 q_1(t) - \alpha_2 q_2(t) - \cdots - \alpha_\rho q_\rho(t) + \kappa_\rho(t); \quad && q_\rho(t) = \frac{d\mathsf{s}^{(\rho-1)}(t)}{dt^{(\rho-1)}}
\end{aligned} \quad , \tag{2.8}$$

where the $\kappa_i(t)$, $i = 1, 2, \ldots, \rho$, denote sparse-in-time sequences of unknown impulses.

Expressions (2.7) and (2.8) can be expressed equivalently in the compact vector-matrix format,

$$\begin{aligned}
&\mathsf{s}(t) = l\,q(t) \\
&\dot{q}(t) = M_0 q(t) + \kappa(t)
\end{aligned} \quad , \tag{2.9}$$

where

$$M_0 = \begin{bmatrix} 0 & 1 & 0 & \cdots & 0 \\ 0 & 0 & 1 & \cdots & 0 \\ \vdots & \vdots & \vdots & \ddots & \vdots \\ 0 & 0 & 0 & \cdots & 1 \\ -\alpha_1 & -\alpha_2 & -\alpha_3 & \cdots & -\alpha_\rho \end{bmatrix}.$$

In the general case where $\mathsf{m} \geq 1$, and each $\mathsf{s}_i(t)$ has a linear waveform model as in (2.3), the corresponding linear state model is

$$\begin{aligned} \mathsf{s}(t) &= Lq(t) \\ \dot{q}(t) &= Mq(t) + \kappa(t) \end{aligned}' \qquad (2.10)$$

where

$\mathsf{s}(t)$ = m-dimensional uncertain vector input (given in (2.4)) which may or may not be accessible for direct on-line measurement,

$q(t)$ = d-dimensional "state" vector of the uncertain input $\mathsf{s}(t)$,

L = m x d constant, real-valued matrix,

M = d x d constant, real-valued matrix, and

$\kappa(t)$ = d-dimensional vector of time-sparse sequences of unknown impulses having completely unknown intensities and arrival-times.

Expression (2.10) constitutes the generic continuous-time state-model for the uncertain servo-commands $y_c(t)$ and disturbances $w(t)$ considered in this report.

2.5.2. An Example

As an example of describing, and obtaining a state model for, an uncertain waveform-structured input, consider the case of an uncertain scalar input $\mathsf{s}(t)$ composed of a random-like, weighted linear combination of step, ramp, and exponential modes of time-behavior. Such an input can be represented as

$$\mathsf{s}(t) = c_1 1 + c_2 t + c_3 e^{-\alpha t}. \qquad (2.11)$$

Comparing (2.11) with (2.3), the basis functions for $\mathsf{s}(t)$ in (2.11) are clearly

$f_1(t) = 1;$

$f_2(t) = t;$

$f_3(t) = e^{-\alpha t}$, where α is assumed known.

A simple method for obtaining the differential equation for $\mathsf{s}(t)$ over the intervals $\{\Delta t_i\}$ is to take the Laplace transform of (2.11), assuming c_1, c_2, c_3 are constant, to obtain

$$\mathsf{s}(s) = \frac{c_1}{s} + \frac{c_2}{s^2} + \frac{c_3}{s+\alpha} = \frac{(c_3 + c_1)s^2 + (c_1\alpha + c_2)s + c_2\alpha}{s^2(s+\alpha)} = \frac{P(s)}{Q(s)} \quad . \qquad (2.12)$$

Following the technique used in [40], imagine that $\mathsf{s}(t)$ is the output of a fictitious linear-dynamical system subject to initial conditions $\mathsf{s}(0), \dot{\mathsf{s}}(0), \ddot{\mathsf{s}}(0)$, which give rise to the term $P(s)$ in (2.12). This imaginary linear-dynamical system has the transfer function

$$G(s) = \frac{1}{Q(s)} \qquad \text{where} \quad Q(s) = s^3 + \alpha s^2 . \tag{2.13}$$

The input $\mathsf{s}(t)$ can now be imagined as satisfying an impulsive forced third-order differential equation of the form

$$\frac{d^3\mathsf{s}(t)}{dt^3} + \alpha \frac{d^2\mathsf{s}(t)}{dt^2} = \omega(t), \tag{2.14}$$

where $\omega(t)$ is an uncertain, impulsive-type external forcing function that mathematically accounts for the sparse-in-time jumping of the c_i coefficients in (2.11). To determine an appropriate state-variable model representing the dynamics of (2.11), the third-order differential equation in (2.14) is rewritten equivalently as the following set of first-order, coupled differential equations having uncertain Dirac impulse sequences as inputs (as described above (2.8))

$$\begin{aligned} \dot{q}_1(t) &= q_2(t) + \kappa_1(t); \qquad & q_1(t) &= \mathsf{s}(t) \\ \dot{q}_2(t) &= q_3(t) + \kappa_2(t); \qquad & q_2(t) &= \dot{\mathsf{s}}(t) \\ \dot{q}_3(t) &= -\alpha q_3(t) + \kappa_3(t); \qquad & q_3(t) &= \ddot{\mathsf{s}}(t) \end{aligned} \quad , \tag{2.15}$$

where the $\kappa_1(t)$, $\kappa_2(t)$, and $\kappa_3(t)$ are unknown, time-sparse sequences of impulses that represent the equivalent action of $\omega(t)$ in (2.14). For convenience, (2.15) can be expressed in the compact vector-matrix format

$$\mathsf{s}(t) = \begin{pmatrix} 1 & 0 & 0 \end{pmatrix} q(t); \qquad q = (q_1, q_2, q_3)$$

$$\dot{q}(t) = \begin{bmatrix} 0 & 1 & 0 \\ 0 & 0 & 1 \\ 0 & 0 & -\alpha \end{bmatrix} q(t) + \kappa(t) \quad , \tag{2.16}$$

which is equivalent to the general continuous-time state-model in (2.10).

2.6. A Discrete-Time Model for the Generic Linear Dynamical Plant in (2.1)

This research effort is concerned with the digital control of continuous-time physical systems with physical inputs $\{u(t), w(t)\}$ and outputs $y(t)$ that are continuous-time variables. In contrast, the inputs $\{y(kT), y_c(kT)\}$ and outputs $u(kT)$ of the digital servo-controller are discrete-time variables (variables that are measured or changed only at the discrete times $t = t_o + kT$, $k = 0, 1, 2, \ldots$). In order to effectively design a digital servo-controller (control algorithm for generating $u(kT)$) for the general class of plants under consideration, the basic continuous-time plant-model in (2.1) must be converted to an equivalent discrete-time model. This discrete-time model is a conventional difference equation which

describes how the values of $x(t)$ and $y(t)$ evolve for the discrete times $t = t_o + kT$, $k = 0, 1, 2, \ldots$. The following development of a discrete-time model for the plant in (2.1) closely follows that presented in [33]. Recall that the general solution of the continuous-time differential equation in (2.1) can be written as

$$x(t) = \Phi(t,t_o)x(t_o) + \int_{t_o}^{t} \Phi(t,\tau)Bu(\tau)d\tau + \int_{t_o}^{t} \Phi(t,\tau)Fw(\tau)d\tau, \tag{2.17}$$

where $\Phi(t,t_o)$ is the state transition matrix for A in (2.1) and is uniquely defined by the matric differential equation

$$\frac{d\Phi(t,t_o)}{dt} = A\Phi(t,t_o),$$

with the special initial condition

$$\Phi(t_o,t_o) = \mathrm{I},$$

where I is the n x n identity matrix.

Now, recalling that T is a fixed positive constant, set $t \to (t_o + T)$, and then set $t_o \to (t_o + kT)$, in (2.17). As is typical in conventional digital control problems, it is assumed that the control action $u(t)$ in (2.17) is of the "zero-order-hold" (z.o.h.) type; i.e., $u(t)$ remains constant ($u(t) = u(kT) =$ a constant) over each sample period, $t_o + kT \le t < t_o + (k+1)T$. This fact allows (2.17) to be written as the following discrete-time state-model (difference equation model) [33]:

$$x((k+1)T) = \tilde{A}x(kT) + \tilde{B}u(kT) + \tilde{v}((k+1)T), \tag{2.18}$$

where kT is hereafter used as shorthand notation for t_o+kT, and

$$\tilde{A} = \Phi((k+1)T,kT) = e^{AT}; \qquad A \text{ is assumed constant,}$$

$$\tilde{B} = \int_{kT}^{(k+1)T} \Phi((k+1)T,\tau)Bd\tau = \int_0^T e^{A(T-\tau)}d\tau B; \qquad B \text{ is assumed constant,}$$

$$\tilde{v}((k+1)T) = \int_{kT}^{(k+1)T} \Phi((k+1)T,\tau)Fw(\tau)d\tau = \int_0^T e^{A(T-\tau)}Fw(\tau+kT)d\tau; \quad F \text{ is assumed constant.}$$

The discrete-time plant-output relationship corresponding to (2.18) is

$$y(kT) = Cx(kT). \tag{2.19}$$

Note that (2.18) relates the "next" value $x((k+1)T)$ of x to the current value $x(kT)$ of x at the time $t = kT$. However, the evaluation of $\tilde{v}((k+1)T)$ in (2.18) requires knowledge of $w(\tau)$ over the entire interval $kT \le \tau \le (k+1)T$. In general, at the time $t = kT$ it is impossible to accurately and consistently predict the time-behavior of the uncertain, unmeasurable disturbances $w(t)$ over the remainder of that sampling-interval. Therefore to make (2.18) practically useful, it is necessary to further investigate and approximate the term $\tilde{v}((k+1)T)$. It will now be shown that the term $\tilde{v}((k+1)T)$ in (2.18) can be simplified by introducing a waveform-model for the time-variations of the uncertain, unmeasurable disturbances $w(\tau)$.

Disturbances were defined in Subsection 1.2.2 as uncontrollable inputs which act on a dynamical system. Unlike the servo-commands, disturbances are usually not directly measurable. For this research, the disturbances $w(t)$ are assumed to have waveform structure and to have a linear state-model (2.10) of the form

$$\begin{aligned} w(t) &= Hz(t) \\ \dot{z}(t) &= Dz(t) + \sigma(t) \end{aligned}, \tag{2.20}$$

as developed in Section 2.5 and where

$w(t)$ = p-dimensional vector of independent disturbances (defined in (2.1)), that are not accessible for direct on-line measurement,

$z(t)$ = ρ-dimensional state-vector for the disturbance $w(t)$,

H = p x ρ real-valued, constant matrix,

D = ρ x ρ real-valued, constant matrix, and

$\sigma(t)$ = a ρ-vector of sparse sequences $\sigma_i(t)$ of unknown impulses having completely unknown intensities and arrival-times.

Expression (2.20) represents the general continuous-time state-model for the uncertain, unmeasurable disturbances considered in this study. Proceeding as in [33], the state model in (2.20) can now be used to simplify the term $\tilde{v}((k+1)T)$ in (2.18). For this purpose one replaces τ by t in (2.20), and substitutes the result into $\tilde{v}((k+1)T)$ in (2.18) to obtain

$$\tilde{v}((k+1)T) = \int_0^T e^{A(T-\tau)} FHz(\tau + kT)d\tau . \tag{2.21}$$

Using (2.20) and methods similar to that used to obtain $x(t)$ in (2.17), the general solution of $z(\tau)$ in (2.21) can be written as

$$z(\tau) = \Phi_D(\tau, kT)z(kT) + \int_{kT}^{\tau} \Phi_D(\tau, \xi)\sigma(\xi)d\xi, \tag{2.22}$$

where Φ_D represents the state transition matrix for matrix D in (2.20). Substituting (2.22) into (2.21) and simplifying terms yields the following result [33] (recall that D is a constant matrix)

$$\tilde{v}((k+1)T) = \tilde{FH}\, z(kT) + \tilde{\gamma}(kT), \tag{2.23}$$

where

$$\tilde{FH} = \int_0^T e^{A(T-\tau)} FHe^{D\tau} d\tau \ ,$$

and

$$\tilde{\gamma}(kT) = \int_0^T e^{A(T-\tau)} FH \int_0^{\tau} e^{D(\tau-\xi)} \sigma(\xi + kT) d\xi d\tau \, .$$

Consolidating (2.18), (2.19), and (2.23) yields the "exact" discrete-time plant-model

$$\begin{aligned} x((k+1)T) &= \tilde{A}x(kT) + \tilde{B}u(kT) + \tilde{FH}\, z(kT) + \tilde{\gamma}(kT) \\ y &= Cx(kT) \end{aligned} \ , \tag{2.24}$$

which is mathematically equivalent to (2.18), under the assumption (2.20).

A discrete-time model for the time evolution of $z(kT)$ can be developed by letting $\tau \to t_o + (k+1)T$ in (2.22) and recalling that $(k+1)T$ denotes $t_o+(k+1)T$ to obtain

$$z((k+1)T) = \tilde{D}z(kT) + \tilde{\sigma}(kT), \tag{2.25}$$

where

$$\tilde{D} = e^{DT} \quad ; \qquad D \text{ is assumed constant,}$$

and

$$\tilde{\sigma}(kT) = \int_0^T e^{D(T-\xi)} \sigma(\xi + kT) d\xi \, .$$

Expressions (2.24) and (2.25) can now be combined to form the "exact" composite discrete-time model

$$\begin{pmatrix} x((k+1)T) \\ \hline z((k+1)T) \end{pmatrix} = \left[\begin{array}{c|c} \widetilde{A} & \widetilde{FH} \\ \hline 0 & \widetilde{D} \end{array}\right] \begin{pmatrix} x(kT) \\ \hline z(kT) \end{pmatrix} + \begin{pmatrix} \widetilde{B} \\ \hline 0 \end{pmatrix} u(kT) + \begin{pmatrix} \widetilde{\gamma}(kT) \\ \hline \widetilde{\sigma}(kT) \end{pmatrix}$$

$$y(kT) = \begin{pmatrix} C & | & 0 \end{pmatrix} \begin{pmatrix} x(kT) \\ \hline z(kT) \end{pmatrix} \tag{2.26}$$

The quantities $\widetilde{\gamma}(kT)$ and $\widetilde{\sigma}(kT)$ in (2.26) are an accumulation, from kT to $(k+1)T$, of the effects of the completely unknown, unpredictable, and unmeasurable sparse impulses $\sigma(t)$ associated with the disturbance model (2.20) and which arrive during the "intersample interval" $kT < t < (k+1)T$ between successive sampling instants [33]. Since the arrival-times and intensities of the $\sigma(t)$ impulses are assumed to be completely unknown, there is no rational, scientific way to predict the values of $\widetilde{\gamma}(kT)$ and $\widetilde{\sigma}(kT)$. Disregarding the $\widetilde{\gamma}(kT)$ and $\widetilde{\sigma}(kT)$ terms will necessarily introduce errors, that accumulate only from kT to $(k+1)T$, in the predicted values of $x((k+1)T)$ and $z((k+1)T)$ as determined by (2.26). To avoid those errors being too significant, it is necessary to invoke the assumption (from Section 2.5) that the $\sigma(t)$ impulses (denoted as $\kappa(t)$ in Section 2.5) occur only occasionally (sparse-in-time), with minimum spacing at Δt_{min} between successive impulses being somewhat larger than the sampling-period T [33]. That assumption results in the $\widetilde{\sigma}(kT)$ and $\widetilde{\gamma}(kT)$ terms remaining "quiet" during most intersample intervals. Consequently, the $\widetilde{\sigma}(kT)$ and $\widetilde{\gamma}(kT)$ terms are disregarded throughout the design process.

2.7. Introduction of a Discrete-Time Evolution Equation for the Servo-Tracking Error

As previously stated, a digital servo-tracking controller $u(kT)$ must achieve closed-loop stability for the (possibly unstable) plant, and simultaneously quickly achieve and maintain accurate servo-tracking. The "tracking-error" in (2.2) is the single most important entity for measuring servo-tracking controller performance. In terms of discrete-time, $t = kT$, that tracking-error is written as

$$\varepsilon_y(kT) = y_c(kT) - y(kT). \tag{2.27}$$

The term $\varepsilon_y(kT)$ will be hereafter referred to as the discrete-time servo-tracking error. Thus, the task of the digital servo-tracking controller is to regulate the tracking-error in (2.27) to zero with a prescribed settling-time and thereafter maintain $\varepsilon_y(kT)$ acceptably near zero in the face of all anticipated uncertainties. That is, the digital controller must achieve

$$\varepsilon_y(kT) \to 0 \; ; \qquad k = 0, 1, 2, \ldots , \tag{2.28}$$

in a sufficiently small amount of time, and maintain $\left\| \varepsilon_y(kT) \right\| \approx 0$ thereafter.

It was shown in [37] that a fundamental necessary condition (called the "trackability condition") for achievement of theoretically exact MIMO servo-tracking, $y(t) \equiv y_c(t), \forall\, t$, is that the vector servo-command input $y_c(t)$ consistently lie in the column range-space of the plant output matrix C in (2.1). This fundamental necessary condition can be expressed as

$$y_c(t) \in \Re[C] \quad \forall\ t\,; \qquad \Re[\bullet] = \text{column range-space of } [\bullet], \tag{2.29}$$

or equivalently,

$$\text{rank}[C \mid y_c(t)] \equiv \text{rank}[C] \quad \forall\, t\,. \tag{2.30}$$

We hereafter assume that (2.29) and (2.30) are satisfied for the $y_c(t)$ being considered. It is remarked that if (2.29) and (2.30) are <u>not</u> satisfied the command $y_c(t)$ is "improper" for the plant in (2.1), in the sense that, even under <u>ideal</u> conditions, it is physically and mathematically impossible for the plant output $y(t)$ to consistently equal $y_c(t)$, for all t.

To proceed with the development of the new digital servo-controller design methodology, it is first necessary to develop a state-model representation of the time-behavior of the uncertain servo-commands $y_c(t)$. The elements $y_{ci}(t)$ of the servo-command vector $y_c(t)$ are assumed to be uncertain time-varying inputs which have "waveform structure" and have a corresponding linear state-model of the form

$$\begin{aligned} y_c(t) &= Gc(t) \\ \dot{c}(t) &= Ec(t) + \mu(t) \end{aligned} \quad , \tag{2.31}$$

as discussed in Section 2.5 and where

$y_c(t)$ = m-vector of independent servo-commands (defined in Section 2.3) accessible for measurement only in discrete real-time,

$c(t)$ = v-dimensional state-vector for the servo-command $y_c(t)$,

G = m x v constant, real-valued matrix,

E = v x v constant, real-valued matrix, and

$\mu(t)$ = a v-vector of sparse-in-time sequences of unknown, unmeasurable impulses $\mu_i(t)$ having completely unknown intensities and arrival-times.

Expression (2.31) constitutes the generic continuous-time state-model for the uncertain servo-commands to be considered in this report.

Substituting (2.31) into (2.29) yields the expression

$$Gc(t) \in \Re[C] \quad \forall\, t\,. \tag{2.32}$$

Recall from Section 2.5 and (2.31) that the "state" $c(t)$ of the servo-command is a completely arbitrary v-vector; therefore the necessary and sufficient condition for achieving exact servo-tracking ($\varepsilon_y(t) \equiv 0$ for some $x(t)$) is equivalent to requiring that [37],

$$\Re[G] \subseteq \Re[C], \tag{2.33}$$

in the state-model (2.31).

Satisfaction of condition (2.33) implies that it is possible to express each column of the matrix G as some linear combination of the columns of C. That is,

$$G = C\theta \quad , \tag{2.34}$$

for some (possibly nonunique) matrix θ. The factorization in (2.34) assures that at each t it is mathematically possible to have

$$\varepsilon_y(t) = y_c(t) - Cx(t) = 0\,, \tag{2.35}$$

for some $x(t)$. However, it is further necessary to invoke the complete controllability condition to assure that the required $x(t)$ in (2.35) can be attained by an admissible control input $u(t)$, in general.

To develop the discrete-time evolution equation for $\varepsilon_y(kT)$ in (2.27), it is necessary to convert the continuous-time servo-command model in (2.31) to an equivalent discrete-time model. A discrete-time model for the time-evolution of the servo-command state $c(kT)$ can be developed by a method similar to that used in Section 2.6 to obtain (2.25). In that way, the final form of the discrete-time state model for the uncertain servo-command, having dynamics modeled by (2.31), is

$$\begin{aligned} y_c(kT) &= Gc(kT) \\ c((k+1)T) &= \widetilde{E}c(kT) + \widetilde{\mu}(kT) \end{aligned} \quad ; \quad \begin{cases} c = (c_1, c_2, \cdots, c_v) \\ \mu = (\mu_1, \mu_2, \cdots, \mu_v) \end{cases} \quad , \tag{2.36}$$

where

$$\widetilde{E} = e^{ET}\,,$$

and

$$\widetilde{\mu}(kT) = \int_0^T e^{E(T-\xi)}\mu(\xi + kT)d\xi\,.$$

The quantity $\widetilde{\mu}(kT)$ in (2.36) is a v-vector of completely unknown, unpredictable, and unmeasurable "residual-effects" caused by the arrival of uncertain $\mu(t)$ impulses (2.31) during the interval between the sampling instants $kT < t < (k+1)T$. Since the arrival-times and intensities of the $\mu(t)$ impulses are completely unknown, there is no rational, scientific way to predict the value of $\widetilde{\mu}(kT)$. Therefore for the reasons discussed below (2.26), and as advocated in [33], the $\widetilde{\mu}(kT)$ term will be ignored throughout the design process.

Substituting (2.19), (2.36), and (2.34) into (2.27) yields

$$\begin{aligned} \varepsilon_y(kT) &= Gc(kT) - Cx(kT) \\ &= C\big(\theta c(kT) - x(kT)\big) \end{aligned} \quad , \tag{2.37}$$

where $c(kT)$ is the state of the servo-command $y_c(t)$ at the discrete time $t = kT$, $k = 0, 1, 2, \ldots$, as indicated in (2.36).

In [37], Johnson developed a novel method for studying and controlling the time-evolution of the servo-tracking error ε_y by introducing what he called the "servo-state" vector $e_{ss}(t)$ associated with the servo-tracking problem. For purposes of the present study the servo-state vector e_{ss} introduced in [37] is expressed (in discrete-time) as

$$e_{ss}(kT) \overset{\Delta}{=} \theta c(kT) - x(kT). \tag{2.38}$$

Thus, $e_{ss}(kT)$ is an n-dimensional vector representing the difference between the n-vector $\theta c(kT)$ and the plant state $x(kT)$. Using (2.38) to express the servo-tracking error $\varepsilon_y(kT)$ in (2.37) turns out to be a key idea in the development of an all-algebraic servo-tracking design technique. In particular, using (2.38), expression (2.37) can be written as

$$\varepsilon_y(kT) = Ce_{ss}(kT). \tag{2.39}$$

It is clear from (2.39) that the servo-tracking error will be zero at each of the sample times $t = kT$, $k = 0, 1, 2, \ldots$, if, and only if, the motions of the vector $e_{ss}(kT)$ remain confined to the null-space of C. The discrete-time servo-tracking control task can now be viewed (ideally) as the design of an algorithm for the digital control $u(kT)$ such that the servo-state vector $e_{ss}(kT)$ rapidly approaches, and thereafter stays within, the nullspace of C, or equivalently, $Ce_{ss}(kT) \to 0$. Therefore, the digital servo-controller design task is reduced to a *discrete-time linear subspace stabilization problem* for the servo-state vector $e_{ss}(kT)$. The linear subspace stabilization problem, introduced in [76], is a generalization of the conventional null-point stabilization problem where the null-point is generalized to an $(n\text{-}m)$-dimensional null-space.

The discrete-time evolution equation for $e_{ss}(kT)$ is determined by forward shifting (2.38) once as follows:

$$e_{ss}((k+1)T) = \theta c((k+1)T) - x((k+1)T). \tag{2.40}$$

Substituting (2.24) and (2.36) into (2.40) yields

$$e_{ss}\big((k+1)T\big) = \theta\tilde{E}c(kT) + \theta\tilde{\mu}(kT) - \tilde{A}x(kT) - \tilde{B}u(kT) - \tilde{FH}z(kT) - \tilde{\gamma}(kT), \tag{2.41}$$

and incorporating (2.38) into (2.41) yields

$$\begin{aligned} e_{ss}\big((k+1)T\big) = {} & \tilde{A}e_{ss}(kT) - \tilde{B}u(kT) + \big(\theta\tilde{E} - \tilde{A}\theta\big)c(kT) - \tilde{FH}z(kT) \\ & + \theta\tilde{\mu}(kT) - \tilde{\gamma}(kT) \end{aligned} \tag{2.42}$$

For reasons discussed below (2.26) and (2.36), the terms $\tilde{\mu}(kT)$ and $\tilde{\gamma}(kT)$ in (2.42) have been disregarded. Ignoring those terms allows one to re-write (2.42) in the truncated form

$$\bar{e}_{ss}\big((k+1)T\big) = \tilde{A}\bar{e}_{ss}(kT) - \tilde{B}u(kT) + \big(\theta\tilde{E} - \tilde{A}\theta\big)c(kT) - \tilde{FH}z(kT), \tag{2.43}$$

where the notation $\bar{e}_{ss}$ indicates that the effect of the terms $\tilde{\mu}(kT)$ and $\tilde{\gamma}(kT)$ have been ignored. Accordingly, (2.39) is re-written as

$$\bar{\varepsilon}_y(kT) = C\bar{e}_{ss}(kT). \tag{2.44}$$

2.8. Information Aspects of the $\bar{e}_{ss}(kT)$ Subspace Stabilization Problem

With respect to (2.43) and (2.44) the task of the digital servo-tracking controller is (ideally) to quickly regulate the servo-state vector $\bar{e}_{ss}(kT)$ in (2.43) to the null-space of the matrix C (e.g., $\bar{e}_{ss}(kT) \to \mathcal{N}[C]$, where, hereafter, $\mathcal{N}[\bullet]$ indicates the null-space of $[\bullet]$) and maintain $\bar{e}_{ss}(kT) \in \mathcal{N}[C]$ thereafter. However, the structure of the matrices $\tilde{A}$, $\tilde{B}$, C, $\tilde{FH}$, and $\tilde{E}$ might not permit $\bar{e}_{ss}(kT)$ to be made invariant with respect to the entire $\mathcal{N}[C]$ for arbitrary disturbances $w(t)$ and servo-commands $y_c(t)$. Consequently, in the most general case, the servo-control designer must strive to control $\bar{e}_{ss}(kT)$ to <u>some</u> subspace $S_\nu \subseteq \mathcal{N}[C]$, $\nu = 0, 1, 2, \ldots, n-m$, where ν indicates the dimension of the subspace S. That is, one should seek a matrix $\bar{C}$ and design $u(kT)$ to achieve

$$\bar{e}_{ss}(kT) \to S_\nu = \mathcal{N}[\bar{C}] \subseteq \mathcal{N}[C]; \qquad k = 0, 1, 2, \ldots \ , \tag{2.45}$$

where $\bar{C}$ is an $(n-\nu) \times n$ partitioned matrix of the form

$$\bar{C} = \begin{bmatrix} C \\ \hline P \end{bmatrix}, \tag{2.46}$$

and where P is any $(n\text{-}m\text{-}\nu)$ x n matrix such that

$$\text{rank}[\bar{C}] = n - \nu, \qquad \text{(since it is assumed that rank}[C] = m\text{, it follows that rank}[P] = n - m - \nu)$$

and

$$\mathcal{N}[\bar{C}] \subseteq \mathcal{N}[C].$$

The columns of $\bar{C}$ so defined form a basis for the "orthogonal complement" of S_ν. To study the dynamics of $\bar{e}_{ss}(kT)$ relative to S_ν it suffices to study $\bar{C}\bar{e}_{ss}(kT)$ (compare to (2.45)). Therefore, it is desirable to find the subspace $S_\nu \subseteq \mathcal{N}[C]$ of <u>largest</u> dimension ν (largest "landing zone" for $\bar{e}_{ss}(kT)$) such that $\bar{e}_{ss}(kT)$ can be stabilized to and thereafter remain within the subspace S_ν as illustrated in Figure 2.5. This latter problem can be stated in terms of the subspace stability concepts introduced in [74] and used in [37]. That is, $u(kT)$ should be designed such that some linear subspace $S_\nu = \mathcal{N}[\bar{C}] \subseteq \mathcal{N}[C]$ is converted into a uniformly asymptotically-stable invariant-subspace for the closed-loop system (2.43) and such that the motions of $\bar{e}_{ss}(kT)$, within the subspace S_ν, remain bounded for all bounded servo-command state motions $c(kT)$ and disturbance state motions $z(kT)$. The choice of P in (2.46) will be explained later in Subsection 2.11.7.

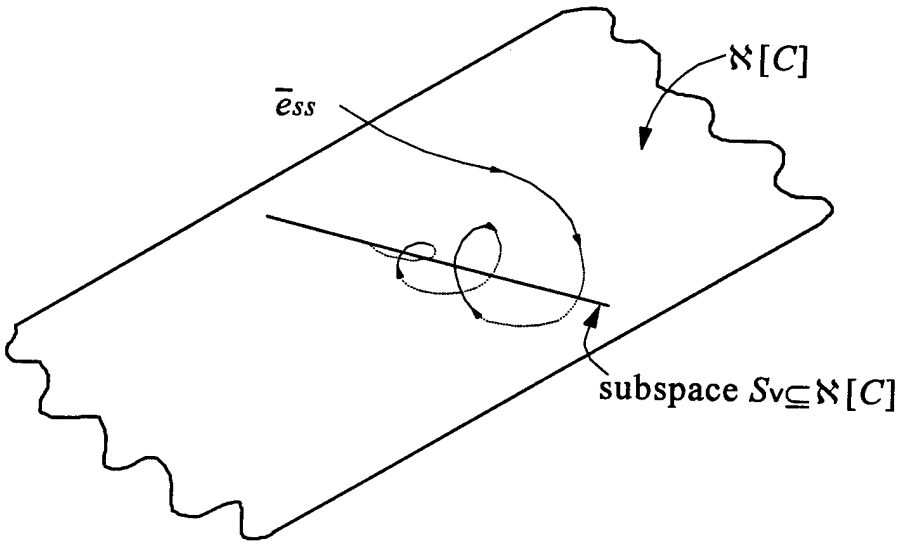

Figure 2.5 Stabilization of $\bar{e}_{ss}$ to Some Linear Subspace $S_v \subseteq \aleph[C]$.

Certain technical conditions must be met in order for there to exist a $u(kT)$ that can make $\bar{e}_{ss}(kT)$ quickly and accurately approach a given subspace $S_v \subseteq \aleph[C]$ and become invariant to S_v in the face of arbitrary, uncertain behaviors of $c(kT)$ and $z(kT)$. These conditions govern the design of the digital servo-tracking controller $u(kT)$ and will be discussed individually as their need arises in the design procedure developed in the following sections.

2.9. Decomposition of the Digital Servo-Tracking Control-Effort

To develop a digital control law (algorithm for generating $u(kT)$), the standard control-effort decomposition as used in DAC theory [40,71,72] will be invoked. This technique consists of splitting the total (vector) control-effort $u(kT)$ into a sum of individual (vector) terms as follows:

$$u(kT) = u_{sc}(kT) + u_p(kT), \tag{2.47}$$

where each term in (2.47) is assigned a specific task.

Collectively, the control terms in (2.47) are responsible for achieving closed-loop stability, and regulating $\bar{e}_{ss}(kT)$ to a subspace $S_v \subseteq \aleph[C]$, thereby controlling the servo-tracking error $\varepsilon_y(kT)$ to zero. The control term $u_{sc}(kT)$ is responsible for counteracting the effects of the disturbances $w(t)$ and the "disturbance-like" effects of the servo-commands $y_c(t)$ on the servo-tracking error in (2.44). The term $u_p(kT)$ is responsible for stabilizing the servo-state vector $\bar{e}_{ss}(kT)$ to a designated subspace $S_v \subseteq \aleph[C]$,

while achieving an acceptable closed-loop settling-time for the servo-tracking error ε_y, assuming $u_{sc}(kT)$ is performing its task. Substituting (2.47) into (2.43), and re-grouping terms, yields

$$\bar{e}_{ss}((k+1)T) = \tilde{A}\bar{e}_{ss}(kT) - \tilde{B}u_p(kT) + \left((\theta\tilde{E} - \tilde{A}\theta)c(kT) - \tilde{F}\tilde{H}z(kT) - \tilde{B}u_{sc}(kT)\right). \qquad (2.48)$$

From consideration of (2.48) and (2.45) it is clear that the individual tasks of u_{sc} and u_p can be expressed mathematically as two conditions which must be satisfied simultaneously. The condition associated with $u_{sc}(kT)$ is

$$\bar{C}\left[\left(\theta\tilde{E} - \tilde{A}\theta\right)c(kT) - \tilde{F}\tilde{H}\,z(kT) - \tilde{B}u_{sc}(kT)\right] \equiv 0; \qquad \forall\, c(kT) \text{ and } z(kT), \qquad (2.49)$$

which can be written as

$$\bar{C}\left\{\left[\theta\tilde{E} - \tilde{A}\theta \;\middle|\; -\tilde{F}\tilde{H}\right]\begin{pmatrix} c(kT) \\ z(kT) \end{pmatrix} - \tilde{B}u_{sc}(kT)\right\} \equiv 0 \qquad . \qquad (2.50)$$

Since $y_c(t)$ and $w(t)$ almost always originate from completely different (and uncorrelated) sources, in general, the necessary and sufficient condition for existence of a $u_{sc}(kT)$ satisfying (2.50), for all $c(kT)$ and $z(kT)$, is

$$\text{rank}\left[\bar{C}\theta\tilde{E} - \bar{C}\tilde{A}\theta \;\middle|\; \bar{C}\tilde{F}\tilde{H} \;\middle|\; \bar{C}\tilde{B}\right] = \text{rank}\left[\bar{C}\tilde{B}\right], \qquad (2.51)$$

which is equivalent to the two simultaneous conditions

$$\text{rank}\left[\bar{C}\theta\tilde{E} - \bar{C}\tilde{A}\theta \mid \bar{C}\tilde{B}\right] = \text{rank}\left[\bar{C}\tilde{B}\right], \qquad (2.52)$$

and

$$\text{rank}\left[\bar{C}\tilde{F}\tilde{H} \;\middle|\; \bar{C}\tilde{B}\right] = \text{rank}\left[\bar{C}\tilde{B}\right]. \qquad (2.53)$$

The decomposition in (2.52) and (2.53) suggests that the control term u_{sc} in (2.48) can be further split into two terms as follows

$$u_{sc}(kT) = u_s(kT) + u_c(kT), \qquad (2.54)$$

allowing (2.47) to be rewritten as

$$u(kT) = u_s(kT) + u_c(kT) + u_p(kT). \qquad (2.55)$$

In (2.55), $u_s(kT)$ is responsible for counteracting the "disturbance-like" effects of the servo-commands $y_c(t)$ and $u_c(kT)$ is responsible for counteracting the effects of the disturbances $w(t)$ as they appear in (2.48). Mathematically, the tasks of $u_s(kT)$ and $u_c(kT)$ are to achieve the identities

$$\overline{C}\left[\tilde{F}\tilde{H}\,z(kT)+\tilde{B}u_c(kT)\right]\equiv 0;\qquad \forall\, z(kT),\qquad k=0,\,1,\,2,\,...,\tag{2.56}$$

and

$$\overline{C}\left[\left(\theta\tilde{E}-\tilde{A}\theta\right)c(kT)-\tilde{B}u_s(kT)\right]\equiv 0;\quad \forall\, c(kT),\qquad k=0,\,1,\,2,\,...\quad .\tag{2.57}$$

The necessary and sufficient conditions for existence of a $u_s(kT)$ satisfying (2.57) and a $u_c(kT)$ satisfying (2.56) for all $c(kT)$ and $z(kT)$ are given in (2.52) and (2.53), respectively.

The task of $u_p(kT)$ is to ensure that all solutions $\bar{e}_{ss}(kT)$ of

$$\bar{e}_{ss}\left((k+1)T\right)=\tilde{A}\bar{e}_{ss}(kT)-\tilde{B}u_p(kT),\tag{2.58}$$

are asymptotically-stable to a designated subspace $S_v\subseteq\aleph[C]$.

It is remarked that, in special cases, it may be possible to satisfy (2.49) even though (2.51) or (2.52) and (2.53) fail to be satisfied. For instance, under the very special case where it naturally turns out that $\overline{C}\left[(\theta\tilde{E}-\tilde{A}\theta)c(kT)-\tilde{F}\tilde{H}\,z(kT)\right]\equiv 0$, it suffices to choose $u_{sc}(kT)\equiv 0$ in (2.49), in which case (2.51) is not necessary. However, such special cases are highly unlikely in practice.

In the next section, the design procedure for $u(kT)$ will be developed for the "ideal case" in which the availability of accurate "sampled" on-line, real-time measurements of the states $x(kT)$, $z(kT)$, and $c(kT)$ are assumed. In practice, this is not a realistic assumption, because the disturbances $w(t)$ are completely unmeasurable and moreover the states $z(kT)$ and $c(kT)$ are related to unmeasurable physical attributes of the usually uncorrelated disturbance and servo-command functions, respectively. Therefore, a physically-realizable approximation of the "ideal solution" will be presented in Subsections 2.13.2 and 2.13.3 at the completion of the idealized design procedure for $u(kT)$.

2.10. Conditions for Complete Cancellation of Disturbance-Like Terms in the Servo-Tracking Error Discrete-Time Evolution Equation

To accomplish the goal of making $\bar{e}_{ss}(kT)$ in (2.48) remain invariant with respect to some subspace $S_v\subseteq\aleph[C]$, it is necessary that the digital-control terms $u_c(kT)$ and $u_s(kT)$ in (2.54) be designed such that the disturbance-like terms in (2.48) have no affect on the behavior of the tracking-error $\varepsilon_y(kT)$. However, recall that the behavior of the external disturbance $w(t)$ and the servo-command $y_c(t)$ is uncertain and time-varying. The disturbance $w(t)$ acts continuously on the plant (and consequently on the tracking-error) and the servo-command $y_c(t)$ continuously affects the servo-tracking error (refer to (2.1) and (2.2)). In addition, recall that the conventional digital-controller maintains a constant control-action between consecutive sampling times $(kT,\,(k+1)T)$. Also recall that the servo-state vector e_{ss} in (2.42) is subjected to the totally unknown, sparse-in-time random-like impulses $\sigma(t)$ and $\mu(t)$ (disregarded for design purposes, but present in application) inherent in the time-behavior of the external disturbance $w(t)$ and servo-command $y_c(t)$, respectively, and that those impulses cause the $\tilde{\gamma}(kT)$ and $\tilde{\mu}(kT)$ terms in

(2.42) to impose a limit on the degree of "disturbance" cancellation that can be obtained. This makes it technically impossible for the stepwise-constant digital control-action $u(kT)$ to completely cancel the effects of a non-constant disturbance $w(t)$ and/or a non-constant servo-command $y_c(t)$ on the continuous-time behavior of $\varepsilon_y(t)$, for all time $kT \le t < (k+1)T$. Therefore, the prudent alternative introduced in discrete-time DAC theory [33] is to define "complete disturbance-cancellation in discrete-time" as (ideally) total cancellation of the effects of the disturbance-related terms $\left(\theta\tilde{E} - \tilde{A}\theta\right)c(kT) - \tilde{FH}z(kT)$ on the motion of $\varepsilon_y(t)$, as they appear at the isolated sample-times $t = kT$, $k = 0, 1, 2, \ldots$. Thus, following this line of reasoning, the task is to design the control terms $u_c(kT)$ and $u_s(kT)$ in (2.54) to achieve complete disturbance-cancellation of $w(t)$ and the disturbance-like effects caused by $y_c(t)$ as they affect the behavior of the servo-tracking error in (2.44).

It is clear from (2.43) and (2.44) that complete disturbance-cancellation on the servo-tracking error $\bar{\varepsilon}_y(kT)$ can be achieved at each sample time $t = kT$, $k = 0, 1, 2, \ldots$, if, and only if, all motions of $\bar{e}_{ss}(kT)$, that can be affected by the disturbance $w(t)$ and the disturbance-like effects of the servo-command $y_c(t)$, are confined to the subspace $S_v = \mathcal{N}\left[\bar{C}\right] \subseteq \mathcal{N}[C]$. For convenience, the term $\bar{C}$ is carried symbolically throughout the computations in this section. A procedure for choosing S_v, computing $\bar{C}$ and designing u_c and u_s for that particular $\bar{C}$ is presented in the next section. Recall from below (2.57) that the control terms $u_c(kT)$ and $u_s(kT)$ satisfying (2.56) and (2.57) exist if, and only if conditions (2.53) and (2.52) are satisfied. Those expressions imply that

$$\bar{C}\left[\tilde{B}\tilde{\Gamma}_c + \tilde{FH}\right] = 0, \tag{2.59}$$

and

$$\bar{C}\left[\theta\tilde{E} - \tilde{A}\theta - \tilde{B}\tilde{\Gamma}_s\right] = 0 \tag{2.60}$$

for some r x ρ matrix $\tilde{\Gamma}_c$, some r x v matrix $\tilde{\Gamma}_s$, and the chosen $\bar{C}$.

If the conditions (2.59) and (2.60) are achieved, the control terms $u_c(kT)$ and $u_s(kT)$ (satisfying (2.56) and (2.57)) may be chosen ideally as

$$u_c(kT) = \tilde{\Gamma}_c z(kT), \tag{2.61}$$

and

$$u_s(kT) = \tilde{\Gamma}_s c(kT). \tag{2.62}$$

2.11. Design of $u(kT)$ to Stabilize the Servo-State $\bar{e}_{ss}(kT)$ to a Subspace $S_v \subseteq \mathcal{N}[C]$ While Achieving an Acceptable Closed-Loop Settling-Time

The structure of the idealized servo-tracking control terms $u_c(kT)$ and $u_s(kT)$ was given in (2.61) and (2.62). The structure of the idealized servo-tracking control term $u_p(kT)$ in (2.47) will be postulated in the linear state-feedback form:

$$\begin{aligned} u_p(kT) &= -\tilde{K}_p \bar{e}_{ss}(kT) \\ &= -\tilde{K}_p\big(\theta c(kT) - x(kT)\big) \end{aligned} \quad , \tag{2.63}$$

where $\tilde{K}_p$ is an r x n constant gain-matrix that is to be designed to achieve $\bar{C}\bar{e}_{ss}(kT) \to 0$, where $\|x(kT)\|$ must remain bounded for all bounded servo-command and disturbance state motions ($c(kT)$ and $z(kT)$). A procedure for designing such a $\tilde{K}_p$ consists of first substituting (2.61), (2.62), and (2.63) into (2.55) and then into (2.43) to obtain

$$\bar{e}_{ss}((k+1)T) = \big(\tilde{A} + \tilde{B}\tilde{K}_p\big)\bar{e}_{ss}(kT) - \hat{\tilde{B}}z(kT) + \hat{\tilde{\chi}}c(kT), \tag{2.64}$$

where, by design, the terms $\hat{\tilde{B}} = \tilde{B}\tilde{\Gamma}_c + \tilde{F}\tilde{H}$ and $\hat{\tilde{\chi}} = \theta\tilde{E} - \tilde{A}\theta - \tilde{B}\tilde{\Gamma}_s$ must satisfy (2.59) and (2.60) for the chosen $\bar{C}$, and consequently have no effect on the time-evolution of the servo-tracking error $\varepsilon_y(t)$ at each discrete sample-time $t = kT$, $k = 0, 1, 2, \ldots$.

Recall that the servo-tracking task is to quickly control the servo-state vector $\bar{e}_{ss}$ in (2.64) to a subspace $S_v \subseteq \mathcal{N}[C]$ having largest dimension v (e.g., $\bar{e}_{ss}(kT) \to S_v = \mathcal{N}[\bar{C}] \subseteq \mathcal{N}[C]$), and keep it there for each subsequent time $t = kT$, $k = 0, 1, 2, \cdots$. Several different approaches to the design of the gain matrices $\tilde{K}_p$, $\tilde{\Gamma}_c$, and $\tilde{\Gamma}_s$ in (2.64) can be considered that will accomplish this task. For example, if the null-point stabilization condition $\bar{e}_{ss}(kT) \to 0 \subset S_v$ is achievable, $\tilde{K}_p$ should be designed to place the eigenvalues of $\big(\tilde{A} + \tilde{B}\tilde{K}_p\big)$ at sufficiently-damped locations inside the unit circle and $\tilde{\Gamma}_c$ and $\tilde{\Gamma}_s$ in (2.59) and (2.60) should be designed to achieve $\left[\tilde{B}\tilde{\Gamma}_c + \tilde{F}\tilde{H}\right] \equiv 0$ and $\left[\theta\tilde{E} - \tilde{A}\theta - \tilde{B}\tilde{\Gamma}_s\right] \equiv 0$. This null-point stabilization approach for designing the matrices $\tilde{K}_p$, $\tilde{\Gamma}_c$, and $\tilde{\Gamma}_s$ regulates $\bar{e}_{ss}(kT)$ to the null state $\bar{e}_{ss} = 0$, which is a "point" that always lies in the null-space of the matrix C (and also $\bar{C}$) (e.g., $0 \in \mathcal{N}[\bar{C}] \subseteq \mathcal{N}[C]$) and hence is more restrictive than regulating $\bar{e}_{ss}(kT) \to S_v = \mathcal{N}[\bar{C}]$ of largest dimension. A procedure for performing the more general subspace stabilization task will be presented in the next section.

2.11.1. Transforming the Servo-State Vector Stabilization Problem to a New Coordinate System

A general mathematical theory for the stabilization of continuous-time linear dynamical systems to arbitrary linear subspaces was developed in [76]. That theory was applied in [37] to asymptotically control the *continuous-time* servo-state vector $\bar{e}_{ss}(t)$ to $\mathcal{N}[C]$, and in [70], to some subspace $S_{\nu} \subseteq \mathcal{N}[C]$. In this section the results and techniques in [37,70,76] will be adapted to our digital servo-control problem of designing $\tilde{K}_P$, $\tilde{\Gamma}_c$, and $\tilde{\Gamma}_s$ in (2.64) so that some subspace $S_{\nu} \subseteq \mathcal{N}[C]$ will become an asymptotically-stable invariant-subspace for all solutions $\bar{e}_{ss}(kT)$ of (2.64). The $\tilde{\Gamma}_c$ and $\tilde{\Gamma}_s$ and the collection of all $\tilde{K}_P$ which allow all solutions of (2.64) to be stabilized to, and become invariant for, some $S_{\nu} \subseteq \mathcal{N}[C]$ can be determined by the following method.

Recall from (2.1) that C is an m x n matrix which is assumed to have maximal rank m. Therefore, it is always possible to select an n x $(n\text{-}m)$ matrix M having maximal rank $(n\text{-}m)$ that satisfies $CM = 0$. Furthermore, the columns of M will form a basis for $\mathcal{N}[C]$. Consequently, any vector in $\mathcal{N}[C]$ can be written as a unique linear combination of the column vectors of M.

Let R be any $(n\text{-}m)$ x ν matrix such that $\nu \leq (n-m)$ and rank$[R]$ = ν. Then the product MR will be an n x ν matrix (rank$[MR]$ = ν) having column vectors which necessarily span some subspace $S_{\nu} \subseteq \mathcal{N}[C]$. That is,

$$S_{\nu} = \mathcal{R}[MR] = \mathcal{N}[\bar{C}] \subseteq \mathcal{N}[C]; \qquad \nu = 0,\ 1,\ 2,\ \ldots,\ n-m. \tag{2.65}$$

By varying the choices of the elements of R, and also varying the number ν of columns of R, one can isolate and designate any subspace $S_{\nu} \in \mathcal{N}[C]$, [37]. A systematic procedure for identifying every subspace $S_{\nu} \in \mathcal{N}[C]$, $\nu = 0,\ 1,\ 2,\ \ldots,\ n-m$, will be presented in Subsection 2.11.7. Hereafter, the chosen subspace S_{ν} will be generically defined as that subspace which is generated by the columns of MR and denoted by $S_{\nu} = \mathcal{R}[MR]$. It follows from (2.65) that $\bar{C}MR = 0$, which is written equivalently as (incorporating (2.46))

$$\bar{C}MR = \begin{bmatrix} C \\ \overline{P} \end{bmatrix} MR = \begin{bmatrix} CM \\ \overline{PM} \end{bmatrix} R = \begin{bmatrix} 0 \\ \overline{PM} \end{bmatrix} R = 0. \tag{2.66}$$

The choices of the elements of R in (2.65) will determine the choice of P in (2.46) and consequently the choice of $\bar{C}$ in (2.46).

Assume that $\bar{C}$ has been so chosen and, proceeding as in [76], consider the invertible linear transformation

$$\bar{e}_{ss} = [\bar{C}^{\#} | MR]\xi_{ss}, \tag{2.67}$$

where $\bar{C}^{\#}$ is the right inverse of $\bar{C}$, defined as

$$\bar{C}^{\#} = \bar{C}^T(\bar{C}\bar{C}^T)^{-1} \quad \text{(such that } \bar{C}\bar{C}^{\#} = \mathrm{I}\text{)}. \tag{2.68}$$

The inverse transformation associated with (2.67) is [76]

$$\xi_{ss} = \begin{pmatrix} \xi_{ss1} \\ \xi_{ss2} \end{pmatrix} = \left[\frac{\overline{C}}{(MR)^{\#}} \right] \overline{e}_{ss}, \tag{2.69}$$

where $(MR)^{\#}$ is the left inverse of (MR) given by (MR has maximal rank ν)

$$(MR)^{\#} = ((MR)^T MR)^{-1} (MR)^T \qquad \text{(such that } (MR)^{\#} MR = \mathrm{I}\text{)}. \tag{2.70}$$

2.11.2. The Discrete-Time Evolution Equation for $\xi_{ss}(kT)$

It follows from (2.69) that the condition $\overline{e}_{ss} \in S_{\nu} = \mathcal{N}[\overline{C}] \subseteq \mathcal{N}[C]$ is realized if, and only if $\xi_{ss1} = \overline{C}\overline{e}_{ss} = 0$. Therefore, in order to stabilize $\overline{e}_{ss}(kT)$ to a subspace S_{ν} we must regulate $\xi_{ss1}(kT) \to 0$ and ideally maintain $\xi_{ss1}(kT) \equiv 0$ for all subsequent $t = kT$, $k = 0, 1, 2, \ldots$. To do this requires examination of the evolution equation governing $\xi_{ss}(kT)$, which is computed from (2.69) as follows

$$\xi_{ss}((k+1)T) = \left[\frac{\overline{C}}{(MR)^{\#}} \right] \overline{e}_{ss}((k+1)T). \tag{2.71}$$

Substituting (2.64) into (2.71) yields

$$\xi_{ss}((k+1)T) = \left[\frac{\overline{C}}{(MR)^{\#}} \right] (\widetilde{A} + \widetilde{B}\widetilde{K}_p)\overline{e}_{ss}(kT) + \left[\frac{\overline{C}}{(MR)^{\#}} \right] \left[\hat{\widetilde{\chi}} c(kT) - \hat{\widetilde{B}} z(kT) \right], \tag{2.72}$$

where $\hat{\widetilde{\chi}} = \theta\widetilde{E} - \widetilde{A}\theta - \widetilde{B}\widetilde{\Gamma}_s$ and $\hat{\widetilde{B}} = \widetilde{B}\widetilde{\Gamma}_c + \widetilde{F}H$. Substituting (2.67) into (2.72), and rearranging terms, results in the vector-matrix difference equation

$$\begin{pmatrix} \xi_{ss1}((k+1)T) \\ \xi_{ss2}((k+1)T) \end{pmatrix} = \left[\begin{array}{c|c} \overline{C}(\widetilde{A} + \widetilde{B}\widetilde{K}_p)\overline{C}^{\#} & \overline{C}(\widetilde{A} + \widetilde{B}\widetilde{K}_p)MR \\ \hline (MR)^{\#}(\widetilde{A} + \widetilde{B}\widetilde{K}_p)\overline{C}^{\#} & (MR)^{\#}(\widetilde{A} + \widetilde{B}\widetilde{K}_p)MR \end{array} \right] \begin{pmatrix} \xi_{ss1}(kT) \\ \xi_{ss2}(kT) \end{pmatrix}$$

$$+ \left[\begin{array}{c|c} \overline{C}\hat{\widetilde{\chi}} & -\overline{C}\hat{\widetilde{B}} \\ \hline (MR)^{\#}\hat{\widetilde{\chi}} & -(MR)^{\#}\hat{\widetilde{B}} \end{array} \right] \begin{pmatrix} c(kT) \\ z(kT) \end{pmatrix}. \tag{2.73}$$

2.11.3. Conditions for Regulating $\bar{e}_{ss}(kT) \rightarrow S_v$

In order to stabilize $\xi_{ss1}(kT)$ to zero, and consequently regulate $\bar{e}_{ss}(kT)$ to the subspace $S_v = \aleph[\bar{C}]$, matrices $\tilde{K}_p$, $\tilde{\Gamma}_c$, and $\tilde{\Gamma}_s$ must exist such that the following conditions are met for the chosen $\bar{C}$ (refer to (2.73)):

a) $\bar{C}(\tilde{A} + \tilde{B}\tilde{K}_p)MR = 0$; (2.74)

b) $\bar{C}\hat{\tilde{\chi}} = 0$ (same as (2.60)),

or equivalently,

$\Re[\hat{\tilde{\chi}}] \subseteq \aleph[\bar{C}]$;

c) $\bar{C}\hat{\tilde{B}} = 0$ (same as (2.59)),

or equivalently,

$\Re[\hat{\tilde{B}}] \subseteq \aleph[\bar{C}]$;

and

d) all solutions $\bar{\xi}_{ss1}(kT)$ of the reduced system

$$\bar{\xi}_{ss1}((k+1)T) = \bar{C}(\tilde{A} + \tilde{B}\tilde{K}_p)\bar{C}^{\#}\bar{\xi}_{ss1}(kT) \,, \tag{2.75}$$

must be asymptotically stable to the null-point $\bar{\xi}_{ss1}(kT) = 0$.

Conditions a), b), and c) are the necessary and sufficient conditions to make the subspace S_v invariant to $\xi_{ss1}(kT)$ with respect to all initial values of $\xi_{ss2} \in S_v$ and all uncertain and unpredictable time-behavior of the disturbance and servo-command states, $z(kT)$ and $c(kT)$, respectively. Expression (2.75) in condition d) is the homogeneous difference equation for ξ_{ss1}, and, together with conditions a), b), and c), condition d) is necessary and sufficient for $\xi_{ss1}(kT) = 0$ to be an asymptotically-stable solution of (2.73).

Condition a) in (2.74) can be stated equivalently as [76]:

i) $$(\tilde{A} + \tilde{B}\tilde{K}_p)MR = MR\Xi \,, \tag{2.76}$$

for some matrix Ξ; or

ii) $$\bar{C}(\tilde{A} + \tilde{B}\tilde{K}_p) = \Omega\bar{C} \,, \tag{2.77}$$

for some Ω.

If conditions a), b), and c) are satisfied, then (2.76) and (2.77) can be used to write (2.73) in the simplified form

$$\begin{pmatrix} \xi_{ss1}((k+1)T) \\ \xi_{ss2}((k+1)T) \end{pmatrix} = \left[\begin{array}{c|c} \Omega & 0 \\ \hline (MR)^{\#}(\tilde{A}+\tilde{B}\tilde{K}_p)\bar{C}^{\#} & \Xi \end{array}\right] \begin{pmatrix} \xi_{ss1}(kT) \\ \xi_{ss2}(kT) \end{pmatrix}$$
$$+ \left[\begin{array}{c|c} 0 & 0 \\ \hline (MR)^{\#}\hat{\tilde{\chi}} & -(MR)^{\#}\hat{\tilde{B}} \end{array}\right] \begin{pmatrix} c(kT) \\ z(kT) \end{pmatrix} \tag{2.78}$$

In view of (2.78), the problem of stabilizing $\bar{e}_{ss} \to S_v = \aleph[\bar{C}] = \Re[MR]$ can be restated as finding the matrices $\tilde{\Gamma}_s$ and $\tilde{\Gamma}_c$ such that conditions b) and c) are satisfied and finding the set $\tilde{\mathbf{K}}$ of all matrices $\tilde{K}_p$ which satisfy (2.74) for the chosen $\bar{C}$ and, when that set is found, determine which, if any, $\tilde{K}_p \in \tilde{\mathbf{K}}$ exist such that condition d) is satisfied

2.11.4. Identification of the Set $\tilde{\mathbf{K}}$ of all Stabilizing Gain-Matrices $\tilde{K}_p$

Proceeding as in [76], the existence of a $\tilde{K}_p$ satisfying (2.74), and subsequently the set $\tilde{\mathbf{K}}$ of all such $\tilde{K}_p$, can be determined by first noticing that (2.74) can be written as

$$-\bar{C}\tilde{A}MR = \bar{C}\tilde{B}\tilde{\Delta}, \quad \text{where } \tilde{\Delta} = \tilde{K}_p MR. \tag{2.79}$$

Then, the necessary and sufficient condition for existence of a $\tilde{\Delta}$ satisfying (2.79) is that

$$\Re[\bar{C}\tilde{A}MR] \subseteq \Re[\bar{C}\tilde{B}], \tag{2.80}$$

or equivalently,

$$\text{rank}\left[\bar{C}\tilde{B} \mid \bar{C}\tilde{A}MR\right] = \text{rank}[\bar{C}\tilde{B}]. \tag{2.81}$$

Note that (2.80) further restricts the choice of R, (originally defined in the text above (2.72)) and consequently the choice of $\bar{C}$. It follows that there exists a matrix $\tilde{K}_p$, satisfying $\tilde{\Delta} = \tilde{K}_p MR$ and (2.74), if, and only if (2.80) (equivalently (2.81)) is satisfied. In that case, the non-unique solutions to (2.79) can be obtained by using the well-known expression for the general solution $h = P^{+}c + \left(\mathrm{I} - P^{+}P\right)g$ (g is an arbitrary vector) of the linear algebraic equation $Ph = c$ when $c \in \Re[P]$. That is, the set of solutions to (2.79) consists of the $\tilde{\Delta}$ defined by

$$\tilde{\Delta} = -(\bar{C}\tilde{B})^{+}\bar{C}\tilde{A}MR + [\mathrm{I} - (\bar{C}\tilde{B})^{+}\bar{C}\tilde{B}]\tilde{Z}, \tag{2.82}$$

where

$\tilde{Z}$ is an arbitrary r x $(n\text{-}m)$ constant matrix to be determined,

I is the identity matrix, and

$(\overline{C}\tilde{B})^{+}$ indicates the Moore-Penrose pseudo inverse [75] of $\overline{C}\tilde{B}$.

Following the development in [76], the set $\tilde{\mathbf{K}}$ of all $\tilde{K}_p$ satisfying (2.74) can be computed directly from (2.79) and (2.82) by again using the results in [75] (since rank[MR]= v, $(MR)^{+} = (MR)^{\#}$, where $(MR)^{+}$ is the Moore-Penrose pseudo inverse of MR).

$$\tilde{\mathbf{K}} = \left\{ \tilde{K}_p \mid \tilde{K}_p = -(\overline{C}\tilde{B})^{+}\overline{C}\tilde{A}MR(MR)^{\#} + [\mathrm{I} - (\overline{C}\tilde{B})^{+}\overline{C}\tilde{B}]\tilde{Z}(MR)^{\#} + \tilde{L}\overline{C} \right\}, \qquad (2.83)$$

where $\tilde{L}$ is an r x $(n\text{-}\mathrm{v})$ constant matrix to be determined. To verify (2.83), substitute the $\tilde{K}_p$ in (2.83) into $\tilde{\Delta} = \tilde{K}_p MR$ from (2.79) and use the relationships in (2.66) and (2.70) to obtain the relationship

$$\begin{aligned}
\tilde{\Delta} &= \tilde{K}_p MR \\
&= -\left(\overline{C}\tilde{B}\right)\overline{C}\tilde{A}MR(MR)^{\#}MR + \left[\mathrm{I} - \left(\overline{C}\tilde{B}\right)^{+}\overline{C}\tilde{B}\right]\tilde{Z}(MR)^{\#}MR + \tilde{L}\overline{C}MR \\
&= -\left(\overline{C}B\right)^{+}\overline{C}\tilde{A}MR + \left[\mathrm{I} - \left(\overline{C}\tilde{B}\right)^{+}\overline{C}\tilde{B}\right]\tilde{Z}
\end{aligned},$$

which is the same as (2.82).

2.11.5. Identification of all $\tilde{K}_p \in \tilde{\mathbf{K}}$ that Satisfy Condition d) Associated With (2.75)

Now that the set $\tilde{\mathbf{K}}$ of all $\tilde{K}_p$ satisfying (2.74) has been found, it remains to identify the subset consisting of those $\tilde{K}_p \in \tilde{\mathbf{K}}$ which <u>also</u> satisfy condition d) associated with (2.75). For this purpose substitute (2.83) into (2.73), and use the relationships in (2.66), (2.68), and (2.70) to obtain the vector-matrix difference equation

$$\begin{aligned}
\begin{pmatrix} \xi_{ss1}((k+1)T) \\ \xi_{ss2}((k+1)T) \end{pmatrix} &= \left[\begin{array}{c|c} \tilde{A}_1 + \tilde{B}_1\tilde{L} & 0 \\ \hline (MR)^{\#}(\tilde{A} + \tilde{B}L\overline{C})\overline{C}^{\#} & \tilde{A}_2 + \tilde{B}_2\tilde{Z} \end{array}\right]\begin{pmatrix} \xi_{ss1}(kT) \\ \xi_{ss2}(kT) \end{pmatrix} \\
&+ \left[\begin{array}{c|c} \overline{C}\hat{\tilde{\chi}} & -\overline{C}\hat{\tilde{B}} \\ \hline (MR)^{\#}\hat{\tilde{\chi}} & -(MR)^{\#}\hat{\tilde{B}} \end{array}\right]\begin{pmatrix} c(kT) \\ z(kT) \end{pmatrix}
\end{aligned}, \qquad (2.84)$$

where

$$\widetilde{A}_1 = \overline{C}\widetilde{A}\overline{C}^{\#},$$

$$\widetilde{A}_2 = (MR)^{\#}(\widetilde{A} - \widetilde{B}(\overline{C}\widetilde{B})^{+}\overline{C}\widetilde{A})MR,$$

$$\widetilde{B}_1 = \overline{C}\widetilde{B},$$

and

$$\widetilde{B}_2 = (MR)^{\#}\widetilde{B}[\mathrm{I} - (\overline{C}\widetilde{B})^{+}\overline{C}\widetilde{B}].$$

The conditions a), b), c), and d) above (2.75), necessary and sufficient for $\overline{e}_{ss}(kT)$ to be asymptotically stabilized to $S_{\mathrm{v}} = \Re[MR]$ for some R (some $\overline{C}$), can now be restated equivalently as (refer to (2.84))

a′) $\Re[\overline{C}\widetilde{A}MR] \subseteq \Re[\overline{C}\widetilde{B}]$ (from (2.80));

b′) there exists a $\widetilde{\Gamma}_s$ such that (2.60) is satisfied. The necessary and sufficient condition for existence of a $\widetilde{\Gamma}_s$ satisfying (2.60) is given in (2.52);

c′) there exists a $\widetilde{\Gamma}_c$ such that (2.59) is satisfied. The necessary and sufficient condition for existence of a $\widetilde{\Gamma}_c$ satisfying (2.59) is given in (2.53);

and

d′) there exists an r x (n-V) constant matrix $\widetilde{L}$ such that solutions to the following homogeneous difference equation are uniformly and asymptotically stable to the null-point $\xi_{ss1}(kT) = 0$:

$$\xi_{ss1}((k+1)T) = \left[\widetilde{A}_1 + \widetilde{B}_1\widetilde{L}\right]\xi_{ss1}(kT). \tag{2.85}$$

If condition a′) (expression (2.80)) is met then $\widetilde{K}_p$ may be chosen such that (2.74) is achieved. The set $\widetilde{\mathbf{K}}$ of all $\widetilde{K}_p$ satisfying (2.74) is given in (2.83). If conditions b′) and c′) are met then a $\widetilde{\Gamma}_s$ and $\widetilde{\Gamma}_c$, may be chosen to satisfy (2.60) and (2.59), respectively. Finally, (2.85) in condition d′) is the homogeneous difference equation for ξ_{ss1} with $\widetilde{K}_p$ from (2.83) substituted into (2.75). In view of conditions a′), b′), and c′), condition d′) is necessary and sufficient for $\xi_{ss1}(kT) = 0$ to be an asymptotically-stable solution of (2.84).

The standard procedure called pole placement [3,20,21,46,47,77] can be used to obtain the null-point stabilization requirement in condition d′). In that way, $\widetilde{L}$ is selected such that the eigenvalues of $\left[\widetilde{A}_1 + \widetilde{B}_1\widetilde{L}\right]$ are at sufficiently-damped locations inside the unit circle. Due to the

nonsingularity of the linear transformation in (2.67) the eigenvalues of $\left[\widetilde{A}_1 + \widetilde{B}_1\widetilde{L}\right]$ (together with those of $\left[\widetilde{A}_2 + \widetilde{B}_2\widetilde{Z}\right]$ in (2.84)) are also eigenvalues of $\left[\widetilde{A} + \widetilde{B}\widetilde{K}_p\right]$ in (2.64).

The existence of a suitable $\widetilde{L}$ that will stabilize $\xi_{ss1}(kT)$ to zero is determined by examining the controllability matrix corresponding to the homogeneous system in (2.85). If the controllability matrix has maximum rank,

$$\text{rank}\left[\widetilde{B}_1 \mid \widetilde{A}_1\widetilde{B}_1 \mid \widetilde{A}_1{}^2\widetilde{B}_1 \mid \cdots \mid \widetilde{A}_1{}^{(n-\nu-1)}\widetilde{B}_1\right] = n - \nu \quad , \tag{2.86}$$

then, and only then, there exists a constant feedback matrix $\widetilde{L}$ such that the eigenvalues of $\left[\widetilde{A}_1 + \widetilde{B}_1\widetilde{L}\right]$ can be arbitrarily assigned [46] subject to conjugacy of complex eigenvalues. If the rank condition in (2.86) is not satisfied, there may still exist a suitable $\widetilde{L}$ that will stabilize $\xi_{ss1}(kT) \to 0$. In particular, if the rank of (2.86) is less than maximum then the system defined by (2.85) can be separated into corresponding completely controllable and totally uncontrollable subsystems [78]. A suitable $\widetilde{L}$ will then exist if and only if all the natural eigenvalues associated with the totally uncontrollable subsystem are inside the unit circle ($|\lambda_i| < 1$). This necessary and sufficient condition for the existence of $\widetilde{L}$ in a system that is not completely controllable can be stated for the discrete-time case by adapting a continuous-time result in [76,78] to obtain the following.

Let $\mathfrak{N}$ be any (n-ν) x (n-ν-ρ) matrix such that the columns of $\mathfrak{N}$ form a basis for the null-space of the (n-v) x r(n-v) matrix:

$$\left[\widetilde{B}_1 \mid \widetilde{A}_1\widetilde{B}_1 \mid \widetilde{A}_1^2\widetilde{B}_1 \mid \cdots \mid \widetilde{A}_1^{(n-\nu-1)}\widetilde{B}_1\right]. \tag{2.87}$$

Then a matrix $\widetilde{L}$ satisfying condition d′) associated with (2.85) exists if, and only if, all roots λ_i of the polynomial $\det(\lambda I - (\mathfrak{N}^T\mathfrak{N})^{-1}\mathfrak{N}^T\widetilde{A}_1\mathfrak{N}) = 0$ satisfy $|\lambda_i| < 1$, i = 1, 2, ..., n-ν-ρ (all eigenvalues of $(\mathfrak{N}^T\mathfrak{N})^{-1}\mathfrak{N}^T\widetilde{A}_1\mathfrak{N}$ are located inside the unit circle). Here, the matrix $(\mathfrak{N}^T\mathfrak{N})^{-1}\mathfrak{N}^T\widetilde{A}_1\mathfrak{N}$ characterizes the dynamics of the totally uncontrollable subsystem of the system in (2.85).

2.11.6. Conditions for Maintaining Bounded Motions of $\bar{e}_{ss}(kT)$ Within S_ν

Conditions (2.80), (2.53), and (2.52) are the necessary and sufficient conditions for the existence of $\widetilde{K}_p$, $\widetilde{\Gamma}_c$, and $\widetilde{\Gamma}_s$ that, for a given R, will stabilize $\bar{e}_{ss}(kT)$ to the subspace $S_\nu = \Re[MR] = \aleph[\overline{C}] \subseteq \aleph[C]$. However, it remains to determine the equations and conditions necessary to satisfactorily maintain bounded motions of $\bar{e}_{ss}(kT)$ within the subspace S_ν. The differential equation describing the continuous-time evolution of the motions $\bar{e}_{ss}(t) \in S_\nu$ was derived in [76]. Assuming the conditions in a′), b′), c′), and d′) above (2.85) are met, the discrete-time counterpart of that evolution equation is obtained from ((2.84) as (recall that condition d′) associated with (2.85) controls $\xi_{ss1}(kT)$ to zero)

$$\bar{\xi}_{ss2}((k+1)T) = \left[\tilde{A}_2 + \tilde{B}_2\tilde{Z}\right]\bar{\xi}_{ss2}(kT) + \tilde{B}_3\left(\frac{c(kT)}{z(kT)}\right), \tag{2.88}$$

where $\tilde{A}_2$ and $\tilde{B}_2$ are defined in (2.84),

$$\tilde{B}_3 = (MR)^{\#}\left[\hat{\tilde{\chi}} \mid -\hat{\tilde{B}}\right],$$

and the norm of the uncertain vector $\left(\frac{c(kT)}{z(kT)}\right)$ is assumed to be uniformly bounded for all $k = 0, 1, 2, \ldots$.

The r x $(n\text{-}m)$ matrix $\tilde{Z}$ in (2.88) should be chosen as any matrix for which all solutions to (2.88) remain bounded [14]. That is, for all $k = 0, 1, 2, \ldots$,

$$\left\|\bar{\xi}_{ss2}(kT)\right\| \le M_1 < \infty \text{ (for some positive } M_1\text{)}.$$

This latter condition will in turn assure that $\|\bar{e}_{ss}(kT)\|$ remains bounded as $k \to \infty$. A necessary and sufficient condition for the existence of an appropriate $\tilde{Z}$ such that all solutions $\xi_{ss2}(kT)$ of (2.88) remain bounded is similar to that given for the existence of a suitable $\tilde{L}$ in (2.85). That is, if the controllability matrix corresponding to the homogeneous portion of the system in (2.88) has maximum rank,

$$\text{rank}\left[\tilde{B}_2 \mid \tilde{A}_2\tilde{B}_2 \mid \tilde{A}_2^2\tilde{B}_2 \mid \cdots \mid \tilde{A}_2^{(\nu-1)}\tilde{B}_2\right] = \nu, \tag{2.89}$$

then, and only then, there exists a constant feedback matrix $\tilde{Z}$ such that the eigenvalues of $\left[\tilde{A}_2 + \tilde{B}_2\tilde{Z}\right]$ can be <u>arbitrarily</u> assigned [46] subject to conjugacy of complex eigenvalues. If the rank condition in (2.89) is not satisfied, there may still exist an appropriate $\tilde{Z}$ such that all solutions $\xi_{ss2}(kT)$ to (2.88) remain bounded. In particular, if the rank of (2.97) is less than maximum then the system defined by (2.88) can be decomposed into corresponding completely controllable and totally uncontrollable subsystems as explained in [78]. An appropriate $\tilde{Z}$ can be found if, and only if all of the eigenvalues associated with the totally uncontrollable subsystem of (2.88) are inside the unit circle ($|\lambda_i| < 1$). A method for determining and representing the completely controllable and totally uncontrollable subsystems associated with (2.88) was given in [76,78]. Using that method, one can let $\mathbf{P}$ be any ν x $(\nu - q)$ matrix such that the columns of $\mathbf{P}$ form a basis for the null-space of

$$\left[\tilde{B}_2 \mid \tilde{A}_2\tilde{B}_2 \mid \tilde{A}_2^2\tilde{B}_2 \mid \cdots \mid \tilde{A}_2^{(\nu-1)}\tilde{B}_2\right]. \tag{2.90}$$

Then a matrix $\tilde{Z}$ such that all solutions of (2.88) become bounded exists if, and only if, all roots λ_i of the polynomial $\det(\lambda I - (\mathbf{P}^T\mathbf{P})^{-1}\mathbf{P}^T\tilde{A}_2\mathbf{P}) = 0$ satisfy $|\lambda_i| < 1$, i = 1, 2, ..., $(\nu\text{-}q)$, (all eigenvalues of $(\mathbf{P}^T\mathbf{P})^{-1}\mathbf{P}^T\tilde{A}_2\mathbf{P}$ are located inside the unit circle). Here, the matrix $(\mathbf{P}^T\mathbf{P})^{-1}\mathbf{P}^T\tilde{A}_2\mathbf{P}$ characterizes the dynamics of the totally uncontrollable subsystem of the system in (2.88).

Notice that if $\left[\overline{C}\widetilde{B}\right]$ has maximal rank r, then $\widetilde{B}_2 = (MR)^{\#}\widetilde{B}\left[I-(\overline{C}\widetilde{B})^{+}\overline{C}\widetilde{B}\right]=0$ (refer to (2.84)), and the solution to (2.88) then becomes completely independent of the matrix $\widetilde{Z}$ [76]. That is, (2.88) becomes

$$\overline{\xi}_{ss2}((k+1)T) = \widetilde{A}_2\overline{\xi}_{ss2}(kT) + \widetilde{B}_3\begin{pmatrix} c(kT) \\ z(kT) \end{pmatrix}. \tag{2.91}$$

In this special case, the motions of $\overline{\xi}_{ss2}(kT)$ in (2.91) will depend on the initial condition $\xi_{ss2}(t_o)$, the matrix $\widetilde{A}_2$, and the behavior of the servo-command and disturbance states, $c(kT)$ and $z(kT)$, respectively.

2.11.7. Systematic Procedure for Identifying the Candidate Subspaces $S_\nu \subseteq \mathcal{N}[C]$

Recall from the text above (2.65) that the n x (n-m) maximal rank matrix M and the (n-m) x ν matrix R are required to satisfy

$$CM = 0, \qquad \text{(the columns of } M \text{ form a basis for } \mathcal{N}[C]) \tag{2.92}$$

$$\text{rank}[M] = n-m, \tag{2.93}$$

and

$$\text{rank}[R] = \nu \le n-m. \tag{2.94}$$

Depending on the choice of R, the columns of the matrix product MR form a basis for some ν-dimensional (ν = 0, 1, 2, ..., n-m) subspace $S_\nu = \mathcal{N}\left[\overline{C}\right] = \mathcal{R}\left[MR\right] \subseteq \mathcal{N}[C]$. The procedure given in this section allows one to systematically represent all R that can be used in conjunction with MR to generate all ν-dimensional subspaces $S_\nu = \mathcal{R}[MR]$. The procedure for identifying candidate R matrices and using those matrices to perform the subspace stabilization technique is as follows. The control designer begins with an R of largest dimension (ν = n-m) such that $S_\nu = \mathcal{R}[MR] = \mathcal{N}\left[C\right]$, forms a P, and subsequently a matrix $\overline{C}$, according to (2.46) and (2.66) ($\overline{C} = C$ when ν = n-m), and then tests R for satisfaction of the four conditions above (2.85) and the one condition associated with (2.88). If those five conditions are met, then the specific ν = n-m dimensional subspace $S_{n\text{-}m}$ is "suitable" in the sense that there then exists three matrices $\widetilde{K}_p$, $\widetilde{\Gamma}_c$, and $\widetilde{\Gamma}_s$, which may be chosen such that the closed-loop motions of $\overline{e}_{ss}(kT)$ in (2.64) are asymptotically stabilized to $S_\nu = S_{n-m} = \mathcal{N}\left[C\right]$ and the subspace $S_{n\text{-}m}$ becomes invariant with respect to the closed-loop motions of $\overline{e}_{ss}(kT)$. If not all of the five referenced conditions are met, the associated $S_{n\text{-}m}$ is not suitable, and the designer must then proceed to the next step which is to test all R having dimension ν = n-m-1, and so on, until the subspace $S = S_\nu$ of largest dimension is found that is "suitable."

To illustrate how one can represent all R of a given dimension ν, let $\alpha = PM$ in (2.66) and let $\beta = (\beta_1, \beta_2, ..., \beta_{n\text{-}m})$ be any general solution vector for the homogeneous system

$$PM\beta = \alpha\beta = \begin{bmatrix} \alpha_{1,1} & \alpha_{1,2} & \cdots & \alpha_{1,(n-m)} \\ \alpha_{2,1} & \alpha_{2,1} & \cdots & \alpha_{2,(n-m)} \\ \vdots & \vdots & \ddots & \vdots \\ \alpha_{(n-m-\nu),1} & \alpha_{(n-m-\nu),2} & \cdots & \alpha_{(n-m-\nu),(n-m)} \end{bmatrix} \begin{pmatrix} \beta_1 \\ \beta_2 \\ \vdots \\ \beta_{n-m} \end{pmatrix} = \begin{pmatrix} 0 \\ 0 \\ \vdots \\ 0 \end{pmatrix}, \qquad (2.95)$$

having $(n\text{-}m\text{-}\nu)$ equations and $(n\text{-}m)$ unknowns β_i, $i = 1, 2, \ldots, n-m$, and where α has maximal rank $n - m - \nu$. From examination of (2.66) ($PMR = 0$) and (2.95) ($PM\beta = 0$), it is clear that $\beta \subseteq \Re[R]$. Now define W as the subspace spanned by the set of all β satisfying (2.95) for a particular matrix α. Then let $R_{\nu j} = [r_1 \mid r_2 \mid \cdots \mid r_\nu]$, $\nu = 0, 1, 2, \ldots, n-m$, $j = 1, 2, \ldots, \dfrac{(n-m)!}{\nu!(n-m-\nu)!}$ where the nonzero solution vectors $r_1, r_2, \ldots, r_\nu$ ($r_i \in$ the set of all β satisfying (2.95)) will form a basis for a subspace W if every solution vector $\beta \in W$ can be expressed uniquely as a linear combination of $r_1, r_2, \ldots, r_\nu$. The number ν of the basis vectors r_i is equal to the dimension of the subspace W. The number $\dfrac{(n-m)!}{\nu!(n-m-\nu)!}$ is the number of unique ν-combinations of an $(n - m)$-set [81], or equivalently, the number of basis sets required to represent all ν-dimensional subspaces of an $(n - m)$ dimension space, in general.

The linearly independent solution vectors $r_1, r_2, \ldots, r_\nu$ of $R_{\nu j}$ can be obtained by the method described in [82]. In that way, assume that the matrix α in (2.95) has been reduced to echelon form, that is, each leading non-zero entry is to the right of the leading non-zero entry in the preceding row. Since any matrix can be put into an echelon form, there is no loss of generality in this assumption. Clearly, there are more unknowns than there are equations to solve: $(n-m) \geq (n-m-\nu)$ (if $\nu = 0$, then the solution to (2.95) is trivial). Therefore, there are ν variables in each solution vector r_i which can be defined arbitrarily. Now let $r_1, r_2, \ldots, r_\nu$ be the β solution vectors obtained by setting one of the free variables equal to one and the remaining free variables equal to zero. Then the ν-dimensional subspace W will have basis vectors $r_1, r_2, \ldots, r_\nu$. Now recall the $(n\text{-}m)$ x ν matrix R from Subsection 2.11.1 defined as any matrix such that $\nu \leq (n-m)$ and rank[R] = ν. Then R may be further specified as consisting of the set of column vectors $r_1, r_2, \ldots, r_\nu$. That is,

$$R = [r_1 \mid r_2 \mid \cdots \mid r_\nu]. \qquad (2.96)$$

The columns of R constructed in this manner form a basis for the ν-dimensional subspace W (i.e., $W = \Re[R]$) corresponding to a particular matrix α in (2.95). For every such ν-dimensional subspace W (or any possible matrix α having rank $n - m - \nu$), a matrix R of column basis vectors r_i, $i = 1, 2, \ldots, \nu$, can be formulated by the method above. The resulting R will have ν^2 elements (each r_i vector has ν free variables and there are ν such vectors) which can be selected as 0 or 1, and $\nu(n\text{-}m\text{-}\nu)$ elements (represented by the notation $r_{\nu h}$, $h = 1, 2, \ldots, \nu(n-m-\nu)$) that are uniquely determined by the individual elements of the matrix $\alpha = PM$ in (2.95). Since each basis vector r_i has dimension $n\text{-}m$, there are then $\dfrac{(n-m)!}{\nu!(n-m-\nu)!}$ possible combinations of free variables associated with all possible subspaces W of dimension ν contained in an $(n\text{-}m)$-dimensional space, in general. In light of this, define $\mathbf{R}_\nu$, $\nu = 0, 1, 2, \ldots, n-m$, as the set of all R which can be used, in general, to generate the ν-dimensional subspaces of an $(n\text{-}m)$-dimension space. Each $R \in \mathbf{R}_\nu$ will have ν^2 elements, defined as 0

or 1, and $\nu(n\text{-}m\text{-}\nu)$ elements represented by the undetermined variables r_{ij}. The set $\mathbf{R}_\nu$ will contain $\frac{(n-m)!}{\nu!(n-m-\nu)!}$ matrices $R=R_{\nu j}$, $j = 1, 2, \ldots, \frac{(n-m)!}{\nu!(n-m-\nu)!}$, each consisting of ν column basis vectors r_i, corresponding to the different combinations of free variables. Now define the set $\mathbf{R}$, consisting of all sets $\mathbf{R}_\nu$. The set $\mathbf{R}$ will then contain all general forms of the column basis vectors that generate any ν-dimensional, $\nu = 0, 1, 2, \ldots, n-m$, subspace $W = \Re[R]$ contained in an $(n\text{-}m)$-dimension space, in general.

Now recall from Subsection 2.11.1 that the subspace $S_\nu \subseteq \aleph[C]$ is generated by the columns of MR (where $S_\nu = \Re[MR]$, rank$[MR] = \nu$, and M is a maximum rank matrix consisting of column basis vectors that generate the entire $\aleph[C]$, i.e., $CM = 0$). Therefore, as each set $\mathbf{R}_\nu$ is identified, beginning with $\mathbf{R}_{n-m}$, every $R = R_{\nu j} \in \mathbf{R}_\nu \in \mathbf{R}$, beginning with $\mathbf{R}_{(n-m)1}$, can be systematically tested for suitability using the technique described in Subsections 2.11.1 through 2.11.6. There are $\nu(n\text{-}m\text{-}\nu)$ elements in each R which may remain undetermined until conditions a'), b'), c'), and d') above (2.85) are established. At that point a value, or range of values, may be determined for each $r_{\nu h}$ such that those conditions are still met. The column vectors in R can be defined as any set of linearly independent vectors containing acceptable values of $r_{\nu h}$, as determined by applying the subspace stabilization technique described in Subsections 2.11.1 through 2.11.6. The columns of R will form a basis for a ν-dimensional subspace W and the columns of the matrix product MR will form a basis for the ν-dimensional subspace $S_\nu = \aleph[\bar{C}] = \Re[MR] \subseteq \aleph[C]$ to which $\bar{e}_{ss}(kT)$ will be stabilized.

2.11.8. An Example

A specific example will assist in clarifying the method described above for identifying the matrices R and subsequently forming a basis for all ν-dimensional subspaces $S_\nu = \Re[MR]$ in the $(n\text{-}m)$-dimensional space $\aleph[C]$. Note that it is not necessary to enumerate all of the sets $\mathbf{R}_\nu$ before performing the subspace stabilization procedure. In practice, the control designer would first obtain the set $\mathbf{R}_{n-m}$ and then test each $R_{n-m,j} \in \mathbf{R}_{n-m}$ in the subspace stabilization procedure. If all of those $R_{n-m,j}$ matrices are unsuitable, the designer then obtains the set $\mathbf{R}_{n-m-1}$ and repeats the procedure. Enumeration of all $\mathbf{R}_\nu$ is given here for illustration purposes only. For this example, suppose that the dimension of $\aleph[C]$ is 3. That is, $n-m=3$. Then the sets $\mathbf{R}_\nu$, $\nu = 0, 1, 2, \ldots, n-m$ will be:

$$\mathbf{R}_0 = \{0\} = \{R_{01}\} \quad \text{(the null-point)}, \tag{2.97}$$

$$\mathbf{R}_1 = \left\{ \begin{pmatrix} r_{11} \\ r_{12} \\ 1 \end{pmatrix}, \begin{pmatrix} r_{11} \\ 1 \\ r_{12} \end{pmatrix}, \begin{pmatrix} 1 \\ r_{11} \\ r_{12} \end{pmatrix} \right\} = \{R_{11}, R_{12}, R_{13}\}, \tag{2.98}$$

$$\mathbf{R}_2 = \left\{ \begin{pmatrix} r_{21} & r_{22} \\ 1 & 0 \\ 0 & 1 \end{pmatrix}, \begin{pmatrix} 1 & 0 \\ r_{21} & r_{22} \\ 0 & 1 \end{pmatrix}, \begin{pmatrix} 1 & 0 \\ 0 & 1 \\ r_{21} & r_{22} \end{pmatrix} \right\} = \{R_{21},\ R_{22},\ R_{23}\} \quad , \tag{2.99}$$

$$\mathbf{R}_3 = \left\{ \begin{pmatrix} 1 & 0 & 0 \\ 0 & 1 & 0 \\ 0 & 0 & 1 \end{pmatrix} \right\} = \{R_{31}\} \tag{2.100}$$

(column basis vectors for the entire (n-m)-dimensional $\mathcal{N}[C]$, hence $\overline{C} = C$),

and

$$\mathbf{R} = \{\mathbf{R}_0, \mathbf{R}_1, \mathbf{R}_2, \mathbf{R}_3\}. \tag{2.101}$$

The notation $R_{\nu j}$, $\nu = 0,\ 1,\ 2,\ \ldots,\ n-m$, $j = 1,\ 2,\ \ldots,\ \dfrac{(n-m)!}{\nu!(n-m-\nu)!}$ in (2.97)-(2.100) is used to denote each $R \in \mathbf{R}_\nu \in \mathbf{R}$. The $\mathbf{R}_0$ in (2.97) is used when trying to stabilize $\bar{e}_{ss}(kT)$ to the null-point ($\overline{C}$ has rank n) as described in Section 2.11. $\mathbf{R}_3$ in (2.100) is used when trying to stabilize $\bar{e}_{ss}(kT)$ to the entire $\mathcal{N}[C]$ ($\overline{C} = C$). Since there are no r_{ij} elements to be determined in $\mathbf{R}_3$, this case, and that of $\mathbf{R}_0$, is relatively straight forward.

Any one of the set of column vectors in $\mathbf{R}_1$ in (2.98) can be used to designate a line (a 1-dimensional subspace) in a 3-dimensional space. For instance, the basis vector

$$R = R_{11} = \begin{pmatrix} r_{11} \\ r_{12} \\ 1 \end{pmatrix}, \quad \text{with} \quad \begin{cases} r_{11} = 0 \\ r_{12} = 0 \end{cases}$$

designates the line along ℓ_1 lying on the e_{ss3} -axis as illustrated in Figure 2.1.

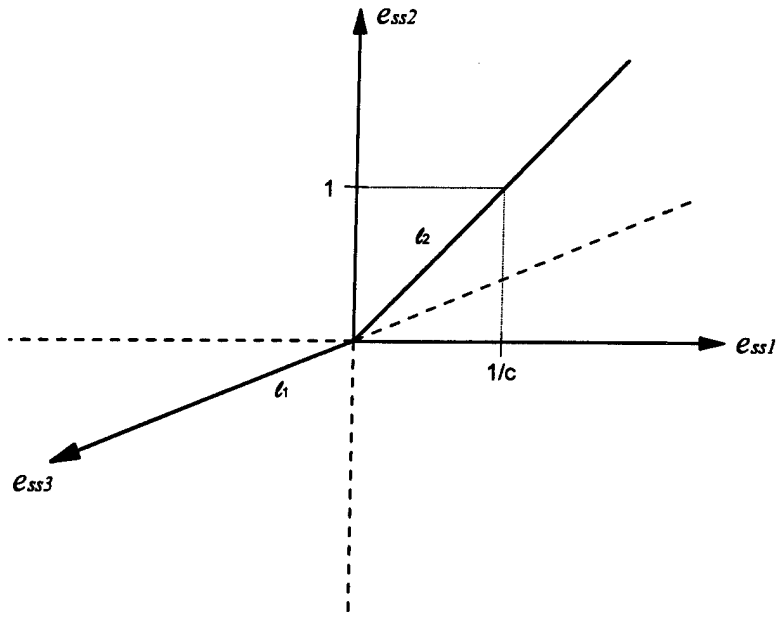

Figure 2.6 Illustration of Two Lines ℓ_1, ℓ_2 (1-Dimensional Subspace) in 3-Space.

Likewise, the vector R_{12} in (2.98)

$$R = R_{12} = \begin{pmatrix} r_{11} \\ 1 \\ r_{12} \end{pmatrix}, \quad \text{with} \quad \begin{cases} r_{11} = \frac{1}{c} \\ r_{12} = 0 \end{cases},$$

designates a line along ℓ_2 in the e_{ss1} - e_{ss2} plane having slope c, as illustrated in Figure 2.1. The alternative basis vector R_{13} in (2.98) can also be used to represent the same line along ℓ_2 in the e_{ss1} - e_{ss2} plane having slope c:

$$R = R_{13} = \begin{pmatrix} 1 \\ r_{11} \\ r_{12} \end{pmatrix}, \quad \text{with} \quad \begin{cases} r_{11} = c \\ r_{12} = 0 \end{cases}.$$

Any one of the basis vectors in $\mathbf{R}_1$ in (2.98) can be used to represent any line in 3-space having non-zero e_{ss1}, e_{ss2}, and e_{ss3} components (except for the point (0,0,0)). Similar logic can be applied to each $R_{vj} \in \mathbf{R}_2$ in (2.99). For instance, the column basis vectors

$$R = R_{22} = \begin{pmatrix} 1 & 0 \\ r_{21} & r_{22} \\ 0 & 1 \end{pmatrix}, \quad \text{with} \quad \begin{cases} r_{21} = 0 \\ r_{22} = 0 \end{cases},$$

will designate a plane (a 2-dimensional subspace) in a 3-dimensional space, namely the e_{ss1} - e_{ss3} plane as illustrated in Figure 2.2.

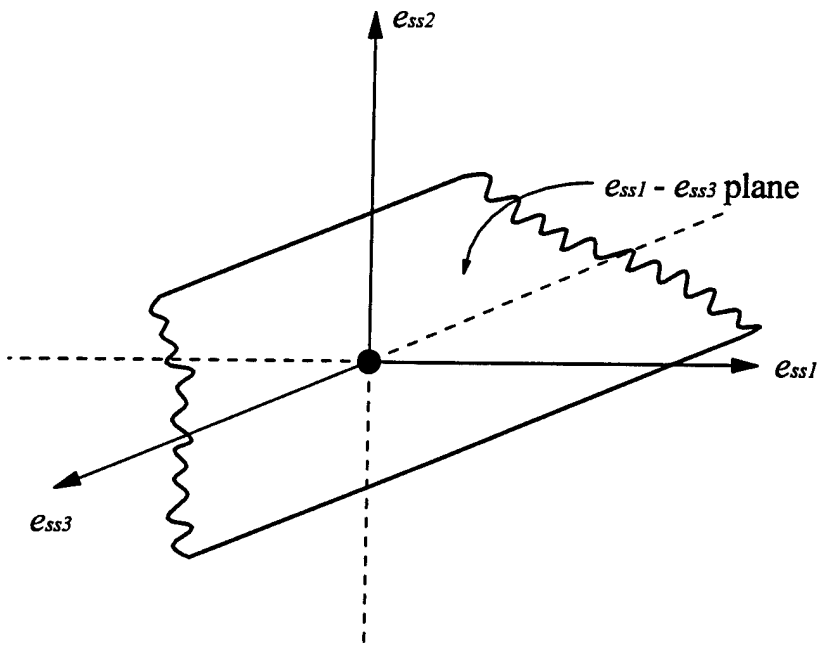

Figure 2.7 Illustration of a Plane (a 2-Dimensional Subspace) in 3-Space.

Beginning with the formulation of the set $\mathbf{R}_3$ in (2.101), the control designer chooses $R = R_{31}$ for the largest subspace W_3 associated with (2.100), determines M from (2.92) and (2.93), and forms the matrix product MR (a basis for the 3-dimensional subspace $S_3 = \mathcal{N}[C]$). The matrix $\overline{C}$ is then formed according to (2.46) and (2.66), and the four conditions above (2.85) and the one condition associated with (2.88) are verified. If those five conditions are met, S_3 is considered suitable and $u_c(kT)$, $u_s(kT)$, and $u_p(kT)$ are chosen according to (2.61), (2.62), and (2.63). If those five conditions are <u>not</u> met, the designer must form the set $\mathbf{R}_2$ in (2.99) and repeat the process with R_{21}, R_{22}, and R_{23}, and so on until a suitable subspace $S_\nu = \mathcal{R}[MR]$ having largest dimension ν is found. A detailed block flow diagram is shown in Figure 2.3 to illustrate the design of a digital servo-tracking controller using the subspace stabilization process presented in this Chapter.

Clearly, the number of elements of $R_{\nu j}$ in $\mathbf{R}$ increases with the dimension of the subspaces $S_\nu \subseteq \mathcal{N}[C]$. Therefore, this technique will become labor-intensive for subspaces S_ν with relatively large dimension. The number of elements N in the set $\mathbf{R}$ can be calculated exactly using the binomial expansion theorem in [81], that is

$$N = \sum_{\nu=0}^{n-m} \frac{(n-m)!}{\nu!(n-m-\nu)!} = 2^{n-m} \qquad (2.102)$$

Therefore, a null-space $\aleph[C]$ of dimension $n-m=5$ would have $N=2^5=32$ candidate R_{vj} matrices to evaluate (including the special cases of $R=0$ (the null-point) and $R=I_{n-m}$, a basis for $\aleph[C]$). Note that the matrix C, and the values of n and m were not needed in representing the set of all R, rather the difference n-m (the dimension of $\aleph[C]$) is the only property of C utilized.

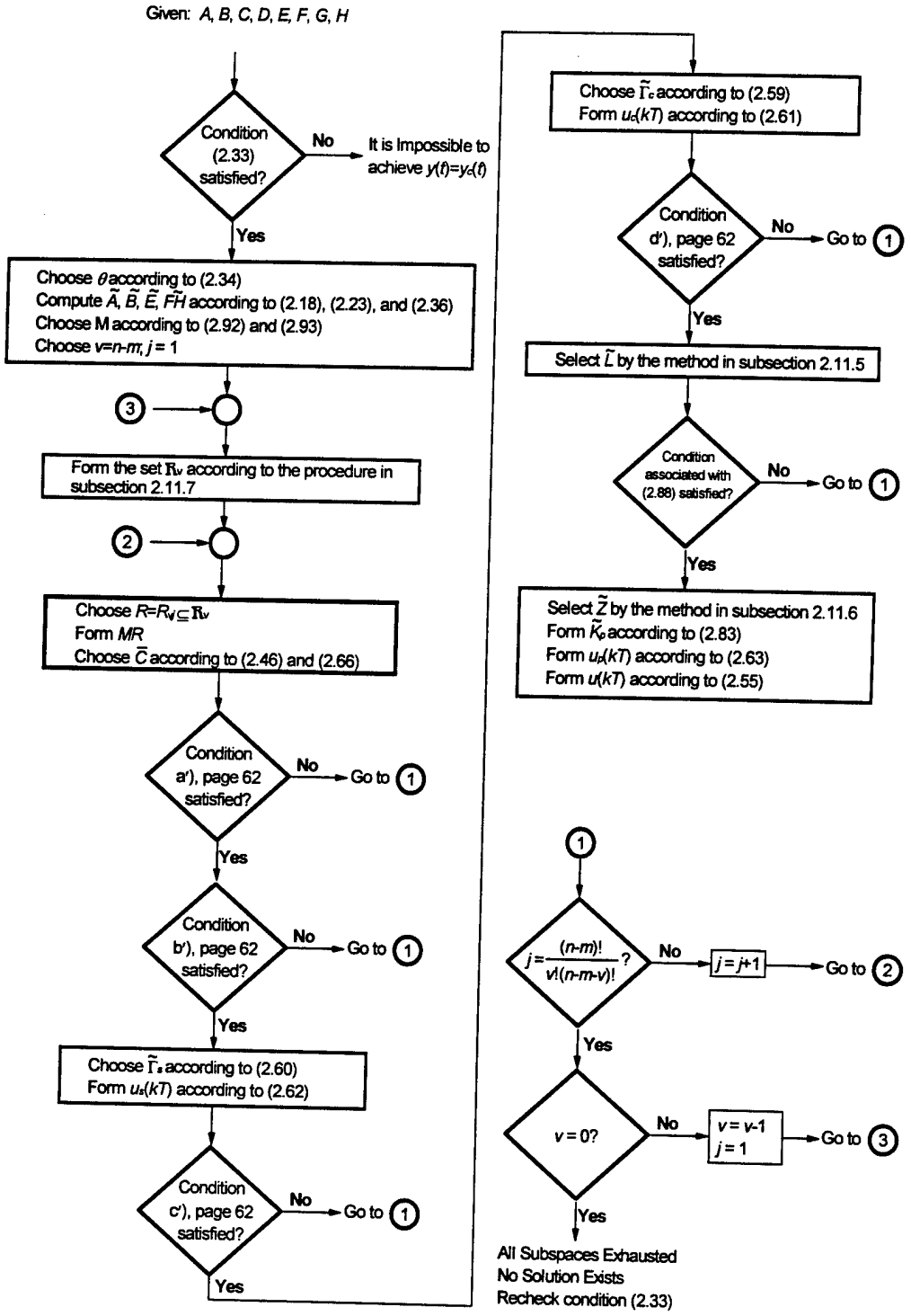

Figure 2.8 Block Flow Diagram for the New Digital Servo-Controller Design Procedure.

2.12. Summary of the New Digital Servo-Controller Design Procedure for the Ideal Case

If the plant, disturbance, and servo-command states $\{x(kT), z(kT), c(kT)\}$ are available for accurate, real-time measurement (the ideal case), then the digital servo-controller chosen as in (2.61), (2.62), and (2.63) can be implemented directly as

$$u(kT) = \tilde{\Gamma}_c z(kT) + \tilde{\Gamma}_s c(kT) - \tilde{K}_p(\theta c(kT) - x(kT)), \tag{2.103}$$

where $\tilde{\Gamma}_c$, $\tilde{\Gamma}_s$, and $\tilde{K}_p$ are selected to satisfy the four conditions above (2.85) and the one condition associated with (2.88).

2.13. Practical Realization of the Discrete-Time Servo-Controller

The digital servo-controller design methodology developed in the previous sections of this chapter is an extended state-feedback design technique. To implement such a state-feedback controller design, the states $x(kT)$ and $z(kT)$ of the composite system and the servo-command state $c(kT)$ must be measurable or estimatable in real-time. The idealized control law in (2.103) uses the real-time value of the disturbance state $z(kT)$, the plant state $x(kT)$, and the servo-command state $c(kT)$. In practical applications, it is rarely possible to measure those three states. Recall that, for this research, it is assumed that the current "sampled" value of the plant output vector $y(kT)$ and the current "sampled" value of the servo-command vector $y_c(kT)$ are the only quantities available for direct measurement. Consequently, discrete-time state estimation algorithms (observers) must be designed to estimate the value of the plant, disturbance, and servo-command states in real-time.

In order to design the composite state-observer and the observer for the servo-command state $c(kT)$, the composite system and the servo-command model must be completely observable. That is, every element of each state $x(kT)$ and $z(kT)$ must affect one or more of the plant outputs and every command state $c(kT)$ must affect one or more of the servo-commands. In that case, an observer can be designed in either a full-order or reduced-order form. A full-order observer reconstructs (estimates), for example, all elements of each of the states $x(kT)$ and $z(kT)$ of the composite system. Thus, if the composite system is $(n + \rho)^{\text{th}}$-order, then a full-order observer will also be $(n + \rho)^{\text{th}}$-order. A reduced-order observer reconstructs, for example, only the state elements of (x, z) that are not directly measurable through the $y(t)$ measurements. An obvious advantage of using a reduced-order observer is that it has lower dimension than a full-order observer.

Two observers will be needed for implementing the digital servo-tracking controller developed in this chapter. The first will be chosen to be a discrete-time full-order observer using "sampled" measurements of the plant output $y(kT)$ and the control input $u(kT)$ to obtain the real-time state estimates $\hat{x}(kT)$, $\hat{z}(kT)$, $\hat{x}((k+1)T)$, and $\hat{z}((k+1)T)$ of $x(kT)$, $z(kT)$, $x((k+1)T)$ and $z((k+1)T)$, respectively. The second observer will be chosen as a discrete-time reduced-order observer and will use the "sampled" measurements of the servo-commands $y_c(kT)$ to obtain the discrete-time estimates $\hat{c}(kT)$ of the servo-command states $c(kT)$. The use of those discrete-time state-estimators will result in a physically-realizable digital servo-tracking control law having the form (refer to (2.55), (2.60), (2.61), and (2.63))

$$u(kT) = \tilde{\Gamma}_c \hat{z}(kT) + \tilde{\Gamma}_s \hat{c}(kT) - \tilde{K}_p(\theta \hat{c}(kT) - \hat{x}(kT)). \tag{2.104}$$

2.13.1. Development of Discrete-Time Composite Models of the Plant, Servo-Command, and Disturbance System

The discrete-time composite plant/disturbance model was given in (2.26). However, for reasons identified in Section 2.6 the terms $\tilde{\gamma}(kT)$ and $\tilde{\sigma}(kT)$ in (2.26) have been disregarded. Ignoring those terms results in the following truncated composite plant/disturbance model which will be used in the discrete-time full-order observer design

$$\begin{aligned} \begin{pmatrix} x((k+1)T) \\ z((k+1)T) \end{pmatrix} &= \left[\begin{array}{c|c} \tilde{A} & \tilde{FH} \\ \hline 0 & \tilde{D} \end{array}\right] \begin{pmatrix} x(kT) \\ z(kT) \end{pmatrix} + \begin{pmatrix} \tilde{B} \\ 0 \end{pmatrix} u(kT) \\ y(kT) &= (C \mid 0) \begin{pmatrix} x(kT) \\ z(kT) \end{pmatrix} \end{aligned} \tag{2.105}$$

The discrete-time state-model for the servo-command in (2.36) will be used in the discrete-time reduced-order observer design. For reasons discussed in Section 2.7, the $\tilde{\mu}(kT)$ term in (2.36) is ignored, resulting in the following truncated servo-command model which will be used in the discrete-time reduced-order observer design

$$\begin{aligned} y_c(kT) &= Gc(kT) \\ c((k+1)T) &= \tilde{E}(kT)c(kT) \end{aligned} \tag{2.106}$$

2.13.2. The Design of a Discrete-Time Full-Order State-Observer for the Composite System in (2.105)

In principle, accurate real-time estimates $\hat{x}(kT)$ and $\hat{z}(kT)$ of the plant states $x(kT)$ and the disturbance states $z(kT)$ can be obtained from "sampled" on-line measurements of $y(kT)$ and $u(kT)$ using conventional observer theories. In [33], a discrete-time DAC composite observer theory is developed which achieves this estimation by extending modern control observer/estimation theory. A unique feature of the DAC observer theory in [33] is the incorporation of the disturbance model (2.25) into the observer dynamics. This is accomplished using the $(n+\rho)$-dimensional composite plant/disturbance model in (2.105). The resulting discrete-time full-order observer for (2.105) has the form [33]

$$\begin{pmatrix} \hat{x}((k+1)T) \\ \hat{z}((k+1)T) \end{pmatrix} = \left[\begin{array}{c|c} \tilde{A} & \tilde{FH} \\ \hline 0 & \tilde{D} \end{array}\right] \begin{pmatrix} \hat{x}(kT) \\ \hat{z}(kT) \end{pmatrix} + \begin{pmatrix} \tilde{B} \\ 0 \end{pmatrix} u(kT) + \left[\begin{array}{c} \tilde{K}_{01} \\ \hline \tilde{K}_{02} \end{array}\right] \left[(C \mid 0) \begin{pmatrix} \hat{x}(kT) \\ \hat{z}(kT) \end{pmatrix} - y(kT) \right], \tag{2.107}$$

where $u(kT)$ is given in (2.103) and $\tilde{K}_0 = \left[\frac{\tilde{K}_{01}}{\tilde{K}_{02}}\right]$ is the observer gain-matrix to be designed.

The time-evolution of the estimation error ε, where ε is defined by

$$\varepsilon = \left[\frac{\varepsilon_x(kT)}{\varepsilon_z(kT)}\right] \stackrel{\Delta}{=} \left(\frac{\hat{x}(kT)}{\hat{z}(kT)}\right) - \left(\frac{x(kT)}{z(kT)}\right), \tag{2.108}$$

for the discrete-time full-order observer (2.107) is determined by forward shifting (2.108). The result is

$$\begin{aligned}\left(\frac{\varepsilon_x((k+1)T)}{\varepsilon_z((k+1)T)}\right) &= \left(\frac{\hat{x}((k+1)T)}{\hat{z}((k+1)T)}\right) - \left(\frac{x((k+1)T)}{z((k+1)T)}\right) \\ &= \left[\begin{array}{c|c} \tilde{A}+\tilde{K}_{01}C & \tilde{FH} \\ \hline \tilde{K}_{02}C & \tilde{D} \end{array}\right]\left(\frac{\varepsilon_x(kT)}{\varepsilon_z(kT)}\right)\end{aligned} \tag{2.109}$$

The observer "gain matrix" $\tilde{K}_o$ should be designed so that the observer error $\left(\frac{\varepsilon_x(kT)}{\varepsilon_z(kT)}\right)$ always converges to zero promptly, from any initial condition. This can be achieved if, and only if, the states $x(kT)$ and $z(kT)$ of (2.105) are completely observable, that is, if, and only if

$$\text{rank}\left[C_0^T \mid \tilde{A}_0^T C_0^T \mid \tilde{A}_0^{T^2} C_0^T \mid \cdots \mid \tilde{A}_0^{T^{n+\rho-1}} C_0^T\right] = n+\rho,$$

where

$$\tilde{A}_0 = \left[\begin{array}{c|c} \tilde{A} & \tilde{FH} \\ \hline 0 & \tilde{D} \end{array}\right],$$

and

$$C_0 = \left(C \mid 0\right).$$

Note that the choice of control sample-period T affects the outcome of the complete observability rank condition. If that rank condition is achieved, standard pole placement techniques [3,20,21,46,47,77] can be used to determine an appropriate $\tilde{K}_o$. In that way, $\tilde{K}_o$ is selected such that the eigenvalues of the matrix (refer to (2.109))

$$\left[\begin{array}{c|c} \tilde{A}+\tilde{K}_{01}C & \tilde{FH} \\ \hline \tilde{K}_{02}C & \tilde{D} \end{array}\right], \tag{2.110}$$

are at sufficiently-damped locations inside the unit circle ($|\lambda_i| < 1$) of the complex-plane. Designing $\tilde{K}_o$ to achieve this latter condition will assure that the estimated values $\hat{x}(kT)$ and $\hat{z}(kT)$ of the plant and disturbance states quickly and accurately track the corresponding actual plant and disturbance states $x(kT)$ and $z(kT)$, respectively.

A detailed block diagram of the discrete-time full-order observer in (2.107) is shown in Figure 2.4. The "unit delayor" shown in Figure 2.4 is a one-step delay commonly denoted by E^{-1} and defined such that $E^{-1}x(kT) = x\big((k-1)T\big)$.

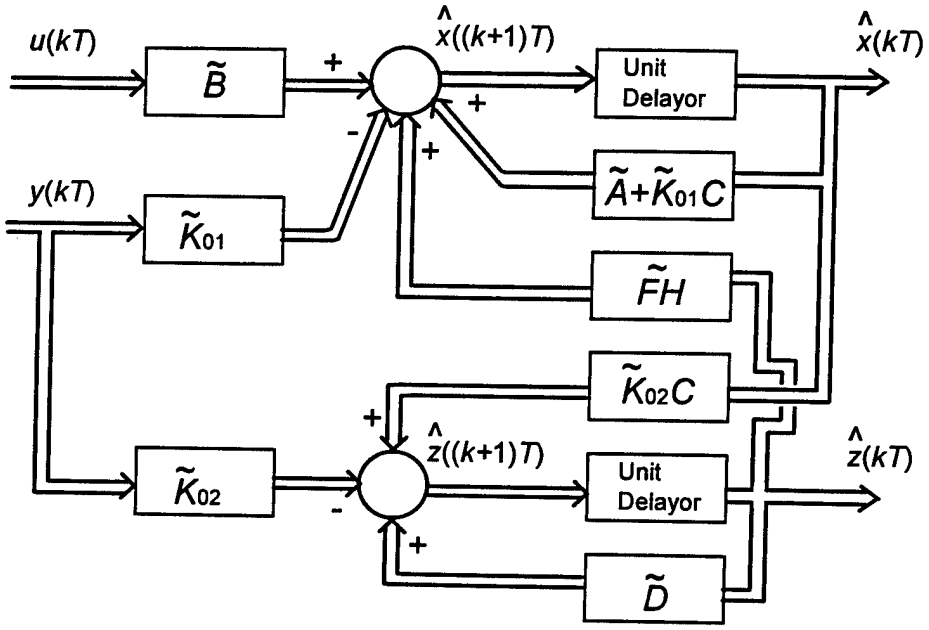

Figure 2.9 A Discrete-Time Full-Order Observer for Generating Real-Time Estimates of the Plant State $x(kT)$ and Disturbance State $z(kT)$.

2.13.3. The Design of a Discrete-Time Reduced-Order State-Observer for Estimating the Servo-Command State $c(kT)$

In this section, a discrete-time reduced-order observer design is presented that will generate servo-command state estimates $\hat{c}(kT)$ from the "sampled" real-time servo-command measurements $y_c(kT)$. An effective "recipe" for designing a discrete-time reduced-order state-observer was developed in [33]. That "recipe" will be used here, with slight modifications to specifically address state estimation for the servo-commands.

The truncated discrete-time state-model in (2.106) for the servo-command is used here in the construction of the discrete-time reduced-order observer. Since the y_{ci}'s, $i = 1, 2, ..., m$, are assumed to be linear independent servo-commands, the matrix G will have rank m.

The following is a summary of the "recipe" presented in [33] for construction of a discrete-time reduced-order observer for the servo-command state $c(kT)$:

Step 1. define T_{12} as any v x $(v\text{-}m)$ maximal rank matrix such that

$$GT_{12} = 0.$$

(The $\Re[T_{12}]$ of the T_{12} which meets this condition will necessarily form a basis for $\aleph[G]$);

Step 2. a) define the $(v\text{-}m)$ x v matrix

$$\overline{T}_{12} = \left(T_{12}^T T_{12}\right)^{-1} T_{12}^T,$$

and

b) define the m x v matrix

$$G^{\#} = \left(GG^T\right)^{-1} G;$$

Step 3. a) construct the $(v\text{-}m)$ x $(v\text{-}m)$ matrix

$$\mathcal{D} = \overline{T}_{12} \widetilde{E} T_{12},$$

and

b) construct the m x $(v\text{-}m)$ matrix

$$\mathcal{H} = G\widetilde{E}T_{12};$$

Step 4. construct the error-dynamics evolution equation

$$\varepsilon_{y_c}((k+1)T) = [\mathcal{D} + \Sigma\mathcal{H}]\varepsilon_{y_c}(kT), \tag{2.111}$$

where Σ is an $(v\text{-}m)$ x m arbitrary observer design matrix to be determined;

Step 5. design Σ in (2.111) such that $\varepsilon_{y_c}(kT) \to 0$ rapidly,

(This can be achieved if, and only if, the servo-command state $c(kT)$ is completely observable, that is, if, and only if

$$\text{rank}\left[G^T \mid \widetilde{E}^T G^T \mid \widetilde{E}^{T^2} G^T \mid \cdots \mid \widetilde{E}^{T^{v-1}} G^T\right] = v.$$

In that case, standard pole placement techniques can be used to place the poles of $[\mathcal{D}+\Sigma\mathcal{H}]$ at sufficiently damped locations inside the unit circle);

Step 6. construct the "filter" part of the reduced-order observer

$$\xi((k+1)T) = (\mathcal{D}+\Sigma\mathcal{H})\xi(kT) + \left[\left(\bar{T}_{12}+\Sigma G\right)\left(\tilde{E}G^{\#^T}\right) - (\mathcal{D}+\Sigma\mathcal{H})\Sigma\right] y_c(kT); \qquad (2.112)$$

and

Step 7. construct the "assembly-equation" portion of the observer

$$\hat{c}(kT) = T_{12}\xi(kT) + \left[G^{\#^T} - T_{12}\Sigma\right] y_c(kT), \qquad (2.113)$$

where

$\hat{c}(kT)$ represents the estimate of the servo-command state vector $c(kT)$, and

ξ is an auxiliary vector defined in step 6 above.

A detailed block diagram of the discrete-time reduced-order observer in (2.112) and (2.113) is shown in Figure 2.5.

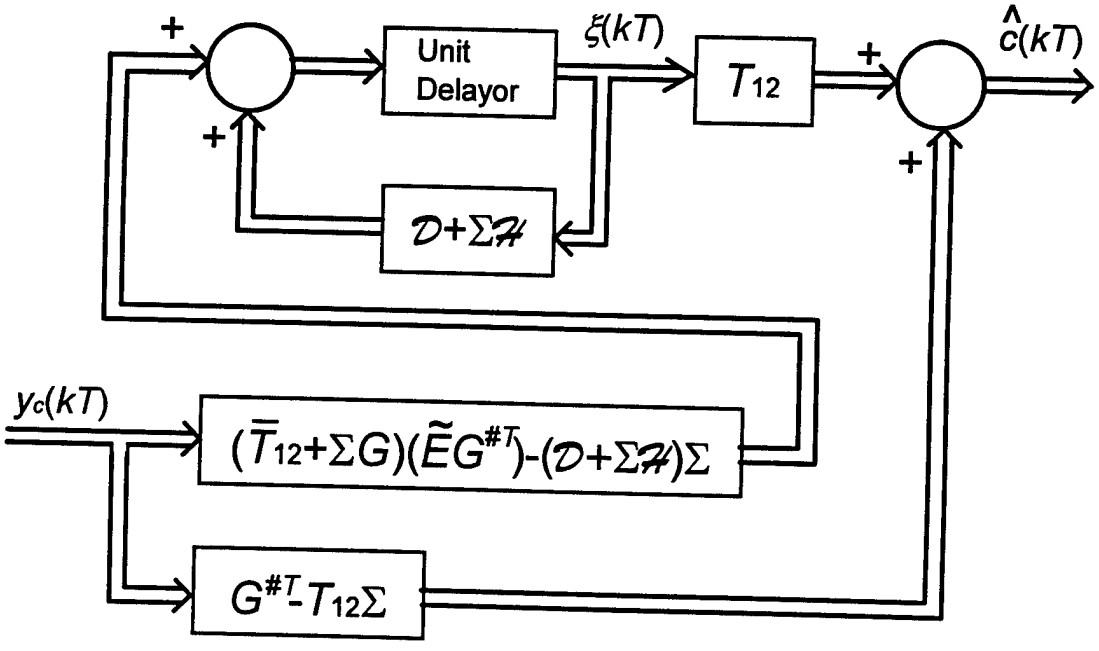

Figure 2.10 A Reduced-Order Discrete-Time Observer for Generating Real-Time Estimates of the Servo-Command State $c(kT)$.

3. ADD-ON ENHANCEMENTS TO THE NEW DIGITAL SERVO-TRACKING CONTROLLER

3.1. Modification of the Digital Servo-Controller Design Procedure to Reduce Intersample Misbehavior

The digital servo-controller terms ($u_c(kT)$, $u_s(kT)$, $u_p(kT)$) developed in Sections 2.10 through 2.11 utilize a stepwise-constant zero-order-hold (z.o.h.) type of control action. This means that the control decision which is made at each sample time $t = kT$, $k = 0, 1, 2, \ldots$, determines a value for $u(kT)$ that remains constant until the beginning of the next sample time. With the exception of the special cases where $w(t)$ and $y_c(t)$ are constants or stepwise-constants, this particular implementation of the digital servo-tracking controller, as developed in Sections 2.10 through 2.11, does not smooth out the stair-step behavior of the control input $u(kT)$ and thus cannot reduce the intersample misbehavior in $y(t)$ that occurs *between* the sample times.

As discussed in Subsection 1.5.2, intersample misbehavior, or "ripple," is the build-up of error between the desired response (servo-command vector $y_c(t)$) and the actual response (plant output vector $y(t)$) that occurs between the sample times $kT < t < (k+1)T$. This error build-up can arise due to intersample time-variations of the uncertain servo-commands and the disturbances or can be due to open-loop instability of the plant. Conventional digital-controllers use holding circuits (first-order hold, second-order hold, exponential hold, etc.) as a means of smoothing out the control input signal before it is applied to the plant as a means of reducing intersample misbehavior of $y(t)$. However, those conventional holding circuits do not attempt to intelligently select the control-action for the next sample-period based on the *intersample* waveform behaviors that $w(t)$ and $y_c(t)$ are anticipated to exhibit. Consequently, those conventional attempts fall short when the plant is subjected to uncertain, time-varying external disturbances, or is required to track uncertain, time-varying servo-commands [38]. In those cases, it is possible to select a smarter holding-strategy that will significantly improve the intersample tracking accuracy of the overall closed-loop system.

In [38], a technique was introduced for computing and implementing an intelligent holding-strategy for discrete-time controlled plants subjected to uncertain, unmeasurable, time-varying disturbances and uncertain, time-varying servo-commands. The technique in [38] achieves a level of robustness to disturbances and a degree of intersample servo-tracking accuracy that is unobtainable by conventional discrete-time control design methods. Specifically, that method provides the capability of intelligently selecting, at each $t = kT$, a time-varying intersample control-action $u(t)$, $kT \le t < (k+1)T$, based on the intersample waveform behaviors that both the servo-command $y_c(t)$ and disturbance $w(t)$ are predicted to exhibit, as determined by current estimates $\hat{z}(kT)$ and $\hat{c}(kT)$ of the disturbance state $z(kT)$ and the servo-command state $c(kT)$ at the sample time $t = kT$, $k = 0, 1, 2, \ldots$. It will now be shown how the intelligent holding-strategy developed in [38] can be incorporated into the new digital servo-controller design technique developed in this report.

3.1.1. Reconsideration of the Servo-Tracking Error Equation

The result in [38] will be incorporated into the new digital servo-controller design technique in this report with the exception that the $u_p(kT)$ control term in (2.63) will remain as it was derived in Chapter 2. The servo-controller design method in [38] is based on the idea of regulating $e_{ss}(t)$ to zero between consecutive samples; however that condition is unnecessarily restrictive in the design of

$u_p(kT)$. It is only necessary to design $u_p(kT)$ to regulate $e_{ss}(t)$ to some subspace $S_v \subseteq \mathcal{N}[C]$. Therefore, the $u_p(kT)$ control term developed in Chapter 2 does not need to be modified when adapting (2.103) to utilize the intersample holding strategy in [38].

The $u_c(kT)$ and $u_s(kT)$ control terms in (2.61) and (2.62) must be modified in order to adapt the intersample holding strategy developed in [38]. To accomplish this modification, it is first necessary to reconsider the servo-tracking error $\varepsilon_y(t)$ in (2.2). Substituting (2.1), (2.31), and (2.34) into (2.2) yields

$$\begin{aligned} \varepsilon_y(t) &= y_c(t) - y(t) \\ &= Gc(t) - Cx(t) \\ &= C\big(\theta c(t) - x(t)\big) \end{aligned} \quad . \tag{3.1}$$

And now introduce the continuous-time servo-state vector $e_{ss}(t)$ (continuous-time counterpart to (2.38)), defined in [37] as

$$e_{ss}(t) \overset{\Delta}{=} \theta c(t) - x(t), \tag{3.2}$$

such that (3.1) can be re-written as

$$\varepsilon_y(t) = Ce_{ss}(t). \tag{3.3}$$

The continuous-time equation for the servo-state vector $e_{ss}(t)$ is of interest because the objective of the intersample holding-strategy is to minimize the continuous-time intersample build-up of tracking error $\varepsilon_y(t)$ that occurs between the sample times. Doing so requires examination of the continuous-time dynamics of $e_{ss}(t)$. Differentiating (3.2) and substituting in (2.1), (2.20), (2.31), and (2.34), yields the following differential equation for the dynamics of the servo-state vector e_{ss} :

$$\begin{aligned} \dot{e}_{ss}(t) &= \theta \dot{c}(t) - \dot{x}(t) \\ &= \theta \dot{c}(t) - \big(Ax(t) + Bu(t) + Fw(t)\big) \\ &= \theta\big(Ec(t) + \mu(t)\big) - \big(Ax(t) + Bu(t) + FHz(t)\big) \end{aligned} \quad . \tag{3.4}$$

Incorporating (3.2) and rearranging terms in (3.4) yields

$$\dot{e}_{ss}(t) = Ae_{ss}(t) - Bu(t) + \big(\theta E - A\theta\big)c(t) - FHz(t) + \theta\mu(t). \tag{3.5}$$

The terms $\big(\theta E - A\theta\big)c(t) - FHz(t) + \theta\mu(t)$ in (3.5) are disturbance-like effects caused by the external disturbance $w(t)$ and the uncertainties of the servo-command $y_c(t)$. The particular term $\theta\mu(t)$ is a consequence of the sparse sequences of totally unknown, random impulses $\mu(t)$ inherent in the servo-command modeled in (2.31). For reasons discussed in Section 2.7, the $\mu(t)$ (and hence the $\theta\mu(t)$ term) is hereafter ignored and (3.4) is rewritten as

$$\dot{e}_{ss}(t) = Ae_{ss}(t) - Bu(t) + \big(\theta E - A\theta\big)c(t) - FHz(t)\,. \tag{3.6}$$

Certain technical conditions must be met in order to cancel the disturbance-like effects of the uncertain motions $c(t)$ and $z(t)$ on the servo-state vector $e_{ss}(t)$ in (3.6) and consequently on the servo-tracking error $\varepsilon_y(t)$ during the intersample interval. Those conditions govern the design of the improved intersample holding-action for the digital servo-tracking control terms u_c and u_s and will be discussed as needed in the design procedure.

3.1.2. Decomposition of the Servo-Tracking Control Effort

In order to develop an enhanced digital servo-control law (algorithm for generating) $u(kT)$ that uses an intelligent holding-strategy to achieve high-performance intersample servo-tracking, a control-effort decomposition similar to the control-effort decomposition in Section 2.9 will be used. This technique consists of splitting the total (vector) control-effort u into a sum of two individual (vector) terms as follows

$$u(\cdot) = u_{sc}(\cdot) + u_p(kT)\,, \tag{3.7}$$

where the notation $u(\cdot)$ is temporarily being used to indicate that the control effort may consist of both discrete and continuous terms, and where

$u_{sc}(\cdot)$ is designed to accomplish reduction of intersample error build-up due to the effects of the disturbance $w(t)$ and the disturbance-like effects of the servo-command $y_c(t)$, and

$u_p(kT)$ is designed by the technique in Section 2.11 and will stabilize $e_{ss}(kT)$ to some subspace $S_v \subseteq \mathcal{N}[C]$ while achieving an acceptable closed-loop settling-time for the servo-tracking error ε_y, assuming $u_{sc}(\cdot)$ is performing its tasks.

The final form of the $u(\cdot)$ in (3.7) will meet the strict definition of a discrete-time controller in the sense that the control action $u(\cdot)$ is updated only at the discrete times $t = kT$, $k = 0, 1, 2, \ldots$, based on real-time measurements (or estimates) of the plant, disturbance, and servo-command states $\{x(kT), z(kT), c(kT)\}$ available at the beginning $t = kT$ of each sample-period. As discussed in Subsection 1.5, the discrete-time servo-control algorithm is realized by digital processors and the resulting servo-controller is referred to as a digital servo-controller. Following a line of development similar to that in Section 2.9, substitute (3.7) into (3.6) and group terms to yield the result

$$\dot{e}_{ss}(t) = Ae_{ss}(t) - Bu_p(\cdot) + \Big(\big(\theta E - A\theta\big)c(t) - FHz(t) - Bu_{sc}(\cdot)\Big)\,. \tag{3.8}$$

The disturbance-cancellation condition governing the ideal design of the control term $u_{sc}(\cdot)$ in (3.8) is the condition for total cancellation of the disturbance-like terms $\big(\theta E - A\theta\big)c(t) - FHz(t)$ in (3.8) over each interval $kT \le t < (k+1)T$. Mathematically speaking, $u_{sc}(\cdot)$ must satisfy

$$\big(\theta E - A\theta\big)c(t) - FHz(t) - Bu_{sc}(t) \equiv 0\,; \quad \forall\, kT \le t < (k+1)T \text{ and } \forall\, c(t) \text{ and } z(t)\,, \tag{3.9}$$

which can be written as

$$\left[\theta E - A\theta \mid -FH\right]\begin{pmatrix} c(t) \\ z(t) \end{pmatrix} - Bu_{sc}(t) \equiv 0. \tag{3.10}$$

Since $y_c(t)$ and $w(t)$ originate from completely different (and uncorrelated) sources, in general, the necessary and sufficient condition for existence of a $u_{sc}(t)$ satisfying (3.10), for all $c(t)$ and $z(t)$, is

$$\text{rank}\left[\theta E - A\theta \mid FH \mid B\right] = \text{rank}\left[B\right], \tag{3.11}$$

which is equivalent to the two simultaneous conditions

$$\text{rank}\left[FH \mid B\right] = \text{rank}\left[B\right], \tag{3.12}$$

and

$$\text{rank}\left[\theta E - A\theta \mid B\right] = \text{rank}\left[B\right]. \tag{3.13}$$

That is, $\Re\left[FH\right] \subseteq \Re\left[B\right]$ and $\Re\left[\theta E - A\theta\right] \subseteq \Re\left[B\right]$.

Proceeding as in Section 2.9, the decomposition in (3.12) and (3.13) suggests that the control term u_{sc} in (3.7) can be further split into two terms as follows

$$u_{sc}(\cdot) = u_c(\cdot) + u_s(\cdot),$$

so that (3.7) is rewritten as

$$u(\cdot) = u_c(\cdot) + u_s(\cdot) + u_p(kT). \tag{3.14}$$

In (3.14), $u_c(\cdot)$ is responsible for reducing the intersample build-up of error due to the effects of the disturbance $w(t)$ and $u_s(\cdot)$ is responsible for reducing the intersample build-up of error due to the disturbance-like effects of the servo-command $y_c(t)$. Mathematically, the tasks of $u_c(\cdot)$ and $u_s(\cdot)$ are, ideally, to achieve the identities

$$FHz(t) + Bu_c(t) \equiv 0; \qquad \forall\, kT \le t < (k+1)T \text{ and } \forall\, z(t), \tag{3.15}$$

and

$$(\theta E - A\theta)c(t) - Bu_s(t) \equiv 0; \qquad \forall\, kT \le t < (k+1)T \text{ and } \forall\, c(t). \tag{3.16}$$

As discussed in Section 2.9, there is a technical possibility that the vectors $c(t)$ and $z(t)$ could be such that $(\theta E - A\theta)c(t) - FHz(t) \equiv 0$. In that fortuitous case the value $u_{sc}(t) \equiv 0$ can be chosen in (3.9) and thus (3.11) is then not necessary. This singular condition is highly unlikely in practical applications and is not addressed further in this report.

The design of the control terms $u_c(\cdot)$ and $u_s(\cdot)$ will be accomplished by first developing the continuous-time cancellation conditions and corresponding continuous-time controller terms $u_c(t)$ and $u_s(t)$, and then discretizing those terms into their digital counterparts $u_c(kT)$ and $u_s(kT)$, respectively.

3.1.3. Conditions for Complete Cancellation of Disturbance-Like Terms on the Servo-State Vector e_{ss}

The control terms u_c and u_s satisfying (3.15) and (3.16) exist if, and only if (3.12) and (3.13) are satisfied. Those expressions imply that

$$FH + B\Gamma_c = 0, \tag{3.17}$$

and

$$(\theta E - A\theta) - B\Gamma_s = 0, \tag{3.18}$$

for some r x ρ matrix Γ_c and some r x ν matrix Γ_s.

Assuming the necessary and sufficient conditions in (3.17) and (3.18) are met, the *continuous-time* control terms $u_c(t)$ and $u_s(t)$ satisfying (3.15) and (3.16), respectively, may be chosen (ideally), during the intersample interval $kT \le t < (k+1)T$, as

$$u_c(t) = \Gamma_c z(t), \tag{3.19}$$

and

$$u_s(t) = \Gamma_s c(t) \quad . \tag{3.20}$$

As discussed in Section 2.13, it is assumed that the digital control decisions at time $t = kT$ must be based on measurements, or estimates, of the states $z(t)$ and $c(t)$ available at each of the times $t = kT$, $k = 0, 1, 2, \ldots$. Therefore, the predicted or forecasted behaviors of $z(t)$ and $c(t)$ across each intersample interval must be represented in terms of $z(kT)$ and $c(kT)$. Proceeding as in [38], that relationship is found in the general solution to (2.20) and (2.31) evaluated at each t over the interval from kT to $t = (k+1)T$. In particular,

$$z(t) = e^{D(t-kT)} z(kT) + r_c(t); \qquad kT \le t < (k+1)T, \tag{3.21}$$

and

$$c(t) = e^{E(t-kT)} c(kT) + r_s(t); \qquad kT \le t < (k+1)T, \tag{3.22}$$

where

$r_c(t)$ is a residual-effect given by $r_c(t) = \int_{kT}^{t} e^{D(t-\tau)} \sigma(\tau) d\tau$,

and

$r_s(t)$ is a residual-effect given by $r_s(t) = \int_{kT}^{t} e^{E(t-\tau)}\mu(\tau)d\tau$.

The residual terms $r_c(t)$ and $r_s(t)$ are an accumulation, from $t = kT$ to t, of the effects of unknown, unpredictable, sparse impulses $\sigma(t)$ and $\mu(t)$ respectively (refer to (2.20) and (2.31)). For reasons discussed in Chapter 2, the $\sigma(t)$ and $\mu(t)$ impulses, and consequently the $r_c(t)$ and $r_s(t)$ terms, are disregarded during the digital-control design process. Substituting (3.21) and (3.22) into (3.19) and (3.20), and disregarding the residual terms, results in the final (idealized) form of the $u_c(t)$ and $u_s(t)$ terms of the enhanced digital servo-tracking controller

$$u_c(t) = \Gamma_c e^{D(t-kT)} z(kT) \quad , \tag{3.23}$$

and

$$u_s(t) = \Gamma_s e^{E(t-kT)} c(kT) . \tag{3.24}$$

The control terms $u_c(t)$ and $u_s(t)$ in (3.23) and (3.24) generate a continuous-time, open-loop control-action where the entire intersample variations of $u_c(t)$ and $u_s(t)$ over each sample interval are determined at the beginning, $t = kT$, of each of the intervals $kT \le t < (k+1)T$. Because those control decisions are updated only at the discrete times $t = kT$, $k = 0, 1, 2, \ldots$, u_s and u_c are, by definition, discrete-time controllers. Since those control terms are both discrete and time-varying they are more appropriately represented by the notation $u_c(t;kT)$ and $u_s(t;kT)$, such that (3.23) and (3.24) are rewritten as

$$u_c(t;kT) = \Gamma_c e^{D(t-kT)} z(kT); \qquad kT \le t < (k+1)T, \tag{3.25}$$

and

$$u_s(t;kT) = \Gamma_s e^{E(t-kT)} c(kT); \qquad kT \le t < (k+1)T. \tag{3.26}$$

The type of control action represented by (3.25) and (3.26) will hereafter be referred to as "digital/continuous" (D/C) control.

The ideal choice for $u_c(t;kT)$ and $u_s(t;kT)$ in (3.25) and (3.26) assumes one can directly measure the states $z(kT)$ and $c(kT)$ in an on-line fashion. In reality, those states are typically not accessible for direct measurement, therefore the solution in (3.25) and (3.26) is not physically-realizable. Consequently, accurate estimates of the states $z(kT)$ and $c(kT)$ must be generated from the real-time "sampled" measurements of $y(kT)$ and $y_c(kT)$. A procedure for generating such estimates $\hat{z}(kT)$ and $\hat{c}(kT)$ and composing the physically-realizable solutions

$$u_c(t;kT) = \Gamma_c e^{D(t-kT)} \hat{z}(kT), \tag{3.27}$$

and

$$u_s(t;kT) = \Gamma_s e^{E(t-kT)} \hat{c}(kT), \tag{3.28}$$

will be presented in Subsection 3.3.3.

3.1.4. Final Form of the Digital/Continuous Servo-Controller for the Ideal Case

If the plant, disturbance, and servo-command states $\{ x(kT), z(kT), c(kT) \}$ are available for direct and accurate measurement (the ideal case), then the digital servo-controller chosen as in (3.25), (3.26), and (2.63) can be expressed as

$$\begin{aligned} u(t;kT) &= u_c(t,kT) + u_s(t,kT) + u_p(kT) \\ &= \Gamma_c e^{D(t-kT)} z(kT) + \Gamma_s e^{E(t-kT)} c(kT) - \tilde{K}_p\big(\theta c(kT) - x(kT)\big) \end{aligned} \quad , \tag{3.29}$$

where the gain matrices Γ_c and Γ_s are selected to satisfy (3.17) and (3.18) and the gain-matrix $\tilde{K}_p$ is selected as described in Section 2.11 with $\tilde{B} = 0$ and $\tilde{\chi} = 0$ throughout the design. Selecting the gain-matrices in this way will stabilize $e_{ss}(t)$ to $S_v = \mathcal{N}[\bar{C}] \subseteq \mathcal{N}[C]$ while achieving an acceptable closed-loop settling-time for $\varepsilon_y = y_c - y$.

3.2. Enhancement of the Digital Servo-Controller Design to Provide Robustness to Plant Parameter-Perturbations

Up to this point, the development of the new digital servo-tracking controller in this report has been carried out under the assumption that the designer has knowledge of the exact values of the plant parameters (the elements of the A, B, C, and F matrices in (2.1)). However, in real-world control problems, knowing the exact values of all those parameters is rarely possible. Uncertain deviations from the nominal design values of the plant parameters is often caused by modeling errors or variations in component hardware characteristics. Whatever the cause, such parameter "perturbations" can significantly reduce the level of closed-loop tracking-performance obtained by a controller that is tuned for nominal parameter values. Consequently, the degree to which a servo-tracking controller-algorithm can resist tracking-performance degradation, and "accommodate" uncertain parameter perturbations, is a measure of the robustness level of the servo-tracking controller. To address parameter uncertainty and achieve robust control, a portion of the linear adaptive control method developed in [34,35,39] will be incorporated into the proposed digital servo-design methodology. For this study, only perturbations (denoted by ΔA) in the nominal value of the A matrix in (2.1) are considered. Methods for modeling and accommodating ΔB, ΔC, and ΔF perturbations are discussed in [34,35,39].

3.2.1. Incorporation of the Plant-Parameter Perturbations ΔA into the Servo-State e_{ss} Dynamics

In order to investigate the effects of plant-parameter perturbations ΔA, it is necessary to look again at the general class of plants in (2.1) and define precisely where the perturbations ΔA arise in the general model of the plant. The plant model as given in (2.1) is

$$\dot{x}(t) = Ax(t) + Bu(t) + Fw(t)$$
$$y(t) = Cx(t) \quad , \tag{3.30}$$

where all components of (3.30) are defined as they were in (2.1) and, in addition, the array of elements a_{ij} in the plant's A matrix are assumed subject to uncertain perturbations ΔA as follows

$$A = A_N + \Delta A \, , \tag{3.31}$$

where

A_N = an n x n known, constant, real-valued matrix representing the nominal A matrix, and

ΔA = an n x n matrix consisting of uncertain and unmeasurable stepwise-constant (or slowly-varying) parameter-perturbations δa_{ij}, $i = 1, 2, \ldots, n$; $j = 1, 2, \ldots, n$.

Substituting (3.31) into (3.30) yields

$$\dot{x}(t) = A_N x(t) + Bu(t) + Fw(t) + \Delta A x(t)$$
$$y(t) = Cx(t) \quad . \tag{3.32}$$

Substituting (3.32) and (3.2) into the differential equation in (3.4) for the servo-state vector $e_{ss}(t)$ yields

$$\begin{aligned} \dot{e}_{ss}(t) &= \theta \dot{c}(t) - \dot{x}(t) \\ &= \theta\big(Ec(t) + \mu(t)\big) - \big(A_N x(t) + Bu(t) + Fw(t) + \Delta A x(t)\big) \\ &= A_N e_{ss}(t) - Bu(t) + (\theta E - A_N \theta)c(t) - FHz(t) - \Delta A x(t) + \theta \mu(t) \end{aligned} \quad . \tag{3.33}$$

For reasons identified below (2.36), the $\mu(t)$ term in (3.33) is ignored and (3.33) is rewritten as

$$\dot{e}_{ss}(t) = A_N e_{ss}(t) - Bu(t) + (\theta E - A\theta)c(t) - FHz(t) - \Delta A x(t) \, . \tag{3.34}$$

3.2.2. Introduction of an Ideal Model for the Servo-Tracking Error $\varepsilon_y(t)$

Following the line of development in [34,35,39], the ideal behavior of (3.34) is assumed to be modeled by the "ideal model"

$$\dot{e}_{ss}(t) = A_m e_{ss}(t)$$
$$\varepsilon_y(t) = C e_{ss}(t) \quad , \tag{3.35}$$

where A_m is a customer or designer-specified "ideal" n x n matrix. In some applications, the matrix A_m may be specified in terms of "ideal" or "desired" eigenvalues of A_m [39]. In that case, the term $P_m(\lambda)$ will hereafter denote the characteristic polynomial of A_m, where

$$P_m(\lambda) = \lambda^n + \beta_n \lambda^{n-1} + \cdots + \beta_2 \lambda + \beta_1, \tag{3.36}$$

and where the β_i in (3.36) are known coefficients corresponding to the specified ideal eigenvalues of A_m. The extended task of the enhanced digital servo-tracking controller is to make (3.34) behave like (3.35) in the face of all anticipated uncertainties and initial conditions.

3.2.3. Introduction of the D/C Control Term u_a to Accommodate Plant Parameter-Perturbations ΔA

Adapting the technique in [34,35,39] for accommodating the ΔA-effects in (3.34) requires that a control term u_a be added to the digital servo-tracking controller expression in (3.14) and that the $u_p(kT)$ control term in (2.63) be redesigned. Thus, (3.14) will be rewritten as

$$u(\cdot) = u_c(\cdot) + u_s(\cdot) + u_p(kT) + u_a(\cdot) \quad , \tag{3.37}$$

where

$u_c(\cdot) = u_c(t;kT)$ as developed in Subsection 3.1.3,

$u_s(\cdot) = u_s(t;kT)$ as developed in Subsection 3.1.3, with A replaced by A_N from (3.31) throughout the design process,

$u_p(kT)$ is designed to stabilize $e_{ss}(kT)$ to $S_v = \aleph[\overline{C}] \subseteq \aleph[C]$ while achieving the specified "ideal model" characteristics in (3.35) for the closed-loop dynamics of the servo-tracking error ε_y,

$u_a(\cdot)$ is designed to accomplish reduction of intersample error build-up due to the disturbance-like effects caused by the uncertain plant-parameter variations ΔA.

Substituting (3.37) into (3.34) and grouping terms yields

$$\begin{aligned} \dot{e}_{ss}(t) = A_N e_{ss}(t) - Bu_p(\cdot) + \big((\theta E - A\theta)c(t) - Bu_s(\cdot)\big) - \big(FHz(t) + Bu_c(\cdot)\big) \\ - \big(\Delta A x(t) + Bu_a(\cdot)\big) \end{aligned} \quad . \tag{3.38}$$

Assuming (3.15) and (3.16) are achieved, it remains to design $u_a(\cdot)$ to cancel the disturbance-like term $\Delta A x(t)$ in (3.38). Mathematically speaking, $u_a(\cdot)$ must satisfy

$$-\big(\Delta A x(t) + Bu_a(t)\big) \equiv 0 . \tag{3.39}$$

The necessary and sufficient condition for existence of a u_a satisfying (3.39) is that

$$\Delta A x(t) \subseteq \Re[B]; \qquad \forall\, t .$$

in which case

$$\Delta Ax(t) = B\gamma(t)\,, \tag{3.40}$$

for some $\gamma(t)$, and thus, theoretically, $u_a(t)$ can be chosen as

$$u_a(t) = -\gamma(t)\,. \tag{3.41}$$

There is no way to predict or directly measure the ΔA-effects as reflected in the $\Delta Ax(t)$ term in (3.40). Therefore, the $u_a(t)$ as chosen in (3.41) is <u>not</u> physically-realizable. Following the line of development in [34,35,39], the design of a physically-realizable control term $u_a(\cdot)$ that satisfies (3.39) is expedited by using a novel dynamical model of the time-evolution of the parameter-perturbation term $\Delta Ax(t)$ as it appears in (3.34). That model is developed in the following Section.

3.2.4. A Dynamic Model for the Time-Evolution of the Plant Parameter-Perturbation Term $\Delta Ax(t)$

Recall from (3.31) that ΔA is a completely unknown and unmeasurable n x n matrix of stepwise-constant perturbations δa_{ij}, written as

$$\Delta A = \begin{bmatrix} \delta a_{11} & \delta a_{12} & \cdots & \delta a_{1n} \\ \delta a_{21} & \delta a_{22} & \cdots & \delta a_{2n} \\ \vdots & \vdots & \ddots & \vdots \\ \delta a_{n1} & \delta a_{n2} & \cdots & \delta a_{nn} \end{bmatrix}\,, \tag{3.42}$$

where some δa_{ij} may be known, a priori, to be zero. As explained in [34,35,39], real-time identification of the perturbations δa_{ij} in (3.42) require complex identification techniques that result in complicated, non-linear data-processing algorithms associated with the control decision process. The unique approach in [34,35,39] to designing a control law for u_a is to view the <u>product</u> $(\Delta A)x(t)$ in (3.34) as an uncertain time-varying parameter disturbance-<u>vector</u> $w_a(t)$ (an uncertain time-varying input as discussed in Section 2.5), written as

$$w_a(t) = \begin{pmatrix} w_{a1}(t) \\ w_{a2}(t) \\ \vdots \\ w_{an}(t) \end{pmatrix} = -(\Delta A)x(t)\,, \tag{3.43}$$

and then to recognize that $w_a(t)$ has a knowable waveform-structure which allows one to estimate the vector $w_a(t)$ in real-time using a disturbance state-observer similar to that used for estimating the external disturbance state $z(kT)$ in Chapter 2.

Let $\hat{w}_a(t)$ represent the observer-generated estimate of $w_a(t)$ obtained from such an observer. It was shown in [39] that, if $\|\Delta A\|$ and/or $\|w_a(t) - \hat{w}_a(t)\|$ are sufficiently small, the <u>closed-loop</u> time variations of the independent elements $w_{ai}(t)$ in (3.43) are closely modeled by the known differential equation

$$\frac{d^n w_{ai}(t)}{dt^n} + \beta_n \frac{d^{n-1} w_{ai}(t)}{dt^{n-1}} + \cdots + \beta_2 \frac{dw_{ai}(t)}{dt} + \beta_1 w_{ai}(t) = 0 \; ; i = 1, 2, ..., n, \qquad (3.44)$$

where the β_i's shown in (3.36) are precisely the same β_i's that appear in (3.44).

Using the technique for representing waveform-structured input behavior, as described in Section 2.5, expression (3.44) can be utilized to develop a model for the dynamic behavior of the uncertain disturbance-term $w_a(t)$ in (3.43). The result is the following n^{th}-order, vector-matrix state-model for $w_a(t)$

$$\begin{aligned} -(\Delta A)x(t) = w_a(t) &= H_a z_a(t) \\ \dot{z}_a(t) &= D_a z_a(t) + \sigma_a(t) \end{aligned} \quad , \qquad (3.45)$$

where $z_a(t)$ represents the "state" of the parameter disturbance-vector $w_a(t)$ and the elements of the vector $\sigma_a(t)$ are unknown, sparse sequences of impulses that are the source of the uncertain, occasional "jumps" that may occur in $(\Delta A)x(t)$. If the perturbation matrix ΔA is completely arbitrary, then the H_a and D_a matrices in (3.45) are specified by the following block diagonal matrices:

$$H_a = \text{diag}(h_o, h_o, \ldots, h_o) \quad ; \qquad (3.46)$$

and

$$D_a = \text{diag}(D_o, D_o, \ldots, D_o); \qquad (3.47)$$

where

H_a is an $n \times n^2$ matrix,

D_a is an $n^2 \times n^2$ matrix,

$h_o = (1,0,\ldots,0)$; an n-dimensional row vector,

and

$$D_o = \begin{bmatrix} 0 & 1 & 0 & \cdots & 0 \\ 0 & 0 & 1 & \cdots & 0 \\ \vdots & & & & \vdots \\ 0 & 0 & 0 & \cdots & 1 \\ -\beta_1 & -\beta_2 & -\beta_3 & \cdots & -\beta_n \end{bmatrix}; \quad \text{an } n \times n \text{ matrix.}$$

If the perturbation matrix ΔA is not completely arbitrary (if certain components of ΔA are known to always be zero), then the vector h_o will only appear in the rows of H_a corresponding to the non-zero rows of ΔA. Similarly, D_o only appears in the corresponding positions in D_a. This will reduce the dimension of the matrices H_a and D_a, and consequently reduce the number of perturbation-related state-variables z_{a_i} that require estimation [34].

3.2.5. Design of the $u_a(t;kT)$ Control Term to Completely Cancel the Parameter-Perturbation Vector $\Delta Ax(t)$

The model in (3.45) can be used as a close approximation of the $\Delta Ax(t)$ effects as they appear in (3.38). Incorporating the $w_a(t)$ model in (3.45) into the cancellation condition in (3.39) yields the requirement on $u_a(t)$ as

$$\left(H_a z_a(t) - Bu_a(t)\right) \equiv 0 . \tag{3.48}$$

Since the state $z_a(t)$ in (3.48) is completely arbitrary, the necessary and sufficient condition for existence of a u_a satisfying (3.48) for all $z_a(t)$ is

$$\text{rank}\left[B | H_a\right] = \text{rank}\left[B\right], \tag{3.49}$$

or equivalently,

$$\Re\left[H_a\right] \subseteq \Re\left[B\right].$$

If (3.49) is satisfied, then it is possible to obtain a (possibly nonunique) matrix Γ_a such that

$$H_a - B\Gamma_a = 0 , \tag{3.50}$$

in which case the control term $u_a(t)$ in (3.48) can be chosen to have the ideal structure

$$u_a(t) = \Gamma_a z_a(t) \quad , \tag{3.51}$$

during the interval $kT \le t < (k+1)T$. Recall, however, that the digital control decisions at time $t = kT$ must be based on measurements, or estimates, of the state $z_a(t)$ available at the beginning of each sample-interval $t = kT$, $k = 0, 1, 2, \ldots$. Therefore, the predicted or forecasted behavior of $z_a(t)$ across each intersample interval must be determined in terms of $z_a(kT)$. This relationship is found in the general solution to (3.45) evaluated at each t over the interval from kT to $t = (k+1)T$

$$z_a(t) = e^{D_a(t-kT)} z_a(kT) + r_a(t) \qquad ; \qquad kT \le t < (k+1)T , \tag{3.52}$$

where $r_a(t)$ is a post-sample residual-effect given by $r_a(t) = \int_{kT}^{t} e^{D_a(t-\tau)} \sigma_a(\tau) d\tau$.

The $r_a(t)$ term is a consequence of the totally unknown, unmeasurable, sparse impulses $\sigma_a(t)$ in (3.45) that may arrive <u>after</u> $t = kT$, and which are the cause of the uncertain, intersample "jumps" that may occur in the parameter disturbance vector $(\Delta A)x(t)$. For reasons discussed below (3.22), the effects of the $\sigma_a(t)$ impulses cannot be predicted or accounted for and consequently the $r_a(t)$ term in (3.52) is ignored. Substituting (3.52) into (3.51), ignoring the residual term, and using the notation $u_a(t;kT)$ to denote "digital/continuous" (D/C) control, results in the following final (idealized) form of the u_a term of the digital servo-tracking controller

$$u_a(t;kT) = \Gamma_a e^{D_a(t-kT)} z_a(kT) . \tag{3.53}$$

3.2.6. Design of the $u_p(kT)$ Control Term to Achieve the Ideal Model Characteristics in (3.35)

The $u_p(kT)$ control term in (2.63) must be redesigned in order to accommodate the ΔA-effects. To accomplish this, $\tilde{K}_p$ in (2.64) is designed to achieve the ideal model characteristics in (3.35). The control designer must choose $\tilde{K}_p$ according to the subspace stabilization technique presented in Subsection 2.11.1, with A replaced by A_N and $\tilde{A}$ replaced by $\tilde{A}_N = e^{A_N T}$ throughout the design process, and with the restriction that the eigenvalues of $\left(\tilde{A}_1 + \tilde{B}_1\tilde{L}\right)$ and $\left(\tilde{A}_2 + \tilde{B}_2\tilde{Z}\right)$ in (2.84) (which are also the eigenvalues of $\left(\tilde{A}_N + \tilde{B}\tilde{K}_p\right)$) are selected to match the eigenvalues of $\tilde{A}_m = e^{A_m T}$ for A_m defined in (3.35). That is, $\tilde{L}$ and $\tilde{Z}$ are chosen to satisfy

$$\det\left[\lambda \mathrm{I} - \left[\begin{array}{c|c} \tilde{A}_1 + \tilde{B}_1\tilde{L} & 0 \\ \hline 0 & \tilde{A}_2 + \tilde{B}_2\tilde{Z} \end{array}\right]\right] = \det\left[\lambda \mathrm{I} - \tilde{A}_m\right], \tag{3.54}$$

where $\tilde{A}_1$, $\tilde{B}_1$, $\tilde{A}_2$, and $\tilde{B}_2$ are defined in (2.84). The (ideal) digital-control term $u_p(kT)$ is then chosen as

$$\begin{aligned} u_p(kT) &= -\tilde{K}_p e_{ss}(kT) \\ &= -\tilde{K}_p\left(\theta c(kT) - x(kT)\right) \end{aligned} \tag{3.55}$$

3.3. Summary of the Enhanced Digital Servo-Controller for the Ideal Case

If the plant, disturbance, servo-command, and parameter disturbance states $\{x(kT),\ z(kT),\ c(kT),\ z_a(kT)\}$ are available for direct, real-time measurement (the ideal case), then the enhanced digital servo-controller can be implemented ideally as

$$u(t;kT) = u_c(t;kT) + u_s(t;kT) + u_p(kT) + u_a(t;kT) \quad , \tag{3.56}$$

where the terms $u_c(t;kT)$ and $u_s(t;kT)$ are given in (3.25) and (3.26), $u_a(t;kT)$ is given in (3.53) when $\Delta A \neq 0$ and $u_a(t,kT) \equiv 0$ when $\Delta A = 0$, and $u_p(kT)$ is designed as in Subsection 3.2.6 when the term $u_a(t;kT)$ is included, or as in Section 2.11 when $u_a(t,kT) \equiv 0$

3.3.1. Practical Realization of the Enhanced Digital Servo-Controller

Two state-observers were designed in Chapter 2. The same discrete-time reduced-order state-observer described in Subsection 2.13.3 is used here to estimate $\hat{c}(kT)$ of the servo-command state $c(kT)$. Estimates $\hat{x}(kT)$, $\hat{z}(kT)$, and $\hat{z}_a(kT)$ of the plant state $x(kT)$, disturbance state $z(kT)$, and

the parameter-perturbation state $z_a(kT)$, respectively, will be obtained from a modified form of the discrete-time full-order state-observer in (2.107). This modified state-observer, called a "hybrid composite state-observer" [33], differs from the discrete-time full-order state-observer described in Subsection 2.13.2 in that the hybrid full-order state-observer uses a D/C control input $u(t;kT)$ as opposed to the stepwise-constant z.o.h.-type of control input $u(kT)$ used by the discrete-time full-order observer. The particular hybrid composite state-observer to be presented in Subsection 3.3.3 is based on the ideas in [33].

3.3.2. A Discrete-Time Composite Model of the Plant, Disturbance, and Parameter-Perturbation Dynamics

In order to design the hybrid full-order state-observer, a composite system must be obtained. Substituting (3.43) into (3.32) yields

$$\dot{x}(t) = A_N x(t) + Bu(t) + Fw(t) - w_a(t). \tag{3.57}$$

A discrete-time model for (3.57) can be determined by the same procedure used in Section 2.6 to obtain (2.18). In that way, the following difference equation is obtained (assuming $u(t) = u(kT) =$ constant):

$$x((k+1)T) = \tilde{A}_N x(kT) + \tilde{B}u(kT) + \tilde{FH}z(kT) + \tilde{\gamma}(kT) - \tilde{v}_a((k+1)T), \tag{3.58}$$

where $\tilde{B}$, $\tilde{FH}$, and $\tilde{\gamma}$ are as derived in (2.18) and (2.23) (with A replaced by A_N), $\tilde{A}_N = e^{A_N T}$, and

$$\tilde{v}_a((k+1)T = \int_0^T e^{A_N(T-\tau)} w_a(\tau + kT) d\tau. \tag{3.59}$$

Note that $\tilde{v}_a((k+1)T)$ is similar to the $\tilde{v}((k+1)T)$-term in (2.18). The term $\tilde{v}_a((k+1)T)$ requires knowledge of $w_a(\tau)$ (actually $(\Delta A)x(\tau)$) over the entire sampling-interval $kT \le \tau \le (k+1)T$. In general, at the time $t = kT$ it is impossible to accurately and consistently predict the time-behavior of the uncertain, unmeasurable quantity $(\Delta A)x(\tau)$ over the remainder of that sampling-interval. Therefore to make (3.58) practically useful, it is necessary to further investigate and approximate the term $\tilde{v}_a((k+1)T)$ in (3.59). The $\tilde{v}_a((k+1)T)$ term can be simplified by incorporating the waveform-model in (3.45) for the time variations of $-(\Delta A)x(\tau) = w_a(\tau)$. Substituting τ for t in (3.45) and substituting the result into (3.59) yields

$$\tilde{v}_a((k+1)T = \int_0^T e^{A_N(T-\tau)} H_a z_a(\tau + kT) d\tau. \tag{3.60}$$

Using (3.45) and methods similar to those used to obtain $z(\tau)$ in (2.22), the general solution of $z_a(\tau)$ is written as

$$z_a(\tau) = \Phi_{Da}(\tau, kT) z_a(kT) + \int_{kT}^{\tau} \Phi_{Da}(\tau, \xi) \sigma_a(\xi) d\xi, \tag{3.61}$$

where Φ_{Da} represents the state-transition matrix for matrix D_a in (3.45). Substituting (3.61) into (3.60) and simplifying terms yields

$$\tilde{v}_a((k+1)T = \tilde{H}_a z_a(kT) + \tilde{\gamma}_a(kT), \tag{3.62}$$

where

$$\tilde{H}_a = \int_0^T e^{A_N(T-\tau)} H_a e^{D a \tau} d\tau,$$

and

$$\tilde{\gamma}_a(kT) = \int_0^T e^{A(T-\tau)} H_a \int_0^\tau e^{D_a(\tau-\xi)} \sigma_a(\xi + kT) d\xi d\tau.$$

Consolidating (3.58) and (3.62) yields the "exact" discrete-time plant-model

$$\begin{aligned} x((k+1)T) &= \tilde{A}_N x(kT) + \tilde{B}u(kT) + \tilde{FH} z(kT) - \tilde{H}_a z_a(kT) + \tilde{\gamma}(kT) - \tilde{\gamma}_a(kT), \\ y &= Cx(kT) \end{aligned} \tag{3.63}$$

which is mathematically equivalent to (3.58) under the model assumption in (3.45) and under the assumption that $u(t) = u(kT) = \text{constant}$.

A discrete-time model for the time-evolution of $z_a(kT)$ can be developed by letting $\tau \to (t_o + (k+1)T)$ in (3.61) and recalling from the comments below (2.18) that $(k+1)T$ denotes $t_o+(k+1)T$ to obtain

$$z_a((k+1)T) = \tilde{D}_a z_a(kT) + \tilde{\sigma}_a(kT), \tag{3.64}$$

where

$$\tilde{D}_a = e^{DT} \quad ; \qquad D_a \text{ is assumed constant,}$$

and

$$\tilde{\sigma}_a(kT) = \int_0^T e^{D_a(\tau-\xi)} \sigma_a(\xi + kT) d\xi.$$

Expressions (2.25), (3.63), and (3.64) can now be combined to form the composite discrete-time model

$$\begin{pmatrix} \dfrac{x((k+1)T)}{z((k+1)T)} \\ \dfrac{}{z_a((k+1)T)} \end{pmatrix} = \left[\begin{array}{c|c|c} \widetilde{A}_N & \widetilde{FH} & -\widetilde{H}_a \\ \hline 0 & \widetilde{D} & 0 \\ \hline 0 & 0 & \widetilde{D}_a \end{array}\right] \begin{pmatrix} \dfrac{x(kT)}{z(kT)} \\ \dfrac{}{z_a(kT)} \end{pmatrix} + \begin{pmatrix} \widetilde{B} \\ \hline 0 \\ \hline 0 \end{pmatrix} u(kT) + \begin{pmatrix} \dfrac{\widetilde{\gamma}(kT) - \widetilde{\gamma}_a(kT)}{\widetilde{\sigma}(kT)} \\ \dfrac{}{\widetilde{\sigma}_a(kT)} \end{pmatrix} \tag{3.65}$$

$$y(kT) = \left(C \mid 0 \mid 0\right) \begin{pmatrix} \dfrac{x(kT)}{z(kT)} \\ \dfrac{}{z_a(kT)} \end{pmatrix}$$

However, the model in (3.65) is obtained under the assumption that the control-action remains constant between the sample times ($u(t) = u(kT)$ = constant) and therefore is not an accurate model when a D/C control-action is used. In that case, (3.65) must be modified to include the time-varying portion of the D/C servo-control in (3.56). Across each of the sampling intervals, the control-action governed by (3.56) can be divided into a discrete-time part $u_p(kT)$, that consists of a stepwise-constant zero-order-hold type control-action, and a continuous "time-varying interpolating" [33] part $u_t(\cdot)$. Thus, $u(\tau)$ can be written as

$$u(\tau) = u_p(kT) + u_t(\tau); \qquad kT \le \tau < (k+1)T, \tag{3.66}$$

where $u_p(kT)$ is constant in value between consecutive sample times and

$$u_t(\tau) = u_a(\tau; kT) + u_c(\tau; kT) + u_s(\tau; kT) \tag{3.67}$$

is the portion of $u(t;kT)$ in (3.56) that is allowed to vary with time across each intersample interval.

The time-varying nature of $u_t(\tau)$ changes the structure of the discrete-time model in (3.65). In order to modify (3.65) to accurately reflect the time-varying nature of the D/C servo-control in (3.56), it is necessary to return to the general solution of (3.57)

$$x((k+1)T)) = e^{A_N T} x(kT) + \int_0^T e^{A_N(T-\tau)} B u(\tau) d\tau + \widetilde{v}((k+1)T) - \widetilde{v}_a((k+1)T), \tag{3.68}$$

and incorporate (2.23), (3.62), and (3.66) to obtain

$$\begin{aligned} x((k+1)T)) = \widetilde{A}_N x(kT) + \int_0^T e^{A_N(T-\tau)} B\left[u_p(kT) + u_t(\tau)\right] d\tau + \widetilde{FH} z(kT) \\ + \widetilde{\gamma}(kT) - \widetilde{H}_a z_a(kT) - \widetilde{\gamma}_a(kT) \end{aligned} \tag{3.69}$$

Since $u_p(kT)$ is constant, it can be factored out of the integral in (3.69), resulting in

$$\begin{aligned} x((k+1)T)) = \widetilde{A}_N x(kT) + \widetilde{B} u_p(kT) + \psi(u_t) + \widetilde{FH} z(kT) + \widetilde{\gamma}(kT) \\ - \widetilde{H}_a z_a(kT) - \widetilde{\gamma}_a(kT) \end{aligned} \tag{3.70}$$

where

$$\psi(u_t) = \int_0^T e^{A_N(T-\tau)} B u_t(\tau) d\tau .$$

Using (3.69), the composite discrete-time model from (3.65) is rewritten to accurately reflect the time-varying nature of the digital servo-controller in (3.56)

For $\Delta A = 0$:

$$\begin{pmatrix} x((k+1)T) \\ \hline z((k+1)T) \end{pmatrix} = \left[\begin{array}{c|c} \widetilde{A} & \widetilde{FH} \\ \hline 0 & \widetilde{D} \end{array}\right] \begin{pmatrix} x(kT) \\ \hline z(kT) \end{pmatrix} + \begin{pmatrix} \widetilde{B} \\ \hline 0 \end{pmatrix} u_p(kT) + \begin{pmatrix} \psi(u_t) \\ \hline 0 \end{pmatrix} + \begin{pmatrix} \widetilde{\gamma}(kT) \\ \hline \widetilde{\sigma}(kT) \end{pmatrix} \quad ; \quad (3.71)$$

$$y(kT) = \begin{pmatrix} C & | & 0 \end{pmatrix} \begin{pmatrix} x(kT) \\ \hline z(kT) \end{pmatrix}$$

and

For $\Delta A \neq 0$:

$$\begin{pmatrix} x((k+1)T) \\ \hline z((k+1)T) \\ \hline z_a((k+1)T) \end{pmatrix} = \left[\begin{array}{c|c|c} \widetilde{A}_N & \widetilde{FH} & -\widetilde{H}_a \\ \hline 0 & \widetilde{D} & 0 \\ \hline 0 & 0 & \widetilde{D}_a \end{array}\right] \begin{pmatrix} x(kT) \\ \hline z(kT) \\ \hline z_a(kT) \end{pmatrix} + \begin{pmatrix} \widetilde{B} \\ \hline 0 \\ \hline 0 \end{pmatrix} u_p(kT) + \begin{pmatrix} \psi(u_t) \\ \hline 0 \\ \hline 0 \end{pmatrix} + \begin{pmatrix} \widetilde{\gamma}(kT) - \widetilde{\gamma}_a(kT) \\ \hline \widetilde{\sigma}(kT) \\ \hline \widetilde{\sigma}_a(kT) \end{pmatrix} \quad . \quad (3.72)$$

$$y(kT) = \begin{pmatrix} C & | & 0 & | & 0 \end{pmatrix} \begin{pmatrix} x(kT) \\ \hline z(kT) \\ \hline z_a(kT) \end{pmatrix}$$

The quantities $\widetilde{\gamma}(kT)$, $\widetilde{\gamma}_a(kT)$, $\widetilde{\sigma}(kT)$, and $\widetilde{\sigma}_a(kT)$ in (3.71) and (3.72) are completely unknown, unpredictable, and unmeasurable "residual-effects" [33,34]. The $\widetilde{\gamma}(kT)$ and $\widetilde{\sigma}(kT)$ are consequences of the sparse, uncertain $\sigma(t)$ impulses associated with the external disturbance model for $w(t)$ in (2.20) and the $\widetilde{\gamma}_a(kT)$ and $\widetilde{\sigma}_a(kT)$ are consequences of the uncertain $\sigma_a(t)$ impulses associated the parameter perturbation model in (3.45), each of which arrive in a random, time-sparse manner during the intervals between each of the sampling instants $kT < t < (k+1)T$. The $\sigma_a(t)$ impulses are similar to the unpredictable and uncontrollable $\sigma(t)$ impulses discussed in Section 2.6. For the reasons stated below (2.26), the $\sigma(t)$ (and also the $\sigma_a(t)$ term), and consequently the $\widetilde{\gamma}(kT)$, $\widetilde{\gamma}_a(kT)$, $\widetilde{\sigma}(kT)$, and $\widetilde{\sigma}_a(kT)$ terms as well, will be ignored. Thus (3.71) and (3.72) are rewritten in the truncated form

For $\Delta A = 0$:

$$\begin{pmatrix} x((k+1)T) \\ z((k+1)T) \end{pmatrix} = \left[\begin{array}{c|c} \widetilde{A}_N & \widetilde{FH} \\ \hline 0 & \widetilde{D} \end{array}\right] \begin{pmatrix} x(kT) \\ z(kT) \end{pmatrix} + \begin{pmatrix} \widetilde{B} \\ 0 \end{pmatrix} u_p(kT) + \begin{pmatrix} \psi(u_t) \\ 0 \end{pmatrix}; \tag{3.73}$$

$$y(kT) = (C \mid 0) \begin{pmatrix} x(kT) \\ z(kT) \end{pmatrix}$$

and

For $\Delta A \neq 0$:

$$\begin{pmatrix} x((k+1)T) \\ z((k+1)T) \\ z_a((k+1)T) \end{pmatrix} = \left[\begin{array}{c|c|c} \widetilde{A}_N & \widetilde{FH} & -\widetilde{H}_a \\ \hline 0 & \widetilde{D} & 0 \\ \hline 0 & 0 & \widetilde{D}_a \end{array}\right] \begin{pmatrix} x(kT) \\ z(kT) \\ z_a(kT) \end{pmatrix} + \begin{pmatrix} \widetilde{B} \\ 0 \\ 0 \end{pmatrix} u_p(kT) + \begin{pmatrix} \psi(u_t) \\ 0 \\ 0 \end{pmatrix} \tag{3.74}$$

$$y(kT) = (C \mid 0 \mid 0) \begin{pmatrix} x(kT) \\ z(kT) \\ z_a(kT) \end{pmatrix}$$

3.3.3. The Design of Hybrid Full-Order State-Observers for the Composite Systems in (3.73) and (3.74)

The hybrid full-order state-observer for the composite system in (3.73) is obtained by adding the control-related term $\begin{pmatrix} \psi(u_t) \\ 0 \end{pmatrix}$ in (3.73) to the discrete-time full-order observer equations in (2.107) as follows:

$$\begin{pmatrix} \hat{x}((k+1)T) \\ \hat{z}((k+1)T) \end{pmatrix} = \left[\begin{array}{c|c} \widetilde{A} & \widetilde{FH} \\ \hline 0 & \widetilde{D} \end{array}\right] \begin{pmatrix} \hat{x}(kT) \\ \hat{z}(kT) \end{pmatrix} + \begin{pmatrix} \widetilde{B} \\ 0 \end{pmatrix} u_p(kT) + \begin{pmatrix} \psi(u_t) \\ 0 \end{pmatrix}$$

$$+ \begin{bmatrix} \widetilde{K}_{01} \\ \widetilde{K}_{02} \end{bmatrix} \left[(C \mid 0) \begin{pmatrix} \hat{x}(kT) \\ \hat{z}(kT) \end{pmatrix} - y(kT) \right] \tag{3.75}$$

where $\widetilde{K}_0 = \begin{bmatrix} \widetilde{K}_{01} \\ \widetilde{K}_{02} \end{bmatrix}$ is precisely the same observer gain-matrix designed in Subsection 2.13.2.

The hybrid full-order state-observer for the composite system in (3.74) is obtained by incorporating the composite model from (3.74) into the discrete-time full-order observer equations in (2.107) and adding the control-related term $\begin{pmatrix} \psi(u_t) \\ \hline 0 \\ \hline 0 \end{pmatrix}$ in (3.74) as follows:

$$\begin{pmatrix} \hat{x}((k+1)T) \\ \hline \hat{z}((k+1)T) \\ \hline \hat{z}_a((k+1)T) \end{pmatrix} = \left[\begin{array}{c|c|c} \widetilde{A}_N & \widetilde{FH} & -\widetilde{H}_a \\ \hline 0 & \widetilde{D} & 0 \\ \hline 0 & 0 & \widetilde{D}_a \end{array}\right] \begin{pmatrix} \hat{x}(kT) \\ \hline \hat{z}(kT) \\ \hline \hat{z}_a(kT) \end{pmatrix} + \begin{pmatrix} \widetilde{B} \\ \hline 0 \\ \hline 0 \end{pmatrix} u_p(kT) + \begin{pmatrix} \psi(u_t) \\ \hline 0 \\ \hline 0 \end{pmatrix}$$

$$+ \begin{bmatrix} \widetilde{K}_{01} \\ \hline \widetilde{K}_{02} \\ \hline \widetilde{K}_{03} \end{bmatrix} \left[(C \mid 0 \mid 0) \begin{pmatrix} \hat{x}(kT) \\ \hline \hat{z}(kT) \\ \hline \hat{z}_a(kT) \end{pmatrix} - y(kT) \right] \quad , \qquad (3.76)$$

where $\widetilde{K}_0 = \begin{bmatrix} \widetilde{K}_{01} \\ \hline \widetilde{K}_{02} \\ \hline \widetilde{K}_{03} \end{bmatrix}$ is an observer gain-matrix to be designed.

The general evolution equation for the error dynamics of the hybrid full-order state-observer in (3.76) is obtained in the same manner as (2.109), using the composite system from (3.74). The result is as follows:

$$\begin{pmatrix} \varepsilon_x((k+1)T) \\ \hline \varepsilon_z((k+1)T) \\ \hline \varepsilon_{z_a}((k+1)T) \end{pmatrix} = \begin{pmatrix} \hat{x}((k+1)T) \\ \hline \hat{z}((k+1)T) \\ \hline \hat{z}_a((k+1)T) \end{pmatrix} - \begin{pmatrix} x((k+1)T) \\ \hline z((k+1)T) \\ \hline z_a((k+1)T) \end{pmatrix}$$

$$= \left[\begin{array}{c|c|c} \widetilde{A}_N + \widetilde{K}_{01}C & \widetilde{FH} & -\widetilde{H}_a \\ \hline \widetilde{K}_{02}C & \widetilde{D} & 0 \\ \hline \widetilde{K}_{03}C & 0 & \widetilde{D}_a \end{array}\right] \begin{pmatrix} \varepsilon_x(kT) \\ \hline \varepsilon_z(kT) \\ \hline \varepsilon_{z_a}(kT) \end{pmatrix} \qquad (3.77)$$

As discussed in Subsection 2.13.2, it is desirable to design $\widetilde{K}_0$ so that the observer error $\begin{pmatrix} \varepsilon_x(kT) \\ \hline \varepsilon_z(kT) \\ \hline \varepsilon_{z_a}(kT) \end{pmatrix}$ approaches zero promptly. This can be achieved if, and only if, the states $x(kT)$, $z(kT)$, and $z_a(kT)$ are completely observable, that is, if, and only if

$$\text{rank}\left[C_0^T \mid \widetilde{A}_0^T C_0^T \mid \widetilde{A}^{T^2} C_0^T \mid \cdots \mid \widetilde{A}^{T^{n+\rho+n^2-1}} C_0^T \right] = n + \rho + n^2$$

where

$$\tilde{A}_0 = \left[\begin{array}{c|c|c} \tilde{A}_N & \tilde{FH} & -\tilde{H}_a \\ \hline 0 & \tilde{D} & 0 \\ \hline 0 & 0 & \tilde{D}_a \end{array}\right],$$

and

$$C_0 = \left(C \mid 0 \mid 0\right).$$

In that case, standard pole placement techniques are used to determine an appropriate $\tilde{K}_0$. In that way, $\tilde{K}_0$ is designed such that the eigenvalues λ_i of the block-matrix (see (3.77))

$$\left[\begin{array}{c|c|c} \tilde{A}_N + \tilde{K}_{01}C & \tilde{FH} & -\tilde{H}_a \\ \hline \tilde{K}_{02}C & \tilde{D} & 0 \\ \hline \tilde{K}_{03}C & 0 & \tilde{D}_a \end{array}\right], \tag{3.78}$$

are at sufficiently-damped locations inside the unit circle ($|\lambda_i| < 1$) of the complex plane. Designing $\tilde{K}_0$ to achieve this latter condition will assure that the estimated values $\hat{x}(kT)$, $\hat{z}(kT)$, and $\hat{z}_a(kT)$ of the plant, external disturbance, and parameter-perturbation states, respectively, quickly converge to and accurately track the corresponding actual plant state $x(kT)$, disturbance state $z(kT)$, and parameter-perturbation state $z_a(kT)$.

A detailed block diagram of the hybrid full-order observers in (3.75) and (3.76) is shown in Figure 3.1. This hybrid full-order observer replaces (2.107) as presented in Subsection 2.13.2, when the add-on enhancements in Chapter 3 are incorporated into the new digital servo-controller. The dashed lines in Figure 3.1 are the components of the hybrid full-order observer in (3.76) that differ from the discrete-time full-order state-observer shown in Figure 2.8.

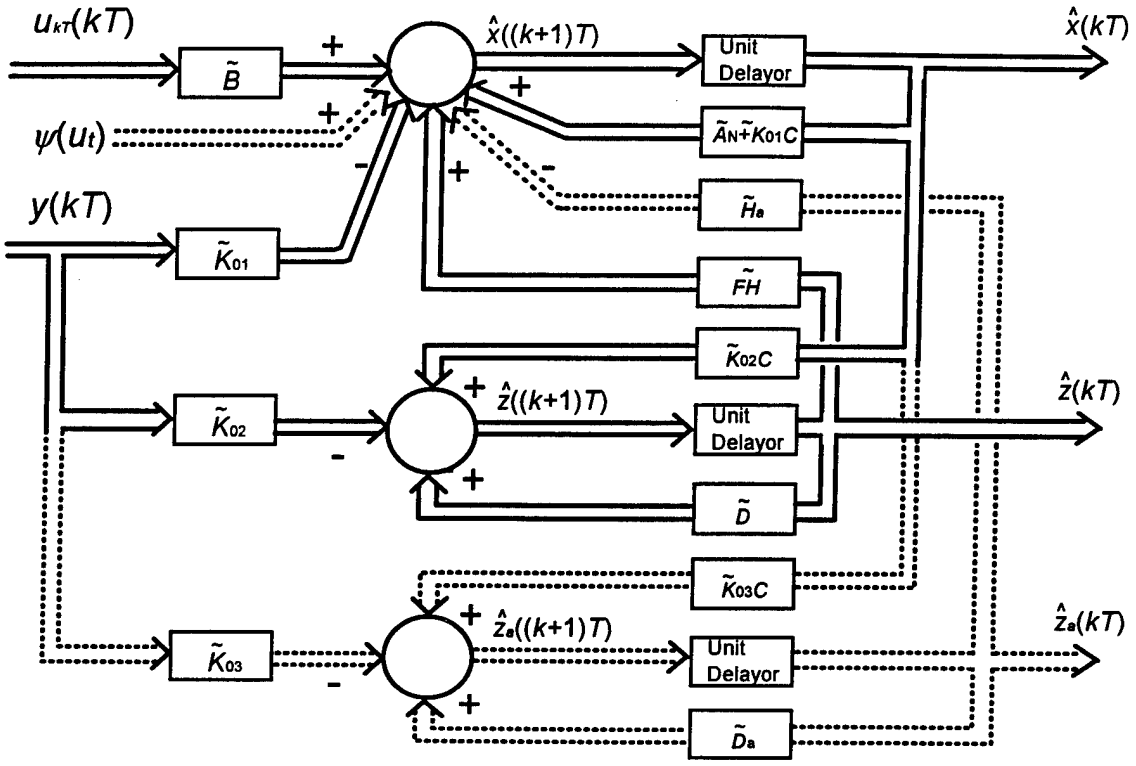

Figure 3.1 A Hybrid Full-Order Observer for Generating Real-Time Estimates of the Plant State $x(kT)$, Disturbance State $z(kT)$, and Parameter-Perturbation State $z_a(kT)$.

Incorporation of the discrete-time reduced-order state-observer (from Subsection 2.13.3) and the hybrid full-order state-observer in (3.75) for $\Delta A = 0$ or in (3.76) for $\Delta A \neq 0$ will result in a physically-realizable implementation of the digital servo-control law in (3.56) having the form

$$u(t;kT) = \Gamma_c e^{D(t-kT)}\hat{z}(kT) + \Gamma_s e^{E(t-kT)}\hat{c}(kT) - \tilde{K}_p\left(\theta\hat{c}(kT) - \hat{x}(kT)\right) + \Gamma_a e^{D_a(t-kT)}\hat{z}_a(kT) \qquad (3.79)$$

3.4. Improved Tracking Performance through Multirate Sampling

Up to this point in the design of the digital servo-tracking controller, the periodic samplers of the system output data $y(t)$ and command input data $y_c(t)$ have been assumed to operate in a fully synchronized manner with the same sampling-period T (sampling-rate $1/T$). In conventional digital-control this is called a *single-rate* system. Although single-rate systems comprise the vast majority of implemented digital control systems, there also exist practical, digitally-controlled systems which utilize two or more synchronized samplers operating at different sampling-rates. Such systems are referred to as *multirate* digital control systems.

Practical applications where a multirate digital-control system is used can be found in aircraft flight-control systems where the flight-control data-link computer typically operates at a rate different from the rate of the radar antenna [80]. Multirate sampling is sometimes introduced deliberately into the controller in order to improve system performance. A digital controller operating at a higher rate than the basic sampling-rate for the system measurements is an example of this sort of situation [79]. It was shown in [58] that properly designed, multirate digital controllers can achieve higher performance than those using single-rate sampling.

In principle, the new digital servo-tracking controller as developed in Chapters 2 and 3 can utilize different sampling-rates to achieve a level of servo-tracking performance that cannot be matched using a single-rate servo-controller. There are many different ways of implementing the digital servo-tracking controller in (3.79) as a multirate servo-controller. For example, each of the control terms in (3.79) could be implemented at a different sample-rate determined by individual design specifications, or by analysis of the problem requirements.

A particular multirate implementation technique that has been used in many practical applications is the technique involving two distinct and synchronized sample-periods, T_c and T_y, associated with the two distinct vector-inputs, y_c and y, to the digital servo-tracking controller $u(t;kT)$. The first sample-period T_c is associated with the real-time measurements, or processing, of the servo-command vector $y_c(t)$. Updates of the servo-command data are assumed to be available every $t = kT_c$, $k = 0, 1, 2, \ldots$. The second sample-period T_y is associated with the measurements, or processing, of the plant-output vector $y(t)$. The sample periods T_c and T_y are synchronized and assumed to have the integer-multiple relationship

$$T_c = \eta T_y \tag{3.80}$$

where η is a positive integer. This particular multirate system is illustrated in Figure 3.2.

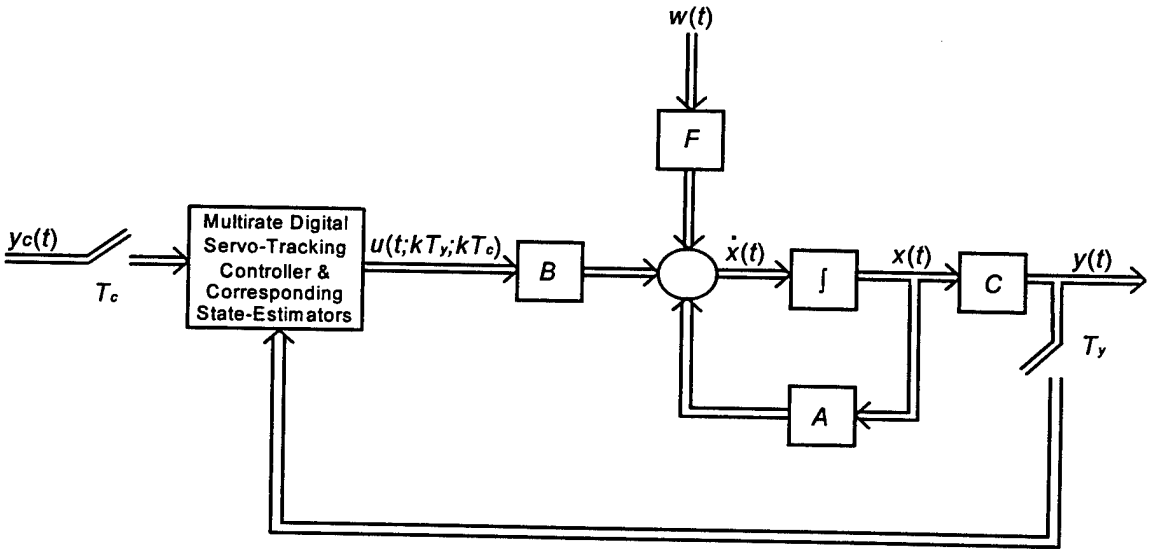

Figure 3.2 Configuration of a Two-Rate Type of Multirate Digital Servo-Tracking Controller.

In the implementation of (3.79) as a two-rate type of multirate digital servo-controller, the control terms associated with the plant run at the sample-rate $1/T_y$ and the control terms primarily associated with the servo-command $y_c(t)$ operate at the different sample-rate $1/T_c = 1/(\eta T_y)$ For example, the control terms u_c and u_a in (3.56) would typically run at a higher sample-rate $1/T_y$ in order to better respond to changes in the external disturbance $w(t)$ and parameter perturbations ΔA. On the other hand, the control terms u_s and u_p in (3.56) would typically not require processing at that same rate and could be implemented to run at the slower rate $1/T_c$. In that case, the physically-realizable digital servo-tracking controller from (3.79) would have the form

$$u(t;kT;kT_y) = u_c(t;kT_y) + u_s(t;kT_c) + u_p(kT_c) + u_a(t;kT_y)$$

$$= \Gamma_c e^{D(t-kT_y)}\hat{z}(kT_y) + \Gamma_s e^{E(t-kT)}\hat{c}(kT_c) - \tilde{K}_p\left(\theta\hat{c}(kT_c) - \hat{x}(kT_c)\right) \qquad (3.81)$$
$$+ \Gamma_a e^{D_a(t-kT_y)}\hat{z}_a(kT_y)$$

For this example, the hybrid full-order state-observer in (3.76) would be implemented using sample-period T_y while the discrete-time reduced-order state-observer in (2.113) would be implemented using sample-period T_c. Those state-observer designs will yield the state estimates $\hat{x}(kT_y)$, $\hat{z}(kT_y)$, $\hat{z}_a(kT_y)$, and $\hat{c}(kT_c)$. If any of the digital-control terms involve intersample, time-varying components, the $\psi(u_t)$ term in the hybrid full-order state-observer design must be computed as (refer to (3.70))

$$\psi(u_t) = \int_{kT_y}^{(k+1)T_y} e^{A_N((k+1)T_y-\tau)} B u_t(\tau) d\tau . \qquad (3.82)$$

Notice that the control term $u_p(kT_c) = -\tilde{K}_p\left(\theta\hat{c}(kT_c) - \hat{x}(kT_c)\right)$ in (3.81) requires estimates $\hat{x}(kT_c)$ of the plant state $x(t)$ at each of the times $t = kT_c$, $k = 0, 1, 2, \ldots$. However, those state estimates are generated for the sample-period T_y by virtue of the hybrid full-order state-observer running at sample-rate $1/T_y$. Also, recall that it is assumed in this Section that the samplers are synchronized and the sample-periods have the integer-multiple relationship given in (3.80). Then the necessary estimate $\hat{x}(kT_c)$ may be obtained by passing $\hat{x}(kT_y)$ through a zero-order-hold device having a hold time of T_c.

The digital servo-tracking control law in (3.56) can be modified to take full benefit of the use of multiple sample-rates. For example, the particular multirate servo-controller in (3.81) can be altered such that an inherently unstable, or highly-oscillatory, plant (A_N matrix having poles in the right-half complex plane or on, or near, the imaginary axis) would be controlled and stabilized at the higher sample-rate $1/T_y$. In that way an additional control term, postulated in continuous-time as $u_{a_m}(t) = K_m x(t)$, should be designed such that the continuous-time homogeneous equation

$$\dot{x}(t) = (A_N + BK_m)x(t), \qquad (3.83)$$

has certain specified eigenvalues. For that purpose, K_m should be selected such that

$$\det\left[\lambda \mathrm{I} - (A_N + BK_m)\right] = P_m(\lambda), \qquad (3.84)$$

where $P_m(\lambda)$ is given in (3.36) and the matrix A_m in (3.35) is replaced by the composite matrix A_N+BK_m,

$$A_m = A_N + BK_m . \tag{3.85}$$

The discrete-time counterpart to the design of K_m in (3.83) is to choose $\tilde{K}_m$ to obtain

$$\det\left[\lambda \mathrm{I} - (\tilde{A}_N + \tilde{B}\tilde{K}_m)\right] = \det\left[\lambda \mathrm{I} - \tilde{A}_m\right], \tag{3.86}$$

where,

$$\tilde{A}_N = e^{A_N T_y},$$

$$\tilde{B} = \int_0^{T_y} e^{A_N (T_y - \tau)} B d\tau,$$

$$\tilde{A}_m = e^{A_m T_y} \text{ ; for } A_m \text{ defined in (3.85),}$$

and select

$$u_{a_m}(kT_y) = \tilde{K}_m x(kT_y) . \tag{3.87}$$

Assuming the ideal choice for $u_{a_m}(kT_y)$ in (3.87) is implemented, the control terms $u_s(t;kT_c)$ in (3.26) and $u_p(kT_c)$ in (3.55) would be designed using the new A matrix. That is, the term A_N (or A) would be replaced by $A_N + B\tilde{K}_m$ (or $A + B\tilde{K}_m$) and $\tilde{A}_N$ (or $\tilde{A}$) would be replaced by the matrix exponential $e^{(A_N + B\tilde{K}_m)T_y}$ (or $e^{(A + B\tilde{K}_m)T_y}$) throughout the design of $u_s(t;kT_c)$ in Subsection 3.1.3 and $u_p(kT_c)$ in Subsection 3.2.6 (for $\Delta A \neq 0$) or Section 2.11 (for $\Delta A = 0$). In that way, the improved ideal multirate servo-controller equation in (3.81) becomes

$$\begin{aligned} u(t;kT_y;kT_c) &= u_c(t;kT_y) + u_s(t;kT_c) + u_p(kT_c) + u_a(t;kT_y) + u_{a_m}(kT_y) \\ &= \Gamma_c e^{D(t-kT_y)} z(kT_y) + \Gamma_s e^{E(t-kT)} c(kT_c) \\ &\quad - \tilde{K}_p\left(\theta c(kT_c) - x(kT_c)\right) + \Gamma_a e^{D_a(t-kT_y)} z_a(kT_y) + \tilde{K}_m x(kT_y) \end{aligned} \tag{3.88}$$

Estimates $\hat{z}(kT_y)$, $\hat{x}(kT_y)$, $\hat{z}_a(kT_y)$, and $\hat{c}(kT_c)$ are obtained from a discrete-time reduced-order and hybrid full-order state-observer as described in Subsections 2.13.3 and 3.3.3, respectively. Incorporation of those state-observers will result in a physically-realizable, multirate servo-tracking control algorithm.

4. SOME ILLUSTRATIVE EXAMPLES AND SIMULATION RESULTS

4.1. Description of the Examples to be Considered

In this chapter the new digital servo-tracking controller design procedure, developed in Chapters 2 and 3, is applied to several specific examples to illustrate the effectiveness of the design process and the closed-loop performance. In particular, the following examples and subcases are considered:

Example 1) An unstable second-order plant with a stepwise-constant disturbance $w(t)$ and a stepwise-constant servo-command $y_c(t)$. A digital servo-tracking controller $u(kT)$ is designed by the subspace stabilization method presented in Chapter 2. Simulation results are presented to illustrate the servo-tracking performance.

Example 2) A third-order plant with a stepwise-constant disturbance $w(t)$ and a stepwise-constant servo-command $y_c(t)$. A digital servo-tracking controller $u(kT)$ is designed by the subspace stabilization method presented in Chapter 2. Simulations results are given to illustrate the servo-tracking performance and to show the motions of the servo-state vector $\bar{e}_{ss}(kT)$ within the $\aleph[\bar{C}]$;

Example 3) A stable first-order plant with a step+ramp disturbance $w(t)$ and a step servo-command $y_c(t)$. A digital servo-tracking controller is designed and simulation results are given for the following four subcases:

Subcase 1) a plant with known, constant parameters controlled by a digital servo-controller $u(kT)$ using conventional stepwise-constant (z.o.h.) control-action (from Chapter 2);

Subcase 2) a plant with known, constant parameters controlled by a digital servo-controller $u(t;kT)$ using one form of digital-continuous control-action (from Chapter 3);

Subcase 3) a plant with constant, uncertain parameters controlled by a digital servo-controller $u(t;kT)$ using digital-continuous control-action (from Chapter 3). This is compared with the results for the same plant and uncertain parameters using stepwise-constant (z.o.h.) control-action $u(kT)$; and

Subcase 4) a plant with constant, uncertain parameters controlled by a multirate servo-controller $u(t;kT_c;kT_y)$ using digital-continuous control-action (from Chapter 3);

Example 4) An unstable first-order plant with a step+ramp disturbance w(t) and a constant+exponential servo-command yc(t). A single-rate u(t;kT) (Subcase 4a) and multirate u(t;kTc;kTy) (Subcase 4b) servo-controller utilizing digital-continuous control-action (from Chapter 3) is designed and simulation results are given for the case of known, constant plant parameters and the case of constant, uncertain plant parameters; and

Example 5) An unstable second-order plant with a (step+ramp) x exponential disturbance w(t) and a stepwise-constant servo-command yc(t). A single-rate u(t;kT) (Subcase 5a) and multirate u(t;kTc;kTy) (Subcase 5b) servo-controller utilizing digital-continuous control-action (from Chapter 3) is designed and simulation results are given for fixed plant parameters and for constant, uncertain plant parameters.

4.2. Example 1: Digital Servo-Tracking Control Design Utilizing a Stepwise-Constant (z.o.h.) Control-Action $u(kT)$ for the Case of a Second-Order Plant and Stepwise-Constant Servo-Command $y_c(t)$ Subjected to a Stepwise-Constant Disturbance $w(t)$

The purpose of Example 1 is to illustrate the digital servo-tracking controller design techniques presented in Chapter 2. This example is worked for the case of a digital servo-controller using stepwise-constant (z.o.h.) control-action $u(kT)$. Simulation results are provided for the example plant.

4.2.1. Plant, Disturbance, and Servo-Command Models for Example 1

The plant for Example 1 is modeled by the following second-order differential equation:

$$\ddot{y}(t) = u(t) + w(t)\,. \tag{4.1}$$

The disturbance $w(t)$ is an uncertain, unmeasurable stepwise-constant disturbance represented by

$$w(t) = c_1, \tag{4.2}$$

where c_1 may "jump" in value from time-to-time. The interval between successive jumps in c_1 is assumed to be somewhat larger than the sampling-period T.

The state model for the plant in (4.1) is easily determined by choosing $x_1(t) = y(t)$, and $x_2 = \dot{y}(t)$ as follows:

$$\begin{aligned} \dot{x}(t) &= Ax(t) + Bu(t) + Fw(t) \\ y(t) &= Cx(t) \end{aligned}\,, \tag{4.3}$$

where

$$A = \begin{bmatrix} 0 & 1 \\ 0 & 0 \end{bmatrix},\ B = \begin{bmatrix} 0 \\ 1 \end{bmatrix},\qquad F = \begin{pmatrix} 0 \\ 1 \end{pmatrix},\qquad C = \begin{pmatrix} 1, & 0, \end{pmatrix}.$$

A similar state model is developed for the disturbance $w(t)$ in (4.2), using the techniques described in Section 2.5, by noting that, between jumps in c_1, the disturbance $w(t)$ is governed by the linear homogeneous differential equation

$$\dot{w}(t) = 0\,. \tag{4.4}$$

Using the methods described in Section 2.5, the state model for $w(t)$ is obtained as

$$\begin{aligned} w(t) &= Hz(t) \\ \dot{z}(t) &= Dz(t) + \sigma(t) \end{aligned}, \tag{4.5}$$

where

$$H = 1,$$

$$D = 0,$$

and

$\sigma(t)$ are uncertain, sparse sequences of impulses that "cause" the occasional "jumps" in the disturbance $w(t)$.

Using the technique described in Section 2.6, discrete-time models are obtained for the plant and the disturbance. Those models are (the sample-period T is held as a variable throughout the computations):

Plant:

$$\begin{aligned} x((k+1)T) &= \tilde{A}x(kT) + \tilde{B}u(kT) + \tilde{FH}z(kT) + \tilde{\gamma}(kT) \\ y(kT) &= Cx(kT) \end{aligned}, \tag{4.6}$$

where

$$\tilde{A} = e^{AT} = \begin{bmatrix} 1 & T \\ 0 & 1 \end{bmatrix},$$

$$\tilde{B} = \int_0^T e^{A(T-\tau)} B d\tau = \begin{bmatrix} \frac{T^2}{2} \\ T \end{bmatrix},$$

$$\tilde{FH} = \int_0^T e^{A(T-\tau)} FH e^{D\tau} d\tau = \begin{bmatrix} \frac{T^2}{2} \\ T \end{bmatrix},$$

$$C = \begin{pmatrix} 1, & 0 \end{pmatrix},$$

$$\tilde{\gamma}(kT) = \int_0^T e^{A(T-\tau)} FH \int_0^{\tau} e^{D(\tau-\xi)} \sigma(\xi) d\xi d\tau;$$

and

Disturbance:

$$\begin{aligned} w(kT) &= Hz(kT) \\ z((k+1)T) &= \tilde{D}z(kT) + \tilde{\sigma}(kT) \end{aligned} \quad , \tag{4.7}$$

where

$$H = 1,$$

$$\tilde{D} = e^{DT} = e^{0T} = 1,$$

$$\tilde{\sigma}(kT) = \int_0^T e^{D(T-\xi)}\sigma(\xi + kT)d\xi .$$

The servo-command $y_c(t)$ is assumed to be an unknown stepwise-constant command represented by

$$y_c(t) = \bar{c}_1 \quad , \tag{4.8}$$

where $\bar{c}_1$ may occasionally jump in value at unknown times.

The linear homogeneous differential equation governing the motions of $y_c(t)$ in (4.8) between jumps in $\bar{c}_1$ is

$$\dot{y}_c(t) = 0 . \tag{4.9}$$

A state model for the servo-command $y_c(t)$ is obtained using (4.9) and the method outlined in Section 2.5. That state model is obtained as

$$\begin{aligned} y_c(t) &= Gc(t) \\ \dot{c}(t) &= Ec(t) + \mu(t) \end{aligned} \quad , \tag{4.10}$$

where

$$G = 1 ,$$

$$E = 0 ,$$

and

$\mu(t)$ are unknown, sparse sequences of impulses that "cause" the sparse uncertain "jumps" in the servo-command $y_c(t)$.

Using the technique described in Section 2.6, a discrete-time model is obtained for the servo-command. In that way, this model is written as

$$\begin{aligned} y_c(kT) &= Gc(kT) \\ c((k+1)T) &= \tilde{E}c(kT) + \tilde{\mu}(kT) \end{aligned} \quad , \tag{4.11}$$

where

$$G = 1,$$

$$\tilde{E} = e^{ET} = e^{0T} = 1,$$

and

$$\tilde{\mu}(kT) = \int_0^T e^{E(T-\xi)}\mu(\xi + kT)d\xi.$$

For reasons discussed in Chapter 2, the unknown, unpredictable terms $\tilde{\gamma}(kT)$, $\tilde{\sigma}(kT)$, and $\tilde{\mu}(kT)$ in (4.6), (4.7), and (4.11) are disregarded throughout the design process.

4.2.2. The Necessary and Sufficient Condition for Achieving Exact Servo-Tracking for Example 1

The objective is to design a digital servo-tracking controller for the plant in (4.1) such that the tracking-error, defined by

$$\varepsilon_y(t) = y_c(t) - y(t), \tag{4.12}$$

goes to zero in the face of arbitrary plant initial conditions and unmeasurable plant disturbances. As first shown in [37], the necessary and sufficient condition for achieving theoretically exact servo-tracking is that the vector servo-command input $y_c(t)$ must consistently lie in the column range-space of the plant-output matrix C in (4.3) for all t. In the present example, satisfaction of this condition requires that (from (2.33))

$$\Re[G] \subseteq \Re[C] \quad . \tag{4.13}$$

If (4.13) is satisfied, then it is possible to express G as some linear combination of the columns of C. That is, $G = C\theta$ for some possibly nonunique θ. Substituting C and G from (4.3) and (4.10) into $G = C\theta$ yields

$$1 = \begin{pmatrix} 1, & 0 \end{pmatrix}\theta. \tag{4.14}$$

Expression (4.14) is satisfied for the following θ:

$$\theta = \begin{pmatrix} 1 \\ 0 \end{pmatrix}. \tag{4.15}$$

The discrete-time models for the plant (4.6), disturbance (4.7), servo-command (4.11), and the θ determined in (4.15) will now be used to design a digital servo-tracking controller using the design techniques presented in Chapter 2 of this report.

4.2.3. The Necessary and Sufficient Conditions for Stabilizing $\bar{e}_{ss}(kT)$ to S_v for Example 1

The control task is to design a discrete-time control algorithm for $u(kT)$ such that the servo-state vector $e_{ss}(kT)$ defined in (2.38) becomes stable to and invariant for a subspace $S_v = \aleph[\bar{C}] \subseteq \aleph[C]$, for some $\bar{C}$ in (2.46), having largest dimension v, $v = 0, 1, \ldots, n-m$. To perform this task, begin by choosing $v = n - m = 2 - 1 = 1$ (the dimension of $\aleph[C]$ is 1). The n x (n-m) maximal rank matrix M is chosen such that (same as (2.92))

$$CM = \begin{pmatrix} 1, & 0 \end{pmatrix} M = 0,$$

where M is selected as

$$M = \begin{pmatrix} 0 \\ 1 \end{pmatrix}. \tag{4.16}$$

Next, form the set $\mathbf{R}_{n-m}$ according to the procedure given in Subsection 2.11.7. For Example 1, that set is

$$\mathbf{R}_{n-m} = \mathbf{R}_1 = \{1\} = \{R_{11}\}. \tag{4.17}$$

Since the $\mathbf{R}_{n-m}$ contains only one element, we choose $R = R_{11}$, form the matrix product

$$MR = \begin{pmatrix} 0 \\ 1 \end{pmatrix},$$

and choose $\bar{C}$ according to (2.46) and (2.66), in which case,

$$\bar{C} = C = \begin{pmatrix} 1, & 0 \end{pmatrix}. \tag{4.18}$$

Now the necessary and sufficient conditions for $\bar{e}_{ss}(kT)$ to be asymptotically stabilized to $S_1 = \aleph[\bar{C}] = \aleph[C]$ for the $\tilde{A}$, $\tilde{B}$, $\tilde{FH}$, $\tilde{E}$, θ, M, R, and $\bar{C}$ in (4.6), (4.11), (4.15), (4.16), (4.17), and (4.18) are as follows (refer to the conditions on page 62)

condition a′: $\Re[\bar{C}AMR] \subseteq \Re[\bar{C}\tilde{B}]$; (from (2.80)),

or equivalently,

$\text{rank}[\bar{C}\tilde{B} \mid \bar{C}\tilde{A}MR] = \text{rank}[\bar{C}\tilde{B}]$; (from (2.81)),

where

$$\text{rank}\left[\overline{C}\widetilde{B} \mid \overline{C}\widetilde{A}MR\right] = \text{rank}\left[\frac{T^2}{2} \mid T\right] = 1,$$

and

$$\text{rank}\left[\overline{C}\widetilde{B}\right] = \text{rank}\left[\frac{T^2}{2}\right] = 1.$$

Clearly, condition a′ is met;

condition b′: there exists a $\widetilde{\Gamma}_s$ such that (2.60) is satisfied. The necessary and sufficient condition for the existence of a $\widetilde{\Gamma}_s$ satisfying (2.60) is (same as (2.52))

$$\text{rank}\left[\overline{C}\theta\widetilde{E} - \overline{C}\widetilde{A}\theta \mid \overline{C}\widetilde{B}\right] = \text{rank}\left[\overline{C}\widetilde{B}\right],$$

where

$$\text{rank}\left[\overline{C}\theta\widetilde{E} - \overline{C}\widetilde{A}\theta \mid \overline{C}\widetilde{B}\right] = \text{rank}\left[0 \mid \frac{T^2}{2}\right] = 1,$$

and $\text{rank}\left[\overline{C}\widetilde{B}\right] = 1$ was determined in condition a′ above. Clearly, condition b′ is met and $\widetilde{\Gamma}_s$ is chosen to satisfy (same as (2.60))

$$\overline{C}\left[\theta\widetilde{E} - \widetilde{A}\theta - \widetilde{B}\widetilde{\Gamma}_s\right] = -\frac{T^2}{2}\widetilde{\Gamma}_s = 0. \tag{4.19}$$

A $\widetilde{\Gamma}_s$ that satisfies (4.19) for Example 1 is

$$\widetilde{\Gamma}_s = 0. \tag{4.20}$$

The digital control term $u_s(kT)$ in (2.62) can thus be chosen ideally as

$$\begin{aligned} u_s(kT) &= \widetilde{\Gamma}_s c(kT) \\ &= 0\, c(kT) \end{aligned}; \tag{4.21}$$

condition c′: there exists a $\widetilde{\Gamma}_c$ such that (2.59) is satisfied. The necessary and sufficient condition for existence of a $\widetilde{\Gamma}_c$ satisfying (2.59) is (same as (2.53))

$$\text{rank}\left[\overline{C}\,\widetilde{FH} \mid \overline{C}\widetilde{B}\right] = \text{rank}\left[\overline{C}\widetilde{B}\right],$$

where

$$\text{rank}\left[\bar{C}\,\tilde{FH} \mid \bar{C}\tilde{B}\right] = \text{rank}\left[\frac{T^2}{2} \mid \frac{T^2}{2}\right] = 1,$$

and $\text{rank}\left[\bar{C}\tilde{B}\right] = 1$ was determined in condition a'. Clearly condition c' is met and $\tilde{\Gamma}_c$ is chosen to satisfy (same as (2.59))

$$\bar{C}\left[\tilde{B}\tilde{\Gamma}_c + \tilde{FH}\right] = \frac{T^2}{2}\tilde{\Gamma}_c + \frac{T^2}{2} = 0. \tag{4.22}$$

A $\tilde{\Gamma}_c$ that satisfies (4.22) for Example 1 is

$$\tilde{\Gamma}_c = -1. \tag{4.23}$$

The digital control term $u_c(kT)$ in (2.61) can thus be chosen ideally as

$$\begin{aligned} u_c(kT) &= \tilde{\Gamma}_c z(kT) \\ &= -1\, z(kT) \end{aligned}; \tag{4.24}$$

condition d': there exists an r x (n - ν) constant $\tilde{L}$ such that solutions $\xi_{ss1}(kT)$ to (2.85) are uniformly and asymptotically stable to the null-point $\xi_{ss1}(kT) = 0$. The characteristic polynomial of the system in (2.85) is

$$\det\left(\lambda \mathrm{I} - (\tilde{A}_1 + \tilde{B}_1\tilde{L})\right) = \lambda - \frac{T^2}{2}\tilde{L} - 1, \tag{4.25}$$

where $\tilde{A}_1$ and $\tilde{B}_1$ are defined in (2.84). One choice for $\tilde{L}$ that will achieve $|\lambda| < 1$ in (4.25) is

$$\tilde{L} = \frac{-2}{T^2}. \tag{4.26}$$

4.2.4. The Necessary and Sufficient Conditions for Maintaining Bounded Motions of $\bar{e}_{ss}(kT)$ within S_1

Conditions a', b', c', and d' in the previous Subsection have been met. It remains to test the condition necessary to satisfactorily maintain bounded motions of $\bar{e}_{ss}(kT)$ within the subspace $S_1 = \aleph\left[\bar{C} = C\right]$. As discussed in Subsection 2.11.6, there must exist an r x (n - m) gain term $\tilde{Z}$ such that all solutions $\xi_{ss2}(kT)$ to (2.88) remain bounded. The characteristic polynomial of the system in (2.88) is

$$\det\left(\lambda \mathrm{I} - (\tilde{A}_2 + \tilde{B}_2\tilde{Z})\right) = \lambda + 1, \tag{4.27}$$

where $\tilde{A}_2 = -1$ and $\tilde{B}_2 = 0$ (refer to (2.84)). Clearly, (4.27) is independent of $\tilde{Z}$ and the choice of $\tilde{Z}$ is arbitrary, assuming the eigenvalue λ of $\tilde{A}_2$ is such that $|\lambda| < 1$. From (4.27) we have $\lambda = -1$, therefore this condition is not satisfied.

4.2.5. The Necessary and Sufficient Conditions and the Digital Servo-Controller Design for Stabilizing $\bar{e}_{ss}(kT)$ to the Nullpoint

In the previous Subsection, the necessary and sufficient condition for maintaining bounded motions of $\bar{e}_{ss}(kT)$ within a subspace S_1 failed to be satisfied. We then proceed to test subspace S_V where $V = n - m - 1 = 2 - 1 - 1 = 0$. The subspace S_0 is the "improper" subspace known as the nullpoint. For the special case of nullpoint stabilization, $\bar{C} = \mathrm{I}$ (where I is the $n \times n$ $(n = 2)$ identity matrix) and the design of $u(kT)$ in (2.55) proceeds as follows.

The necessary and sufficient conditions for existence of the control terms $u_c(kT)$ satisfying (2.56) and $u_s(kT)$ satisfying (2.57) is given in (2.53) and (2.52), respectively. Satisfaction of those conditions is shown as follows (where $\bar{C} = \mathrm{I}$):

for $u_c(kT)$:
$$\mathrm{rank}\left[\bar{C}\tilde{F}\tilde{H} \mid \bar{C}\tilde{B}\right] = \mathrm{rank}\left[\bar{C}\tilde{B}\right]; \qquad \text{(same as (2.53))}, \tag{4.28}$$

where

$$\mathrm{rank}\left[\bar{C}\tilde{F}\tilde{H} \mid \bar{C}\tilde{B}\right] = \mathrm{rank}\begin{bmatrix} \frac{T^2}{2} & \frac{T^2}{2} \\ T & T \end{bmatrix} = 1,$$

and

$$\mathrm{rank}\left[\bar{C}\tilde{B}\right] = \mathrm{rank}\begin{bmatrix} \frac{T^2}{2} \\ T \end{bmatrix} = 1;$$

for $u_s(kT)$:
$$\mathrm{rank}\left[\bar{C}\theta\tilde{E} - \bar{C}\tilde{A}\theta \mid \bar{C}\tilde{B}\right] = \mathrm{rank}\left[\bar{C}\tilde{B}\right]; \qquad \text{(same as (2.52))}, \tag{4.29}$$

where

$$\mathrm{rank}\left[\bar{C}\theta\tilde{E} - \bar{C}\tilde{A}\theta \mid \bar{C}\tilde{B}\right] = \mathrm{rank}\begin{bmatrix} 0 & \frac{T^2}{2} \\ 0 & T \end{bmatrix} = 1,$$

and $\text{rank}\left[\overline{C}\tilde{B}\right]$ is given below (4.28).

The rank conditions in (4.28) and (4.29) are met and $\tilde{\Gamma}_c$ and $\tilde{\Gamma}_s$ are designed to satisfy (2.59) and (2.60), respectively. That is,

for $\tilde{\Gamma}_c$: $$\overline{C}\left(\tilde{B}\tilde{\Gamma}_c + \tilde{F}\tilde{H}\right) = \begin{bmatrix} \frac{T^2}{2} \\ T \end{bmatrix}\tilde{\Gamma}_c + \begin{bmatrix} \frac{T^2}{2} \\ T \end{bmatrix} = 0; \tag{4.30}$$

for $\tilde{\Gamma}_s$: $$\overline{C}\left(\theta\tilde{E} - \tilde{A}\theta - \tilde{B}\tilde{\Gamma}_s\right) = -\begin{bmatrix} \frac{T^2}{2} \\ T \end{bmatrix}\tilde{\Gamma}_s = 0. \tag{4.31}$$

The $\tilde{\Gamma}_c$ and $\tilde{\Gamma}_s$ that satisfy (4.30) and (4.31) are

$$\tilde{\Gamma}_c = -1, \tag{4.32}$$

and

$$\tilde{\Gamma}_s = 0. \tag{4.33}$$

The ideal digital-control terms $u_c(kT)$ and $u_s(kT)$ in (2.61) and (2.62) can thus be written as

$$\begin{aligned} u_c(kT) &= \tilde{\Gamma}_c z(kT) \\ &= -1 z(kT) \end{aligned}, \tag{4.34}$$

and

$$\begin{aligned} u_s(kT) &= \tilde{\Gamma}_s c(kT) \\ &= 0 c(kT) \end{aligned}. \tag{4.35}$$

The $u_p(kT)$ control term is postulated as in (2.63), where the gain-matrix $\tilde{K}_p$ is designed to place the eigenvalues of $(\tilde{A} + \tilde{B}\tilde{K}_p)$ in (2.64) at sufficiently damped locations inside the unit circle $|\lambda_i| < 1$. For the present example, the gain-matrix $\tilde{K}_p$ is designed such that all eigenvalues of $(\tilde{A} + \tilde{B}\tilde{K}_p)$ in (2.64) are at zero. The design of $\tilde{K}_p$ is shown as follows:

$$\begin{aligned} \det\left(\lambda \mathrm{I} - (\tilde{A} + \tilde{B}\tilde{K}_p)\right) &= \lambda^2 - \left(2 + \frac{T^2}{2}\tilde{K}_{p1} + T\tilde{K}_{p2}\right)\lambda + \left(1 - \frac{T^2}{2}\tilde{K}_{p1} + T\tilde{K}_{p2}\right). \\ &= 0 \end{aligned} \tag{4.36}$$

The appropriate choice of $\widetilde{K}_p$ for achieving $\lambda_i = 0$ (deadbeat response) in (4.36) is to choose $\widetilde{K}_p$ as

$$\widetilde{K}_p = \left(\frac{-1}{T^2},\ \frac{-3}{2T}\right), \tag{4.37}$$

such that the ideal choice for $u_p(kT)$ in (2.63) becomes

$$\begin{aligned} u_p(kT) &= -\widetilde{K}_p e_{ss}(kT) \\ &= \left(\frac{1}{T^2},\ \frac{3}{2T}\right) e_{ss}(kT) \\ &= \left(\frac{1}{T^2},\ \frac{3}{2T}\right)\left(\theta_c(kT) - x(kT)\right) \\ &= \frac{1}{T^2}\left(y_c(kT) - y(kT)\right) - \frac{3}{2T}x_2(kT) \end{aligned} \tag{4.38}$$

4.2.6. Practical Realization of the Digital Servo-Tracking Controller for Example 1

The ideal digital servo-tracking control law designed using the methods described in Sections 2.9 through 2.11 for Example 1 described by the plant, disturbance, and servo-command in (4.1), (4.2), and (4.8), is as follows

$$u(kT) = u_c(kT) + u_s(kT) + u_p(kT), \tag{4.39}$$

where $u_c(kT)$, $u_s(kT)$, and $u_p(kT)$ are given in (4.34), (4.35), and (4.38), respectively.

The digital servo-tracking controller in (4.39) is designed for the ideal case where exact measurements of $x(kT)$, $z(kT)$, and $c(kT)$ are assumed available. For this example, $y_c(t)$ is a stepwise-constant which is directly measurable at each of the times $t = kT$, $k = 0, 1, 2, \ldots$. Thus, estimates of $c(kT)$ are not needed ($y_c(kT) = c(kT)$). On the other hand, the state vectors $z(kT)$ and $x(kT)$ (with the exception $x_1(kT) = y(kT)$) are not available for measurement and must be estimated. Estimates $\hat{z}(kT)$ and $\hat{x}(kT)$ of $z(kT)$ and $x(kT)$, respectively, can be generated by a discrete-time full-order state-observer as described in Subsection 2.13.2. The general form for the discrete-time full-order state-observer is (same as (2.107))

$$\begin{pmatrix} \hat{x}((k+1)T) \\ \hat{z}((k+1)T) \end{pmatrix} = \left[\begin{array}{c|c} \widetilde{A} & \widetilde{FH} \\ \hline 0 & \widetilde{D} \end{array}\right] \begin{pmatrix} \hat{x}(kT) \\ \hat{z}(kT) \end{pmatrix} + \begin{pmatrix} \widetilde{B} \\ 0 \end{pmatrix} u(kT) + \begin{bmatrix} \widetilde{K}_{01} \\ \widetilde{K}_{02} \end{bmatrix} \left[(C \mid 0) \begin{pmatrix} \hat{x}(kT) \\ \hat{z}(kT) \end{pmatrix} - y(kT) \right], \tag{4.40}$$

where $\widetilde{K}_0 = \begin{bmatrix} \widetilde{K}_{01} \\ \widetilde{K}_{02} \end{bmatrix}$ is an observer gain-matrix to be designed, and $\widetilde{A}$, $\widetilde{FH}$, $\widetilde{B}$, C, and $\widetilde{D}$ are defined in (4.6) and (4.7).

The general discrete-time evolution equation for the error dynamics of the discrete-time full-order state-observer is (same as (2.109))

$$\begin{pmatrix} \varepsilon_x((k+1)T) \\ \varepsilon_z((k+1)T) \end{pmatrix} = \begin{pmatrix} \hat{x}((k+1)T) \\ \hat{z}((k+1)T) \end{pmatrix} - \begin{pmatrix} x((k+1)T) \\ z((k+1)T) \end{pmatrix}$$
$$= \left[\begin{array}{c|c} \tilde{A}+\tilde{K}_{01}C & \tilde{FH} \\ \hline \tilde{K}_{02}C & \tilde{D} \end{array}\right] \begin{pmatrix} \varepsilon_x(kT) \\ \varepsilon_z(kT) \end{pmatrix} . \tag{4.41}$$

It is desirable to design $\tilde{K}_0$ so that the observer error $\begin{pmatrix} \varepsilon_x(kT) \\ \varepsilon_z(kT) \end{pmatrix}$ always converges to zero promptly, from any initial condition. Pole placement techniques can be used to determine an appropriate $\tilde{K}_0$. The characteristic polynomial of the observer error in (4.41) is

$$\det\left[\lambda I - \left[\begin{array}{c|c} \tilde{A}+\tilde{K}_{01}C & \tilde{FH} \\ \hline \tilde{K}_{02}C & \tilde{D} \end{array}\right]\right] = \det\begin{bmatrix} 1 & T & \frac{T^2}{2} \\ 0 & 1 & T \\ 0 & 0 & 1 \end{bmatrix}$$
$$= \lambda^3 - \left(\tilde{K}_{01}+3\right)\lambda^2 + \left(2\tilde{K}_{01} - T\tilde{K}_{02_1} - \frac{T^2}{2}\tilde{K}_{02_2} + 3\right)\lambda \tag{4.42}$$
$$-\left(\tilde{K}_{01} - T\tilde{K}_{02_1} + \frac{T^2}{2}\tilde{K}_{02_2} + 1\right)$$

For the present example, $\tilde{K}_0$ is designed such that the roots of the characteristic polynomial in (4.42) are at $\lambda_i = 0$ (deadbeat response). A $\tilde{K}_0$ that achieves deadbeat observer response is:

$$\tilde{K}_0 = \begin{bmatrix} \tilde{K}_{01} \\ \tilde{K}_{02} \end{bmatrix} = \begin{pmatrix} -3 \\ -\frac{5}{2T} \\ -\frac{1}{T^2} \end{pmatrix} . \tag{4.43}$$

The discrete-time full-order state-observer for $\hat{x}(kT)$ and $\hat{z}(kT)$ is then obtained by substituting values from (4.6) and (4.7) into (4.40). The result is

$$\begin{pmatrix} \hat{x}_1((k+1)T) \\ \hat{x}_2((k+1)T) \\ \hat{z}((k+1)T) \end{pmatrix} = \begin{bmatrix} 1 & T & \frac{T^2}{2} \\ 0 & 1 & T \\ 0 & 0 & 1 \end{bmatrix} \begin{pmatrix} \hat{x}(kT) \\ \hat{z}_1(kT) \\ \hat{z}_2(kT) \end{pmatrix} + \begin{pmatrix} \frac{T^2}{2} \\ T \\ 0 \end{pmatrix} u(kT) + \left(\tilde{K}_0\right)\left(\hat{x}(kT) - y(kT)\right) , \tag{4.44}$$

where $y(kT)$ and $u(kT)$ in (4.44) are the inputs and $\hat{x}(kT)$, $\hat{z}(kT)$, $\hat{x}((k+1)T)$, and $\hat{z}((k+1)T)$ are the outputs of the discrete-time full-order state-observer, and $\widetilde{K}_0$ is given in (4.43).

4.2.7. Simulation Results for Example 1

Incorporation of the discrete-time full-order state-observer equations in (4.44) into (4.39) results in the following physically-realizable digital servo-tracking control law for Example 1:

$$\begin{aligned} u(kT) &= u_c(kT) + u_s(kT) + u_p(kT) \\ &= -\hat{z}(kT) + \frac{1}{T^2}\big(y_c(kT) - y(kT)\big) - \frac{3}{2T}\hat{x}_2(kT) \end{aligned} \tag{4.45}$$

Simulations results were obtained for the unstable, second-order plant (4.1), stepwise-constant disturbance (4.2), and stepwise-constant servo-command (4.8), compensated by the digital servo-controller in (4.45) using a control sample-period of $T = 0.1$. The simulation results shown in Figure 4.1 illustrate the plant output $y(t)$, the disturbance $w(t)$, and the servo-command $y_c(t)$ for Example 1. The simulation plot in Figure 4.2 shows the servo-tracking error $\varepsilon_y(t) = y_c(t) - y(t)$ for Example 1. The large "jumps" in the servo-tracking error $\varepsilon_y(t)$ ($|\varepsilon_y(t)| > 1$) are caused by the unexpected jumps in the servo-command $y_c(t)$. The small fluctuations in $\varepsilon_y(t)$ are caused by the uncertain jumping of the disturbance $w(t)$. In both cases, the servo-controller in (4.45) compensates for the sudden changes in $y_c(t)$ and $w(t)$ and controls the tracking-error $\varepsilon_y(t) \to 0$ within a finite amount of time ("settling-time").

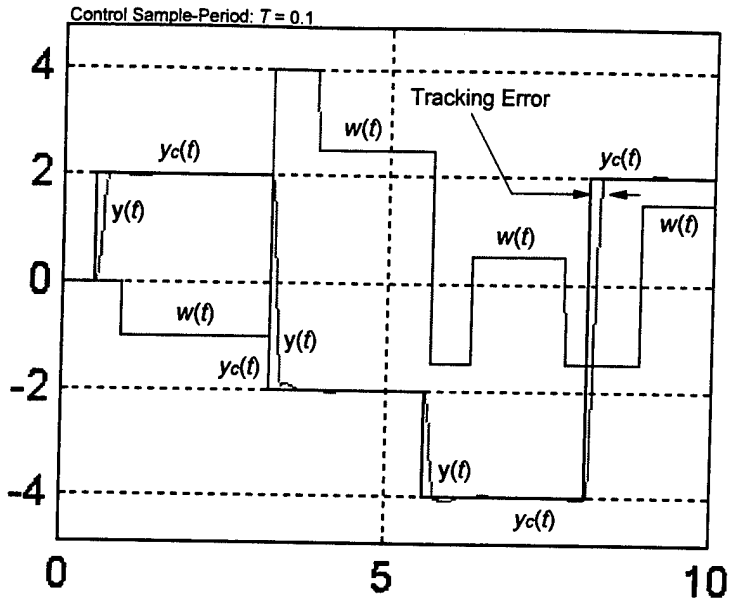

Figure 4.1 Illustration of the Plant Output $y(t)$, Disturbance $w(t)$, and Servo-Command $y_c(t)$ for Example 1.

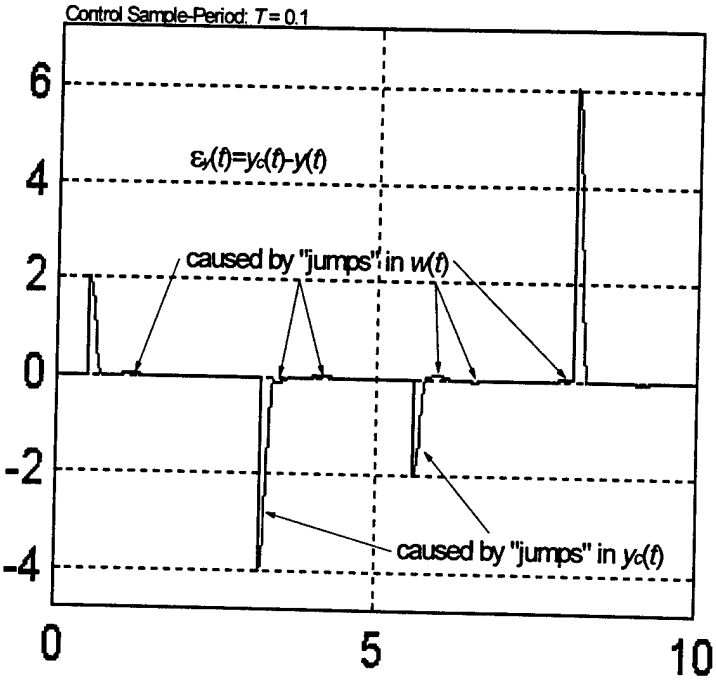

Figure 4.2 Illustration of the Servo-Tracking Error $\varepsilon_y(t) = y_c(t) - y(t)$ for Example 1.

4.3. Example 2: Digital Servo-Tracking Control Design Utilizing a Stepwise Constant Control-Action $u(kT)$ for the Case of a Third-Order Plant and Stepwise-Constant Servo-Command $y_c(t)$ Subjected to a Stepwise-Constant Disturbance $w(t)$

The purpose of Example 2 is to illustrate the subspace stabilization procedure presented in Chapter 2. This example is worked for the case of a digital servo-controller using stepwise-constant (z.o.h.) control-action $u(kT)$. Simulation results are provided for the example plant.

4.3.1. Plant, Disturbance, and Servo-Command Models for Example 2

The plant for Example 2 is modeled by the following third order differential equation[1]:

$$\dddot{y}(t) = \ddot{y}(t) - 0.5\dot{y}(t) - y(t) + \ddot{u}_1(t) - \dot{u}_1(t) + 0.5u_1(t) + u_2(t) + w(t). \tag{4.46}$$

The disturbance $w(t)$ is an uncertain, unmeasurable stepwise-constant disturbance represented by (4.2) and having continuous-time and discrete-time state models given in (4.5) and (4.7), respectively.

The state model for the plant is easily determined by choosing $x_1(t) = y(t)$, $x_2 = \dot{y}(t)$, and $x_3 = \ddot{y}(t)$ as follows:

$$\begin{aligned} \dot{x}(t) &= Ax(t) + Bu(t) + Fw(t) \\ y(t) &= Cx(t) \end{aligned}, \tag{4.47}$$

where

$$A = \begin{bmatrix} 0 & 1 & 0 \\ 0 & 0 & 1 \\ -1 & -0.5 & 1 \end{bmatrix}, B = \begin{bmatrix} 1 & 0 \\ 0 & 0 \\ 0 & 1 \end{bmatrix}, \quad F = \begin{pmatrix} 0 \\ 0 \\ 1 \end{pmatrix}, \quad C = \begin{pmatrix} 1, & 0, & 0 \end{pmatrix}.$$

Using the technique described in Section 2.6, a discrete-time model is obtained for the plant. Assuming a control sample-period of $T = 0.1$, this model is:

$$\begin{aligned} x((k+1)T) &= \tilde{A}x(kT) + \tilde{B}u(kT) + \tilde{F}\tilde{H}z(kT) + \tilde{\gamma}(kT) \\ y(kT) &= Cx(kT) \end{aligned}, \tag{4.48}$$

where

$$\tilde{A} = e^{AT} = \begin{bmatrix} 0.9998 & 0.0999 & 0.0052 \\ -0.0052 & 0.9972 & 0.1051 \\ -0.1051 & -0.0577 & 1.1023 \end{bmatrix},$$

$$\widetilde{B} = \int_0^T e^{A(T-\tau)} B d\tau = \begin{bmatrix} 0.1000 & 0.0002 \\ -0.0002 & 0.0052 \\ -0.0052 & 0.1051 \end{bmatrix},$$

$$\widetilde{FH} = \int_0^T e^{A(T-\tau)} FH e^{D\tau} d\tau = \begin{bmatrix} 0.0002 \\ 0.0052 \\ 0.1051 \end{bmatrix},$$

$$C = \begin{pmatrix} 1, & 0, & 0 \end{pmatrix},$$

and

$$\widetilde{\gamma}(kT) = \int_0^T e^{A(T-\tau)} FH \int_0^\tau e^{D(\tau-\xi)} \sigma(\xi) d\xi d\tau .$$

The servo-command $y_c(t)$ is assumed to be an unknown stepwise-constant command represented by (4.8) and having continuous-time and discrete-time state models given in (4.10) and (4.11), respectively.

4.3.2. The Necessary and Sufficient Condition for Achieving Exact Servo-Tracking for Example 2

The objective is to design a digital servo-tracking controller for the plant in (4.46) such that the tracking-error, defined by

$$\varepsilon_y(t) = y_c(t) - y(t), \tag{4.49}$$

goes to zero in the face of arbitrary plant initial conditions and unmeasurable plant disturbances. As first shown in [37], the necessary and sufficient condition for achieving theoretically exact servo-tracking is that the vector servo-command input $y_c(t)$ must consistently lie in the column range-space of the plant-output matrix C in (4.47) for all t. In the present example, satisfaction of this condition requires that (from (2.33))

$$\Re[G] \subseteq \Re[C] \quad . \tag{4.50}$$

If (4.50) is satisfied, then there exists a (possibly nonunique) matrix θ such that $G = C\theta$. Substituting C and G from (4.47) and (4.10) into $G = C\theta$ yields

$$1 = \begin{pmatrix} 1, & 0, & 0 \end{pmatrix} \theta . \tag{4.51}$$

Expression (4.51) is satisfied for some θ. In particular,

$$\theta = \begin{pmatrix} 1 \\ 0 \\ 0 \end{pmatrix}. \tag{4.52}$$

The discrete-time models for the plant (4.48), disturbance (4.7), servo-command (4.11), and the θ determined in (4.52) will now be used to design a digital servo-tracking controller using the design techniques presented in Chapter 2 of this report.

4.3.3. The Necessary and Sufficient Conditions for Stabilizing $\bar{e}_{ss}(kT)$ to S_{v} for Example 2

The control task is to design a discrete-time control algorithm for $u(kT)$ such that the servo-state vector $e_{ss}(kT)$ defined in (2.38) becomes stable to and invariant for a subspace $S_{\mathsf{v}} = \mathcal{N}[\overline{C}] \subseteq \mathcal{N}[C]$ (for some choice of $\overline{C}$ in (2.46)) having largest dimension v, $\mathsf{v} = 0, 1, \ldots, n-m$. To perform this task, begin by choosing $\mathsf{v} = n - m = 3 - 1 = 2$ (the dimension of $\mathcal{N}[C]$ is 2). The maximal rank matrix M is chosen such that (same as (2.92))

$$CM = \begin{pmatrix} 1, & 0, & 0 \end{pmatrix} M = 0,$$

where M is selected as

$$M = \begin{pmatrix} 0 & 0 \\ 1 & 0 \\ 0 & 1 \end{pmatrix}. \tag{4.53}$$

Next, form the set $\mathbf{R}_{n-m}$ according to the procedure given in Subsection 2.11.7. For Example 2, that set is

$$\mathbf{R}_{n-m} = \left\{ \begin{pmatrix} 1 & 0 \\ 0 & 1 \end{pmatrix} \right\} = \{R_{21}\}. \tag{4.54}$$

Since the $\mathbf{R}_{n-m}$ contains only one matrix, we choose $R = R_{21}$, form the matrix product

$$MR = \begin{pmatrix} 0 & 0 \\ 1 & 0 \\ 0 & 1 \end{pmatrix},$$

and choose $\overline{C}$ according to (2.46) and (2.66), in which case,

$$\overline{C} = C = \begin{pmatrix} 1, & 0, & 0 \end{pmatrix}. \tag{4.55}$$

Now the necessary and sufficient conditions for $\bar{e}_{ss}(kT)$ to be asymptotically stabilized to $S_2 = \aleph[\bar{C}] = \aleph[C]$ for the $\tilde{A}$, $\tilde{B}$, $\tilde{FH}$, $\tilde{E}$, θ, M, R, and $\bar{C}$ in (4.48), (4.11), (4.52), (4.53), (4.54), and (4.55) are as follows (refer to the conditions on page 62)

condition a′: $\Re[\bar{C}AMR] \subseteq \Re[\bar{C}\tilde{B}]$ (from (2.80)),

or equivalently,

$$\text{rank}\left[\bar{C}\tilde{B} \mid \bar{C}\tilde{A}MR\right] = \text{rank}\left[\bar{C}\tilde{B}\right]; \qquad \text{(from (2.81))},$$

where

$$\text{rank}\left[\bar{C}\tilde{B} \mid \bar{C}\tilde{A}MR\right] = \text{rank}\left[0.1,\ 0.0002 \mid 0.1,\ 0.0052\right] = 1,$$

and

$$\text{rank}\left[\bar{C}\tilde{B}\right] = \text{rank}\left[0.1,\ \ 0.0002\right] = 1.$$

Clearly, condition a′ is met;

condition b′: there exists a $\tilde{\Gamma}_s$ such that (2.60) is satisfied. The necessary and sufficient condition for the existence of a $\tilde{\Gamma}_s$ satisfying (2.60) is (same as (2.52))

$$\text{rank}\left[\bar{C}\theta\tilde{E} - \bar{C}\tilde{A}\theta \mid \bar{C}\tilde{B}\right] = \text{rank}\left[\bar{C}\tilde{B}\right],$$

where

$$\text{rank}\left[\bar{C}\theta\tilde{E} - \bar{C}\tilde{A}\theta \mid \bar{C}\tilde{B}\right] = \text{rank}\left[0.0002 \mid 0.1,\ 0.0002\right] = 1,$$

and $\text{rank}\left[\bar{C}\tilde{B}\right] = 1$ was determined in condition a′. Clearly, condition b′ is met and $\tilde{\Gamma}_s$ is chosen to satisfy (same as (2.60))

$$\bar{C}\left[\theta\tilde{E} - \tilde{A}\theta - \tilde{B}\tilde{\Gamma}_s\right] = 0.0002 - 0.01\tilde{\Gamma}_{s1} - 0.0002\tilde{\Gamma}_{s2} = 0. \tag{4.56}$$

A $\tilde{\Gamma}_s$ that satisfies (4.56) for Example 2 is

$$\tilde{\Gamma}_s = \begin{pmatrix} 0 \\ 1 \end{pmatrix}. \tag{4.57}$$

The digital control term $u_s(kT)$ in (2.62) can thus be chosen ideally as

$$u_s(kT) = \tilde{\Gamma}_s c(kT)$$
$$= \begin{pmatrix} 0 \\ 1 \end{pmatrix} c(kT) \quad ; \tag{4.58}$$
$$= \begin{pmatrix} 0 \\ 1 \end{pmatrix} y_c(kT)$$

condition c′: there exists a $\tilde{\Gamma}_c$ such that (2.59) is satisfied. The necessary and sufficient condition for existence of a $\tilde{\Gamma}_c$ satisfying (2.59) is (same as (2.53))

$$\text{rank}\left[\bar{C}\tilde{FH} \mid \bar{C}\tilde{B}\right] = \text{rank}\left[\bar{C}\tilde{B}\right],$$

where

$$\text{rank}\left[\bar{C}\tilde{FH} \mid \bar{C}\tilde{B}\right] = \text{rank}\left[0.0002 \mid 0.1,\ 0.0002\right] = 1,$$

and $\text{rank}\left[\bar{C}\tilde{B}\right] = 1$ was determined in condition a′. Clearly condition c′ is met and $\tilde{\Gamma}_c$ is chosen to satisfy (same as (2.59))

$$\bar{C}\left[\tilde{B}\tilde{\Gamma}_c + \tilde{FH}\right] = 0.01\tilde{\Gamma}_{c1} + 0.0002\tilde{\Gamma}_{c2} + 0.0002 = 0. \tag{4.59}$$

A $\tilde{\Gamma}_c$ that satisfies (4.59) for Example 2 is

$$\tilde{\Gamma}_c = \begin{pmatrix} 0 \\ -1 \end{pmatrix}. \tag{4.60}$$

The digital control term $u_c(kT)$ in (2.61) can thus be chosen ideally as

$$u_c(kT) = \tilde{\Gamma}_c z(kT)$$
$$= \begin{pmatrix} 0 \\ -1 \end{pmatrix} z(kT) \quad ; \tag{4.61}$$

condition d′: there exists an r x (n - v) constant matrix $\tilde{L} = \begin{bmatrix} \tilde{L}_1 \\ \tilde{L}_2 \end{bmatrix}$ such that solutions $\xi_{ss1}(kT)$ to (2.85) are uniformly and asymptotically stable to the null-point $\xi_{ss1}(kT) = 0$. The characteristic polynomial of the system in (2.85) is

$$\det\left(\lambda \mathrm{I} - (\tilde{A}_1 + \tilde{B}_1\tilde{L})\right) = \lambda - 0.1\tilde{L}_1 - 0.0002\tilde{L}_2 - 0.9998, \tag{4.62}$$

where $\tilde{A}_1$ and $\tilde{B}_1$ are defined in (2.84). One choice for $\tilde{L}$ that will achieve $|\lambda_i| < 1$ in (4.62) is

$$\tilde{L} = \begin{bmatrix} -10 \\ 0 \end{bmatrix}. \tag{4.63}$$

4.3.4. The Necessary and Sufficient Conditions for Maintaining Bounded Motions of $\bar{e}_{ss}(kT)$ within S_1 for Example 2

Conditions a′, b′, c′, and d′ in the previous Subsection have been met. It remains to test the condition necessary to satisfactorily maintain bounded motions of $\bar{e}_{ss}(kT)$ within the subspace $S_v = \mathcal{N}[\bar{C} = C]$. As discussed in Subsection 2.11.6, there must exist an r x (n - m) matrix $\tilde{Z} = \begin{bmatrix} \tilde{Z}_{11} & \tilde{Z}_{12} \\ \tilde{Z}_{21} & \tilde{Z}_{22} \end{bmatrix}$ such that all solutions $\xi_{ss2}(kT)$ to (2.88) remain bounded. The characteristic polynomial of the system in (2.88) is

$$\begin{aligned} \det\left(\lambda \mathrm{I} - (\tilde{A}_2 + \tilde{B}_2\tilde{Z})\right) = \lambda^2 + \left(0.0002\,\tilde{Z}_{12} - 0.0052\,\tilde{Z}_{21} - 0.1051\,\tilde{Z}_{22} - 2.1\right)\lambda \\ + \left(0.1051\,\tilde{Z}_{22} - 0.0053\,\tilde{Z}_{21} - 0.0002\,\tilde{Z}_{12} + 1.1053\right) \end{aligned}, \tag{4.64}$$

where $\tilde{A}_2$ and $\tilde{B}_2$ are defined in (2.84). One choice for $\tilde{Z}$ that will achieve $|\lambda_i| < 1$ in (4.64) is

$$\tilde{Z} = \begin{bmatrix} 0 & 0 \\ 0 & -11 \end{bmatrix}. \tag{4.65}$$

4.3.5. Calculation of the Gain-Matrix $\tilde{K}_p$ and the Idealized Digital Control Term $u_p(kT)$ for Example 2

The gain-matrix $\tilde{K}_p$ can be computed from (2.83) by incorporating $\tilde{A}$, $\tilde{B}$, M, R, $\bar{C}$, $\tilde{L}$, and $\tilde{Z}$ from (4.48), (4.53), (4.54), (4.55), (4.63), and (4.65) to obtain the gain-matrix

$$\begin{aligned} \tilde{K}_p &= -(\bar{C}\tilde{B})^{+}\bar{C}\tilde{A}MR(MR)^{\#} + [\mathrm{I} - (\bar{C}\tilde{B})^{+}\bar{C}\tilde{B}]\tilde{Z}(MR)^{\#} + \tilde{L}\bar{C} \\ &= \begin{bmatrix} -10 & -0.9991 & -0.0329 \\ 0 & -0.0017 & -11.0001 \end{bmatrix} \end{aligned} \tag{4.66}$$

Substituting (4.66) into (2.62) yields the idealized form of the control term $u_p(kT)$,

$$u_p(kT) = -\tilde{K}_p \bar{e}_{ss}(kT)$$

$$= \begin{bmatrix} 10 & 0.9991 & 0.0329 \\ 0 & 0.0017 & 11.0001 \end{bmatrix} e_{ss}(kT) \tag{4.67}$$

4.3.6. Practical Realization of the Digital Servo-Tracking Controller for Example 2

The ideal digital servo-tracking control law designed using the methods described in Sections 2.9 through 2.11 for Example 2 described by (4.46), (4.2), and (4.8), is as follows

$$u(kT) = u_c(kT) + u_s(kT) + u_p(kT), \tag{4.68}$$

where $u_c(kT)$, $u_s(kT)$, and $u_p(kT)$ are given in (4.61), (4.58), and (4.67), respectively.

The digital servo-tracking controller in (4.68) is designed for the ideal case where exact measurements of $x(kT)$, $z(kT)$, and $c(kT)$ are available. For this example, $y_c(t)$ is a stepwise-constant which is directly measurable at each of the times $t = kT$, $k = 0, 1, 2, \ldots$, thus, estimates of $c(kT)$ are not needed ($y_c(kT) = c(kT)$). On the other hand, the state vectors $z(kT)$ and $x(kT)$ (with the exception $x_1(kT) = y(kT)$) are not available for measurement and must be estimated in order for the digital servo-controller to be physically realizable. Estimates $\hat{z}(kT)$ and $\hat{x}(kT)$ of $z(kT)$ and $x(kT)$, respectively, are generated by a discrete-time full-order state-observer as described in Subsection 2.13.2. For purposes of illustration and to reduce the computational complexity, a discrete-time full-order observer is not computed for the present example.

4.3.7. Simulation Results for Example 2

Simulations results were obtained for the third-order plant (4.46), stepwise-constant disturbance (4.2), and stepwise-constant servo-command (4.8), compensated by the digital servo-controller in (4.68) using control sample-period $T = 0.1$. The simulation results shown in Figure 4.3 illustrate the plant output $y(t)$, the disturbance $w(t)$, and the servo-command $y_c(t)$ for Example 2. The simulation plot in Figure 4.2 shows the servo-tracking error $\varepsilon_y(t) = y_c(t) - y(t)$ for Example 2. The servo command $y_c(t)$ "jumps" at the times $t = 0.5$, 1.4, 5.6, and 8.1. At each of those jumps, the tracking error $\varepsilon_y(t) = y_c(t) - y(t)$ also jumps, equivalent to the total jump in the servo-command.

The plot in Figure 4.5 illustrates the motions of $e_{ss2}(t)$ and $e_{ss3}(t)$ projected onto $\aleph[C]$ (the $e_{ss2} - e_{ss3}$ plane). Examination of the plot in Figure 4.5 reveals jumps in $e_{ss2}(t)$ and $e_{ss3}(t)$ corresponding to the times of the servo-command "jumps" ($t = 0.5$, 1.4, 5.6, and 8.1). When the tracking-error $\varepsilon_y(t) = 0$, the servo-state $e_{ss3} \approx 0$ and $e_{ss2}(t)$ is increasing at a very slow rate. The 3-dimensional view of the motions of the servo-state vector $e_{ss}(t)$ are shown in Figure 4.6. As long as the motions of $e_{ss}(t)$ remain in the $\aleph[C]$ (the shaded area in Figure 4.6), the tracking error $\varepsilon_y(t)$ will be zero.

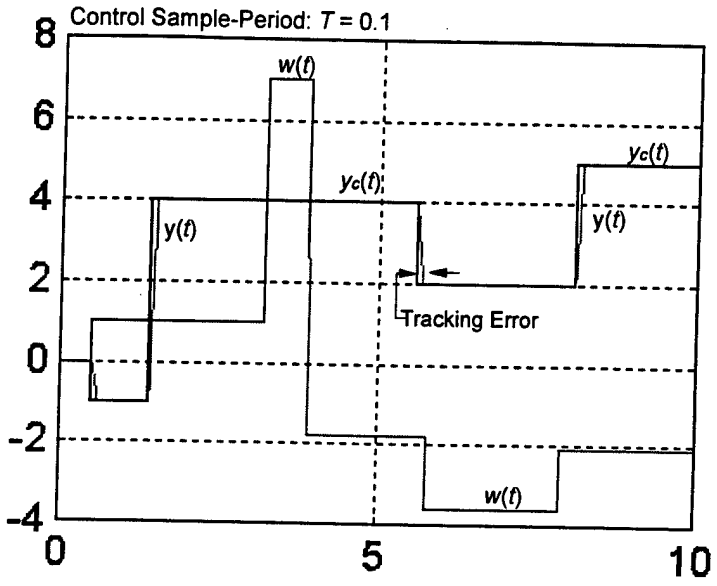

Figure 4.3 Illustration of the Plant Output $y(t)$, Disturbance $w(t)$, and Servo-Command $y_c(t)$ for Example 2.

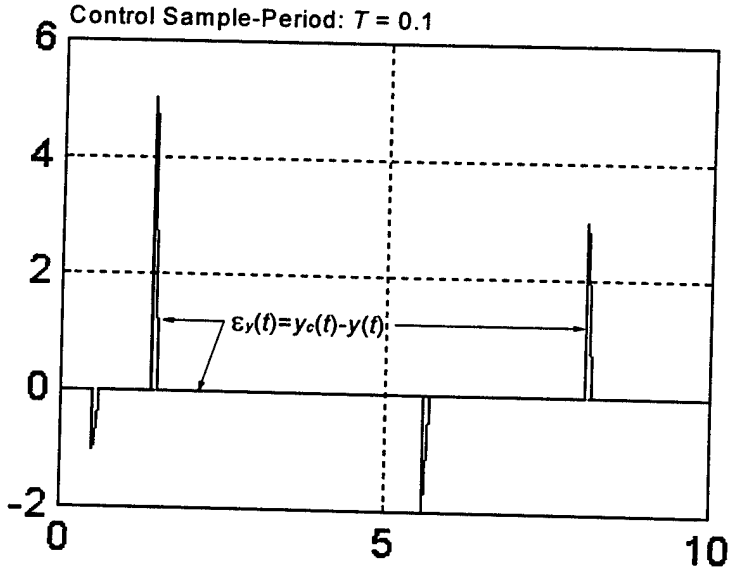

Figure 4.4 Illustration of the Servo-Tracking Error $\varepsilon_y(t) = y_c(t) - y(t)$ for Example 2.

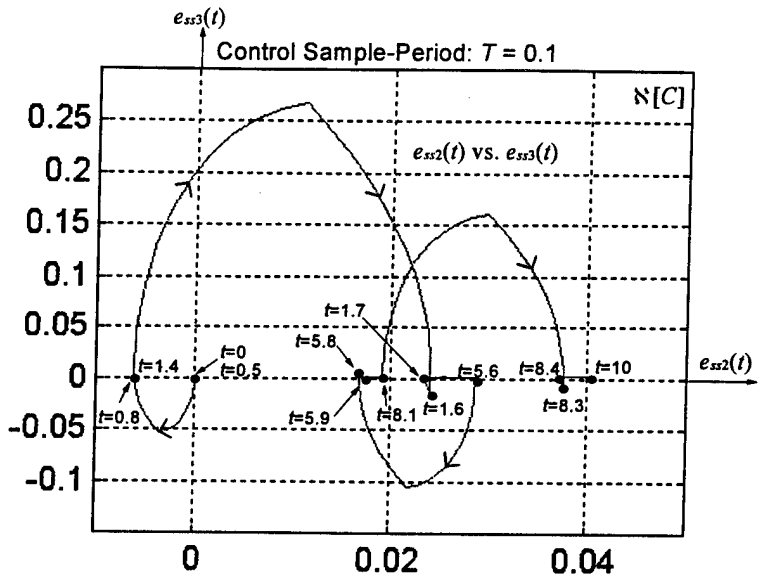

Figure 4.5 Illustration of the Motions of $e_{ss2}(t)$ and $e_{ss3}(t)$ Projected Onto $\aleph[C]$ for Example 2.

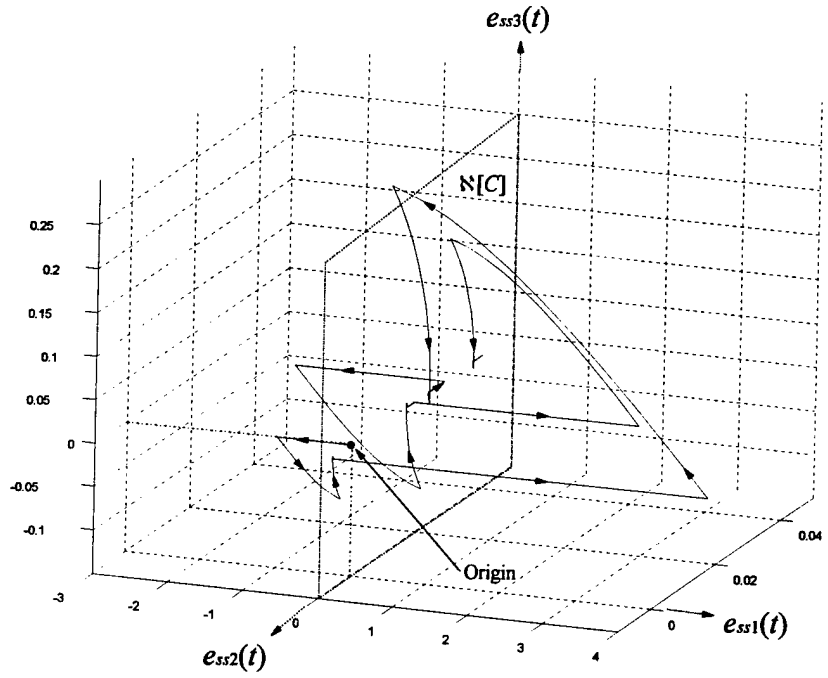

Figure 4.6 3-Dimensional View of the Servo-State $e_{ss}(t)$ Motions for Example 2.

Recall from Subsection 4.3.6 that, in order to reduce the computational complexity, no observer was designed for the present example and exact measurements of the plant state $x(kT)$ and disturbance state $z(kT)$ were assumed available. The disturbance accommodating control term $u_c(kT)$ in (4.61) was designed to completely cancel the effects of the disturbance $w(t)$ on the servo-tracking error $\varepsilon_y(kT)$ at each of the times $t = kT$, $k = 0, 1, 2, \ldots$, assuming exact measurements of $z(kT)$. Consequently, no disturbance effects due to $w(t)$ are present in the simulation plots shown in Figure 4.3 through Figure 4.5.

In order to show the effects of the disturbance $w(t)$ and the difference that the control term $u_c(kT)$ has on the present example, simulation results were obtained for the example plant (4.46), disturbance (4.2), and servo-command (4.8), compensated by the digital servo-controller in (4.68) with $u_c(kT) = 0$ and using control sample-period $T = 0.1$. The simulation results shown in Figure 4.7 illustrate the plant output $y(t)$, the disturbance $w(t)$, and the servo-command $y_c(t)$ for Example 2 with $u_c(kT) = 0$. The simulation plot in Figure 4.8 shows the servo-tracking error $\varepsilon_y(t) = y_c(t) - y(t)$ for Example 2 with $u_c(kT) = 0$. Notice that Figure 4.7 appears identical to Figure 4.3 and Figure 4.8 appears identical to Figure 4.2, even though the disturbance-related control term $u_c(kT) = 0$ and the disturbance $w(t) \neq 0$ in Figure 4.7 and Figure 4.8. Due to the nature of the plant dynamics in (4.46), the motions of the disturbance are primarily confined to $\mathcal{N}[C]$ and have virtually no effect on the plant output $y(t)$ and consequently, no noticeable effect on the servo-tracking error $\varepsilon_y(t)$ (i.e., no $w(t)$ disturbance effects appear in Figure 4.7 or Figure 4.8). Recall from (2.43) that the disturbance-effects of $w(t)$ on the servo-state vector $\bar{e}_{ss}(kT)$ are represented by the term $\tilde{FH}z(kT)$ and that the servo-tracking error $\bar{\varepsilon}_y(kT)$ and the servo-state vector $\bar{e}_{ss}(kT)$ are related by $\bar{\varepsilon}_y(kT) = C\bar{e}_{ss}(kT)$ (same as (2.44)). Then the total effect of the disturbance $w(t)$ on the servo-tracking error $\bar{\varepsilon}_y(kT)$ is determined by the matrix product

$$C\tilde{FH}z(kT) = \begin{pmatrix} 1, & 0, & 0 \end{pmatrix} \begin{bmatrix} 0.0002 \\ 0.0052 \\ 0.1051 \end{bmatrix} z(kT)$$

$$= 0.0002\, z(kT)$$

where C and $\tilde{FH}$ are given in (4.48). Clearly the effect of the disturbance on the servo-tracking error is negligible.

The plot in Figure 4.9 illustrates the motions of $e_{ss2}(t)$ and $e_{ss3}(t)$ projected onto $\mathcal{N}[C]$ (the $e_{ss2} - e_{ss3}$ plane) for the case of $u_c(kT) = 0$ in (4.68). Examination of the plot shown in Figure 4.9 reveals sudden jumps in $e_{ss2}(t)$ and $e_{ss3}(t)$ corresponding to the times of the servo-command "jumps" ($t = 0.5$, 1.4, 5.6, and 8.1) and the times of the disturbance "jumps" ($t = 0.5$, 3.2, 3.9, 5.8, and 7.9). From examination of (2.43), the matrix $\tilde{FH}$ in (4.48), and the plot shown in Figure 4.9, it is clear that the majority of the disturbance-effects due to $w(t)$ are on the servo-state $e_{ss3}(t)$.

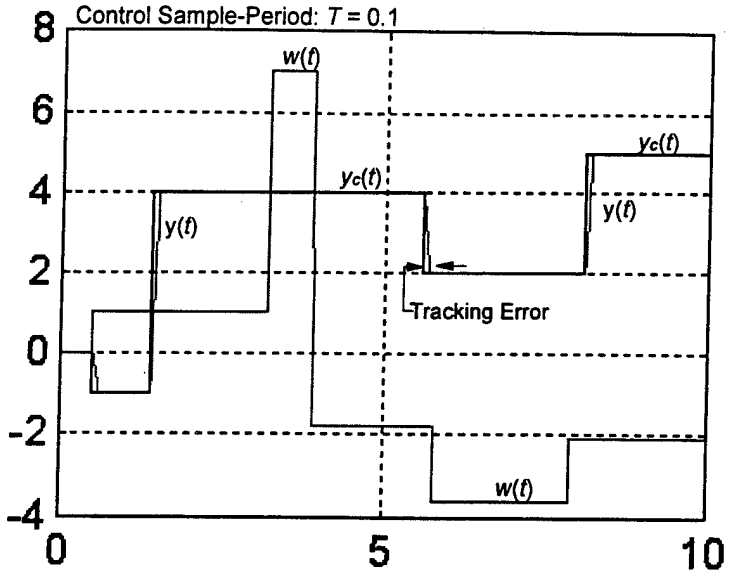

Figure 4.7 Illustration of the Plant Output $y(t)$, Disturbance $w(t)$, and Servo-Command $y_c(t)$ for Example 2 with $u_c(kT) = 0$.

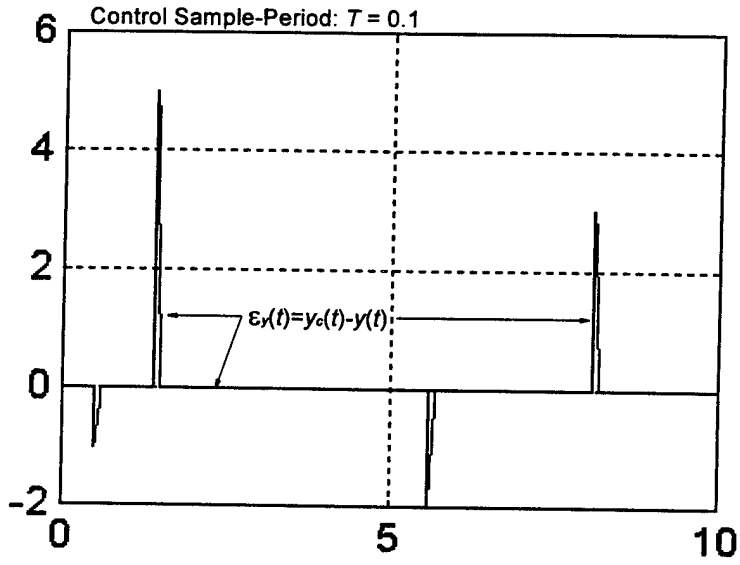

Figure 4.8 Illustration of the Servo-Tracking Error $\varepsilon_y(t) = y_c(t) - y(t)$ for Example 2 with $u_c(kT) = 0$.

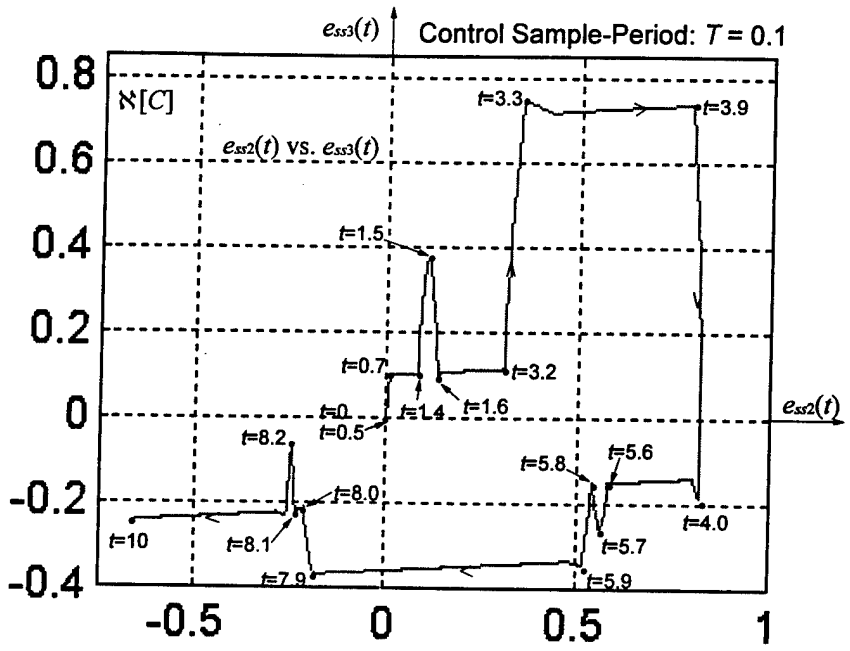

Figure 4.9 Illustration of the Motions of $e_{ss2}(t)$ and $e_{ss3}(t)$ Projected Onto $\aleph[C]$ for Example 2 with $u_c(kT) = 0$.

To further illustrate the variety of motions that can occur in the $\aleph[C]$ (the $e_{ss2} - e_{ss3}$ plane), different values for $\tilde{L}$ in (4.62) and $\tilde{Z}$ in (4.64) were chosen to achieve a different set of eigenvalues for the homogeneous closed-loop system (the homogeneous portion of (2.64))

$$\bar{e}_{ss}((k+1)T) = \left[\tilde{A} + \tilde{B}\tilde{K}_p\right]\bar{e}_{ss}(kT). \tag{4.69}$$

Choosing the gain-matrix $\tilde{L}$ as in (4.63) again and the $\tilde{Z}$ gain-matrix

$$\tilde{Z} = \begin{bmatrix} 7 & 1 \\ -7 & -20 \end{bmatrix},$$

in (4.64) results in the $\tilde{K}_p$ gain-matrix

$$\tilde{K}_p = -(\overline{C}\tilde{B})^{+}\overline{C}\tilde{A}MR(MR)^{\#} + [\mathrm{I} - (\overline{C}\tilde{B})^{+}\overline{C}\tilde{B}]\tilde{Z}(MR)^{\#} + \tilde{L}\overline{C}$$

$$= \begin{bmatrix} -10 & -0.9872 & -0.0175 \\ 0 & -7.0137 & -20.0017 \end{bmatrix} \tag{4.70}$$

The control term $u_p(kT)$ in (4.67) is thus rewritten as

$$u_p(kT) = -\tilde{K}_p e_{ss}(kT)$$
$$= \begin{bmatrix} 10 & 0.9872 & 0.0175 \\ 0 & 7.0137 & 20.0017 \end{bmatrix} e_{ss}(kT) \quad , \tag{4.71}$$

and the digital servo-tracking control law $u(kT)$ in (4.68) is rewritten as

$$u(kT) = u_s(kT) + u_c(kT) + u_p(kT), \tag{4.72}$$

where $u_s(kT)$, $u_c(kT)$, and $u_p(kT)$ are given in (4.58), (4.61), and (4.71).

The factored characteristic polynomial of the closed-loop system in (4.69) using the $\tilde{K}_p$ computed in (4.70) is

$$\det\left(\lambda \mathrm{I} - (\tilde{A} + \tilde{B}\tilde{K}_p)\right) = (\lambda + 0.0001)(\lambda + 0.9987)(\lambda - 0.9605).$$

A third choice for the gain-matrices $\tilde{L}$ and $\tilde{Z}$ is as follows. Choosing the gain-matrix

$$\tilde{L} = \begin{bmatrix} -8 \\ 8 \end{bmatrix},$$

in (4.62) and the gain-matrix

$$\tilde{Z} = \begin{bmatrix} 0 & 3 \\ -33 & -5 \end{bmatrix},$$

in (4.64) results in the $\tilde{K}_p$ gain-matrix

$$\tilde{K}_p = -(\overline{C}\tilde{B})^{+}\overline{C}\tilde{A}MR(MR)^{\#} + [\mathrm{I} - (\overline{C}\tilde{B})^{+}\overline{C}\tilde{B}]\tilde{Z}(MR)^{\#} + \tilde{L}\overline{C}$$
$$= \begin{bmatrix} -8 & -0.9428 & -0.0431 \\ 8 & -33.0016 & -5.0052 \end{bmatrix} \tag{4.73}$$

The control term $u_p(kT)$ in (4.67) is thus rewritten as

$$u_p(kT) = -\tilde{K}_p e_{ss}(kT)$$
$$= \begin{bmatrix} 8 & 0.9428 & 0.04314 \\ -8 & 33.0016 & 5.0052 \end{bmatrix} e_{ss}(kT) \quad , \tag{4.74}$$

and the digital servo-tracking control law $u(kT)$ in (4.68) is rewritten as

$$u(kT) = u_s(kT) + u_c(kT) + u_p(kT), \tag{4.75}$$

where $u_s(kT)$, $u_c(kT)$, and $u_p(kT)$ are given in (4.58), (4.61), and (4.74).

The factored characteristic polynomial of the closed-loop system in (4.69) using the $\tilde{K}_p$ computed in (4.73) is

$$\det\left(\lambda \mathrm{I} - (\tilde{A}+\tilde{B}\tilde{K}_p)\right) = (\lambda - 0.2012)(\lambda - 0.7017 + 0.5131i)(\lambda - 0.7017 - 0.5131i),$$

where $i = \sqrt{-1}$.

Simulation results showing the plant output $y(t)$, disturbance $w(t)$, and servo-command $y_c(t)$ are illustrated in Figure 4.10 (for $u(kT)$ in (4.72)) and Figure 4.14 (for $u(kT)$ in (4.75)). The simulation results in Figure 4.11 (for $u(kT)$ in (4.72)) and Figure 4.15 (for $u(kT)$ in (4.75)) illustrate the servo-tracking error $\varepsilon_y(t) = y_c(t) - y(t)$. The motions of the servo-states $e_{ss2}(t)$ and $e_{ss3}(t)$ projected onto $\aleph[C]$ (the $e_{ss2} - e_{ss3}$ plane) are illustrated in the simulation plots in Figure 4.12 (for $u(kT)$ in (4.72)) and Figure 4.16 (for $u(kT)$ in (4.75)). The $e_{ss2} - e_{ss3}$ plane results shown in Figure 4.12 and Figure 4.16 are clearly labeled to illustrate the periods of time when $y_c(t)$ is constant. The simulation plot in Figure 4.12, for example, shows slowly decaying oscillations of the servo-state motions, even though the tracking error $\varepsilon_y(t)$ is zero during those times. At each time the servo-command $y_c(t)$ "jumps" (at the times $t = 0.5$, 1.4, 5.6, and 8.1), a different set of oscillations is invoked. In contrast, the servo-state motions shown in Figure 4.16 spiral toward the origin ($e_{ss2} = e_{ss3} = 0$) when $y_c(t)$ is constant and jump away from the origin whenever the command $y_c(t)$ jumps in value. The 3-dimensional view of the motions of the servo-state vector $e_{ss}(t)$ are shown in Figure 4.13 (for $u(kT)$ in (4.72)) and Figure 4.17 (for $u(kT)$ in (4.75)). As long as the motions of $e_{ss}(t)$ remain in the $\aleph[C]$ (the shaded area in Figure 4.13 and Figure 4.17), the tracking error $\varepsilon_y(t)$ will be zero.

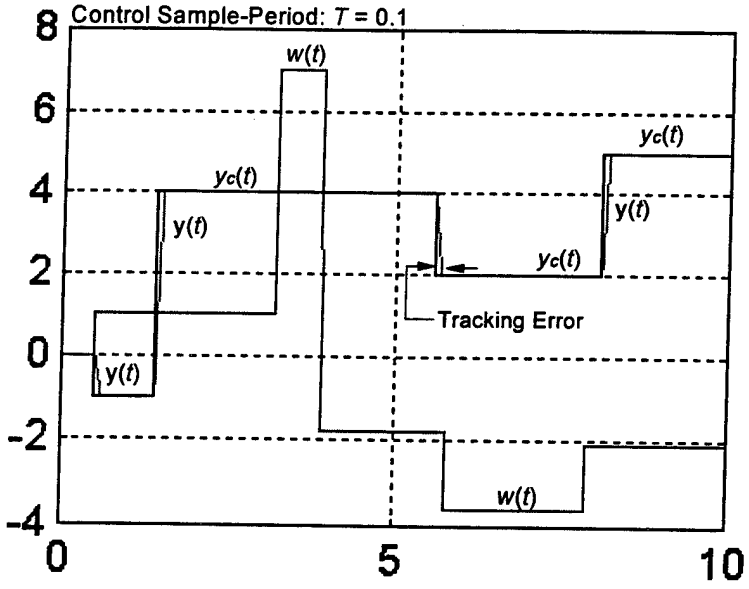

Figure 4.10 Illustration of the Plant Output $y(t)$, Disturbance $w(t)$, and Servo-Command $y_c(t)$ for Example 2 using $u(kT)$ in (4.72).

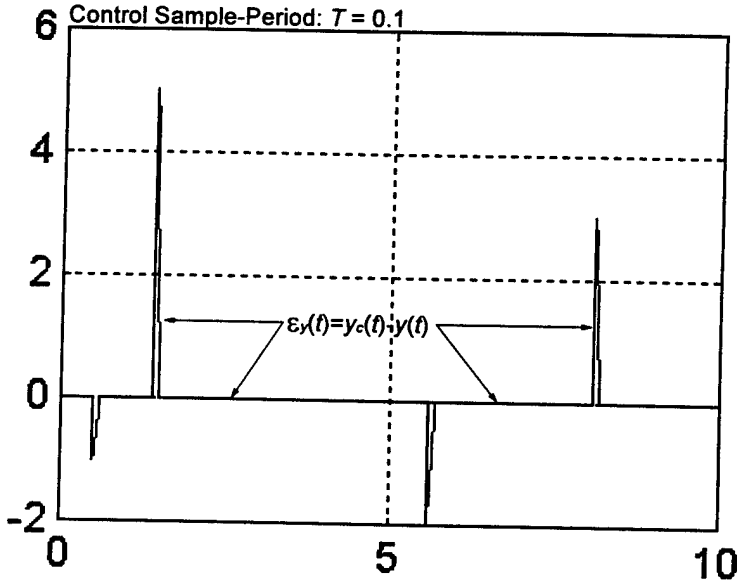

Figure 4.11 Illustration of the Servo-Tracking Error $\varepsilon_y(t) = y_c(t) - y(t)$ for Example 2 using $u(kT)$ in (4.72).

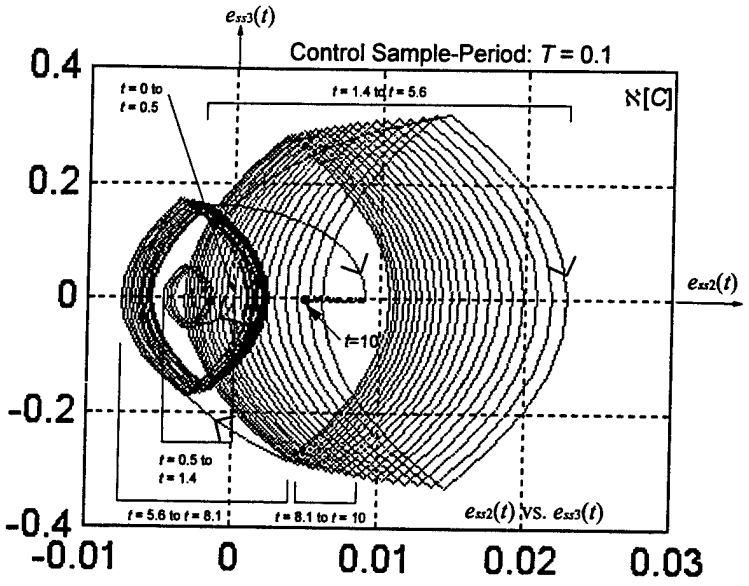

Figure 4.12 Illustration of the Motions of $e_{ss2}(t)$ and $e_{ss3}(t)$ Projected Onto $\aleph[C]$ for Example 2 using $u(kT)$ in (4.72).

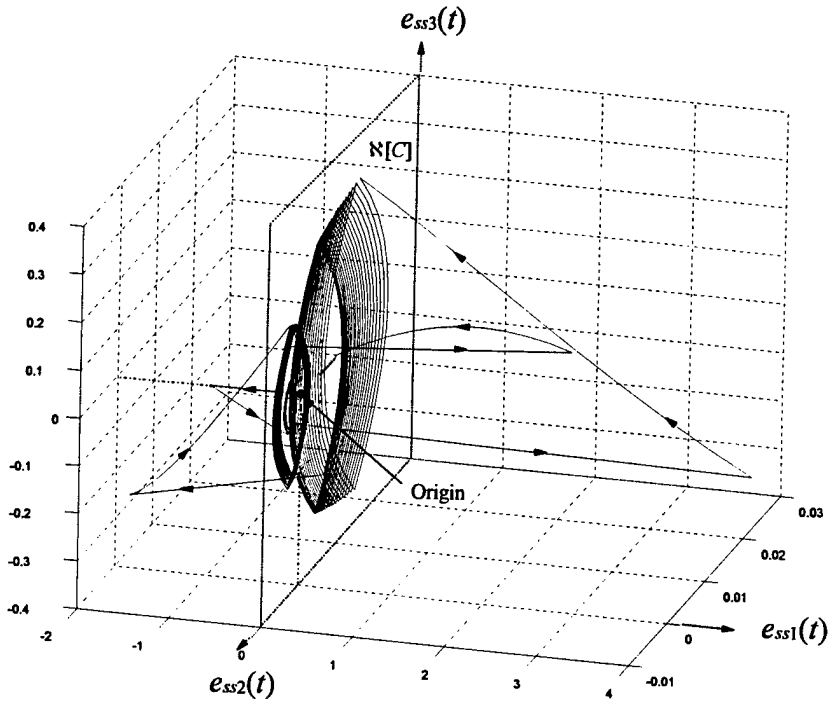

Figure 4.13 3-Dimensional View of the Servo-State $e_{ss}(t)$ Motions for Example 2 with Discrete-Time Closed-Loop Poles at λ = -0.0001, -0.9987, -0.9605.

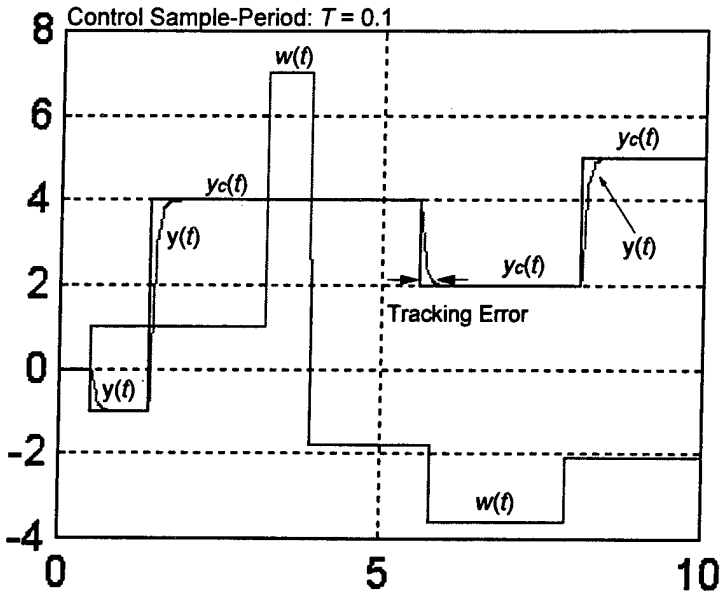

Figure 4.14 Illustration of the Plant Output $y(t)$, Disturbance $w(t)$, and Servo-Command $y_c(t)$ for Example 2 using $u(kT)$ in (4.75).

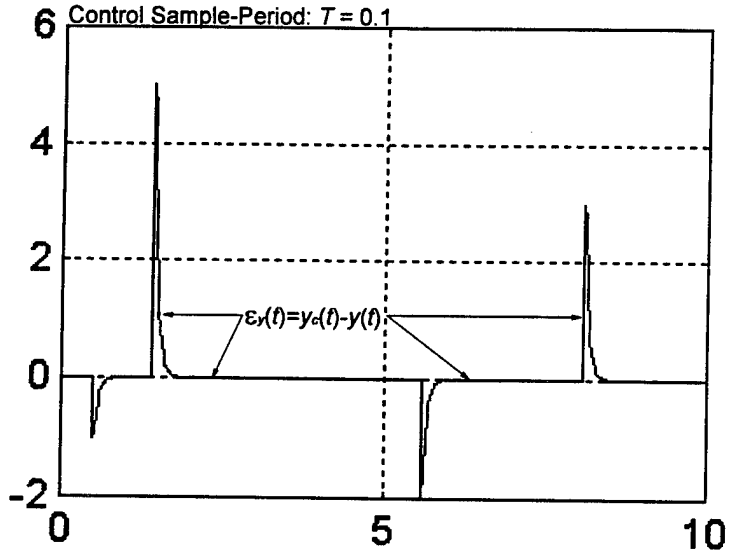

Figure 4.15 Illustration of the Servo-Tracking Error $\varepsilon_y(t) = y_c(t) - y(t)$ for Example 2 Using $u(kT)$ in (4.75).

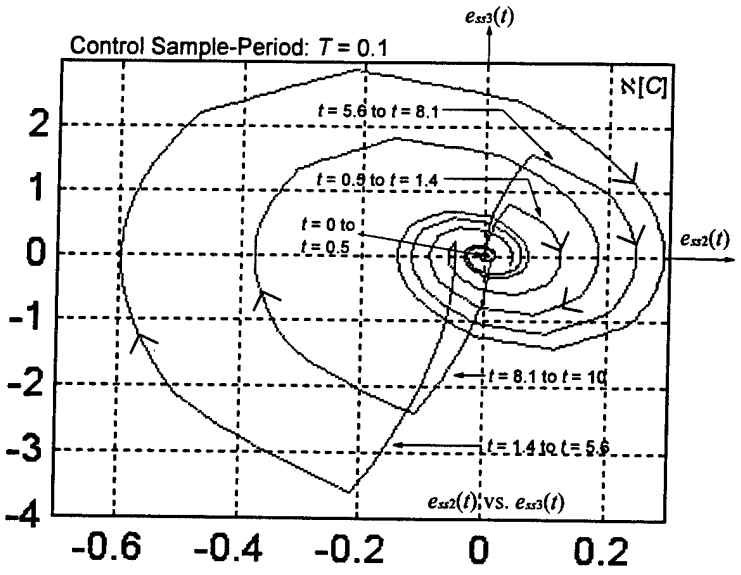

Figure 4.16 Illustration of the Motions of $e_{ss2}(t)$ and $e_{ss3}(t)$ Projected Onto $\aleph[C]$ for Example 2 Using $u(kT)$ in (4.75).

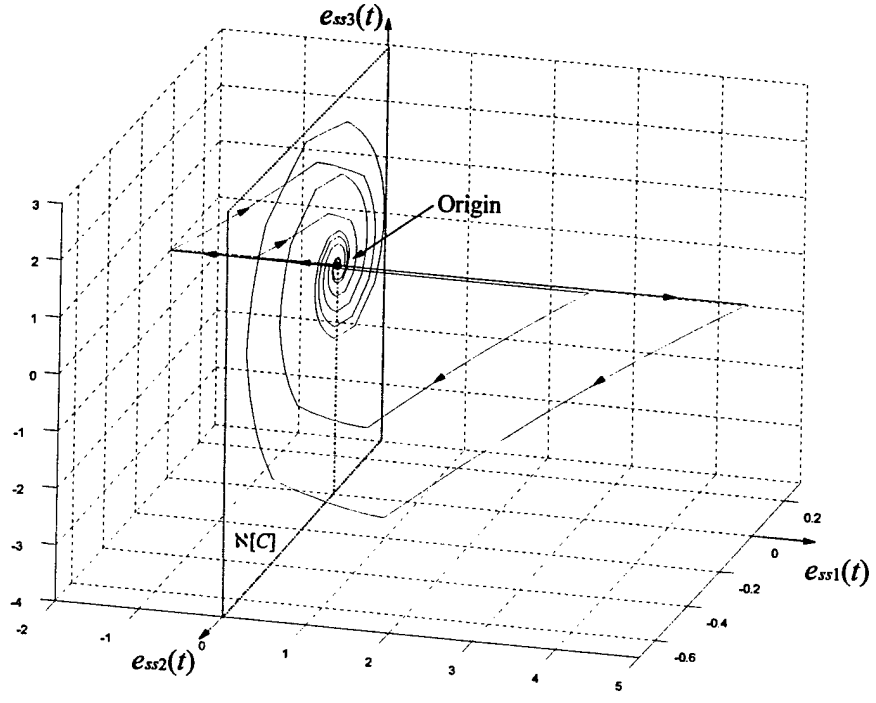

Figure 4.17 3-Dimensional View of the Servo-State $e_{ss}(t)$ Motions for Example 2 with Discrete-Time Closed-Loop Poles at $\lambda = 0.2012,\ 0.7017 \pm 0.5131i$

4.4. Example 3: A First-Order Plant and Step Servo-Command $y_c(t)$ Subjected to a Step+Ramp Disturbance $w(t)$ and Parameter-Perturbation Δa

The purpose of Example 3 is to illustrate and compare each of the digital servo-controller design techniques presented in Chapters 2 and 3. This example is worked for the case of a digital servo-controller using stepwise-constant (z.o.h.) control-action $u(kT)$ and then worked for a digital servo-controller using D/C control-action $u(t;kT)$. Simulation results are provided for the example plant with both perturbed ($\Delta a \neq 0$) and unperturbed ($\Delta a = 0$) plant parameters, and using both single-rate and multirate digital servo-controllers.

4.4.1. Plant, Disturbance, and Servo-Command Models for Example 3

The plant for Example 3 is modeled by the following first-order differential equation:

$$\dot{y}(t) = ay(t) + u(t) + w(t). \tag{4.76}$$

The disturbance $w(t)$ is an uncertain, unmeasurable constant-plus-ramp disturbance represented by

$$w(t) = c_1 + c_2 t, \tag{4.77}$$

where c_1 and c_2 are unknown stepwise-constants which may "jump" in value from time-to-time. The interval between successive jumps in c_1 and c_2 is assumed to be somewhat larger than the sampling-period T.

The state model for the plant is easily determined by choosing $x(t) = y(t)$ as follows:

$$\begin{aligned} \dot{x}(t) &= ax(t) + bu(t) + fw(t) \\ y(t) &= cx(t) \end{aligned}, \tag{4.78}$$

where $b = 1$,

$f = 1$,

$c = 1$,

and the a parameter is left undetermined until specified in Subsection 4.4.3.2.

A similar state model is developed for the disturbance $w(t)$ in (4.77), using the techniques described in Section 2.5, by noting that, between jumps in the c_i, the disturbance $w(t)$ is governed by the linear homogeneous differential equation

$$\ddot{w}(t) = 0. \tag{4.79}$$

Using the methods described in Section 2.5, the state model for $w(t)$ is obtained as

$$\begin{aligned} w(t) &= Hz(t) \\ \dot{z}(t) &= Dz(t) + \sigma(t) \end{aligned}, \tag{4.80}$$

where

$$H = \begin{pmatrix} 1, & 0 \end{pmatrix},$$

$$D = \begin{bmatrix} 0 & 1 \\ 0 & 0 \end{bmatrix},$$

and

$\sigma(t)$ are uncertain, sparse sequences of impulses that "cause" the occasional "jumps" in the disturbance $w(t)$.

Using the technique described in Section 2.6, discrete-time models are obtained for the plant and the disturbance. Those models are (the sample-period T is held as a variable throughout the computations):

Plant:

$$\begin{aligned} x((k+1)T) &= \tilde{A}x(kT) + \tilde{B}u(kT) + \tilde{FH}z(kT) + \tilde{\gamma}(kT), \\ y(kT) &= Cx(kT) \end{aligned} \tag{4.81}$$

where

$$\tilde{A} = e^{AT} = e^{aT},$$

$$\tilde{B} = \int_0^T e^{a(T-\tau)} b d\tau = \begin{cases} \dfrac{e^{aT}-1}{a}; & \text{if } a \neq 0 \\ T \quad ; & \text{if } a = 0 \end{cases},$$

$$\tilde{FH} = \int_0^T e^{a(T-\tau)} fHe^{D\tau} d\tau = \begin{cases} \left(\dfrac{e^{aT}-1}{a}, \quad \dfrac{e^{aT}-aT-1}{a^2} \right); & \text{if } a \neq 0 \\ \left(T, \quad \dfrac{T^2}{2} \right) \quad ; & \text{if } a = 0 \end{cases},$$

$$C = 1,$$

$$\tilde{\gamma}(kT) = \int_0^T e^{a(T-\tau)} fH \int_0^\tau e^{D(\tau-\xi)} \sigma(\xi) d\xi d\tau;$$

and

Disturbance:

$$w(kT) = Hz(kT)$$
$$z((k+1)T) = \tilde{D}z(kT) + \tilde{\sigma}(kT) \quad , \tag{4.82}$$

where

$$H = \begin{pmatrix} 1, & 0 \end{pmatrix},$$

$$\tilde{D} = e^{DT} = \begin{bmatrix} 1 & T \\ 0 & 1 \end{bmatrix},$$

$$\tilde{\sigma}(kT) = \int_0^T e^{D(T-\xi)}\sigma(\xi + kT)d\xi \, .$$

It is hereafter assumed that $a \neq 0$ throughout the design procedure in the four subcases of Example 3.

The servo-command $y_c(t)$ for this example is assumed to be an unknown stepwise-constant command represented by (4.8) and having continuous-time and discrete-time state models as determined in (4.10) and (4.11), respectively.

4.4.2. The Necessary and Sufficient Condition for Achieving Exact Servo-Tracking for Example 3

The objective is to design a digital servo-tracking controller for the plant in (4.76) such that the tracking-error, defined by

$$\varepsilon_y(t) = y_c(t) - y(t), \tag{4.83}$$

goes to zero in the face of arbitrary plant initial conditions and unmeasurable plant disturbances. As first shown in [37], the necessary and sufficient condition for achieving theoretically exact servo-tracking is that the vector servo-command input $y_c(t)$ must consistently lie in the column range-space of the plant-output matrix C in (4.81) for all t. In the present example, satisfaction of this condition requires that (from (2.33))

$$\Re[G] \subseteq \Re[C]. \tag{4.84}$$

If (4.84) is satisfied, then it is possible to express G as some linear combination of the columns of C. That is, $G = C\theta$ for some possibly nonunique θ. Substituting C and G from (4.81) and (4.11) into $G = C\theta$ yields

$$1 = 1\theta. \tag{4.85}$$

Clearly, (4.85) is satisfied for some θ; namely

$$\theta = 1 \, . \tag{4.86}$$

The control task is to design a discrete-time control algorithm for $u(kT)$ such that the servo-state vector $e_{ss}(kT)$ in (2.38) becomes stable to and invariant for a subspace $S_v = \mathcal{N}[\overline{C}] \subseteq \mathcal{N}[C]$ for some choice of $\overline{C}$ in (2.46). Since $C = 1$ in (4.81), we have the special case of stabilizing $e_{ss}(kT)$ to the nullpoint. The single choice for $\overline{C}$ in (2.46) is then $\overline{C} = C = 1$.

The discrete-time models for the plant (4.81), disturbance (4.82), and servo-command (4.11) and the θ determined in (4.86), will now be used in a series of four subcases of Example 3 in which digital servo-tracking controllers will be designed using the techniques presented in Chapters 2 and 3 of this report.

4.4.3. Subcase 3a: Digital Servo-Tracking Control Design Utilizing Stepwise-Constant (z.o.h.) Control-Action $u(kT)$ for the Case of a First-Order Plant and a Step Servo-Command $y_c(t)$ Subjected to a Step+Ramp Disturbance $w(t)$

In this Subsection a digital servo-tracking controller $u(kT)$ is designed for Example 3 using the conventional zero-order-hold type control-action design technique presented in Sections 2.9 through 2.11. The necessary and sufficient conditions for existence, and the subsequent design, of the digital control terms $u_c(kT)$, $u_s(kT)$, and $u_p(kT)$ in (2.55) are as follows.

The necessary and sufficient conditions for existence of the control terms $u_c(kT)$ satisfying (2.56) and $u_s(kT)$ satisfying (2.57) are given in (2.53) and (2.52), respectively. Satisfaction of those conditions is shown as follows (assuming $a \neq 0$ for Example 3):

for $u_c(kT)$:
$$\text{rank}\left[\overline{C}\,\tilde{F}\tilde{H} \mid \overline{C}\tilde{B}\right] = \text{rank}\left[\overline{C}\tilde{B}\right]; \qquad \text{(same as (2.53))}, \tag{4.87}$$

where

$$\text{rank}\left[\overline{C}\,\tilde{F}\tilde{H} \mid \overline{C}\tilde{B}\right] = \text{rank}\left[\frac{e^{aT}-1}{a}, \frac{e^{aT}-T-1}{a^2} \;\middle|\; \frac{e^{aT}-1}{a}\right] = 1,$$

and

$$\text{rank}\left[\overline{C}\tilde{B}\right] = \text{rank}\left[\frac{e^{aT}-1}{a}\right] = 1;$$

for $u_s(kT)$:
$$\text{rank}\left[\overline{C}\theta\tilde{E} - \overline{C}\tilde{A}\theta \mid \overline{C}\tilde{B}\right] = \text{rank}\left[\overline{C}\tilde{B}\right]; \qquad \text{(same as (2.52))}, \tag{4.88}$$

where

$$\text{rank}\left[\overline{C}\theta\tilde{E} - \overline{C}\tilde{A}\theta \mid \overline{C}\tilde{B}\right] = \text{rank}\left[1 - e^{aT} \;\middle|\; \frac{e^{aT}-1}{a}\right] = 1,$$

and rank$\left[\overline{C}\tilde{B}\right]$ is given below (4.87).

Clearly the rank conditions in (4.87) and (4.88) are met and $\tilde{\Gamma}_c$ and $\tilde{\Gamma}_s$ are designed to satisfy (2.59) and (2.60), respectively. That is,

for $\tilde{\Gamma}_c$:
$$\overline{C}\left(\tilde{B}\tilde{\Gamma}_c + \tilde{F}\tilde{H}\right) = \left(\left(\frac{e^{aT}-1}{a}\right)\left(\tilde{\Gamma}_{c1},\ \tilde{\Gamma}_{c2}\right) + \left(\frac{e^{aT}-1}{a},\ \frac{e^{aT}-T-1}{a^2}\right)\right) = 0; \tag{4.89}$$

for $\tilde{\Gamma}_s$:
$$\overline{C}\left(\theta\tilde{E} - \tilde{A}\theta - \tilde{B}\tilde{\Gamma}_s\right) = 1 - e^{aT} - \left(\frac{e^{aT}-1}{a}\right)\tilde{\Gamma}_s = 0. \tag{4.90}$$

The $\tilde{\Gamma}_c$ and $\tilde{\Gamma}_s$ that satisfy (4.89) and (4.90) are

$$\tilde{\Gamma}_c = \left(-1,\ \frac{aT+1-e^{aT}}{a(e^{aT}-1)}\right), \tag{4.91}$$

and

$$\tilde{\Gamma}_s = -a. \tag{4.92}$$

The ideal digital-control terms $u_c(kT)$ and $u_s(kT)$ in (2.61) and (2.62) can thus be written as

$$\begin{aligned} u_c(kT) &= \tilde{\Gamma}_c z(kT) \\ &= -z_1(kT) + \frac{aT+1-e^{aT}}{a(e^{aT}-1)} z_2(kT) \end{aligned}, \tag{4.93}$$

and

$$\begin{aligned} u_s(kT) &= \tilde{\Gamma}_s c(kT) \\ &= -ac(kT) \\ &= -ay_c(kT) \end{aligned}. \tag{4.94}$$

The $u_p(kT)$ control term is postulated as in (2.63), where the gain-matrix $\tilde{K}_p$ is designed by the technique of pole placement to place the eigenvalue λ of $\left(\tilde{A} + \tilde{B}\tilde{K}_p\right)$ in (2.64) at a sufficiently-damped location inside the unit circle $\left(|\lambda| < 1\right)$. For subcase 3a,

$$\det\left(\lambda \mathrm{I} - \left(\tilde{A} + \tilde{B}\tilde{K}_p\right)\right) = \lambda - e^{aT} - \left(\tfrac{e^{aT}-1}{a}\right)\tilde{K}_p = 0, \tag{4.95}$$

and the appropriate choice for achieving $\lambda = 0$ (deadbeat response) in (4.95) is to choose $\tilde{K}_p$ as

$$\tilde{K}_p = \frac{ae^{aT}}{1-e^{aT}} \quad , \tag{4.96}$$

such that the ideal choice for $u_p(kT)$ in (2.63) becomes

$$\begin{aligned} u_p(kT) &= -\tilde{K}_p e_{ss}(kT) \\ &= \tfrac{ae^{aT}}{e^{aT}-1} e_{ss}(kT) \\ &= \tfrac{ae^{aT}}{e^{aT}-1}\big(\theta c(kT) - x(kT)\big) \\ &= \tfrac{ae^{aT}}{e^{aT}-1}\big(y_c(kT) - y(kT)\big) \end{aligned} \tag{4.97}$$

The ideal digital servo-tracking control law designed using the methods described in Sections 2.9 through 2.11 for Subcase 3a described by (4.76), (4.77), and (4.8), is as follows

$$u(kT) = u_c(kT) + u_s(kT) + u_p(kT), \tag{4.98}$$

where $u_c(kT)$, $u_s(kT)$, and $u_p(kT)$ are given in (4.93), (4.94), and (4.97), respectively.

4.4.3.1. Practical Realization of the Digital Servo-Tracking Controller for Subcase 3a

The digital servo-tracking controller in (4.98) is designed for the ideal case where exact measurements of $x(kT)$, $z(kT)$, and $c(kT)$ are assumed available. For this example, $y(kT)=x(kT)$ in (4.81) and $y_c(t)$ is a stepwise-constant which, along with $y(t)$, is directly measurable at each of the times $t = kT$, $k = 0, 1, 2, \ldots$. Thus, estimates of $c(kT)$ and $x(kT)$ are not needed ($c(kT) = y_c(kT)$, $x(kT) = y(kT)$). On the other hand, the disturbance state $z(kT)$ is not available for measurement and must be estimated. Estimates $\hat{z}(kT)$ of $z(kT)$ can be generated by a discrete-time full-order state-observer as described in Subsection 2.13.2. The general form for the discrete-time full-order state-observer is (same as (2.107))

$$\begin{pmatrix} \hat{x}((k+1)T) \\ \hat{z}((k+1)T) \end{pmatrix} = \left[\begin{array}{c|c} \tilde{A} & \tilde{FH} \\ \hline 0 & \tilde{D} \end{array}\right] \begin{pmatrix} \hat{x}(kT) \\ \hat{z}(kT) \end{pmatrix} + \begin{pmatrix} \tilde{B} \\ 0 \end{pmatrix} u(kT) + \begin{bmatrix} \tilde{K}_{01} \\ \tilde{K}_{02} \end{bmatrix} \left[(C \mid 0) \begin{pmatrix} \hat{x}(kT) \\ \hat{z}(kT) \end{pmatrix} - y(kT) \right], \tag{4.99}$$

where $\tilde{K}_0 = \begin{bmatrix} \tilde{K}_{01} \\ \tilde{K}_{02} \end{bmatrix}$ is an observer gain-matrix to be designed, and $\tilde{A}$, $\tilde{FH}$, $\tilde{B}$, C, and $\tilde{D}$ are defined in (4.81) and (4.82).

The general discrete-time evolution equation for the error dynamics of the discrete-time full-order state-observer is (same as (2.109))

$$\begin{pmatrix}\varepsilon_x((k+1)T)\\ \varepsilon_z((k+1)T)\end{pmatrix}=\begin{pmatrix}\hat{x}((k+1)T)\\ \hat{z}((k+1)T)\end{pmatrix}-\begin{pmatrix}x((k+1)T)\\ z((k+1)T)\end{pmatrix}$$

$$=\left[\begin{array}{c|c}\tilde{A}+\tilde{K}_{01}C & \tilde{FH}\\ \hline \tilde{K}_{02}C & \tilde{D}\end{array}\right]\begin{pmatrix}\varepsilon_x(kT)\\ \varepsilon_z(kT)\end{pmatrix} \qquad (4.100)$$

It is desirable to design $\tilde{K}_0$ so that the observer error $\begin{pmatrix}\varepsilon_x(kT)\\ \varepsilon_z(kT)\end{pmatrix}$ always converges to zero promptly, from any initial condition. Pole placement techniques can be used to determine an appropriate $\tilde{K}_0$. In that way, the gain-matrix $\tilde{K}_0$ is designed to place the roots of the polynomial

$$\det\left[\lambda \mathrm{I}-\left[\begin{array}{c|c}\tilde{A}+\tilde{K}_{01}C & \tilde{FH}\\ \hline \tilde{K}_{02}C & \tilde{D}\end{array}\right]\right]=\det\begin{bmatrix}\lambda-e^{aT}-\tilde{K}_{01} & \dfrac{1-e^{aT}}{a} & \dfrac{1+aT-e^{aT}}{a^2}\\ -\tilde{K}_{02_1} & \lambda-1 & -T\\ -\tilde{K}_{02_2} & 0 & \lambda-1\end{bmatrix}$$

$$\begin{aligned}&=\lambda^3-\left(\tilde{K}_{01}+e^{aT}+2\right)\lambda^2\\ &+\left(2\tilde{K}_{01}+2e^{aT}+1+\frac{1-e^{aT}}{a}\tilde{K}_{02_1}+\frac{1+aT-e^{aT}}{a^2}\tilde{K}_{02_2}\right)\lambda\\ &-\left(\tilde{K}_{01}+\frac{1-e^{aT}}{a}\tilde{K}_{02_1}+\frac{1+aTe^{aT}-e^{aT}}{a^2}\tilde{K}_{02_2}+e^{aT}\right)\end{aligned} \qquad (4.101)$$

at sufficiently-damped locations inside the unit circle. A $\tilde{K}_0$ that achieves deadbeat observer response ($\lambda_i = 0$ in (4.101)) is (assuming $a \neq 0$):

$$\tilde{K}_0=\begin{bmatrix}\tilde{K}_{01}\\ \tilde{K}_{02}\end{bmatrix}=\begin{pmatrix}-\left(2+e^{aT}\right)\\ \dfrac{2aT-1+e^{aT}(1-3aT)}{T\left(e^{aT}-1\right)^2}\\ \dfrac{a}{T\left(1-e^{aT}\right)}\end{pmatrix}; \qquad a\neq 0. \qquad (4.102)$$

The discrete-time full-order state-observer for $\hat{x}(kT)$ and $\hat{z}(kT)$ is then obtained by substituting values from (4.81) and (4.82) into (4.99). The result is

$$\begin{pmatrix} \hat{x}((k+1)T) \\ \hat{z}_1((k+1)T) \\ \hat{z}_2((k+1)T) \end{pmatrix} = \begin{bmatrix} e^{aT} & \frac{e^{aT}-1}{a} & \frac{e^{aT}-1-aT}{a^2} \\ 0 & 1 & T \\ 0 & 0 & 1 \end{bmatrix} \begin{pmatrix} \hat{x}(kT) \\ \hat{z}_1(kT) \\ \hat{z}_2(kT) \end{pmatrix} + \begin{pmatrix} \left(\frac{e^{aT}-1}{a}\right) \\ 0 \\ 0 \end{pmatrix} u(kT)$$

$$+\left(\tilde{K}_0\right)\left(\hat{x}(kT) - y(kT)\right) \quad , \qquad (4.103)$$

where $y(kT)$ and $u(kT)$ in (4.103) are the inputs and $\hat{x}(kT)$, $\hat{z}(kT)$, $\hat{x}((k+1)T)$, and $\hat{z}((k+1)T)$ are the outputs of the discrete-time full-order state-observer, and $\tilde{K}_0$ is given in (4.102).

4.4.3.2. Simulation Results for Subcase 3a

Incorporation of the discrete-time full-order state-observer equations in (4.103) into (4.98) results in the following physically-realizable digital servo-tracking control law for Subcase 3a.

$$u(kT) = u_c(kT) + u_s(kT) + u_p(kT)$$

$$= -\hat{z}_1(kT) + \frac{aT+1-e^{aT}}{a(e^{aT}-1)}\hat{z}_2(kT) - ay_c(kT) + \frac{ae^{aT}}{e^{aT}-1}\left(y_c(kT) - y(kT)\right) \quad . \qquad (4.104)$$

Simulations results were obtained for Subcase 3a, where the plant's a term in (4.76) and control sample-period T were chosen as

$$a = -3 \qquad \text{(an inherently stable plant);}$$

and

$$T = 1.$$

The sample-period $T = 1$ was chosen so that the intersample behavior of the plant output $y(t)$ could be easily viewed.

The simulation results in Figure 4.18 illustrate the plant output $y(t)$, the disturbance $w(t)$, and the servo-command $y_c(t)$ for Subcase 3a. Notice the intersample misbehavior (ripple) during the periods $t = 4$ to $t = 6$ and the periods $t = 9$ to $t = 15$. This misbehavior is the result of the ramp-type time-varying nature of the disturbance $w(t)$ and the stepwise-constant (z.o.h.) nature of $u(kT)$. The simulation results in Figure 4.19 show the digital control-effort $u(kT)$ and the servo-tracking error $\varepsilon_y(t) = y_c(t) - y(t)$ for Subcase 3a. The stepwise constant control-action (zero-order-hold type) can not eliminate the intersample misbehavior of the plant output $y(t)$ when the disturbance $w(t)$ is not a constant. Consequently, zero tracking-error cannot be achieved between the sample times.

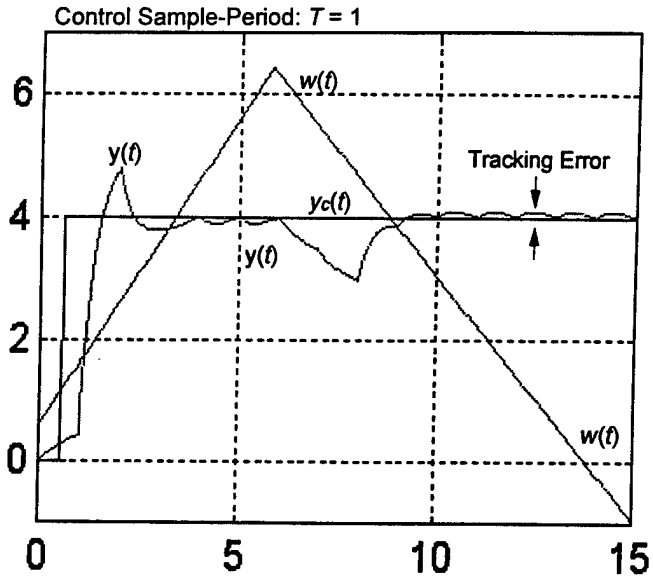

Figure 4.18 Illustration of the Plant Output $y(t)$, Disturbance $w(t)$, and Servo-Command $y_c(t)$ for Subcase 3a.

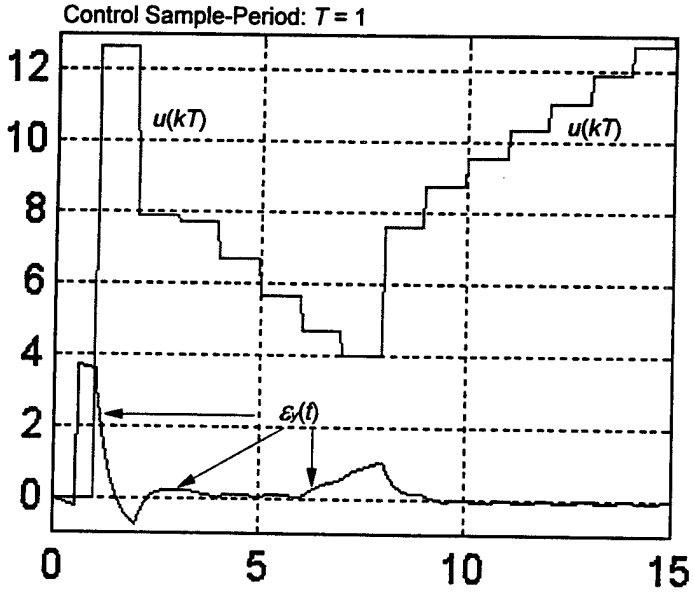

Figure 4.19 Illustration of the Digital Control-Action $u(kT)$ and Tracking-Error $\varepsilon_y(t) = y_c(t) - y(t)$ for Subcase 3a.

4.4.4. Subcase 3b: Digital Servo-Tracking Control Design Utilizing D/C Control-Action $u(t;kT)$ for the Case of a First-Order Plant and a Step Servo-Command $y_c(t)$ Subjected to a Step+Ramp Disturbance $w(t)$

In this Subsection the digital servo-tracking controller in (4.98) of Subcase 3a is modified to utilize the D/C intersample holding-action, as described in Section 3.1. In that way, the control terms $u_c(kT)$ in (4.93) and $u_s(kT)$ in (4.94) are modified to provide intersample accommodation for the effects of the disturbance $w(t)$ and the disturbance-like effects of the servo-command $y_c(t)$.

The necessary and sufficient conditions for existence of the control terms $u_c(t;kT)$ satisfying (3.15) and $u_s(t;kT)$ satisfying (3.16) are given in (3.12) and (3.13), respectively. Satisfaction of those conditions is shown as follows:

for $u_c(t;kT)$: $\text{rank}[FH \mid B] = \text{rank}[B]$; (same as (3.12)), (4.105)

where

$$\text{rank}[FH \mid B] = \text{rank}[1,0 \mid 1] = 1,$$

and

$$\text{rank}[B] = \text{rank}[1] = 1;$$

for $u_s(t;kT)$: $\text{rank}[\theta E\text{-}A\theta \mid B] = \text{rank}[B]$ (same as (3.12)), (4.106)

where

$$\text{rank}[\theta E\text{-}A\theta \mid B] = \text{rank}[-a \mid 1]$$

and $\text{rank}[B]$ is given below (4.105).

Clearly the rank conditions in (4.105) and (4.106) are met and Γ_c and Γ_s are designed to satisfy (3.17) and (3.18), respectively. That is,

for Γ_c: $$FH + B\Gamma_c = (1,0) + (\Gamma_{c1}, \Gamma_{c2}) = 0; \tag{4.107}$$

for Γ_s: $$(\theta E - A\theta) - B\Gamma_s = -a - \Gamma_s = 0. \tag{4.108}$$

The Γ_c and Γ_s that satisfy (4.107) and (4.108) are

$$\Gamma_c = (-1, \quad 0), \tag{4.109}$$

and

$$\Gamma_s = -a. \tag{4.110}$$

The ideal continuous-time control terms $u_c(t)$ and $u_s(t)$ in (3.19) and (3.20) can thus be chosen ideally as

$$\begin{aligned} u_c(t) &= \Gamma_c z(t) \\ &= -z_1(t) \end{aligned} \quad , \tag{4.111}$$

and

$$\begin{aligned} u_s(t) &= \Gamma_s c(t) \\ &= -ac(t) \end{aligned} \quad . \tag{4.112}$$

Recall, however, that it is assumed that the digital control decisions at time $t = kT$ must be based on measurements, or estimates, of the states $z(t)$ and $c(t)$ available at each of the times $t = kT$, $k = 0, 1, 2, \ldots$. Therefore, the projected or forecasted behaviors of $z(t)$ and $c(t)$ across each intersample interval must be represented in terms of $z(kT)$ and $c(kT)$. This relationship is found in the general solution to (4.80) and (4.10) evaluated at each t over the interval from kT to $t = (k+1)T$. In particular,

Disturbance state-vector:

$$\begin{aligned} z(t) &= e^{D(t-kT)} z(kT) + r_c(t) \\ &= \begin{bmatrix} 1 & t-kT \\ 0 & 1 \end{bmatrix} z(kT) + r_c(t) \end{aligned} \quad ; \tag{4.113}$$

and

Servo-command state-vector:

$$\begin{aligned} c(t) &= e^{E(t-kT)} c(kT) + r_s(t) \\ &= c(kT) + r_s(t) \end{aligned} \quad , \tag{4.114}$$

where

$r_c(t)$ is a residual-effect given by $r_c(t) = \int_{kT}^{t} e^{D(t-\tau)} \sigma(\tau) d\tau$,

and

$r_s(t)$ is a residual-effect given by $r_s(t) = \int_{kT}^{t} e^{E(t-\tau)} \mu(\tau) d\tau$.

As discussed below (3.22) in Subsection 3.1.3, the $r_c(t)$ and $r_s(t)$ terms are excluded from the design process.

Substituting (4.113) and (4.114) into (4.111) and (4.112), and disregarding the residual terms, results in the final (idealized) form of the u_c and u_s digital-continuous (D/C) control terms of the digital servo-tracking controller

$$\begin{aligned} u_c(t;kT) &= \Gamma_c e^{D(t-kT)} z(kT) \\ &= \begin{pmatrix} -1, & 0 \end{pmatrix} \begin{bmatrix} 1 & (t-kT) \\ 0 & 1 \end{bmatrix} z(kT) \\ &= -z_1(kT) - (t-kT) z_2(kT) \end{aligned} \quad , \tag{4.115}$$

and

$$\begin{aligned} u_s(t;kT) &= \Gamma_s e^{E(t-kT)} c(kT) \\ &= -ac(kT) \\ &= -ay_c(kT) \end{aligned} \quad . \tag{4.116}$$

The (ideal) digital servo-tracking control law for Subcase 3b is as follows:

$$u(t;kT) = u_c(t,kT) + u_s(t,kT) + u_p(kT), \tag{4.117}$$

where $u_c(t;kT)$, $u_s(t;kT)$ and $u_p(kT)$ are given by (4.115), (4.116), and (4.97).

4.4.4.1. Practical Realization of the Digital Servo-Tracking Controller for Subcase 3b

The digital servo-tracking controller in (4.117) is designed for the ideal case where exact measurements of $x(kT)$, $z(kT)$, and $c(kT)$ are assumed available. For Example 3, the single state $c(kT)$ of the step servo-command and the plant state $x(kT) = y(kT)$ (refer to (4.81)) can be directly measured on-line. However, the disturbance state-vector $z(kT)$ must be estimated by a composite discrete-time full-order state-observer.

The discrete-time full-order state-observer designed in Subsection 4.4.3.1 must be modified to include the time-varying portions of the D/C motions of the servo-controller in (4.117). In that way, (4.117) is rewritten equivalently as (refer to (3.66))

$$u(t;kT) = u_p(kT) + u_t(t); \quad kT \le t < (k+1)T, \tag{4.118}$$

where $u_p(kT)$ in (4.97) is the portion of $u(t;kT)$ in (4.118) which is held constant between sample times, and

$$u_t(t) = u_c(t;kT) + u_s(t;kT); \; kT \le t < (k+1)T,$$

is the portion of $u(t;kT)$ that varies with time between each successive sample-time.

The time-varying nature of $u_t(t)$ changes the calculation of the discrete-time full-order state-observer designed in Subsection 4.4.3.1 where the control action was held constant between the sample times. The hybrid full-order state-observer described in Subsection 3.3.3 must be used instead so that accurate estimates $\hat{z}(kT)$ of $z(kT)$ may be obtained. The resulting hybrid state-observer has the form (same as (3.75))

$$\begin{pmatrix} \hat{x}((k+1)T) \\ \hat{z}((k+1)T) \end{pmatrix} = \left[\begin{array}{c|c} \widetilde{A} & \widetilde{FH} \\ \hline 0 & \widetilde{D} \end{array}\right] \begin{pmatrix} \hat{x}(kT) \\ \hat{z}(kT) \end{pmatrix} + \begin{pmatrix} \widetilde{B} \\ 0 \end{pmatrix} u_p(kT) + \begin{pmatrix} \psi(u_t) \\ 0 \end{pmatrix} + \begin{bmatrix} \widetilde{K}_{01} \\ \widetilde{K}_{02} \end{bmatrix} \left[(C \mid 0) \begin{pmatrix} \hat{x}(kT) \\ \hat{z}(kT) \end{pmatrix} - y(kT) \right] , \quad (4.119)$$

where $\widetilde{A}$, $\widetilde{FH}$, $\widetilde{B}$, C, and $\widetilde{D}$ are defined in (4.81) and (4.82), $\widetilde{K}_0 = \begin{bmatrix} \widetilde{K}_{01} \\ \widetilde{K}_{02} \end{bmatrix}$ is the same observer gain-matrix obtained in (4.102), and $\psi(u_t)$ is determined to be (refer to (3.70), incorporate (4.115) and (4.116), and recall from Subsection 4.4.1 that $a \neq 0$ is assumed)

$$\begin{aligned} \psi(u_t) &= \int_0^T e^{A(T-\tau)} B u_t(\tau) d\tau \\ &= -\int_0^T e^{a(T-\tau)} \left(z_1(kT) + \tau z_2(kT) + a y_c(kT) \right) d\tau \\ &= \frac{1-e^{aT}}{a} z_1(kT) + \frac{aT+1-e^{aT}}{a^2} z_2(kT) + \left(1-e^{aT}\right) y_c(kT) \end{aligned} \quad . \quad (4.120)$$

The term $\psi(u_t)$ becomes physically-realizable when $\hat{z}_1(kT)$ and $\hat{z}_2(kT)$ (generated by (4.119)) is substituted in for $z_1(kT)$ and $z_2(kT)$ in (4.120).

The evolution equation for the hybrid full-order state-observer for Subcase 3b can now be written as (substitute (4.81) and (4.82) into (4.119))

$$\begin{pmatrix} \hat{x}((k+1)T) \\ \hat{z}_1((k+1)T) \\ \hat{z}_2((k+1)T) \end{pmatrix} = \begin{bmatrix} e^{aT} & \left(\frac{e^{aT}-1}{a}\right) & \frac{e^{aT}-aT-1}{a^2} \\ 0 & 1 & T \\ 0 & 0 & 1 \end{bmatrix} \begin{pmatrix} \hat{x}(kT) \\ \hat{z}_1(kT) \\ \hat{z}_2(kT) \end{pmatrix} + \begin{pmatrix} \left(\frac{e^{aT}-1}{a}\right) \\ 0 \\ 0 \end{pmatrix} u_p(kT) + \begin{pmatrix} \psi(u_t) \\ 0 \\ 0 \end{pmatrix} + \left(\widetilde{K}_0\right)\left(\hat{x}(kT) - y(kT)\right) , \quad (4.121)$$

where $u_p(kT)$, $\psi(u_t)$, and $\tilde{K}_0$ are given in (4.97), (4.120), and (4.102), respectively, and $y(kT)$, $\psi(u_t)$, and $u_p(kT)$ are the inputs and $\hat{x}(kT)$, $\hat{z}(kT)$, $\hat{x}((k+1)T)$, and $\hat{z}((k+1)T)$ are the outputs of the hybrid full-order state-observer.

4.4.4.2. Simulation Results for Subcase 3b

Incorporation of the hybrid full-order state-observer equations in (4.121) into $u(t;kT)$ in (4.117) results in the physically-realizable digital servo-tracking control law for Subcase 3b

$$\begin{aligned} u(kT) &= u_c(t;kT) + u_s(t;kT) + u_p(kT) \\ &= -\hat{z}_1(kT) - (t-kT)\hat{z}_2(kT) - a y_c(kT) + \frac{ae^{aT}}{e^{aT}-1}\left(y_c(kT) - y(kT)\right) \end{aligned} \quad . \quad (4.122)$$

Simulation results were obtained for Subcase 3b, where the plant's a parameter in (4.76) and control sample-period T were chosen as (same parameters as in Subcase 3a)

$$a = -3,$$

and

$$T = 1.$$

The simulation results shown in Figure 4.18 illustrate the plant output $y(t)$, the step+ramp-type disturbance $w(t)$, and the step servo-command $y_c(t)$ for Subcase 3b. Similar to the results in Subcase 3a (Figures 4.18 and 4.19) the tracking error $\varepsilon_y(t)$ (shown in Figure 4.21 for Subcase 3b) is zero at each of the sample instants $t = kT = 4$, 5, 6, 9, 10, 11, 12, 13, 14, and 15. In addition, notice that, in the plot of $y(t)$ in Figure 4.18, the intersample misbehavior during the periods $t = 4$ to $t = 6$ and the periods $t = 9$ to $t = 15$ has been completely eliminated by the digital servo-controller $u(t;kT)$ in (4.122) (compare the simulation plots in Figure 4.18 to those in Figure 4.18). The digital-continuous (D/C) control-action $u(t;kT)$ illustrated in Figure 4.21 is smoother than the zero-order-hold (stepwise-constant) type control-action shown in Figure 4.19. It is that type of continuous action between the sample-times that smooths out the control-action and regulates the tracking-error $\varepsilon_y(t)$ to zero during those intersample intervals.

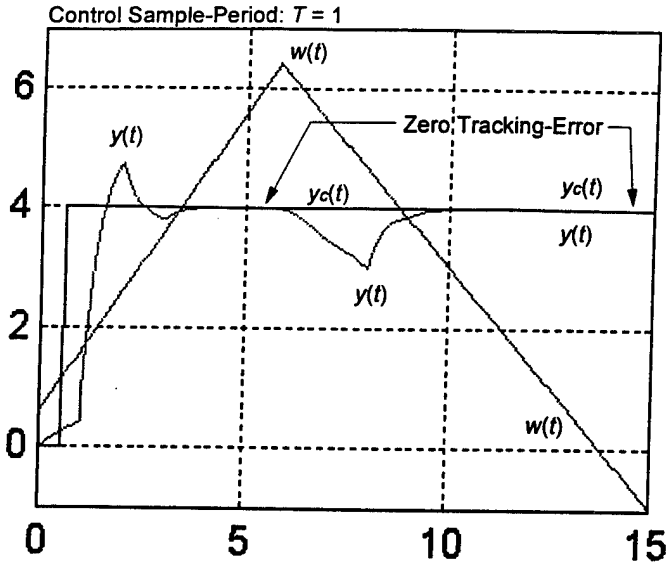

Figure 4.20 Illustration of the Plant Output $y(t)$, Disturbance $w(t)$, and Servo-Command $y_c(t)$ for Subcase 3b.

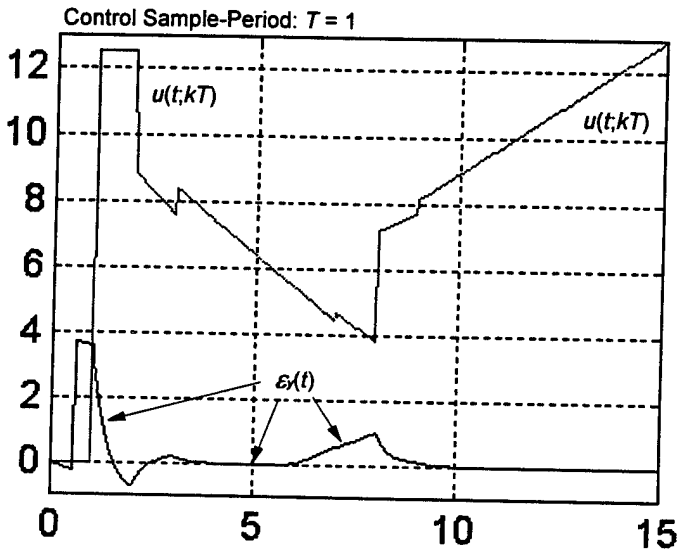

Figure 4.21 Illustration of the D/C Control-Action of $u(t;kT)$ and Tracking-Error $\varepsilon_y(t) = y_c(t) - y(t)$ for Subcase 3b.

4.4.5. Subcase 3c: Digital Servo-Tracking Control Design Utilizing D/C Control-Action $u(t;kT)$ for the Case of a First-Order Plant and a Step Servo-Command $y_c(t)$ Subjected to Parameter-Perturbation Δa and a Step+Ramp Disturbance $w(t)$

In this Subsection the digital servo-tracking control-algorithm in (4.117) is modified to provide robustness to uncertain variations in the value of the plant's a parameter in (4.76). The additional control term $u_a(t;kT)$ and the modified term $u_p(kT)$ that provide this robustness are designed using the method developed in Section 3.2. Expression (4.78) is rewritten to reflect the uncertain parameter-perturbation as follows:

$$\begin{aligned} \dot{x}(t) &= (a_n + \Delta a)x(t) + bu(t) + fw(t) \\ y(t) &= cx(t) \end{aligned} \tag{4.123}$$

Recall from Subsection 3.2.1 that Δa represents deviations to the nominal value of a $(a = a_n + \Delta a)$.

The ideal model behavior for this example is assumed to be

$$\dot{e}_{ss} = a_m e_{ss}(t) . \tag{4.124}$$

The characteristic polynomial $P_m(\lambda)$ of the system in (4.124) is

$$P_m(\lambda) = \lambda - a_m \tag{4.125}$$

where a_m represents the "desired" root of $P_m(\lambda)$ and is left undetermined until specified in Subsection 4.4.5.2.

The approach used in [34,35,39] to designing the control term u_a is to model the product $-(\Delta a)x(t)$ as an uncertain time-varying parameter-disturbance vector $w_a(t)$ as given in (3.43). The term $w_a(t)$ is closely approximated by the known differential equation in (3.44) having coefficient β corresponding to the a_m coefficient in (4.125).

Following the method described in Subsection 3.2.4, the dynamic behavior of the parameter disturbance term $(\Delta a)x(t)$ is expressed by the state model (refer to (3.45))

$$\begin{aligned} -(\Delta a)x(t) &= w_a(t) = H_a z_a(t) \\ \dot{z}_a(t) &= D_a z_a(t) + \sigma_a(t) \end{aligned} \tag{4.126}$$

The procedure for determining H_a and D_a was presented in Subsection 3.2.4. For this particular example

$$H_a = 1 , \tag{4.127}$$

and

$$D_a = a_m . \tag{4.128}$$

The term $\sigma_a(t)$ in (4.126) represents a sparse sequence of impulses that are the source of the uncertain intersample "jumps" that may occasionally occur in the disturbance vector $(\Delta a)x(t)$.

The necessary and sufficient condition for existence of the control term $u_a(t;kT)$ satisfying (3.48) is (same as (3.49))

$$\text{rank}[B \mid H_a] = \text{rank}[B], \tag{4.129}$$

where

$$\text{rank}[B \mid H_a] = \text{rank}[1 \mid 1] = 1,$$

and

$$\text{rank}[B] = \text{rank}[1] = 1.$$

Clearly the rank condition in (4.129) is met. Then there exists a Γ_a such that (same as (3.50))

$$H_a - B\Gamma_a = 1 - \Gamma_a = 0. \tag{4.130}$$

The Γ_a that satisfies (4.130) is

$$\Gamma_a = 1\ , \tag{4.131}$$

and the control term $u_a(t)$ in (3.51) can thus be ideally chosen as

$$\begin{aligned} u_a(t) &= \Gamma_a z_a \\ &= z_a(t) \end{aligned}\ , \tag{4.132}$$

during the intervals $kT \le t < (k+1)T$. Recall, however, that the digital control decisions at time $t = kT$ must be based on measurements, or estimates, of the states $z_a(t)$ available at the beginning of each sample interval $t = kT$, $k = 0, 1, 2, \ldots$. Therefore, the predicted or forecasted behavior of $z_a(t)$ across each intersample interval must be determined in terms of $z_a(kT)$. This relationship is found in the general solution to (4.126) evaluated at each t over the interval from kT to $t = (k+1)T$

$$\begin{aligned} z_a(t) &= e^{D_a(t-kT)} z_a(kT) + r_a(t) \\ &= e^{a_m(t-kT)} z_a(kT) + r_a(t) \end{aligned}\ , \tag{4.133}$$

where $r_a(t)$ is a residual-effect given by $r_a(t) = \int_{kT}^{t} e^{D_a(t-\tau)} \sigma_a(\tau) d\tau$.

As discussed in Subsection 3.2.5, the $r_a(t)$ term is disregarded throughout the design process. Substituting (4.133) into (4.132), and ignoring the residual term, results in the final (idealized) form of the $u_a(t;kT)$ control term

$$u_a(t;kT) = \Gamma_a e^{a_m(t-kT)} z_a(kT)$$
$$= e^{a_m(t-kT)} z_a(kT) \qquad (4.134)$$

The $u_p(kT)$ control term in (4.97) must be redesigned to accommodate the Δa-effects. In that case, the gain-matrix $\tilde{K}_p$ is designed to achieve null-point stabilization and the ideal model characteristics in (4.124) and (4.125). That is, $\tilde{K}_p$ is designed to achieve

$$\lambda - \left(\tilde{A}_N + \tilde{B}\tilde{K}_p\right) = \lambda - \tilde{A}_m \,, \qquad (4.135)$$

where

$$\tilde{A}_N = e^{a_n T}, \qquad \tilde{A}_M = e^{a_m T},$$

and $\tilde{B}$ is given in (4.81) (with a replaced by a_n). In that way, (4.135) becomes (assuming $a_n \neq 0$)

$$\lambda - e^{a_n T} - \left(\frac{e^{a_n T} - 1}{a_n}\right)\tilde{K}_p = \lambda - e^{a_m T}, \qquad (4.136)$$

and $\tilde{K}_p$ in (4.136) is computed to be

$$\tilde{K}_p = \frac{a_n\left(e^{a_m T} - e^{a_n T}\right)}{e^{a_n T} - 1} \qquad (4.137)$$

Given (4.137), the control term $u_p(kT)$ in (4.97) can thus be chosen ideally as

$$u_p(kT) = -\tilde{K}_p e_{ss}(kT)$$
$$= \frac{-a_n\left(e^{a_m T} - e^{a_n T}\right)}{e^{a_n T} - 1} e_{ss}(kT) \qquad (4.138)$$
$$= \frac{-a_n\left(e^{a_m T} - e^{a_n T}\right)}{e^{a_n T} - 1}\left(y_c(kT) - x(kT)\right)$$

The ideal digital servo-tracking control law for Subcase 3c can now be written as (combining (4.115), (4.116), (4.138), and (4.134) and replacing a by a_n in (4.116) and recalling the assumption that $a_n \neq 0$)

$$u(t;kT) = u_c(t;kT) + u_s(t;kT) + u_p(kT) + u_a(t;kT), \qquad (4.139)$$

where

$$u_c(t;kT) = -z_1(kT) - (t - kT)z_2(kT),$$

$$u_s(t;kT) = -a_n c(kT),$$

$$u_p(kT) = -\frac{a_n(e^{a_m T} - e^{a_n T})}{e^{a_n T} - 1}\big(y_c(kT) - x(kT)\big),$$

and

$$u_a(t;kT) = e^{a_m(t-kT)} z_a(kT).$$

4.4.5.1. Practical Realization of the Digital Servo-Tracking Controller for Subcase 3c

The digital servo-control law in (4.139) assumes the availability of the real-time values of the external disturbance state $z(kT)$, the plant state $x(kT)$, the servo-command state $c(kT)$, and the related parameter-perturbation state $z_a(kT)$. The single servo-command state $c(kT)$ and the single plant state $x(kT)$ are obtained directly from on-line measurements of $y_c(kT)$ and $y(kT)$. Estimates $\hat{z}(kT)$ and $\hat{z}_a(kT)$ of $z(kT)$ and $z_a(kT)$, respectively, can be generated by a hybrid full-order state-observer similar to that developed for Subcase 3b in Subsection 4.4.4.1.

In order to design the hybrid full-order state-observer, the control law in (4.139) must be divided into a discrete part $u_p(kT)$ and a continuous time-varying part u_t, written as

$$u(t;kT) = u_p(kT) + u_t(t); \qquad kT \le t < (k+1)T, \tag{4.140}$$

where $u_p(kT)$ in (4.138) is the portion of $u(t;kT)$ in (4.140) that is held constant between sample times, and

$$u_t(t) = u_c(t;kT) + u_s(t;kT) + u_a(t;kT); \qquad kT \le t < (k+1)T, \tag{4.141}$$

is the portion of $u(t;kT)$ in (4.140) that varies with time across each successive sample-time. The resulting hybrid full-order state-observer has the form (same as (3.76))

$$\begin{pmatrix} \hat{x}((k+1)T) \\ \hat{z}((k+1)T) \\ \hat{z}_a((k+1)T) \end{pmatrix} = \left[\begin{array}{c|c|c} \widetilde{A}_N & \widetilde{FH} & -\widetilde{H}_a \\ \hline 0 & \widetilde{D} & 0 \\ \hline 0 & 0 & \widetilde{D}_a \end{array}\right] \begin{pmatrix} \hat{x}(kT) \\ \hat{z}(kT) \\ \hat{z}_a(kT) \end{pmatrix} + \begin{pmatrix} \widetilde{B} \\ \hline 0 \\ \hline 0 \end{pmatrix} u_p(kT) + \begin{pmatrix} \psi(u_t) \\ \hline 0 \\ \hline 0 \end{pmatrix}$$

$$+ \begin{bmatrix} \widetilde{K}_{01} \\ \hline \widetilde{K}_{02} \\ \hline \widetilde{K}_{03} \end{bmatrix} \Big[(C \mid 0 \mid 0) \begin{pmatrix} \hat{x}(kT) \\ \hat{z}(kT) \\ \hat{z}_a(kT) \end{pmatrix} - y(kT) \Big], \tag{4.142}$$

where $\widetilde{A}_N$, $\widetilde{B}$, $\widetilde{FH}$, and $\widetilde{D}$ are given in (4.81) (with a replaced by a_n), (4.82), and (4.135) and (assuming $a_n \neq 0$)

$$\widetilde{D}_a = e^{D_a T} = e^{a_m T},$$

$$\tilde{H}_a = \int_0^T e^{A_N(T-\tau)} H_a e^{D_a \tau} d\tau$$

$$= \int_0^T e^{a_n(T-\tau)} e^{a_m \tau} d\tau = \begin{cases} \dfrac{e^{a_m T} - e^{a_n T}}{a_m - a_n} & \text{if } a_m \neq a_n \\ Te^{a_n T} & \text{if } a_m = a_n \end{cases},$$

$$\psi(u_t) = \int_0^T e^{a_n(T-\tau)} b u_t(\tau) d\tau$$

$$= \frac{(a_n T + 1 - e^{a_n T})}{a_n^2} z_2(kT) + Te^{a_m T} z_a(kT) + \frac{1 - e^{a_n T}}{a_n} z_1(kT) + \left(1 - e^{a_n T}\right) y_c(kT),$$

and $\tilde{K}_0 = \begin{bmatrix} \tilde{K}_{01} \\ \tilde{K}_{02} \\ \tilde{K}_{03} \end{bmatrix}$ is an observer gain-matrix to be designed.

The general discrete-time evolution equation for the error dynamics of the hybrid full-order state-observer is (same as (3.77))

$$\begin{pmatrix} \varepsilon_x((k+1)T) \\ \varepsilon_z((k+1)T) \\ \varepsilon_{z_a}((k+1)T) \end{pmatrix} = \begin{pmatrix} \hat{x}((k+1)T) \\ \hat{z}((k+1)T) \\ \hat{z}_a((k+1)T) \end{pmatrix} - \begin{pmatrix} x((k+1)T) \\ z((k+1)T) \\ z_a((k+1)T) \end{pmatrix}$$

$$= \left[\begin{array}{c|c|c} \tilde{A}_N + \tilde{K}_{01} C & \tilde{FH} & -\tilde{H}_a \\ \hline \tilde{K}_{02} C & \tilde{D} & 0 \\ \hline \tilde{K}_{03} C & 0 & \tilde{D}_a \end{array}\right] \begin{pmatrix} \varepsilon_x(kT) \\ \varepsilon_z(kT) \\ \varepsilon_{z_a}(kT) \end{pmatrix} \quad . \tag{4.143}$$

It is desirable to design $\tilde{K}_0$ so that the observer error $\begin{pmatrix} \varepsilon_x(kT) \\ \varepsilon_z(kT) \\ \varepsilon_{z_a}(kT) \end{pmatrix}$ goes to zero promptly. Pole placement is used to determine a suitable $\tilde{K}_0$, where the roots of the characteristic polynomial

$$\det\left[\lambda \mathrm{I} - \left[\begin{array}{c|c|c} \tilde{A} + \tilde{K}_{01} C & \tilde{FH} & -\tilde{H}_a \\ \hline \tilde{K}_{02} C & \tilde{D} & 0 \\ \hline \tilde{K}_{03} C & 0 & \tilde{D}_a \end{array}\right]\right] = P(\lambda)_{desired} . \tag{4.144}$$

are such that the observer estimated value of the plant state $\hat{x}(kT)$, disturbance state $\hat{z}(kT)$, and parameter-perturbation state $\hat{z}_a(kT)$, quickly and accurately track the actual corresponding plant, disturbance, and parameter-perturbation states $x(kT)$, $z(kT)$, and $z_a(kT)$, respectively. This means that the roots λ_i of $P(\lambda)_{desired}$ are placed at sufficiently-damped locations inside the unit circle ($|\lambda_i| < 1$). A good choice for $P(\lambda)_{\text{desired}}$, which achieves deadbeat response, is

$$P(\lambda)_{\text{desired}} = \lambda^4 . \tag{4.145}$$

The corresponding observer gain-matrix $\tilde{K}_0$ in (4.144) that achieves (4.145) is (assuming $a_n \neq 0$ and $a_m \neq 0$)

$$\tilde{K}_0 = \begin{bmatrix} \tilde{K}_{01} \\ \tilde{K}_{021} \\ \tilde{K}_{022} \\ \tilde{K}_{03} \end{bmatrix} = \begin{bmatrix} -2(1+e^{a_nT}) \\ \dfrac{2a_nT(1-3e^{a_nT}+2e^{2a_nT})-(e^{a_nT}-1)^2}{T(e^{a_nT}-1)^4} \\ \dfrac{a_n}{T(e^{a_nT}-1)^2} \\ \dfrac{e^{3a_mT}}{T(1-e^{a_mT})^2} \end{bmatrix} . \tag{4.146}$$

4.4.5.2. Simulation Results for Subcase 3c

Incorporation of the hybrid full-order state-observer in (4.142) into (4.139) results in a physically-realizable digital servo-control law for Subcase 3c having the form

$$\begin{aligned} u(t;kT) &= \Gamma_c e^{D(t-kT)}\hat{z}(kT) + \Gamma_s e^{E(t-kT)} y_c(kT) - \tilde{K}_p\big(y_c(kT) - y(kT)\big) \\ &\quad + \Gamma_a e^{D_a(t-kT)}\hat{z}_a(kT) \\ &= -\hat{z}_1(kT) - (t-kT)\hat{z}_2(kT) - a_n y_c(kT) \\ &\quad - \frac{a_n\left(e^{a_mT} - e^{a_nT}\right)}{\left(e^{a_nT}-1\right)}\big(y_c(kT) - y(kT)\big) + e^{a_m(t-kT)}\hat{z}_a(kT) \end{aligned} \tag{4.147}$$

To fully comprehend the level of robustness that is provided by the control term $u_a(t;kT)$ in (4.134), it is necessary to first view the effects of a parameter-perturbation Δa on the example plant utilizing a digital servo-controller which does not compensate for a change in parameter value. To show this, a 50% parameter-perturbation ($\Delta a = 1.5$ in (4.123)) and the digital servo-controller in (4.104) from Subcase 3a (Subsection 4.4.3) is used. The control sample-period is chosen as $T = 0.2$ and the nominal plant-parameter value a_n is chosen as $a_n = -3$.

The simulation results shown in Figure 4.22 illustrate the plant output $y(t)$, the step+ramp-type disturbance $w(t)$, and the step servo-command $y_c(t)$. The digital servo-controller $u(kT)$ in (4.104) for this plant assumes a nominal value of a_n = -3, but in fact, the actual value of this parameter is

$$a = a_n + \Delta a = -3 + 1.5$$
$$= -1.5$$

The simulation results in Figure 4.23 illustrate the control-effort $u(kT)$ and the servo-tracking error $\varepsilon_y(t) = y_c(t) - y(t)$ for the plant and digital servo-controller in Subcase 3a subjected to parameter-perturbation Δa = 1.5. The digital controller is exerting considerable effort, early on, in an attempt to control the plant output $y(t)$ into agreement with the servo-command $y_c(t)$. This additional control-effort can be attributed to the inappropriate control-action that is generated due to the digital servo-controller being tuned to an incorrect parameter value (a_n = -3).

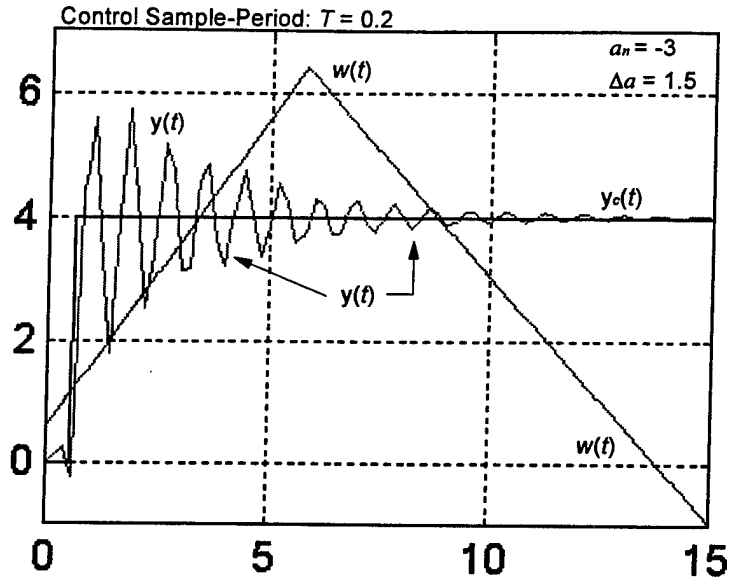

Figure 4.22 Illustration of the Plant Output $y(t)$, Disturbance $w(t)$, and Servo-Command $y_c(t)$ for the Example Plant Subjected to a 50% Parameter-Perturbation Δa (a_n = -3, Δa = 1.5) and Using the Digital Servo-Controller $u(kT)$ Derived in Subcase 3a.

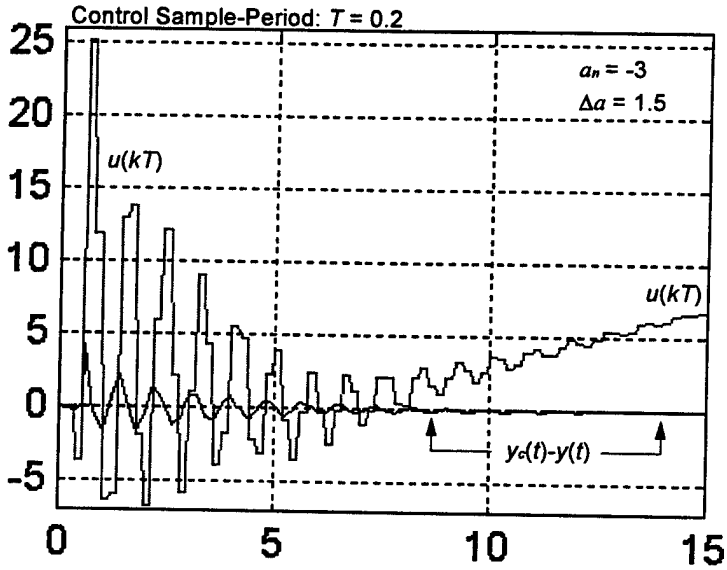

Figure 4.23 Illustration of the Digital Control-Action $u(kT)$ (from Subcase 3a) and Tracking-Error $\varepsilon_y(t) = y_c(t) - y(t)$ for the Example Plant Subjected to a 50% Parameter-Perturbation Δa (a_n = -3, Δa = 1.5).

Simulation results for Subcase 3c were obtained for the example plant, disturbance, and servo-command represented by (4.123), (4.77), and (4.8), where the plant's a_n parameter, parameter-perturbation Δa, ideal model parameter a_m, and control sample-period T were chosen as

$$a_n = -3\,, \qquad \Delta a = 1.5\,,$$

$$a_m = -3, \qquad T = 0.2\,.$$

The simulation results shown in Figure 4.24 illustrate the plant output $y(t)$, the disturbance $w(t)$, and servo-command $y_c(t)$. The digital control terms $u_p(kT)$ and $u_s(t;kT)$ in (4.139) are tuned to the nominal a_n parameter value, however, this parameter is experiencing a perturbation Δa of 50% $\left(a = a_n + \Delta a = -3 + 1.5\right)$. The control term $u_a(t;kT)$ in (4.134) provides robustness to those Δa-effects. The benefits of the $u_a(t;kT)$ control term can be seen by comparing the simulation plots in Figure 4.24 with those in Figure 4.22.

The simulation results in Figure 4.25 show the digital control-effort $u(t;kT)$ from (4.147) and the servo-tracking error $\varepsilon_y(t) = y_c(t) - y(t)$ for Subcase 3c. This digital servo-controller is providing intersample accommodation of the external disturbance $w(t)$ and parameter-perturbation vector $\Delta\alpha x(t)$. The intelligent D/C holding-action reduces ripple and provides robustness to fluctuations, or uncertainties, in plant parameter values (compare the simulation plots in Figure 4.24 with those in Figure 4.22 and the simulation plots in Figure 4.25 with those in Figure 4.23).

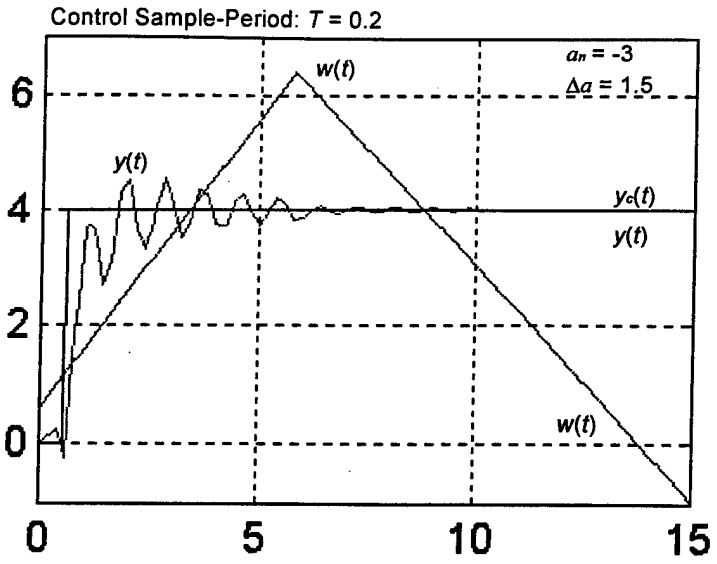

Figure 4.24 Illustration of the Plant Output $y(t)$, Disturbance $w(t)$, and Servo-Command $y_c(t)$ for the Example Plant Subjected to a 50% Parameter-Perturbation Δa (a_n = -3, Δa = 1.5) and Using the Digital Servo-Controller $u(t;kT)$ Derived in Subcase 3c.

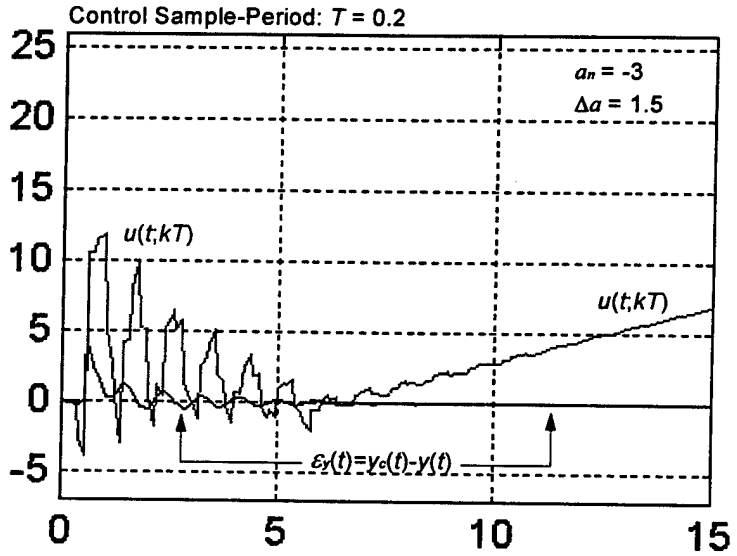

Figure 4.25 Illustration of the D/C Control-Action $u(t;kT)$ (from Subcase 3c) and Tracking-Error $\varepsilon_y(t) = y_c(t) - y(t)$ for the Example Plant Subjected to a 50% Parameter-Perturbation Δa (a_n = -3, Δa = 1.5).

4.4.6. Subcase 3d: Digital Servo-Tracking Control Design Utilizing Multirate Sampling and D/C Control-Action $u(t;kT_c;kT_y)$ for the Case of a First-Order Plant and a Step Servo-Command $y_c(t)$, Subjected to Parameter-Perturbation Δa and a Step+Ramp Disturbance $w(t)$

The digital servo-tracking controller in (4.139) designed in Subcase 3c can be modified to use multiple sampling rates to achieve a level of servo-tracking performance that cannot be matched using a single-rate servo-controller. One method of implementing (4.139) as a multirate servo-controller is to let the controller terms associated with the plant, $u_c(t;kT)$ and $u_a(t;kT)$, operate at sample-rate $1/T_y$ and let the controller term associated with the servo-command, $u_s(t;kT)$, operate at sample-rate $1/T_c$ (note that $u_p(kT) = 0$ in Subcase 3c since $a_n = a_m$). In that way, the ideal digital servo-controller in (4.139) is rewritten as (assuming $a \neq 0$)

$$u(t;kT_c;kT_y) = u_c(t;kT_y) + u_s(t;kT_c) + u_p(kT_c) + u_a(t;kT_y), \tag{4.148}$$

where

$$u_c(t;kT_y) = -z_1(kT_y) - (t - kT_y)z_2(kT_y),$$

$$\begin{aligned} u_s(t;kT_c) &= -a_n c(kT_c) \\ &= -a_n y_c(kT_c) \end{aligned},$$

$$u_p(kT_c) = -\frac{a_n(e^{a_m T_c} - e^{a_n T_c})}{e^{a_n T_c} - 1}\left(y_c(kT_c) - x(kT_c)\right) = 0 \qquad \text{for } a_n = a_m,$$

and

$$u_a(t;kT_y) = e^{a_m(t-kT_y)} z_a(kT_y).$$

4.4.6.1. Practical Realization of the Digital Servo-Tracking Controller for Subcase 3d

The digital servo-controller in (4.148) is realized by substituting T_y for T in the hybrid full-order state-observer in (4.142) for Subcase 3c and by using direct measurements of the servo-command $y_c(t)$. Incorporating (4.142) into (4.148) yields the physically-realizable digital servo-controller

$$u(t;kT_c;kT_y) = -\hat{z}_1(kT_y) - (t - kT_y)\hat{z}_2(kT_y) - a_n y_c(kT_c) + e^{a_m(t-kT_y)}\hat{z}_a(kT_y). \tag{4.149}$$

4.4.6.2. Simulation Results for Subcase 3d

Simulation results were obtained for Subcase 3d, where the plant's nominal a_n parameter, parameter-perturbation Δa in (4.123), ideal parameter a_m in (4.124), and control sample-periods T and T_y were selected as

$$a_n = -3,$$

$$\Delta a = 1.5,$$

$$a_m = -3,$$

$$T_y = 0.1,$$

and

$$T_c = 0.5 .$$

The simulation results shown in Figure 4.26 illustrate the plant output $y(t)$, the step+ramp-type disturbance $w(t)$, and the step servo-command $y_c(t)$ for Subcase 3d. The multirate D/C servo-control action $u(t;kT_y;kT_c)$ and the servo-tracking error $\varepsilon_y(t) = y_c(t) - y(t)$ for Subcase 3d are shown in Figure 4.27. A 50% decrease in the sample-period (from $T = 0.2$ in Subcase 3c to $T_y = 0.1$) for the u_c and u_a control terms has allowed a 250% increase in the sample-period T_c (from $T = 0.2$ in Subcase 3c to $T_c = 0.5$) in the control term $u_s(t;kT_c)$ (associated with the servo-command $y_c(t)$). The overall tracking and system performance has improved over that obtained in Subcase 3c. A comparison of the simulation plots in Figure 4.26 to those in Figure 4.24 and the simulation plots in Figure 4.27 to those in Figure 4.25 shows less ringing and a faster settling-time in the plant output $y(t)$ and a sizeable reduction in the servo-tracking error $\varepsilon_y(t) = y_c(t) - y(t)$. This increased performance can be attributed to the intelligent use of multiple sampling-rates. A particular application of this dual-rate system is the case in which the plant output $y(t)$ is available for measurement at each of the times $t = kT_y$, $k = 0, 1, 2, \ldots$, while the servo-command $y_c(t)$ is available less frequently, at each of the times $t = kT_c$, $k = 0, 1, 2, \ldots$ (recall that T_c and T_y are related by (3.80)).

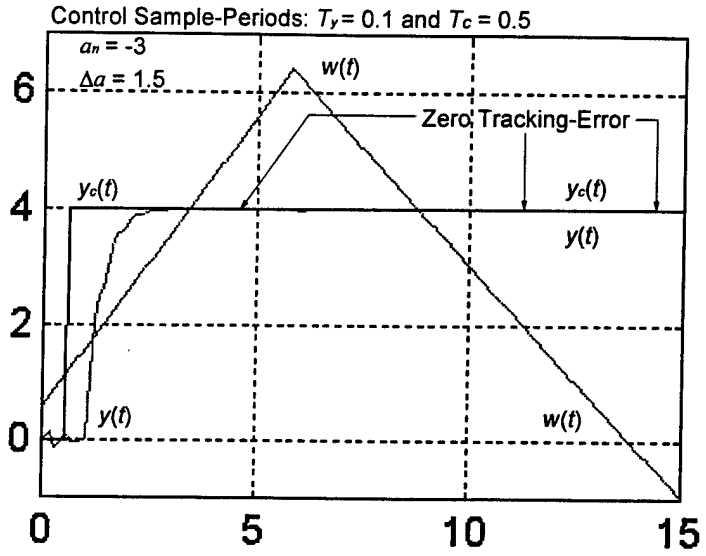

Figure 4.26 Illustration of the Plant Output $y(t)$, Disturbance $w(t)$, and Servo-Command $y_c(t)$ for the Example Plant Subjected to a 50% Parameter-Perturbation Δa (a_n = -3, Δa = 1.5) and Using the Multirate Digital Controller $u(t;kT_y;kT_c)$ from Subcase 3d.

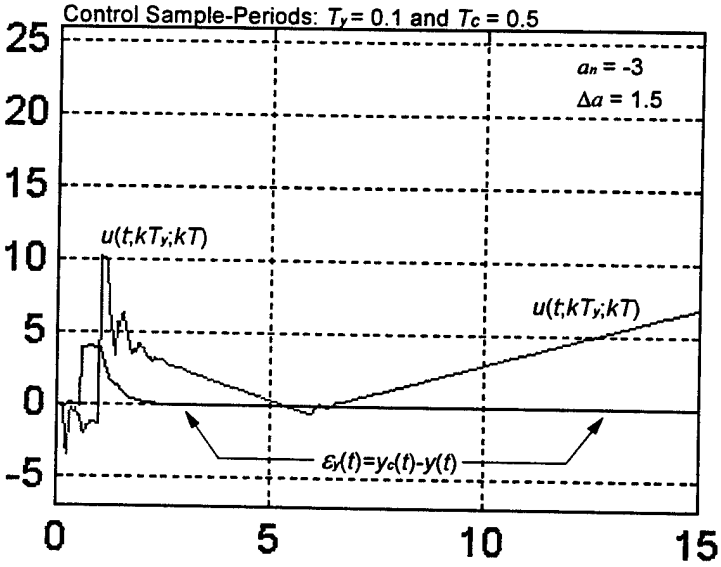

Figure 4.27 Illustration of the Multirate D/C Control-Action $u(t;kT_y;kT_c)$ (Controller from Subcase 3c, using Multirate from Subcase 3d) and Tracking-Error $\varepsilon_y(t) = y_c(t) - y(t)$ for the Example Plant Subjected to a 50% Parameter-Perturbation Δa (a_n = -3, Δa = 1.5).

4.5. Example 4: An Unstable First-Order Plant and Step+Exponential Servo-Command $y_c(t)$ Subjected to a Step+Ramp Disturbance $w(t)$ and Parameter-Perturbation Δa

The purpose of Example 4 is to illustrate that

i) due to the decomposition of the digital control-effort, only the control term $u_s(t;kT)$ in (4.116) from Subcase 3b that is affected by the change in servo-command model need to be designed;

ii) control terms designed previously in Example 3 are valid for a stable, as well as an unstable plant;

iii) the hybrid full-order state-observer in (4.142) from Subcase 3c need not be re-designed;

iv) a control term $u_{a_m}(kT)$ can be added to the digital servo-controller algorithm in (4.148) to take maximum benefit of multiple sample-rates;

v) intersample misbehavior can be eliminated in the case of non-conventional servo-commands (not a Type 1, 2, or 3 command); and

vi) a reduced-order state-observer may be used to estimate the servo-command state $c(kT)$.

4.5.1. Plant, Disturbance, Parameter-Perturbation, and Servo-Command Models for Example 4

Example 4 will use the same first-order plant in (4.76), step+ramp disturbance $w(t)$ in (4.77), and parameter-perturbation vector $\Delta\alpha x(t)$ model in (4.126) as was used in Example 3, with the exception that the plant has a pole in the right-half plane ($a_n = 1$ in (4.123), an inherently unstable plant). The servo-command $y_c(t)$ is assumed to be an unknown stepwise-constant-plus-exponential (hereafter called step+exponential) command represented by

$$y_c(t) = \bar{c}_1 + \bar{c}_2 e^{-\alpha t} \quad , \tag{4.150}$$

where $\bar{c}_1$ and $\bar{c}_2$ may occasionally jump in value at unknown times, and α is a known quantity given later in Subsection 4.5.3.2.

The linear homogeneous differential equation governing the motions of $y_c(t)$ in (4.150) between jumps in the $\bar{c}_i$ is

$$\ddot{y}_c(t) + \alpha \dot{y}_c(t) = 0 \, . \tag{4.151}$$

A state model for the servo-command $y_c(t)$ is obtained using (4.151) and the method outlined in Section 2.5. That state model is

$$\begin{aligned} y_c(t) &= Gc(t) \\ \dot{c}(t) &= Ec(t) + \mu(t) \end{aligned}, \tag{4.152}$$

where

$$G = \begin{pmatrix} 1, & 0 \end{pmatrix},$$

$$E = \begin{bmatrix} 0 & 1 \\ 0 & -\alpha \end{bmatrix},$$

and

$\mu(t)$ are unknown, sparse sequences of impulses that "cause" the uncertain "jumps" in the servo-command $y_c(t)$.

Using the technique described in Section 2.6, a discrete-time model is obtained for the servo-command. In that way, this model is written as

$$\begin{aligned} y_c(kT) &= Gc(kT) \\ c((k+1)T) &= \widetilde{E}c(kT) + \widetilde{\mu}(kT) \end{aligned}, \tag{4.153}$$

where

$$G = \begin{pmatrix} 1, & 0 \end{pmatrix},$$

$$\widetilde{E} = e^{ET} = \begin{cases} \begin{bmatrix} 1 & \dfrac{1-e^{-\alpha T}}{\alpha} \\ 0 & e^{-\alpha T} \end{bmatrix} & \text{if} \quad \alpha \neq 0 \\ \begin{bmatrix} 1 & T \\ 0 & 1 \end{bmatrix} & \text{if} \quad \alpha = 0 \end{cases},$$

and

$$\widetilde{\mu}(kT) = \int_0^T e^{E(T-\xi)} \mu(\xi + kT) d\xi .$$

It is hereafter assumed that $\alpha \neq 0$ throughout Example 4. For reasons discussed in Chapter 2, the term $\widetilde{\mu}(kT)$ in (4.153) is disregarded throughout the design process.

4.5.2. The Necessary and Sufficient Condition for Achieving Exact Servo-Tracking for Example 4

The objective is to design a digital servo-tracking controller for the given plant such that the tracking-error, defined by

$$\varepsilon_y(t) = y_c(t) - y(t), \tag{4.154}$$

goes to zero in the face of arbitrary plant initial conditions and unmeasurable plant disturbances. As first shown in [37], the necessary and sufficient condition for achieving theoretically exact servo-tracking is that the vector servo-command input $y_c(t)$ must consistently lie in the column range-space of the plant-output matrix C in (4.81) for all t. In the present example, satisfaction of this condition requires that (from (2.33))

$$\Re[G] \subseteq \Re[C] \quad . \tag{4.155}$$

If (4.155) is satisfied, then it is possible to express G as some linear combination of the columns of C. That is, $G = C\theta$ for some (possibly nonunique) θ. Substituting C and G from (4.81) and (4.152) into $G = C\theta$ yields

$$\begin{pmatrix} 1, & 0 \end{pmatrix} = 1\begin{pmatrix} \theta_1 & \theta_2 \end{pmatrix} . \tag{4.156}$$

Clearly, (4.156) is satisfied for some θ; namely

$$\theta = \begin{pmatrix} 1, & 0 \end{pmatrix} . \tag{4.157}$$

The control task is to design a discrete-time control algorithm for $u(kT)$ such that the servo-state vector $e_{ss}(kT)$ in (3.38) becomes stable to and invariant for a subspace $S_v = \aleph[\overline{C}] \subseteq \aleph[C]$ for some $\overline{C}$ in (2.46). As discussed below (4.86), $\overline{C} = C = 1$ in (2.45) and we have the special case of stabilizing $e_{ss}(kT)$ to the nullpoint.

The discrete-time models for the plant (4.81), disturbance (4.82), and servo-command (4.153), and the θ determined in (4.157), will now be used in two subcases which utilize the D/C servo-tracking controller design techniques presented in Chapter 3 of this report.

4.5.3. Subcase 4a: Digital Servo-Tracking Control Design Utilizing D/C Control-Action $u(t;kT)$ for the Case of an Unstable First-Order Plant and Step+Exponential Servo-Command $y_c(t)$, and Subjected to a Step+Ramp Disturbance $w(t)$ and Parameter-Perturbation Δa

In this Subsection, a digital servo-controller is designed using the D/C servo-controller design techniques presented in Sections 3.1 through 3.3. The ideal form of the digital servo-tracking control law for Subcase 4a is written as

$$u(t;kT) = u_c(t;kT) + u_s(t;kT) + u_p(kT) + u_a(t;kT), \tag{4.158}$$

where $u_c(t;kT)$, $u_p(kT)$, and $u_a(t;kT)$ are the same as those designed in Subcases 3b and 3c and given in (4.115), (4.138), and (4.134), respectively. Only the control term $u_s(t;kT)$ in (4.116) needs to be redesigned such that intersample accommodation is provided for the disturbance-like effects of the step+exponential servo-command $y_c(t)$ in (4.150).

The necessary and sufficient condition for existence of the control term $u_s(t;kT)$ satisfying (3.16) is (same as (3.13))

$$\text{rank}\left[\theta E - A\theta \mid B\right] = \text{rank}\left[B\right], \tag{4.159}$$

where

$$\text{rank}\left[\theta E - A\theta \mid B\right] = \text{rank}\left[-a_n, 1 \mid 1\right] = 1,$$

and

$$\text{rank}\left[B\right] = \text{rank}\left[1\right] = 1.$$

Clearly the rank condition in (4.159) is met and Γ_s is designed such that (same as (3.18))

$$\left(\theta E - A\theta\right) - B\Gamma_s = \left(-a_n, 1\right) - \left(\Gamma_{s1}, \Gamma_{s2}\right) = 0. \tag{4.160}$$

The Γ_s that will satisfy (4.160) is

$$\Gamma_s = \left(-a_n, \quad 1\right). \tag{4.161}$$

The ideal continuous-time control term $u_s(t)$ in (3.20) can thus be ideally chosen as

$$\begin{aligned} u_s(t) &= \Gamma_s c(t) \\ &= -a_n c_1(t) + c_2(t) \end{aligned} \tag{4.162}$$

Recall, however, that the digital control decisions at time $t = kT$ must be based on measurements, or estimates, of the state $c(t)$ available at each of the times $t = kT$, $k = 0, 1, 2, \cdots$. Therefore, the projected or forecasted behavior of $c(t)$ across each intersample interval must be represented in terms of $c(kT)$. This relationship is found in the general solution to (4.152) evaluated at each t over the interval from kT to $t = (k+1)T$ (assuming $\alpha \neq 0$)

$$\begin{aligned} c(t) &= e^{E(t-kT)} c(kT) + r_s(t) \\ &= \begin{bmatrix} 1 & \dfrac{1 - e^{-\alpha(t-kT)}}{\alpha} \\ 0 & e^{-\alpha(t-kT)} \end{bmatrix} c(kT) + r_s(t) \end{aligned} \tag{4.163}$$

where

$r_s(t)$ is a residual-effect given by $r_c(t) = \int_{kT}^{t} e^{E(t-kT)}\mu(\tau)d\tau$.

As discussed in Subsection 3.1.3, the $r_s(t)$ term is excluded from the design process.

Substituting (4.163) into (4.162), and ignoring the residual term, results in the final (idealized) form of the u_s control term

$$u_s(t;kT) = \Gamma_s e^{E(t-kT)}c(kT)$$

$$= \begin{pmatrix} -a_n, & 1 \end{pmatrix} \begin{bmatrix} 1 & \dfrac{1-e^{-\alpha(t-kT)}}{\alpha} \\ 0 & e^{-\alpha(t-kT)} \end{bmatrix} c(kT) \qquad (4.164)$$

$$= -a_n c_1(kT) + \left(\frac{e^{-\alpha(t-kT)}(a_n+\alpha) - a_n}{\alpha} \right) c_2(kT)$$

The final form of the (ideal) digital-continuous servo-controller equation for Subcase 4a is given in (4.158) where $u_c(t;kT)$, $u_s(t;kT)$, $u_p(kT)$, and $u_a(t;kT)$ are given in (4.115), (4.164), (4.138), and (4.134), respectively.

4.5.3.1. Practical Realization of the Digital Servo-Tracking Controller for Subcase 4a

The digital control law in (4.158) assumes availability of the real-time value of the external disturbance state $z(kT)$, the plant state $x(kT)$, the servo-command state $c(kT)$, and the related parameter-perturbation state $z_a(kT)$. Estimates of the plant state $x(kT)$, disturbance state $z(kT)$, and the parameter-perturbation state $z_a(kT)$, are generated by the hybrid full-order state-observer in (4.142) developed for Subcase 3c with $u(t;kT)$ from (4.158) used for the digital servo-controller. Estimates of the servo-command state $c(kT)$ are generated by a discrete-time reduced-order state-observer as described in Subsection 2.13.3. The states $c_1(kT)$ and $x_1(kT)$ can be obtained directly from measurements of $y_c(kT)$ and $y(kT)$, respectively (refer to (4.153) and (4.81)).

In order to compute $\psi(u_t)$ for (4.158), the control task $u(t;kT)$ in (4.158) must be divided into a discrete part $u_p(kT)$ and a continuous time-varying part u_t. In that way, (4.158) is rewritten as

$$u(t;kT) = u_p(kT) + u_t(t); \qquad kT \le t < (k+1)T, \qquad (4.165)$$

where $u_p(kT)$ in (4.138) is the portion of $u(t;kT)$ that is held constant between sample times, and

$$u_t(t) = u_c(t;kT) + u_s(t;kT) + u_a(t;kT) \quad , \qquad (4.166)$$

is the portion of $u(t;kT)$ that varies with time between each successive sample-time.

The $u_t(t)$ in (4.166) changes the value of $\psi(u_t)$ determined in Subcase 3c in (4.142). The new value of $\psi(u_t)$ is computed as

$$\psi(u_t) = \int_0^T e^{a_n(T-\tau)} b u_t(\tau) d\tau$$

$$= \frac{(a_n T + 1 - e^{a_n T})}{a_n^2} z_2(kT) + \frac{\left(e^{a_n T} - e^{a_m T}\right)}{(a_n - a_m)} z_a(kT) \quad , \qquad (4.167)$$

$$+ \frac{\left(e^{a_n T} - e^{-\alpha T}\right)}{\alpha} c_2(kT) + \frac{1 - e^{a_n T}}{a_n} z_1(kT) + \left(1 - e^{a_n T}\right) y_c(kT) + \frac{\left(1 - e^{a_n T}\right)}{2} c_2(kT)$$

where $a_n \neq a_m$, $a_n \neq 0$, and $\alpha \neq 0$. To physically realize $\psi(u_t)$ in (4.167), the estimates $\hat{z}_1(kT)$, $\hat{z}_2(kT)$, and $\hat{z}_a(kT)$ are used from the hybrid full-order state-observer and the estimate $\hat{c}_2(kT)$ must be obtained.

A discrete-time reduced-order state-observer design is used to generate the state estimate $\hat{c}(kT)$ based solely on the sampled real-time measurement of $y_c(kT)$. The "recipe" for this design was developed in [33] and is described in Subsection 2.13.3 . The discrete-time reduced-order state-observer design proceeds as follows (assuming $\alpha \neq 0$):

Step 1. define T_{12} as any v x (v-m) maximal rank matrix such that

$$GT_{12} = 0$$

The $\Re[T_{12}]$ of a T_{12} which meets this condition will necessarily form a basis for the $\aleph[G]$. For this example,

$$GT_{12} = \begin{pmatrix} 1, & 0 \end{pmatrix} \begin{pmatrix} T_{12_1} \\ T_{12_2} \end{pmatrix},$$

$$= T_{12_1}$$

and T_{12} can be selected as

$$T_{12} = \begin{pmatrix} 0 \\ 1 \end{pmatrix};$$

Step 2. a) define the (v-m) x v matrix

$$\overline{T}_{12} = \left(T_{12}^T T_{12}\right)^{-1} T_{12}^T$$

$$= \left[\begin{pmatrix} 0, & 1 \end{pmatrix} \begin{pmatrix} 0 \\ 1 \end{pmatrix} \right]^{-1} \begin{pmatrix} 0, & 1 \end{pmatrix},$$

$$= \begin{pmatrix} 0, & 1 \end{pmatrix}$$

and

b) define the m x v matrix $G^{\#}$ as

$$G^{\#} = \left(GG^{T}\right)^{-1} G$$

$$= \left[\begin{pmatrix} 1, & 0 \end{pmatrix} \begin{pmatrix} 1 \\ 0 \end{pmatrix} \right]^{-1} \begin{pmatrix} 1, & 0 \end{pmatrix};$$

$$= \begin{pmatrix} 1, & 0 \end{pmatrix}$$

Step 3. a) construct the (v-m) x (v-m) matrix

$$\mathcal{D} = \overline{T}_{12} \widetilde{E} T_{12}$$

$$= \begin{pmatrix} 0 & 1 \end{pmatrix} \begin{bmatrix} 1 & \dfrac{1 - e^{-\alpha T}}{\alpha} \\ 0 & e^{-\alpha T} \end{bmatrix} \begin{pmatrix} 0 \\ 1 \end{pmatrix},$$

$$= e^{-\alpha T}$$

and

b) construct the m x (v-m) matrix

$$\mathcal{H} = G \widetilde{E} T_{12}$$

$$= \begin{pmatrix} 1, & 0 \end{pmatrix} \begin{bmatrix} 1 & \dfrac{1 - e^{-\alpha T}}{\alpha} \\ 0 & e^{-\alpha T} \end{bmatrix} \begin{pmatrix} 0 \\ 1 \end{pmatrix} \quad ;$$

$$= \frac{1 - e^{-\alpha T}}{\alpha}$$

Step 4. construct the error-dynamics discrete-time evolution equation

$$\varepsilon_{y_c}((k+1)T) = [\mathcal{D} + \Sigma \mathcal{H}] \varepsilon_{y_c}(kT)$$

$$= \left[e^{-\alpha T} + \Sigma \left(\frac{1 - e^{-\alpha T}}{\alpha} \right) \right] \varepsilon_{y_c}(kT) \quad ;$$

Step 5. design Σ such that $\varepsilon_{y_c}(kT) \to 0$ rapidly,

For this example, the poles of $\left[\mathcal{D}+\Sigma\mathcal{H}\right]$ in Step 4 are placed at zero ($\lambda = 0$). In that way,

$$\lambda-\left[\mathcal{D}+\Sigma\mathcal{H}\right]=\lambda-\left[e^{-\alpha T}+\Sigma\left(\frac{1-e^{-\alpha T}}{\alpha}\right)\right]=0\,,$$

and Σ is chosen as

$$\Sigma=\frac{\alpha e^{-\alpha T}}{e^{-\alpha T}-1} \quad ;$$

Step 6. construct the "filter" part of the discrete-time reduced-order state-observer

$$\begin{aligned}\xi((k+1)T) &= (\mathcal{D}+\Sigma\mathcal{H})\xi(kT) \\ &\quad +\left[\left(\overline{T}_{12}+\Sigma G\right)\left(\widetilde{E}G^{\#^T}\right)-(\mathcal{D}+\Sigma\mathcal{H})\Sigma\right]y_c(kT) \\ &= 0\,\xi(kT)+\left(\frac{e^{-\alpha T}\left(1+(\alpha-1)e^{-\alpha T}\right)}{e^{-\alpha T}-1}\right)y_c(kT)\end{aligned} \quad ; (4.168)$$

and

Step 7. construct the "assembly-equation" portion of the discrete-time reduced-order state-observer

$$\begin{aligned}\hat{c}(kT) &= T_{12}\xi(kT)+\left[G^{\#^T}-T_{12}\Sigma\right]y_c(kT) \\ &= \begin{pmatrix}0\\1\end{pmatrix}\xi(kT)+\begin{pmatrix}1\\ \frac{\alpha e^{-\alpha T}}{1-e^{-\alpha T}}\end{pmatrix}y_c(kT)\end{aligned} \quad . \quad (4.169)$$

4.5.3.2. Simulation Results for Subcase 4a

Incorporation of the hybrid full-order in (4.142) with $\psi(u_t)$ from (4.167) and discrete-time reduced-order in (4.169) state-observers will result in a physically-realizable digital servo-control law having the form

$$\begin{aligned}u(t;kT) &= \Gamma_c e^{D(t-kT)}\hat{z}(kT)+\Gamma_s e^{E(t-kT)}\hat{c}(kT)-\widetilde{K}_p\left(y_c(kT)-y(kT)\right) \\ &\quad +\Gamma_a e^{D_a(t-kT)}\hat{z}_a(kT)\end{aligned} \quad . \quad (4.170)$$

where Γ_c, Γ_s, $\widetilde{K}_p$, Γ_a are given in Equations (4.109), (4.161), (4.137), and (4.131), respectively.

Simulation results were obtained for two different sample-periods ($T = 0.1, 0.2$) and for the case of no parameter-perturbation ($\Delta a = 0$) and +/-100% parameter-perturbation ($\Delta a = \pm 1$). In the simulations for Subcase 4a, the nominal value of the plant's a_n parameter in (4.123), ideal model parameter a_m in (4.124), and exponential decay α on the servo-command $y_c(t)$ in (4.150) were chosen as

$$a_n = 1; \qquad \text{(an inherently unstable plant),}$$

$$a_m = -3,$$

and

$$\alpha = 1.$$

The plant output $y(t)$, the step+ramp disturbance $w(t)$, and the step+exponential servo-command $y_c(t)$ for the simulation using a control sample-period of $T = 0.2$ is illustrated in Figure 4.28 and Figure 4.30. The illustration in Figure 4.28 represents the nominal case of no parameter-perturbation ($\Delta a = 0$). The illustration in Figure 4.30 represents the case of parameter-perturbation $\Delta a = -1$ and $\Delta a = 1$ overlayed on top of the nominal case (shown in Figure 4.28). The simulation results in Figure 4.29 and Figure 4.31 show the corresponding servo-tracking error $\varepsilon_y(t)$ for Subcase 4a.

The plots in Figure 4.32 and Figure 4.34 show the plant output $y(t)$, the step+ramp disturbance $w(t)$, and the step+exponential servo-command $y_c(t)$ for a simulation using a control sample-period of $T = 0.1$. The simulation results in Figure 4.32 illustrate the case of no parameter-perturbation ($\Delta a = 0$). The simulation results in Figure 4.34 illustrate the case of parameter-perturbation $\Delta a = -1$ and $\Delta a = 1$ overlayed on top of the nominal case (shown in Figure 4.32). The simulation plots in Figure 4.33 and Figure 4.35 show the corresponding servo-tracking error $\varepsilon_y(t)$ for Subcase 4a.

As expected, the settling-time and servo-tracking error decreases as the sample-period is reduced (from $T = 0.2$ to $T = 0.1$). The digital servo-controller and the hybrid and discrete-time reduced-order state-observers did not need to be recomputed for the different sample-periods because the sample-period T was carried throughout the calculations as a variable. The decomposition of the total control-effort greatly reduces the complexity of the design, allowing for this type of symbolic computation on relatively simple systems. Also note that the control term $u_p(kT)$ in (4.158) did not have to be recomputed from (4.138), even though the value of the plant's a_n term changed from stable ($a_n = -3$) to unstable ($a_n = 1$). This example illustrates that the same digital servo-controller equation can be used for both stable and unstable plants, providing the plant-parameter values are carried symbolically throughout the calculations. The control terms $u_c(t;kT)$ and $u_a(t;kT)$ in (4.158) were reused from Subcase 3c (4.139) since the general form of the disturbance $w(t)$ and the characteristics of the parameter-perturbation vector $\Delta\alpha x(t)$ are the same in Example 4 as they were in Example 3.

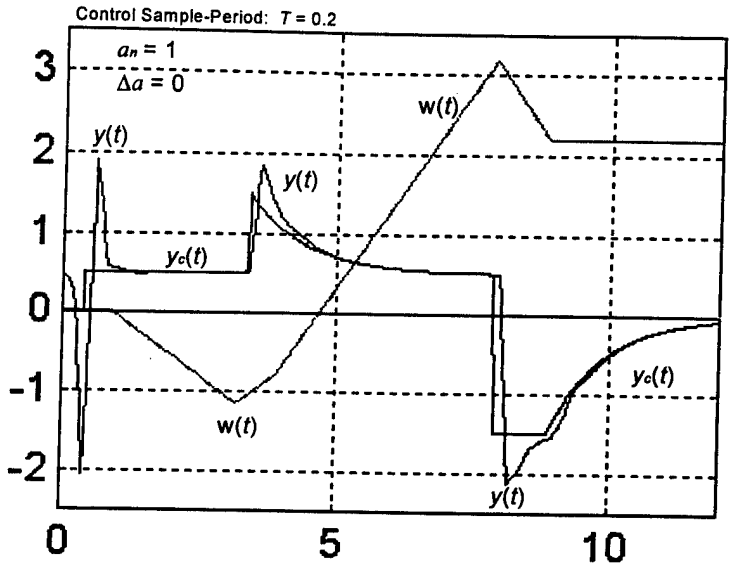

Figure 4.28 Illustration of the Plant Output $y(t)$, Disturbance $w(t)$, and Servo-Command $y_c(t)$ for Subcase 4a With an Unstable Plant, $a_n = 1$, $\Delta a = 0$, and Control Sample-Period $T = 0.2$.

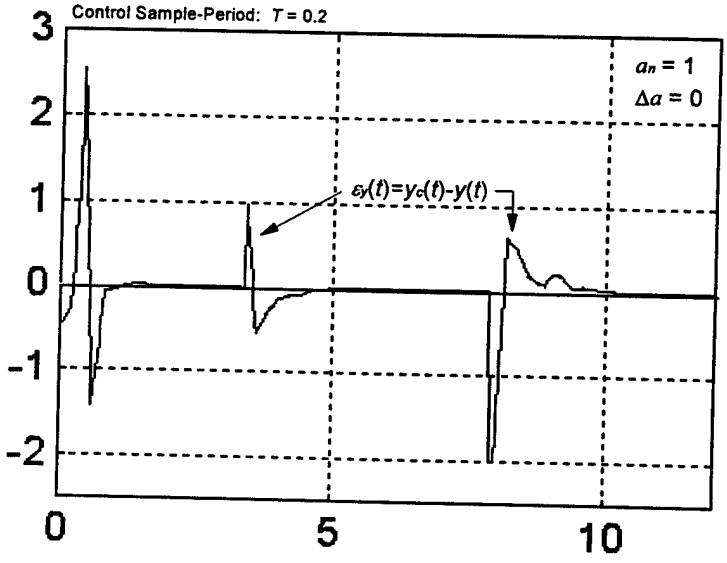

Figure 4.29 Illustration of the Servo-Tracking Error $\varepsilon_y(t)$ for Subcase 4a With an Unstable Plant, $a_n = 1$, $\Delta a = 0$, and Control Sample-Period $T = 0.2$.

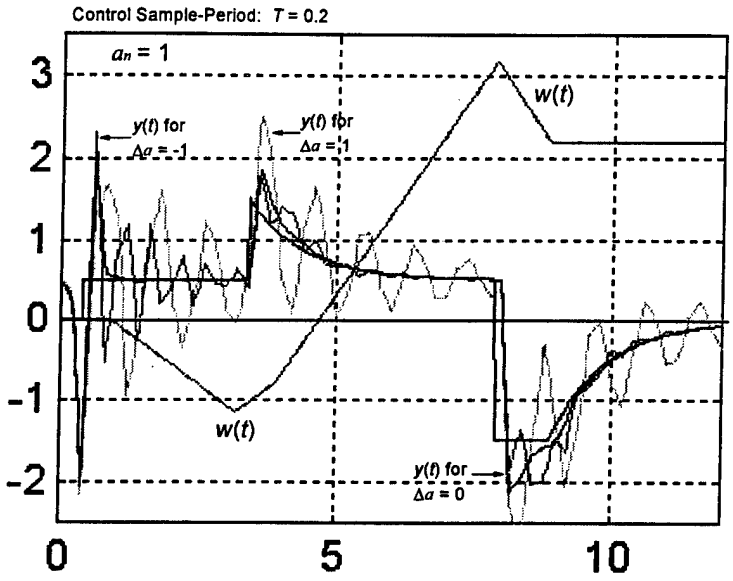

Figure 4.30 Illustration of the Plant Output $y(t)$, Disturbance $w(t)$, and Servo-Command $y_c(t)$ for Subcase 4a With an Unstable Plant, $a_n = 1$, Control Sample-Period $T = 0.2$, and $\Delta a = -1$ and 1, Overlayed on Nominal Case of $\Delta a = 0$.

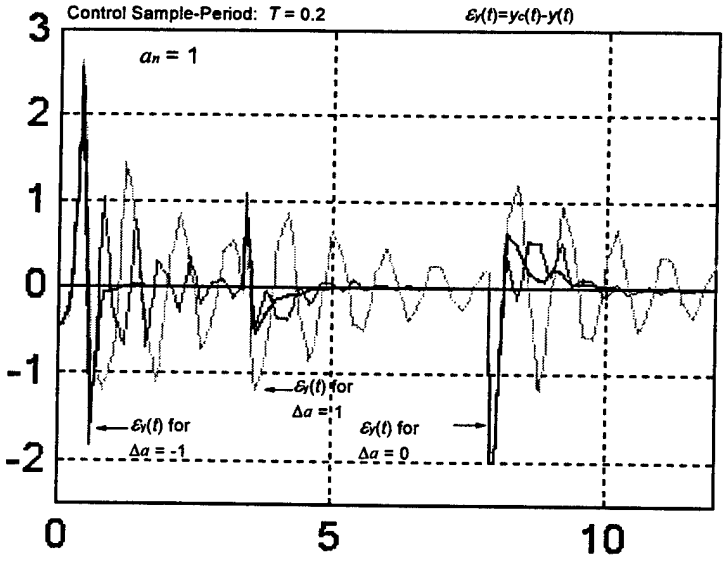

Figure 4.31 Illustration of the Servo-Tracking Error $\varepsilon_y(t)$ for Subcase 4a With an Unstable Plant, $a_n = 1$, Control Sample-Period $T = 0.2$, and $\Delta a = -1$ and 1, Overlayed on Nominal Case of $\Delta a = 0$.

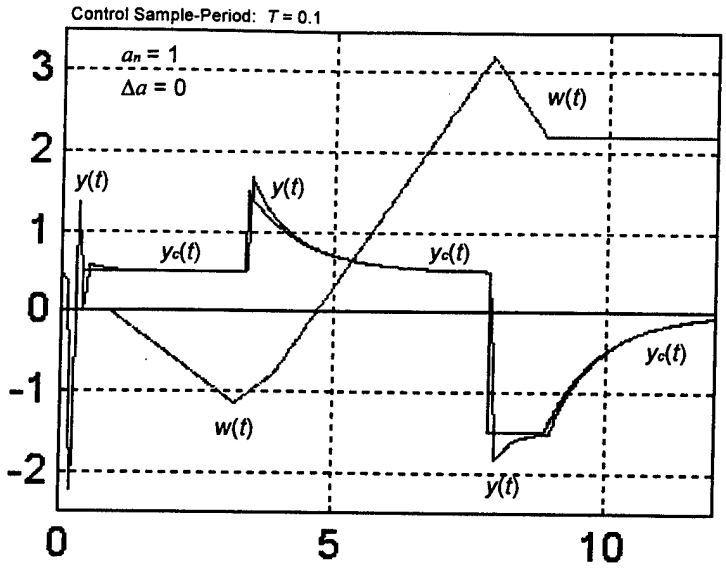

Figure 4.32 Illustration of the Plant Output $y(t)$, Disturbance $w(t)$, and Servo-Command $y_c(t)$ for Subcase 4a With an Unstable Plant, $a_n = 1$, Control Sample-Period $T = 0.1$, and $\Delta a = 0$ (compare to Figure 4.28).

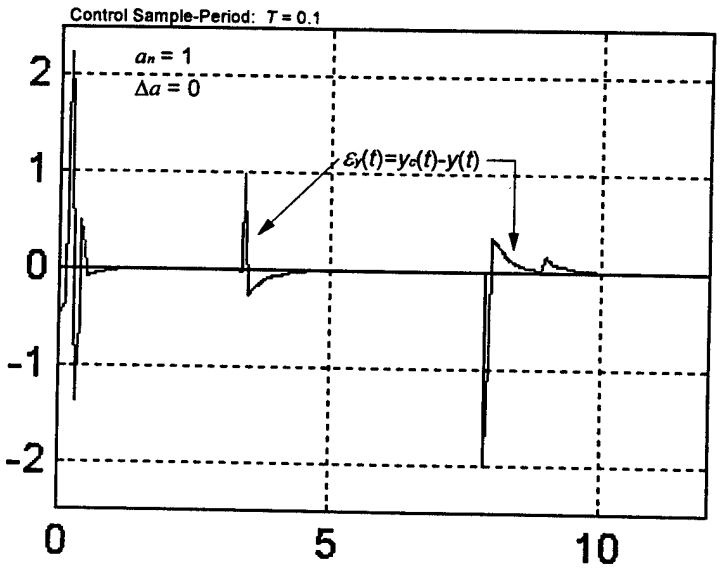

Figure 4.33 Illustration of the Servo-Tracking Error $\varepsilon_y(t)$ for Subcase 4a With an Unstable Plant, $a_n = 1$, Control Sample-Period $T = 0.1$, and $\Delta a = 0$ (compare to Figure 4.29).

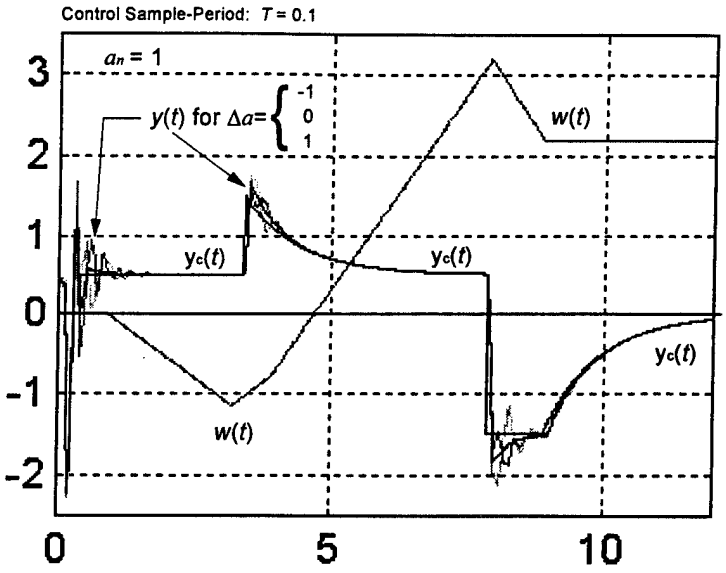

Figure 4.34 Illustration of the Plant Output $y(t)$, Disturbance $w(t)$, and Servo-Command $y_c(t)$ for Subcase 4a With an Unstable Plant, $a_n = 1$, Control Sample-Period $T = 0.1$, and $\Delta a = -1$ and 1, Overlayed on Nominal Case of $\Delta a = 0$ (compare to Figure 4.30).

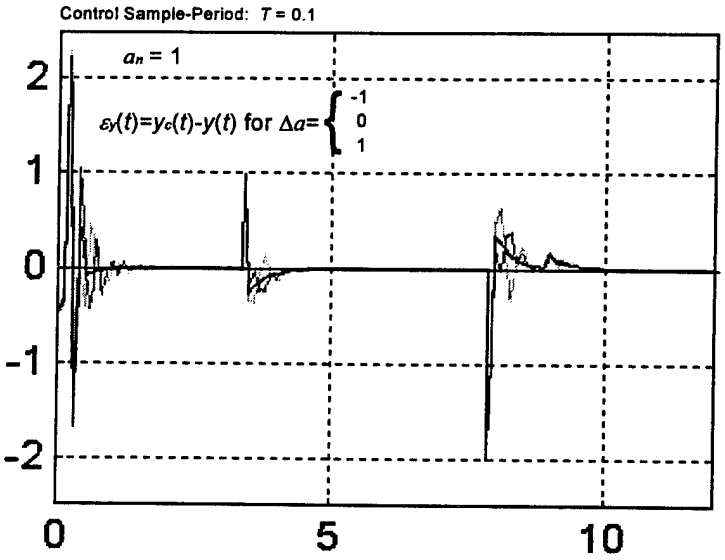

Figure 4.35 Illustration of the Servo-Tracking Error $\varepsilon_y(t)$ for Subcase 4a With an Unstable Plant, $a_n = 1$, Control Sample-Period $T = 0.1$, and $\Delta a = -1$ and 1, Overlayed on Nominal Case of $\Delta a = 0$ (compare to Figure 4.31).

4.5.4. Subcase 4b: Digital Servo-Tracking Control Design Utilizing Multirate Sampling and D/C Control-Action $u(t;kT_c;kT_y)$ for the Case of an Unstable First-Order Plant and Step+Exponential Servo-Command $y_c(t)$, and Subjected to a Step+Ramp Disturbance $w(t)$ and Parameter-Perturbation Δa

The digital servo-tracking controller in (4.158) designed in Subcase 4a can be modified to use different sampling-rates to achieve a level of servo-tracking performance that cannot be matched using a single-rate servo-controller. The digital servo-tracking controller $u(t;kT)$ in (4.158) from Subcase 4a is implemented in this Subsection such that the control terms $u_c(t;kT)$ and $u_a(t;kT)$ run at sample-rate $1/T_y$ and the control terms $u_s(t;kT)$ and $u_p(kT)$ run at sample-rate $1/T_c$. It is assumed that measurements of the plant output $y(t)$ are available every $t = kT_y$ and measurements of the servo-command $y_c(t)$ are available every $t = kT_c$ and the sample-periods T_c and T_y are related by (3.80). In that way, the ideal digital-continuous digital servo-controller equation in (4.158) is rewritten as (assuming $\alpha \neq 0$ and $a_n = 1$)

$$u(t;kT_c;kT_y) = u_c(t;kT_y) + u_s(t;kT_c) + u_p(kT_c) + u_a(t;kT_y), \tag{4.171}$$

where

$$u_c(t;kT_y) = -z_1(kT_y) - (t - kT_y)z_2(kT_y),$$

$$u_s(t;kT_c) = -a_n y_c(kT_c) + \left(\frac{e^{-\alpha(t-kT)}(a_n + \alpha) - a_n}{\alpha}\right)c_2(kT_c),$$

$$u_p(kT_c) = -\frac{a_n(e^{a_m T} - e^{a_n T})}{e^{a_n T} - 1}\left(y_c(kT_c) - y(kT_c)\right),$$

and

$$u_a(t;kT_y) = e^{a_m(t-kT_y)}z_a(kT_y).$$

The digital servo-tracking control law in (4.158) can be modified to take full benefit of the use of multiple sample-rates. For example, the particular multirate implementation in (4.171) can be altered such that an inherently unstable, or highly-oscillatory, plant (a_n=1 for Example 4) is controlled and stabilized at the higher sample-rate $1/T_y$. In that way an additional control term, postulated in continuous-time as $u_{a_m}(t) = K_m x(t)$, is designed such that the continuous-time homogeneous equation (refer to (3.83))

$$\dot{x}(t) = (a_n + bK_m)x(t) \quad , \tag{4.172}$$

has certain specified eigenvalues. For that purpose, K_m is selected such that

$$\det\left[\lambda \mathrm{I} - (a_n + bK_m)\right] = P_m(\lambda) \tag{4.173}$$

where $P_m(\lambda)$ is given in (4.125) and the term a_m in (4.124) is replaced by the composite term $a_n + bK_m$,

$$a_m = a_n + bK_m . \tag{4.174}$$

The discrete-time counterpart to the design of K_m in (4.172) is to choose $\tilde{K}_m$ to obtain

$$\det\left[\lambda \mathrm{I} - (\tilde{A}_N + \tilde{B}\tilde{K}_m)\right] = \det\left[\lambda \mathrm{I} - \tilde{A}_m\right], \tag{4.175}$$

where $\tilde{A}_N$ and $\tilde{B}$ are defined in (4.135) (with T replaced by T_y) and $\tilde{A}_m = e^{a_m T_y}$ for a_m defined in (4.174).

For this example, $\tilde{K}_m$ is designed to satisfy

$$\lambda - e^{a_n T_y} - \frac{e^{a_n T_y} - 1}{a_n}\tilde{K}_m = \lambda - e^{a_m T_y} . \tag{4.176}$$

Solving for $\tilde{K}_m$ in (4.176) yields the result ($a_n = 1$ and $a_n \neq a_m$)

$$\tilde{K}_m = \frac{a_n\left(e^{a_m T_y} - e^{a_n T_y}\right)}{e^{a_n T_y} - 1} . \tag{4.177}$$

The (ideal) control term $u_{a_m}(kT_y)$ in (3.87) can thus be chosen as

$$\begin{aligned} u_{a_m}(kT_y) &= \tilde{K}_m x(kT_y) \\ &= \frac{a_n\left(e^{a_m T_y} - e^{a_n T_y}\right)}{e^{a_n T_y} - 1} x(kT_y) \end{aligned} \tag{4.178}$$

Assuming the ideal choice for $u_{a_m}(kT_y)$ in (4.178) is implemented, the control terms $u_s(t;kT_c)$ and $u_p(kT_c)$ in (4.171) would be designed using the "new" a_n parameter. That is, the term a_n would be replaced by $a_n + b\tilde{K}_m$ and $\tilde{a}_n$ would be replaced by the exponential $e^{(a_n + b\tilde{K}_m)T_c}$ throughout the design of $u_s(t;kT_c)$ and $u_p(kT_c)$ in Subsections 4.5.3 and 4.4.5. In that way, the improved ideal multirate servo-controller equation becomes ($\alpha \neq 0$)

$$u(t;kT_y;kT_c) = u_c(t;kT_y) + u_s(t;kT_c) + u_p(kT_c) + u_a(t;kT_y) + u_{a_m}(kT_y) . \tag{4.179}$$

where

$$u_s(t;kT_c) = -\left(a_n + b\tilde{K}_m\right)y_c(kT_c) + \left(\frac{e^{-\alpha(t-kT)}\left(a_n + b\tilde{K}_m + \alpha\right) - a_n - b\tilde{K}_m}{\alpha}\right)c_2(kT_c) ,$$

$$u_p(kT_c) = -\frac{\left(a_n + b\tilde{K}_m\right)\left(e^{a_m T_c} - e^{\left(a_n + b\tilde{K}_m\right)T_c}\right)}{e^{\left(a_n + b\tilde{K}_m\right)T_c} - 1}\left(y_c(kT_c) - y(kT_c)\right), \quad \text{where} \quad \left(a_n + b\tilde{K}_m\right) \neq 0,$$

and $u_c(t;kT_y)$ and $u_a(t;kT_y)$ are given in (4.171) and $u_{a_m}(kT_y)$ is given in (4.178).

4.5.4.1. Practical Realization of the Digital Servo-Tracking Controller for Subcase 4b

The digital servo-controller in (4.179) is realized by utilizing the discrete-time reduced-order state-observer in (4.169) obtained in Subcase 4a (with T replaced by T_c), by substituting T_y for T in the hybrid full-order state-observer in (4.142) computed for Subcase 3c, and by modifying the term $\psi(u_t)$ in (4.167) in the following way.

Divide the control task in (4.179) into a discrete part $u_{kT}(kT)$ and a continuous time-varying part $u_t(t)$

$$u(t;kT_c;kT_y) = u_{kT}(kT_c) + u_t(t); \qquad kT \le t < (k+1)T, \tag{4.180}$$

where

$$u_{kT}(kT_c;kT_y) = u_p(kT_c) + u_{a_m}(kT_y),$$

and

$$u_t(t) = u_c(t;kT_y) + u_s(t;kT_c) + u_a(t;kT_y).$$

The $u_t(t)$ in (4.180) changes the value of $\psi(u_t)$ in (4.167). The new value of $\psi(u_t)$ is computed as

$$\psi(u_t) = \int_{kT_y}^{(k+1)T_y} e^{a_n((k+1)T_y - \tau)} b u_t(\tau) d\tau$$

$$= \frac{(a_n T_y + 1 - e^{a_n T_y})}{a_n^2} z_2(kT_y) + \frac{\left(e^{a_n T_y} - e^{a_m T_y}\right)}{\left(a_n - a_m\right)} z_a(kT_y) \qquad ; \tag{4.181}$$

$$+ \frac{\left(a_n + b\tilde{K}_m + \alpha\right)\left(e^{a_n T_y} e^{-\alpha(kT_y - kT_c)} - e^{-\alpha((k+1)T_y - kT_c)}\right)}{\alpha(a_n + \alpha)} c_2(kT_c) + \left(\frac{1 - e^{a_n T_y}}{a_n}\right) z_1(kT_y)$$

$$+ \frac{\left(1 - e^{a_n T_y}\right)}{a_n}\left(a_n + b\tilde{K}_m\right) y_c(kT_c) + \frac{\left(1 - e^{a_n T_y}\right)\left(a_n + b\tilde{K}_m\right)}{a_n \alpha} c_2(kT_c)$$

where $a_n = 1$, $a_n \neq a_m$, $\alpha \neq 0$, and $\alpha \neq -a_n$.

To physically realize $\psi(u_t)$, the estimates $\hat{z}_1(kT_y)$, $\hat{z}_2(kT_y)$ and $\hat{z}_a(kT_y)$ are used from the hybrid full-order state-observer (4.142) and the estimate $\hat{c}_2(kT_c)$ is obtained from the output of the discrete-time reduced-order state-observer (4.169).

4.5.4.2. Simulation Results for Subcase 4b

Simulation results were obtained for Subcase 4b using the plant, disturbance, and servo-command, given in (4.76), (4.77), and (4.150) where the value of the plant's a_n parameter, parameter-perturbation Δa in (4.123), ideal model parameter a_m in (4.124), exponential decay α on the servo-command $y_c(t)$ in (4.150), and control sample-periods T_c and T_y were chosen as

$$a_n = 1$$

$$a_m = -3,$$

$$\alpha = 1,$$

and

$$\text{Control Sample-Period: } \begin{cases} T_y = 0.01, & T_c = 1 \\ T_y = 0.05, & T_c = 0.2 \\ T_y = 0.01, & T_c = 0.2 \\ T_y = 0.01, & T_c = 0.1 \end{cases} \text{ for the cases } \begin{cases} \Delta a = 0 \\ \Delta a = -3, -1, 0, 1, 3 \\ \Delta a = -3, -1, 0, 1, 3 \\ \Delta a = -3, -1, 0, 1, 3 \end{cases}$$

The simulation results in Figure 4.36, Figure 4.38, Figure 4.40, and Figure 4.42 illustrate the plant output $y(t)$, the step+ramp disturbance $w(t)$, and the step+exponential servo-command $y_c(t)$ and the simulation plots in Figure 4.37, Figure 4.39, Figure 4.41, and Figure 4.43 show the servo-tracking error $\varepsilon_y(t) = y_c(t) - y(t)$ for Subcase 4b. In particular, the simulation plots in Figure 4.36 and Figure 4.37 are for the nominal case ($\Delta a = 0$). This subcase is provided to illustrate the added benefits that can be obtained by incorporating the additional control term $u_{a_m}(kT_y)$ in (4.178). In that way, the simulation result shown in Figure 4.36 graphs the plant outputs and the result shown in Figure 4.37 graphs the servo-tracking errors for the case of the servo-controllers $u(t;kT_y;kT_c)$, as given in (4.171) (where $u_{a_m}(kT_y) = 0$), and $u(t;kT_y;kT_c)$, as given in (4.179). The improvement provided by the control term $u_{a_m}(kT_y)$ can be seen by examining the performance between the sample times kT_c and $(k+1)T_c$, where $T_c = 1$. For the most part, the tracking error is smaller for the case when the control term $u_{a_m}(kT_y)$ is included. The simulations results shown in Figure 4.38 through Figure 4.43 utilize the multirate control law in (4.179) where $u_{a_m}(kT_y)$ is included. The simulation plots in Figure 4.38 through Figure 4.43 illustrate the performance of the plant in Subcase 4b for a variety of parameter-perturbations Δa, including perturbations as large as +/- 300% of the a_n parameter. A variety of sample periods are used to illustrate the level of performance that can be achieved by combining the sample rates in different ways. The performance of the multirate servo-controller in (4.179) (Figure 4.38 through Figure 4.43) can be compared to the performance of the single-rate servo-controller in (4.170) used in Subcase 4a (see Figure 4.28 through Figure 4.35).

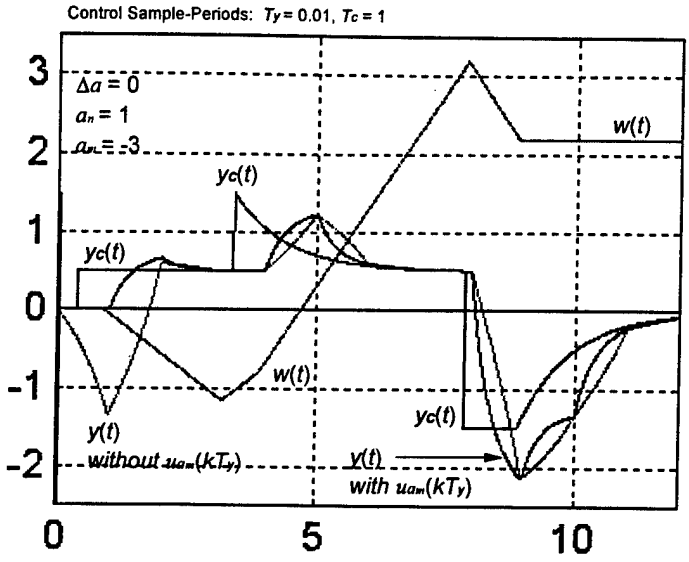

Figure 4.36 Illustration of the Plant Output $y(t)$, Disturbance $w(t)$, and Servo-Command $y_c(t)$ for Subcase 4b: An Unstable Plant ($a_n = 1$) With Known Parameters ($\Delta a = 0$) and Compensated by a Multirate Controller Using Sample Periods $T_y = 0.01$ and $T_c = 1$, With and Without the $u_{a_m}(kT_y)$ Control Term Included.

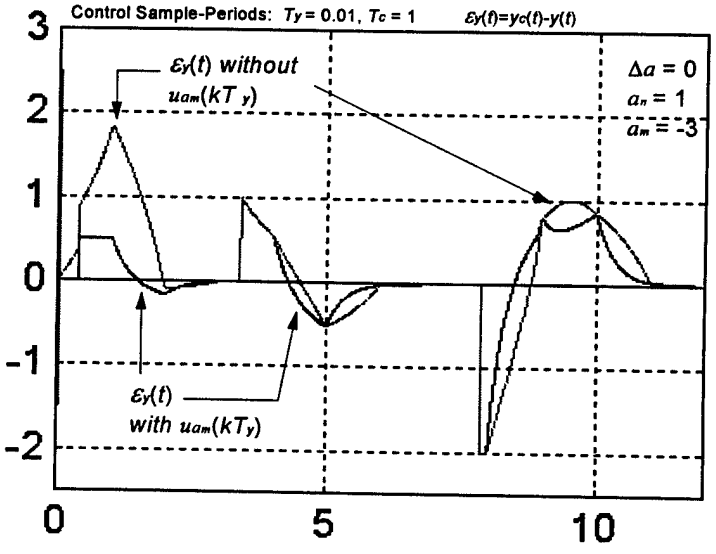

Figure 4.37 Illustration of the Servo-Tracking Error $\varepsilon_y(t)$ for Subcase 4b With An Unstable Plant ($a_n = 1$) With Known Parameters ($\Delta a = 0$) and Compensated by a Multirate Controller Using Sample Periods $T_y = 0.01$ and $T_c = 1$, With and Without the $u_{a_m}(kT_y)$ Control Term Included.

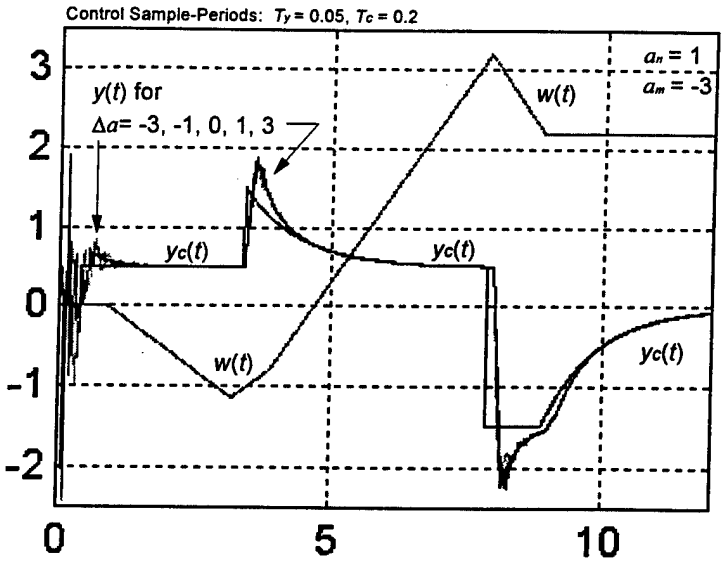

Figure 4.38 Illustration of the Plant Output $y(t)$, Disturbance $w(t)$, and Servo-Command $y_c(t)$ for Subcase 4b With An Unstable Plant (a_n = 1) Subjected to Parameter-Perturbations $\Delta a = -3, -1, 0, 1,$ and 3, and Compensated by a Multirate Controller Using Sample Periods $T_y = 0.05$ and $T_c = 0.2$.

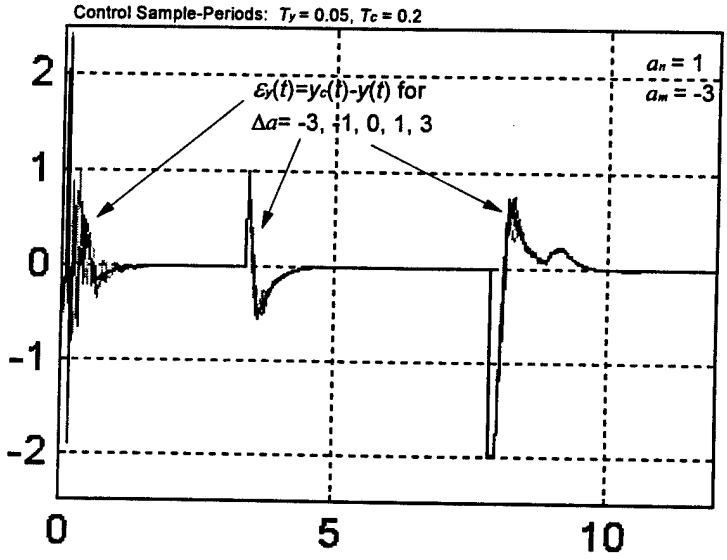

Figure 4.39 Illustration of the Servo-Tracking Error $\varepsilon_y(t)$ for Subcase 4b With An Unstable Plant ($a_n = 1$) Subjected to Parameter-Perturbations $\Delta a = -3, -1, 0, 1,$ and 3, and Compensated by a Multirate Controller Using Sample Periods $T_y = 0.05$ and $T_c = 0.2$.

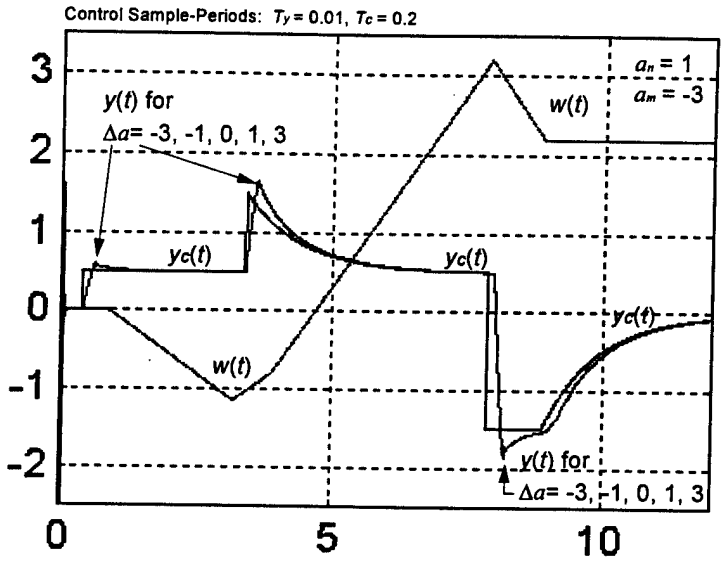

Figure 4.40 Illustration of the Plant Output $y(t)$, Disturbance $w(t)$, and Servo-Command $y_c(t)$ for Subcase 4b With An Unstable Plant $(a_n = 1)$ Subjected to Parameter-Perturbations $\Delta a = -3, -1, 0, 1,$ and 3, and Compensated by a Multirate Controller Using Sample Periods $T_y = 0.01$ and $T_c = 0.2$.

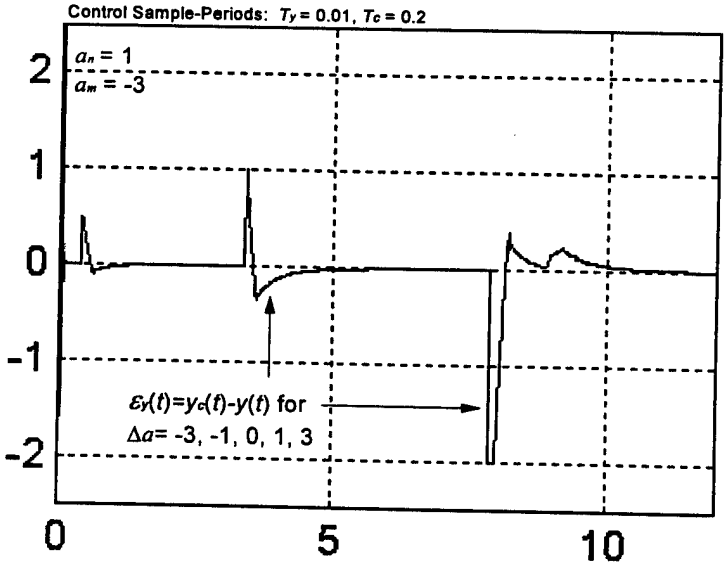

Figure 4.41 Illustration of the Servo-Tracking Error $\varepsilon_y(t)$ for Subcase 4b With An Unstable Plant $(a_n = 1)$ Subjected to Parameter-Perturbations $\Delta a = -3, -1, 0, 1,$ and 3, and Compensated by a Multirate Controller Using Sample Periods $T_y = 0.01$ and $T_c = 0.2$.

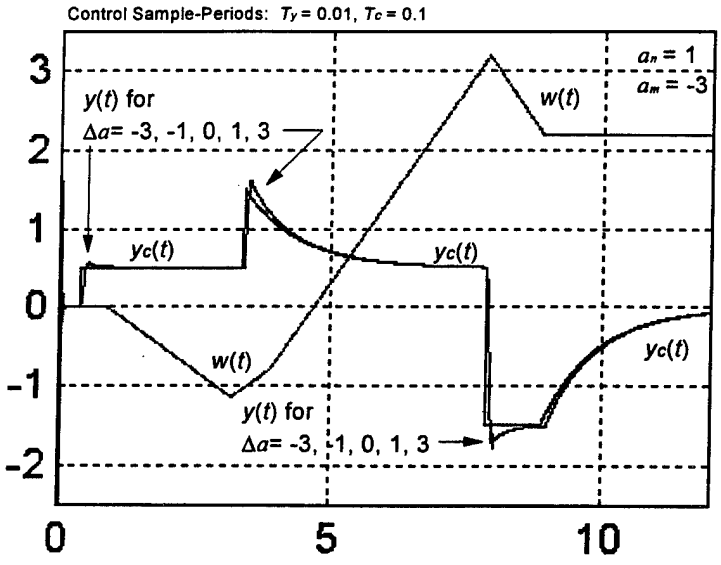

Figure 4.42 Illustration of the Plant Output $y(t)$, Disturbance $w(t)$, and Servo-Command $y_c(t)$ for Subcase 4b With An Unstable Plant ($a_n = 1$) Subjected to Parameter-Perturbations $\Delta a = -3, -1, 0, 1,$ and 3, and Compensated by a Multirate Controller Using Sample Periods $T_y = 0.01$ and $T_c = 0.1$.

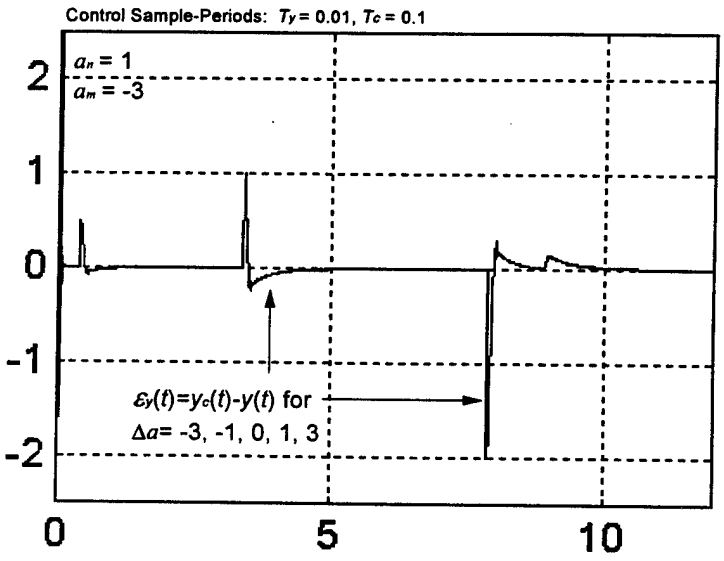

Figure 4.43 Illustration of the Servo-Tracking Error $\varepsilon_y(t)$ for Subcase 4b With An Unstable Plant ($a_n = 1$) Subjected to Parameter-Perturbations $\Delta a = -3, -1, 0, 1,$ and 3, and Compensated by a Multirate Controller Using Sample Periods $T_y = 0.01$ and $T_c = 0.1$.

4.6. Example 5: An Unstable Second-Order Plant and Stepwise-Constant Servo-Command $y_c(t)$, and Subjected to a (Step+Ramp)xDecaying-Exponential Disturbance $w(t)$ and Parameter-Perturbations ΔA

This numerical example illustrates an unstable second-order plant that is required to track a servo-command $y_c(t)$ composed of stepwise-constants. The disturbance $w(t)$ is composed of a stepwise-constant decaying-exponential and a ramp multiplied by a decaying exponential. The plant's A matrix is perturbed. A physically-realizable digital servo-controller $u(t;kT)$ having D/C holding-action is designed for Example 5, and simulation results are presented using both single-rate and multirate digital servo-controllers.

4.6.1. State Models for the Plant, Disturbance, Parameter-Perturbation, and Servo-Command for Example 5

The plant for this example is modeled by the following second-order differential equation:

$$\ddot{y}(t) = (2+\Delta a_2)\dot{y}(t) + (-1+\Delta a_1)y(t) + u(t) + w(t). \tag{4.182}$$

The disturbance $w(t)$ is known to have the following form:

$$w(t) = \left(c_1 + c_2 t\right)e^{-\alpha t}, \tag{4.183}$$

where c_1 and c_2 are unknown stepwise-constants which may "jump" in value from time-to-time, and α is a known quantity. The interval between successive jumps in c_1 and c_2 is assumed to be somewhat larger than the sampling-period T.

The state model for the plant is easily determined by choosing $x_1(t) = y(t)$ and $x_2(t) = \dot{y}(t)$ as follows:

$$\begin{aligned} \dot{x}(t) &= A_N x(t) + Bu(t) + Fw(t) + \Delta A x(t) \\ y(t) &= Cx(t) \end{aligned}, \tag{4.184}$$

where

$$A_N = \begin{bmatrix} 0 & 1 \\ -1 & 2 \end{bmatrix}, \qquad B = \begin{pmatrix} 0 \\ 1 \end{pmatrix}, \qquad F = \begin{pmatrix} 0 \\ 1 \end{pmatrix},$$

$$\Delta A = \begin{bmatrix} 0 & 0 \\ \Delta a_1 & \Delta a_2 \end{bmatrix}, \quad C = \begin{pmatrix} 1 & 0 \end{pmatrix}.$$

A similar state model is developed for the disturbance $w(t)$ in (4.183), using the techniques described in Section 2.5 by noting that between jumps in the c_i, the disturbance $w(t)$ is governed by the linear homogeneous differential equation

$$\ddot{w}(t) + 2\alpha\dot{w}(t) + \alpha^2 w(t) = 0. \tag{4.185}$$

Using the methods described in Section 2.5 the state model for the disturbance $w(t)$ in (4.185) is obtained as

$$\begin{aligned} w(t) &= Hz(t) \\ \dot{z}(t) &= Dz(t) + \sigma(t) \end{aligned}, \tag{4.186}$$

where

$$H = \begin{pmatrix} 1, & 0 \end{pmatrix},$$

$$D = \begin{bmatrix} 0 & 1 \\ -\alpha^2 & -2\alpha \end{bmatrix},$$

and

$\sigma(t)$ are uncertain, sparse impulses that "cause" the occasional "jumps" in the disturbance $w(t)$.

The parameter disturbance-effects $\Delta A x(t)$ in (4.184) are modeled as described in Subsection 3.2.4 as

$$w_a(t) = -(\Delta A)x(t). \tag{4.187}$$

As shown in [39], $w_a(t)$ is closely approximated by the known differential equation model (in (3.44)) where the coefficients β_i in (3.44) are obtained from the characteristic polynomial in (3.36) for the "ideal" closed-loop dynamics of the servo-state vector $e_{ss}(t)$ in (3.35). The ideal model in (3.35) is chosen for Example 5 as

$$\begin{aligned} \dot{e}_{ss}(t) &= A_m e_{ss}(t) \\ &= \begin{bmatrix} 0 & 1 \\ -36 & -12 \end{bmatrix} e_{ss}(t) \end{aligned}. \tag{4.188}$$

The desired characteristic equation in (3.36) is computed from (4.188) as

$$\begin{aligned} P_m(\lambda) &= \det(\lambda \mathrm{I} - A_m) \\ &= \lambda^2 + 12\lambda + 36 \\ &= (\lambda + 6)^2 \end{aligned}. \tag{4.189}$$

Proceeding as in Subsection 3.2.4, the dynamic behavior of the parameter disturbance term $(\Delta A)x(t)$ is expressed by the state model (same as (3.45))

$$\begin{aligned} -(\Delta A)x(t) = w_a(t) &= H_a z_a(t) \\ \dot{z}_a(t) &= D_a z_a(t) + \sigma_a(t) \end{aligned}, \tag{4.190}$$

where the procedure for determining H_a and D_a is given in Subsection 3.2.4. For this particular example

$$H_a = \begin{bmatrix} 0 & 0 \\ 1 & 0 \end{bmatrix}, \tag{4.191}$$

and

$$D_a = \begin{bmatrix} 0 & 1 \\ -36 & -12 \end{bmatrix}. \tag{4.192}$$

The term $\sigma_a(t)$ in (4.190) represents sporadic, sparse-in-time impulses that are the source of the uncertain intersample "jumps" that may occasionally occur in the disturbance vector $(\Delta A)x(t)$. As discussed below (3.72), the $\sigma_a(t)$ term is disregarded throughout the design process.

Using the techniques described in Section 2.6 and Subsection 3.3.2, discrete-time models can be obtained for the plant, disturbance, and parameter-disturbance vector. Those models are

Plant:

$$\begin{aligned} x((k+1)T) &= \tilde{A}_N x(kT) + \tilde{B}u_p(kT) + \psi(u_t) + \tilde{FH}z(kT) \\ &\quad - \tilde{H}_a z_a(kT) + \tilde{\gamma}(kT) - \tilde{\gamma}_a \end{aligned}, \tag{4.193}$$

$$y(kT) = Cx(kT)$$

where

$$\tilde{A}_N = e^{A_N T} = \begin{bmatrix} e^T(1-T) & Te^T \\ -Te^T & e^T(1+T) \end{bmatrix},$$

$$\tilde{B} = \int_0^T e^{A_N(T-\tau)} B d\tau = \begin{pmatrix} 1 + e^T(T-1) \\ Te^T \end{pmatrix},$$

$$\tilde{FH} = \int_0^T e^{A_N(T-\tau)} FHe^{D\tau} d\tau = \begin{bmatrix} fh_{11} & fh_{12} \\ fh_{21} & fh_{22} \end{bmatrix},$$

where

$$fh_{11} = \begin{cases} \dfrac{e^{-\alpha T}\left((\alpha+1)\alpha T + 3\alpha + 1\right) + e^T\left((T-1)(3\alpha+1) + 2T\alpha^2\right)}{(1+\alpha)^3} & \text{if } \alpha \neq -1 \\ \dfrac{T^2}{2}e^T\left(1 - \dfrac{T}{3}\right) & \text{if } \alpha = -1 \end{cases};$$

$$fh_{12} = \begin{cases} \dfrac{\left(e^{T} + e^{-\alpha T}\right)T(\alpha+1) - 2\left(e^{T} - e^{-\alpha T}\right)}{(1+\alpha)^{3}} & \text{if } \alpha \neq -1 \\ \dfrac{T^{3}}{6}e^{T} & \text{if } \alpha = -1 \end{cases};$$

$$fh_{21} = \begin{cases} \dfrac{-e^{-\alpha T}(2\alpha^{2} + \alpha^{2}T(1+\alpha)) + e^{T}(T(3\alpha+1+2\alpha^{2}) + 2\alpha^{2})}{(1+\alpha)^{3}} & \text{if } \alpha \neq -1 \\ Te^{T}\left(1 - \dfrac{T^{2}}{6}\right) & \text{if } \alpha = -1 \end{cases};$$

and

$$fh_{22} = \begin{cases} \dfrac{\left(e^{-\alpha T} - e^{T}\right)(1-\alpha(1+T)) + T(e^{T} - \alpha^{2}e^{-\alpha T})}{(1+\alpha)^{3}} & \text{if } \alpha \neq -1 \\ \dfrac{T^{2}}{2}e^{T}\left(1 + \dfrac{T}{3}\right) & \text{if } \alpha = -1 \end{cases};$$

$$\tilde{H}_{a} = \int_{0}^{T} e^{A_{N}(T-\tau)} H_{a} e^{D_{a}\tau} d\tau = \begin{bmatrix} \tilde{h}_{a11} & \tilde{h}_{a12} \\ \tilde{h}_{a21} & \tilde{h}_{a22} \end{bmatrix},$$

where

$$\tilde{h}_{a11} = e^{-6T}(0.1224T + 0.0554) + e^{T}(0.2653T - 0.0554),$$

$$\tilde{h}_{a12} = e^{-6T}(0.0204T + 0.0058) + e^{T}(0.0204T - 0.0058),$$

$$\tilde{h}_{a21} = -e^{-6T}(0.7347T + 0.2099) + e^{T}(0.2653T + 0.2099),$$

and

$$\tilde{h}_{a22} = -e^{-6T}(0.1224T + 0.0146) + e^{T}(0.0204T + 0.0146),$$

$$C = \begin{pmatrix} 1 & 0 \end{pmatrix},$$

$$\tilde{\gamma}(kT) = \int_{0}^{T} e^{A_{N}(T-\tau)} FH \int_{0}^{\tau} e^{D(\tau-\xi)} \sigma(\xi + kT) d\xi d\tau,$$

and

$$\tilde{\gamma}_{a}(kT) = \int_{0}^{T} e^{A_{N}(T-\tau)} H_{a} \int_{0}^{\tau} e^{D_{a}(\tau-\xi)} \sigma_{a}(\xi + kT) d\xi d\tau \ ;$$

Disturbance:

$$\begin{aligned} w(kT) &= Hz(kT) \\ z((k+1)T) &= \tilde{D}z(kT) + \tilde{\sigma}(kT) \end{aligned}, \tag{4.194}$$

where

$$H = \begin{pmatrix} 1, & 0 \end{pmatrix},$$

$$\tilde{D} = e^{DT} = \begin{bmatrix} e^{-\alpha T}(1+\alpha T) & Te^{-\alpha T} \\ -\alpha^2 Te^{-\alpha T} & e^{-\alpha T}(1-\alpha T) \end{bmatrix},$$

and

$$\tilde{\sigma}(kT) = \int_0^T e^{D(T-\xi)}\sigma(\xi + kT)d\xi;$$

and

Parameter-perturbation vector:

$$\begin{aligned} -\Delta Ax(t) &= w_a(kT) = H_a z_a(kT) \\ z_a((k+1)T) &= \tilde{D}_a z_a(kT) + \tilde{\sigma}_a(kT) \end{aligned}, \tag{4.195}$$

where

$$H_a = \begin{pmatrix} 0 & 0 \\ 1 & 0 \end{pmatrix},$$

$$\tilde{D}_a = e^{D_a T} = \begin{bmatrix} e^{-6T}(1+6T) & Te^{-6T} \\ -36Te^{-6T} & e^{-6T}(1-6T) \end{bmatrix},$$

and

$$\tilde{\sigma}_a(kT) = \int_0^T e^{D_a(T-\xi)}\sigma_a(\xi + kT)d\xi \quad .$$

It is hereafter assumed that $\alpha \neq 1$ throughout Example 5.

The servo-command $y_c(t)$ is assumed to be an unknown stepwise-constant command as given in (4.8). The continuous and discrete-time models for this command were obtained in (4.10) and (4.11) in Example 1.

4.6.2. The Necessary and Sufficient Condition for Achieving Exact Servo-Tracking for Example 5

The objective is to design a digital servo-tracking controller for the plant in (4.182) such that the tracking-error, defined by

$$\varepsilon_y(t) = y_c(t) - y(t), \tag{4.196}$$

goes to zero in the face of arbitrary plant initial conditions and unmeasurable plant disturbances. As first shown in [37], the necessary and sufficient conditions for achieving theoretically exact servo-tracking is that the servo-command input $y_c(t)$ must consistently lie in the column range-space of the plant-output matrix C in (4.184) for all t. In the present problem, satisfaction of this condition requires that (from (2.33))

$$\Re[G] \subseteq \Re[C] \quad . \tag{4.197}$$

If (4.197) is satisfied, then it is possible to express G as some linear combination of the columns of C. That is, $G = C\theta$ for some possibly nonunique θ. Substituting G and C from (4.10) and (4.184) into $G = C\theta$ yields

$$1 = \begin{pmatrix} 1 & 0 \end{pmatrix} \begin{pmatrix} \theta_1 \\ \theta_2 \end{pmatrix}. \tag{4.198}$$

One choice for θ satisfying (4.198) is

$$\theta = \begin{pmatrix} 1 \\ 0 \end{pmatrix}. \tag{4.199}$$

The control task is to design $u(t;kT)$ such that the servo-state vector $e_{ss}(t)$ defined by (3.2) is controlled to $\aleph[C]$. For the present example, we have chosen to stabilize $e_{ss}(t)$ to the nullpoint. In this special case, $\overline{C} = \mathrm{I}$ in (2.46), where I is the n x n ($n = 2$) identity matrix.

The plant, disturbance, and servo-command in (4.182), (4.183), and (4.8), respectively, the θ determined in (4.199), and the ideal model in (4.188) will now be used in two subcases of Example 5 using the digital servo-control techniques presented in Chapters 2 and 3 of this report.

4.6.3. Subcase 5a: Digital Servo-Tracking Control Design Utilizing D/C Control-Action $u(t;kT)$ for the Case of an Unstable Second-Order Plant and Stepwise-Constant Servo-Command $y_c(t)$, and Subjected to a (Step+Ramp)*Decaying-Exponential Disturbance $w(t)$ and Parameter-Perturbations ΔA

The ideal digital servo-tracking control law for Subcase 5 is written as

$$u(t;kT) = u_c(t;kT) + u_s(t;kT) + u_p(kT) + u_a(t;kT), \tag{4.200}$$

The D/C control terms $u_c(t;kT)$, and $u_s(t;kT)$, and $u_a(t;kT)$ are designed to provide intersample accommodation of the effects of the external disturbance and disturbance-like effects of the servo-command and parameter-perturbations. The control term $u_p(kT)$ is designed to regulate the servo-state vector $e_{ss}(t)$ to the nullpoint.

4.6.3.1. The Design of the Control Terms $u_c(t;kT)$, $u_s(t;kT)$, and $u_a(t;kT)$ to Provide Intersample Accommodation of the Effects of the Disturbance $w(t)$, Servo-Command $y_c(t)$, and Parameter-Perturbations ΔA.

The necessary and sufficient conditions for existence of the control terms $u_c(t;kT)$ satisfying (3.15), $u_s(t;kT)$ satisfying (3.16), and $u_a(t;kT)$ satisfying (3.48) are given in (3.12), (3.13), and (3.49), respectively. Satisfaction of those conditions is shown as follows:

for $u_c(t;kT)$: $\text{rank}[FH \mid B] = \text{rank}[B]$; (same as (3.12)), (4.201)

where

$$\text{rank}[FH \mid B] = \text{rank}\left[\begin{array}{cc|c} 0 & 0 & 0 \\ 1 & 0 & 1 \end{array}\right] = 1,$$

and

$$\text{rank}[B] = \text{rank}\begin{bmatrix} 0 \\ 1 \end{bmatrix} = 1;$$

for $u_s(t;kT)$: $\text{rank}[\theta E - A\theta \mid B] = \text{rank}[B]$; (same as (3.13)), (4.202)

where

$$\text{rank}[\theta E - A\theta \mid B] = \text{rank}\left[\begin{array}{c|c} 0 & 0 \\ 1 & 1 \end{array}\right] = 1,$$

and $\text{rank}[B]$ is given below (4.201);

for $u_a(t;kT)$: $\text{rank}[H_a \mid B] = \text{rank}[B]$; (same as (3.49)), (4.203)

where

$$\text{rank}[H_a \mid B] = \text{rank}\left[\begin{array}{cc|c} 0 & 0 & 0 \\ 1 & 0 & 1 \end{array}\right] = 1,$$

and $\text{rank}[B]$ is given below (4.201).

Clearly the rank conditions in (4.201), (4.202), and (4.203) are met and there exists gain matrices Γ_c, Γ_s, Γ_a such that

for Γ_c:
$$FH + B\Gamma_c = \begin{bmatrix} 0 & 0 \\ 1 & 0 \end{bmatrix} + \begin{bmatrix} 0 & 0 \\ \Gamma_{c1} & \Gamma_{c2} \end{bmatrix} = 0; \tag{4.204}$$

for Γ_s:
$$\theta E - A\theta - B\Gamma_s = \begin{pmatrix} 0 \\ 1 \end{pmatrix} - \begin{pmatrix} 0 \\ \Gamma_s \end{pmatrix} = 0; \tag{4.205}$$

for Γ_a:
$$H_a - B\Gamma_a = \begin{bmatrix} 0 & 0 \\ 1 & 0 \end{bmatrix} - \begin{bmatrix} 0 & 0 \\ \Gamma_{a1} & \Gamma_{a2} \end{bmatrix} = 0; \tag{4.206}$$

A suitable choice for Γ_c, Γ_s, and Γ_a satisfying (4.204), (4.205), and (4.206) is

$$\Gamma_c = \begin{pmatrix} -1, & 0 \end{pmatrix}, \tag{4.207}$$

$$\Gamma_s = 1, \tag{4.208}$$

and

$$\Gamma_a = \begin{pmatrix} 1, & 0 \end{pmatrix}. \tag{4.209}$$

The *continuous-time* control terms $u_c(t)$, $u_s(t)$, and $u_a(t)$ in (3.19), (3.20), and (3.51) can thus be chosen (ideally) as

$$\begin{aligned} u_c(t) &= \Gamma_c z(t) \\ &= -z_1(t) \end{aligned}, \tag{4.210}$$

$$\begin{aligned} u_s(t) &= \Gamma_s c(t) \\ &= c(t) \end{aligned}, \tag{4.211}$$

and

$$\begin{aligned} u_a(t) &= \Gamma_a z_a(t) \\ &= z_{a1}(t) \end{aligned}, \tag{4.212}$$

during the interval $kT \le t < (k+1)T$. Recall, again, that the digital controller is only allowed to use measurements, or estimates, of the states $z(t)$, $c(t)$ and $z_a(t)$ at times $t = kT$, $k = 0, 1, 2, \ldots$. Therefore, the projected or forecasted behaviors of $z(t)$, $c(t)$, and $z_a(t)$ across each intersample interval must be represented in terms of $z(kT)$, $c(kT)$, and $z_a(kT)$, respectively. This relationship is found in the general solution to (4.186), (4.10), and (4.190) evaluated at each t over the interval from kT to $t = (k+1)T$. In particular,

Disturbance state-vector:

$$z(t) = e^{D(t-kT)}z(kT) + r_c(t)$$

$$= \begin{bmatrix} e^{-\alpha(t-kT)}(1+\alpha(t-kT)) & (t-kT)e^{-\alpha(t-kT)} \\ -\alpha^2(t-kT)e^{-\alpha(t-kT)} & e^{-\alpha(t-kT)}(1-\alpha(t-kT)) \end{bmatrix} z(kT) + r_c(t) \quad ; \quad (4.213)$$

Servo-command state-vector:

$$c(t) = e^{E(t-kT)}c(kT) + r_s(t)$$

$$= c(kT) + r_s(t) \quad ; \quad (4.214)$$

Parameter-disturbance vector:

$$z_a(t) = e^{D_a(t-kT)}z_a(kT) + r_a(t)$$

$$= \begin{bmatrix} e^{-6(t-kT)}(1+6(t-kT)) & (t-kT)e^{-6(t-kT)} \\ -36(t-kT)e^{-6(t-kT)} & e^{-6(t-kT)}(1-6(t-kT)) \end{bmatrix} z_a(kT) + r_a(t) \quad ; \quad (4.215)$$

where

$r_c(t)$ is a residual-effect given by $r_c(t) = \int_{kT}^{t} e^{D(t-\tau)}\sigma(\tau)d\tau$,

$r_s(t)$ is a residual-effect given by $r_s(t) = \int_{kT}^{t} e^{E(t-\tau)}\mu(\tau)d\tau$,

and

$r_a(t)$ is a residual-effect given by $r_a(t) = \int_{kT}^{t} e^{D_a(t-\tau)}\sigma_a(\tau)d\tau$.

As discussed below (3.22) and (3.52), the $r_c(t)$, $r_s(t)$, and $r_a(t)$ terms are excluded from the design process. Substituting (4.213), (4.214), and (4.215), into (4.210), (4.211), and (4.212), respectively, and disregarding the residual terms, yields the final (idealized) form of the u_c, u_s, and u_a control terms

$$u_c(t;kT) = \Gamma_c e^{D(t-kT)}z(kT)$$

$$= \begin{pmatrix} -1, & 0 \end{pmatrix} \begin{bmatrix} e^{-\alpha(t-kT)}(1+\alpha(t-kT)) & (t-kT)e^{-\alpha(t-kT)} \\ -\alpha^2(t-kT)e^{-\alpha(t-kT)} & e^{-\alpha(t-kT)}(1-\alpha(t-kT)) \end{bmatrix} z(kT), \quad (4.216)$$

$$= -e^{-\alpha(t-kT)}(1+\alpha(t-kT))z_1(kT) - (t-kT)e^{-\alpha(t-kT)}z_2(kT)$$

$$u_s(t;kT) = \Gamma_s e^{E(t-kT)} c(kT)$$

$$= c(kT) \quad , \tag{4.217}$$

$$= y_c(kT)$$

and

$$u_a(t;kT) = \Gamma_a e^{D_a(t-kT)} z_a(kT)$$

$$= \begin{pmatrix} 1 & 0 \end{pmatrix} \begin{bmatrix} e^{-6(t-kT)}(1+6(t-kT)) & (t-kT)e^{-6(t-kT)} \\ -36(t-kT)e^{-6(t-kT)} & e^{-6(t-kT)}(1-6(t-kT)) \end{bmatrix} z_a(kT). \tag{4.218}$$

$$= e^{-6(t-kT)}(1+6(t-kT))z_{a1}(kT) + (t-kT)e^{-6(t-kT)} z_{a2}(kT)$$

4.6.3.2. The Design of the Control Term $u_p(kT)$ for Subcase 5a

The structure of the idealized servo-tracking control term $u_p(kT)$ is postulated as in (2.63). The method for designing $u_p(kT)$ was presented in Subsection 3.2.6 where $\tilde{K}_p$ in (2.63) is designed to achieve the ideal model characteristics in (4.188). In that way, the matrix $\tilde{K}_p$ is chosen to obtain the following

$$\begin{aligned} \det\left[\lambda \mathrm{I} - \left(\tilde{A}_N + \tilde{B}\tilde{K}_p\right)\right] &= \det\left(\lambda \mathrm{I} - \tilde{A}_m\right) \\ &= \lambda^2 - 2e^{-6T}\lambda + e^{-12T} \quad , \\ &= (\lambda - e^{-6T})^2 \end{aligned} \tag{4.219}$$

where $\tilde{A}_N$ and $\tilde{B}$ are defined in (4.193) and $\tilde{A}_m = e^{A_m T}$ for A_m in (4.188). In that way, (4.219) becomes

$$\begin{aligned} &\lambda^2 + \left(\left(e^T(1-T)-1\right)\tilde{K}_{p1} - e^T(T\tilde{K}_{p2}+2)\right)\lambda \\ &+ e^T(1+T-e^T)\tilde{K}_{p1} + e^T(T\tilde{K}_{p2}+e^T) = \lambda^2 - 2e^{-6T}\lambda + e^{-12T} \end{aligned} \quad , \tag{4.220}$$

and the matrix $\tilde{K}_p$ satisfying (4.220) is selected as

$$\tilde{K}_p = \left(\tilde{K}_{p1}, \quad \tilde{K}_{p2}\right), \tag{4.221}$$

where

$$\tilde{K}_{p1} = \frac{e^{2T} - e^{-12T} - 2(e^{T} - e^{-6T})}{\left(1 - e^{T}\right)^{2}},$$

and

$$\tilde{K}_{p2} = \frac{\left(e^{2T} - 2e^{T} + 2e^{-6T}\right)(T+1) + e^{-12T}(1-T) - 2e^{-5T} + e^{T}}{-T(e^{T}-1)^{2}}.$$

The control term $u_p(kT)$ postulated in (2.63) can thus be chosen (ideally) as

$$\begin{aligned} u_p(kT) &= -\tilde{K}_p e_{ss}(kT) \\ &= -\tilde{K}_p(\theta c(kT) - x(kT)) \\ &= -\frac{e^{2T} - e^{-12T} - 2(e^{T} - e^{-6T})}{\left(1 - e^{T}\right)^{2}}\left(y_c(kT) - x_1(kT)\right) \\ &\quad + \frac{\left(e^{2T} - 2e^{T} + 2e^{-6T}\right)(T+1) + e^{-12T}(1-T) - 2e^{-5T} + e^{T}}{-T(e^{T}-1)^{2}} x_2(kT) \end{aligned} \qquad (4.222)$$

The (ideal) digital servo-tracking control law in (4.200) for Subcase 5a can now be written as

$$u(t;kT) = u_c(t;kT) + u_s(t;kT) + u_p(kT) + u_a(t;kT), \qquad (4.223)$$

where $u_c(t;kT)$, $u_s(t;kT)$, $u_p(kT)$, and $u_a(t;kT)$ are given in (4.216), (4.217), (4.222), and (4.218), respectively.

4.6.3.3. Practical Realization of the Digital Servo-Tracking Controller for Subcase 5a

Estimates of the single servo-command state $c(kT)$ can be obtained directly from on-line measurements of $y_c(kT)$. Estimates of the plant state $x(kT)$, disturbance state $z(kT)$, and the parameter-perturbation state $z_a(kT)$ are generated from a hybrid full-order observer similar to that developed for Subcase 3c. The plant state $x_1(kT)$ can be obtained directly from on-line measurements of $y(kT)$ (refer to (4.193)). The hybrid full-order observer developed in this Subsection uses measurements of the plant output $y(kT)$ to obtain the real-time state estimates $\hat{x}(kT)$, $\hat{z}(kT)$, $\hat{z}_a(kT)$, $\hat{x}((k+1)T)$, $\hat{z}((k+1)T)$, and $\hat{z}_a((k+1)T)$ of $x(kT)$, $z(kT)$, $z_a(kT)$, $x((k+1)T)$, $z((k+1)T)$, and $z_a((k+1)T)$.

In order to design the hybrid full-order state-observer, a composite system must be obtained. As in Subcase 3c, the control task must be divided into a discrete part $u_p(kT)$ and a continuous time-varying part $u_t(\bullet)$, such that (4.223) is rewritten as

$$u(t;kT) = u_p(kT) + u_t(t); \qquad kT \le t < (k+1)T, \tag{4.224}$$

where $u_p(kT)$ is the portion of $u(t;kT)$ in (4.224) that is held constant between sample times, and

$$u_t(t) = u_c(t;kT) + u_s(t;kT) + u_a(t;kT) \quad , \tag{4.225}$$

is the portion of $u(t;kT)$ in (4.224) that varies with time between each successive sample-time.

Recall the discrete-time composite plant/disturbance model from (3.72),

$$\begin{pmatrix} \frac{x((k+1)T)}{z((k+1)T)} \\ \hline z_a((k+1)T) \end{pmatrix} = \left[\begin{array}{c|c|c} \tilde{A}_N & \tilde{FH} & -\tilde{H}_a \\ \hline 0 & \tilde{D} & 0 \\ \hline 0 & 0 & \tilde{D}_a \end{array}\right] \begin{pmatrix} \frac{x(kT)}{z(kT)} \\ \hline z_a(kT) \end{pmatrix} + \begin{pmatrix} \frac{\tilde{B}}{0} \\ \hline 0 \end{pmatrix} u_p(kT) + \begin{pmatrix} \frac{\psi(u_t)}{0} \\ \hline 0 \end{pmatrix}$$

$$+ \begin{pmatrix} \frac{\tilde{\gamma}(kT) - \tilde{\gamma}_a(kT)}{\tilde{\sigma}(kT)} \\ \hline \tilde{\sigma}_a(kT) \end{pmatrix} \quad , \tag{4.226}$$

where $\tilde{A}_N$, $\tilde{B}$, $\tilde{FH}$, $\tilde{H}_a$, $\tilde{D}$, $\tilde{D}_a$, $\tilde{\gamma}(kT)$, $\tilde{\gamma}_a(kT)$, $\tilde{\sigma}(kT)$, and $\tilde{\sigma}_a(kT)$ are given in (4.193), (4.194), and (4.195) and $\psi(u_t)$ is computed as (assuming $\alpha \neq -1$)

$$\psi(u_t) = \int_0^T e^{A_N(T-\tau)} B u_t(\tau) d\tau = \begin{pmatrix} \psi_1 \\ \psi_2 \end{pmatrix} \quad , \tag{4.227}$$

where

$$\begin{aligned} \psi_1 = & \frac{-e^{-\alpha T}(\alpha T(1+\alpha)+1+3\alpha) - e^{T}(T(1+3\alpha+2\alpha^2)-1-3\alpha)}{(1+\alpha)^3} z_1(kT) \\ & + \frac{-e^{-\alpha T}(T(1+\alpha)+2) - e^{T}(T(1+\alpha)-2)}{(1+\alpha)^3} z_2(kT) \\ & + \left(e^{-6T}(0.0554 + 0.1224T) + e^{T}(0.2653T - 0.0554)\right) z_{a1}(kT) \\ & + \left(e^{-6T}(0.00583 + 0.0204T) + e^{T}(0.0204T - 0.00583)\right) z_{a2}(kT) \\ & + \left(1 + e^{T}(T-1)\right) y_c(kT) \end{aligned} \quad ,$$

and

$$\psi_2 = \frac{\alpha^2 e^{-\alpha T}(2+T(1+\alpha)-e^T(2\alpha^2(1+T)+T(1+3\alpha)}{(1+\alpha)^3} z_1(kT)$$
$$+\frac{T(1+\alpha)(\alpha e^{-\alpha T}-e^T)+(\alpha-1)(e^{-\alpha T}-e^T)}{(1+\alpha)^3} z_2(kT)$$
$$+\left(e^T(0.0379+0.2099)-e^{-6T}(0.7347T-0.2099)\right) z_{a1}(kT)$$
$$+\left(e^T(0.0204T+0.0146)+e^{-6T}(0.1225T+0.0146)\right) z_{a2}(kT)$$
$$+Te^T y_c(kT)$$

The hybrid full-order state-observer equations are given in (3.76) as

$$\begin{pmatrix} \hat{x}((k+1)T) \\ \hat{z}((k+1)T) \\ \hat{z}_a((k+1)T) \end{pmatrix} = \left[\begin{array}{c|c|c} \widetilde{A}_N & \widetilde{FH} & -\widetilde{H}_a \\ \hline 0 & \widetilde{D} & 0 \\ \hline 0 & 0 & \widetilde{D}_a \end{array}\right] \begin{pmatrix} \hat{x}(kT) \\ \hat{z}(kT) \\ \hat{z}_a(kT) \end{pmatrix} + \begin{pmatrix} \widetilde{B} \\ \hline 0 \\ \hline 0 \end{pmatrix} u_p(kT) + \begin{pmatrix} \psi(u_t) \\ \hline 0 \\ \hline 0 \end{pmatrix}$$
$$+ \left[\begin{array}{c} \widetilde{K}_{01} \\ \hline \widetilde{K}_{02} \\ \hline \widetilde{K}_{03} \end{array}\right] \left[(C \mid 0 \mid 0) \begin{pmatrix} \hat{x}(kT) \\ \hat{z}(kT) \\ \hat{z}_a(kT) \end{pmatrix} - y(kT) \right] \quad , \quad (4.228)$$

where $\widetilde{A}_N$, $\widetilde{B}$, $\widetilde{FH}$, C, $\widetilde{H}_a$, $\widetilde{D}$, $\widetilde{D}_a$, and $\psi(u_t)$ are given in (4.193), (4.194), (4.195), and (4.227) and where $\widetilde{K}_0 = \left[\begin{array}{c} \widetilde{K}_{01} \\ \hline \widetilde{K}_{02} \\ \hline \widetilde{K}_{03} \end{array}\right]$ is an observer gain-matrix to be determined.

The general discrete-time evolution equations for the error dynamics of the hybrid full-order observer are given in (3.77) as

$$\begin{pmatrix} \varepsilon_x((k+1)T) \\ \varepsilon_z((k+1)T) \\ \varepsilon_{z_a}((k+1)T) \end{pmatrix} = \begin{pmatrix} \hat{x}((k+1)T) \\ \hat{z}((k+1)T) \\ \hat{z}_a((k+1)T) \end{pmatrix} - \begin{pmatrix} x((k+1)T) \\ z((k+1)T) \\ z_a((k+1)T) \end{pmatrix}$$
$$= \left[\begin{array}{c|c|c} \widetilde{A}_N + \widetilde{K}_{01}C & \widetilde{FH} & -\widetilde{H}_a \\ \hline \widetilde{K}_{02}C & \widetilde{D} & 0 \\ \hline \widetilde{K}_{03}C & 0 & \widetilde{D}_a \end{array}\right] \begin{pmatrix} \varepsilon_x(kT) \\ \varepsilon_z(kT) \\ \varepsilon_{z_a}(kT) \end{pmatrix} \quad (4.229)$$

As before, it is desirable to design $\tilde{K}_0$ so that the observer error $\begin{pmatrix} \varepsilon_x(kT) \\ \varepsilon_z(kT) \\ \varepsilon_{z_a}(kT) \end{pmatrix}$ goes to zero promptly. Pole placement is used to determine an appropriate $\tilde{K}_0$, where the roots of the characteristic polynomial

$$\det\left[\lambda \mathrm{I} - \left[\begin{array}{c|c|c} \tilde{A} + \tilde{K}_{01}C & \tilde{FH} & -\tilde{H}_a \\ \hline \tilde{K}_{02}C & \tilde{D} & 0 \\ \hline \tilde{K}_{03}C & 0 & \tilde{D}_a \end{array}\right]\right] = P(\lambda)_{desired} . \tag{4.230}$$

are such that the observer estimated value of the plant state $\hat{x}(kT)$, disturbance state $\hat{z}(kT)$, and parameter-perturbation state $\hat{z}_a(kT)$, quickly and accurately track the actual corresponding plant, disturbance, and parameter-perturbation states $x(kT)$, $z(kT)$, and $z_a(kT)$. This means that the roots of $P(\lambda)_{desired}$ in (4.230) can placed at sufficiently-damped locations inside the unit circle ($|\lambda_i| < 1$). For the present example, $P(\lambda)_{\text{desired}}$ is chosen as

$$P(\lambda)_{\text{desired}} = \lambda^6 . \tag{4.231}$$

For Subcase 5a, there are six observer gain values that must be obtained. Computation of those observer gains is greatly simplified by selecting the sample-period T and the decay-rate α on the exponential portion of the disturbance. For the present example, $T = 0.1$ and $\alpha = 1$. Substituting those values and (4.231) into (4.230) and solving for $\tilde{K}_0$ yields

$$\tilde{K}_{0\,(T\,=\,0.1,\,\alpha\,=\,1)} = \begin{bmatrix} \tilde{K}_{011} \\ \tilde{K}_{012} \\ \tilde{K}_{021} \\ \tilde{K}_{022} \\ \tilde{K}_{031} \\ \tilde{K}_{032} \end{bmatrix} = \begin{bmatrix} -5.1176 \\ -66.3346 \\ 23.6918 \\ -4792.8605 \\ 509.7822 \\ -2436.9102 \end{bmatrix} . \tag{4.232}$$

4.6.3.4. Simulation Results for Subcase 5a

Incorporation of the hybrid full-order observer in (4.228) and substituting (4.216), (4.217), (4.218), and (4.222) into (4.200) will result in the physically-realizable digital servo-control law for Subcase 5a

$$u(t;kT) = u_c(t;kT) + u_s(t;kT) + u_p(kT) + u_a(t;kT)$$

$$= -e^{-\alpha(t-kT)}(1+\alpha(t-kT))\hat{z}_1(kT) - (t-kT)e^{-\alpha(t-kT)}\hat{z}_2(kT)$$

$$+ c(kT) - \frac{e^{2T} - e^{-12T} - 2(e^T - e^{-6T})}{\left(1-e^T\right)^2}\left(y_c(kT) - y(kT)\right) \qquad (4.233)$$

$$+ \frac{\left(e^{2T} - 2e^T + 2e^{-6T}\right)(T+1) + e^{-12T}(1-T) - 2e^{-5T} + e^T}{-T(e^T-1)^2}\hat{x}_2(kT)$$

$$+ e^{-6(t-kT)}(1+6(t-kT))\hat{z}_{a1}(kT) + (t-kT)e^{-6(t-kT)}\hat{z}_{a2}(kT)$$

Simulations results were obtained for the unstable, second-order plant, (step+ramp) x exponential disturbance, and stepwise-constant servo-command given in (4.182), (4.183), and (4.8). As stated above (4.232), the control sample-period for Subcase 5a is $T = 0.1$ and the exponential decay on the disturbance is $\alpha = 1$.

The simulation results shown in Figure 4.44 and Figure 4.46 illustrate the plant output $y(t)$, the disturbance $w(t)$, and the servo-command $y_c(t)$. The simulation results in Figure 4.44 illustrate the case of no parameter-perturbations ($\Delta a_1 = \Delta a_2 = 0$). The simulation results in Figure 4.46 illustrate the case of parameter-perturbations $\Delta a = (\Delta a_1, \Delta a_2) = (0.4, -0.8)$, and $(-0.4, 0.8)$, overlayed on the nominal case of $\Delta a = (0,0)$. The simulation results in Figure 4.45 (for the case $\Delta a = (0,0)$) and Figure 4.47 show the corresponding servo-tracking error $\varepsilon_y(t) = y_c(t) - y(t)$ for Subcase 5a.

Notice the oscillations in the plant output $y(t)$ shown in Figure 4.46 for the case of $\Delta a = (0.4, -0.8)$. Those oscillations (due primarily to the uncertainty of parameters in the A matrix in (4.184)), are growing, thus preventing the plant output $y(t)$ from achieving and maintaining a zero tracking-error. As will be seen in the next example, those oscillations can be eliminated by implementing certain control terms at a higher sample-rate.

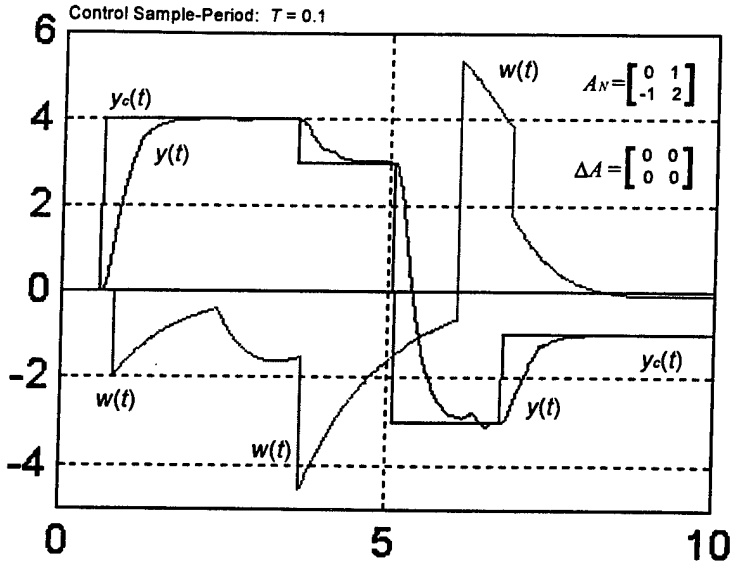

Figure 4.44 Illustration of the Plant Output $y(t)$, Disturbance $w(t)$, and Servo-Command $y_c(t)$ for Subcase 5a With an Unstable Plant, No Parameter-Perturbations and Control Sample-Period $T = 0.1$.

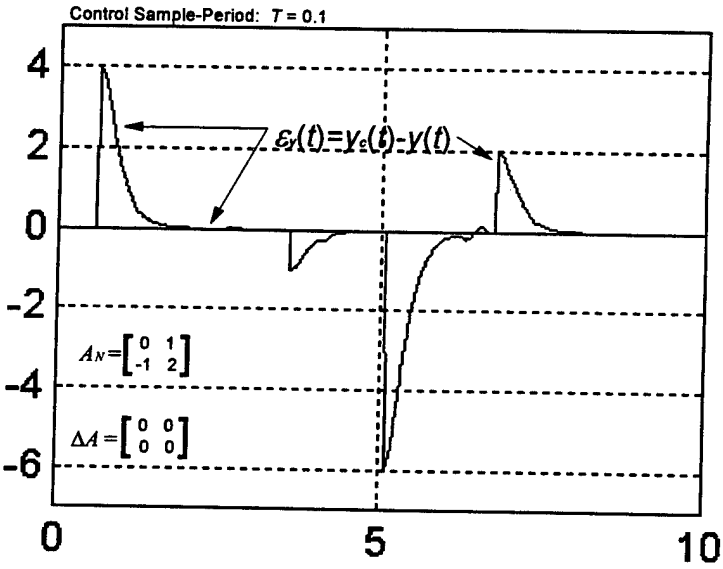

Figure 4.45 Illustration of the Tracking-Error $\varepsilon_y(t)$ for Subcase 5a With an Unstable Plant, No Parameter-Perturbations and Control Sample-Period $T = 0.1$.

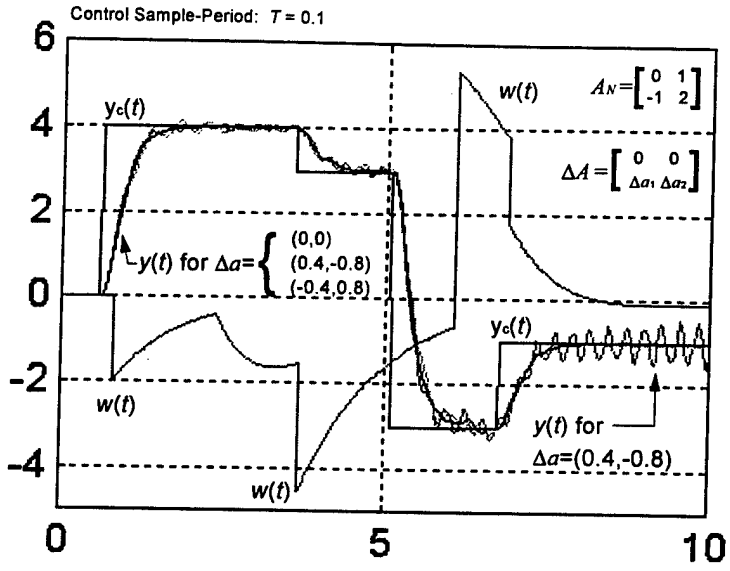

Figure 4.46 Illustration of the Plant Output $y(t)$, Disturbance $w(t)$, and Servo-Command $y_c(t)$ for Subcase 5a With an Unstable Second-Order Plant, Control Sample-Period $T = 0.1$, and Parameter-Perturbations $(\Delta a = (\Delta a_1, \Delta a_2) = (0.4, -0.8)$, and $(-0.4, 0.8))$ Overlayed on Nominal Case of $\Delta a_1 = \Delta a_2 = 0$.

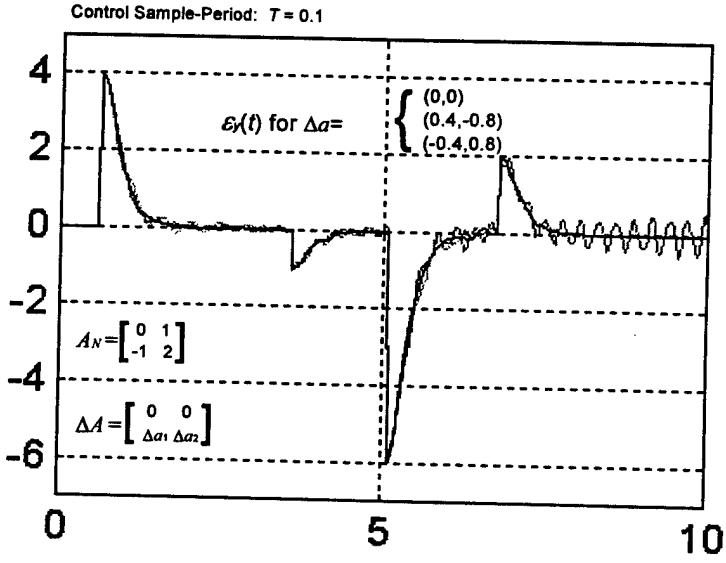

Figure 4.47 Illustration of the Tracking-Error $\varepsilon_y(t)$ for Subcase 5a With an Unstable Second-Order Plant, Control Sample-Period $T = 0.1$, and Parameter-Perturbations $(\Delta a = (\Delta a_1, \Delta a_2) = (0.4, -0.8)$, and $(-0.4, 0.8))$ Overlayed on Nominal Case of $\Delta a_1 = \Delta a_2 = 0$.

4.6.4. Subcase 5b: Digital Servo-Tracking Control Design Utilizing Multirate Sampling and D/C Control-Action $u(t;kT_c;kT_y)$ for the Case of an Unstable Second-Order Plant and Stepwise-Constant Servo-Command $y_c(t)$, and Subjected to a (Step+Ramp)xDecaying Exponential Disturbance $w(t)$ and Parameter-Perturbations ΔA

The digital servo-tracking control algorithm in (4.233), designed in Subcase 5a, can utilize multiple sampling-periods to achieve a level of high-performance servo-tracking that cannot be matched by a single-rate controller. In this Subsection, the digital servo-tracking controller from Subcase 5a is implemented such that the control terms associated with the plant, $u_c(t;kT)$ and $u_a(t;kT)$, operate at one sample-period T_y and the control terms associated with the servo-command, $u_s(t;kT)$ and $u_p(kT)$, operate at another sample-period T_c . In that way, the ideal digital servo-controller in (4.233) becomes

$$u(t;kT_c;kT_y) = u_c(t;kT_y) + u_s(t;kT_c) + u_p(kT_c) + u_a(t;kT_y), \tag{4.234}$$

where

$$u_c(t;kT_y) = -e^{-\alpha(t-kT_y)}(1+\alpha(t-kT_y))\hat{z}_1(kT_y) - (t-kT_y)e^{-\alpha(t-kT_y)}\hat{z}_2(kT_y),$$

$$u_s(t;kT_c) = c(kT_c) = y_c(kT_c),$$

$$u_p(kT_c) = -\frac{e^{2T} - e^{-12T_c} - 2(e^{T_c} - e^{-6T_c})}{\left(1-e^{T_c}\right)^2}\left(y_c(kT_c) - y(kT_c)\right)$$

$$+\frac{\left(e^{2T_c} - 2e^{T_c} + 2e^{-6T_c}\right)(T_c+1) + e^{-12T_c}(1-T_c) - 2e^{-5T_c} + e^{T_c}}{-T_c(e^{T_c}-1)^2}\hat{x}_2(kT_c),$$

and

$$u_a(t;kT_y) = e^{-6(t-kT_y)}(1+6(t-kT_y))\hat{z}_{a1}(kT_y) + (t-kT_y)e^{-6(t-kT_y)}\hat{z}_{a2}(kT_y).$$

The design of the digital servo-tracking controller can be modified to take additional benefit of the use of multiple sample-rates. For example, the particular multirate implementation discussed above can be altered such that the inherently unstable plant (A_N matrix in (4.184) having poles in the right-half plane) can be brought under control at the higher sample-rate $1/T_y$. In that way an additional control term, postulated in continuous-time as $u_{a_m}(t) = K_m x(t)$, is designed such that the homogeneous equation

$$\dot{x}(t) = (A_N + BK_m)x(t) \quad , \tag{4.235}$$

has certain specified eigenvalues. Following the method described in Section 3.4, K_m should be selected such that

$$\det\left[\lambda \mathrm{I} - (A_N + BK_m)\right] = P_m(\lambda) \tag{4.236}$$

where $P_m(\lambda)$ is given in (4.189).

The discrete-time counterpart to the design of K_m in (4.236) is to choose $\widetilde{K}_m$ to obtain

$$\begin{aligned}\det\left[\lambda \mathrm{I} - \left(\widetilde{A}_N + \widetilde{B}\widetilde{K}_m\right)\right] &= \det\left[\lambda \mathrm{I} - \widetilde{A}_m\right] \\ &= \lambda^2 - 2e^{-6T_y}\lambda + e^{-12T_y}\ , \\ &= (\lambda - e^{-6T_y})^2\end{aligned} \tag{4.237}$$

where $\widetilde{A}_N$, and $\widetilde{B}$ are given in (4.193) (with T replaced by T_y) and $\widetilde{A}_m = e^{A_m T_y}$ for A_m in (4.188).

For the present example, $\widetilde{K}_m$ is designed to achieve (incorporating the values of $\widetilde{A}_N$ and $\widetilde{B}$ into (4.237))

$$\begin{aligned}&\lambda^2 + \left(\left(e^{T_y}(1 - T_y) - 1\right)\widetilde{K}_{m1} - e^{T_y}(T_y\widetilde{K}_{m2} + 2)\right)\lambda \\ &+ e^{T_y}(1 + T_y - e^{T_y})\widetilde{K}_{m1} + e^{T_y}(T_y\widetilde{K}_{m2} + e^{T_y}) = \lambda^2 - 2e^{-6T_y}\lambda + e^{-12T_y}\end{aligned} \tag{4.238}$$

A $\widetilde{K}_m$ satisfying (4.238) is

$$\widetilde{K}_m = \left(\widetilde{K}_{m1},\ \ \widetilde{K}_{m2}\right), \tag{4.239}$$

where

$$\widetilde{K}_{m1} = \frac{e^{2T_y} - e^{-12T_y} - 2(e^{T_y} - e^{-6T_y})}{\left(1 - e^{T_y}\right)^2},$$

and

$$\widetilde{K}_{m2} = \frac{\left(e^{2T_y} - 2e^{T_y} + 2e^{-6T_y}\right)(T_y + 1) + e^{-12T_y}(1 - T_y) - 2e^{-5T_y} + e^{T_y}}{-T_y(e^{T_y} - 1)^2}.$$

The idealized control term $u_{a_m}(kT_y)$ is thus chosen (ideally) as (same as 3.87)

$$u_{a_m}(kT_y) = \widetilde{K}_m x(kT_y), \tag{4.240}$$

where $\widetilde{K}_m$ is given in (4.239).

Assuming the ideal choice for $u_{a_m}(kT_y)$ in (4.240) is implemented, the control terms $u_s(t;kT_c)$ and $u_p(kT_c)$ in (4.234) would be re-computed using the "new" A matrix. That is, the term A_N would be replaced by $A_N + B\widetilde{K}_m$ and $\widetilde{A}_N$ would be replaced by the matrix exponential $e^{(A_N+B\widetilde{K}_m)T_y}$ throughout the design of $u_s(t;kT_c)$ and $u_p(kT_c)$ in Subsections 4.6.3.1 and 4.6.3.2. In order to simplify the calculations for $u_p(kT_c)$ and $u_{a_m}(kT_y)$, it is hereafter assumed that the sample-period $T_y = 0.04$ and the multirate digital servo-controller will be obtained for the cases $T_c = 0.08, 0.1, 0.2,$ and 0.8. In that way, the multirate servo-controller equation in (4.234) is recomputed as

$$u(t;kT_y;kT_c) = u_c(t;kT_y) + u_s(t;kT_c) + u_p(kT_c) + u_a(t;kT_y) + u_{a_m}(kT_y), \qquad (4.241)$$

where $u_c(t;kT_y)$ and $u_a(t;kT_y)$ are given in (4.234), and

$$u_s(t;kT_c) = 27.335y_c(kT_c),$$

$$u_p(kT_c) = \begin{cases} 0.0214\big(y_c(kT_c) - y(kT_c)\big) + 0.0026\hat{x}_2(kT_c) & \text{for } T_c = 0.8 \\ -0.9122\big(y_c(kT_c) - y(kT_c)\big) - 0.3185\hat{x}_2(kT_c) & \text{for } T_c = 0.2 \\ -2.9306\big(y_c(kT_c) - y(kT_c)\big) - 0.8594\hat{x}_2(kT_c) & \text{for } T_c = 0.1 \\ -3.6533\big(y_c(kT_c) - y(kT_c)\big) - 1.0465\hat{x}_2(kT_c) & \text{for } T_c = 0.08 \end{cases},$$

and

$$u_{a_m}(kT_y) = -26.3354y(kT_y) - 11.6911\hat{x}_2(kT_y).$$

Estimates $\hat{z}(kT_y)$, $\hat{x}(kT_y)$, and $\hat{z}_a(kT_y)$, are obtained from the hybrid full-order observer described in the following Subsection.

4.6.4.1. Practical Realization of the Digital Servo-Tracking Controller for Subcase 5b

The digital servo-controller in (4.241) can be realized by substituting T_y for T in the hybrid full-order observer in (4.228) and the $\psi(u_t)$ in (4.227) computed for Subcase 5a, re-calculating the observer gain-matrix $\widetilde{K}_0$ in (4.232) for the appropriate value of T_y, and by replacing $u_p(kT)$ in (4.228) with $u_p(kT_y) + u_{a_m}(kT_y)$ in (4.241) (with T_c replaced by T_y in $u_p(kT_c)$). The necessary estimate $\hat{x}(kT_c)$ is then obtained by passing $\hat{x}(kT_y)$ through a zero-order-hold device having a hold time of T_c.

The observer gain-matrix $\widetilde{K}_0$ in (4.232) in Subcase 5a was computed for a sample period of $T = 0.1$ and $\alpha = 1$. In this example, a sample period of $T_y = 0.04$ was chosen. The observer gain-matrix for the sample-period $T_y = 0.04$ was computed and is given as

$$\widetilde{K}_{0\,(T=0.4,\,\alpha=1)} = \begin{bmatrix} \widetilde{K}_{011} \\ \widetilde{K}_{012} \\ \widetilde{K}_{021} \\ \widetilde{K}_{022} \\ \widetilde{K}_{031} \\ \widetilde{K}_{032} \end{bmatrix} = \begin{bmatrix} -5.5765 \\ -192.0704 \\ 101{,}503.1367 \\ -523{,}029.3915 \\ 106{,}033.9770 \\ -447{,}932.2637 \end{bmatrix} . \tag{4.242}$$

4.6.4.2. Simulation Results for Subcase 5b

Simulation results were obtained for the example plant, disturbance, and servo-command, given in (4.182), (4.183), and (4.8), where the parameter-perturbation Δa and control sample-periods T_c, T_y, and T_s are given by

Control Sample-Periods:

$$\begin{cases} T_y = 0.04,\ T_c = 0.8 \\ T_y = 0.04,\ T_c = 0.1 \\ T_y = 0.04,\ T_c = 0.2,\ T_s = 0.8 \text{ for the cases} \\ T_y = 0.04,\ T_c = 0.08 \\ T_y = 0.04,\ T_c = 0.08 \end{cases} \begin{cases} \Delta a = (0,0),(0.4,-0.8),(-0.4,0.8),(0.8,-1.8) \\ \Delta a = (0,0),(0.4,-0.8),(-0.4,0.8),(0.8,-1.8) \\ \Delta a = (0,0),(20,1.6),(-18,-1.3),(-27,1.9) \\ \Delta a = (0,0),(0.4,-0.8),(-0.4,0.8),(0.8,-1.8) \\ \Delta a = (0,0),(-1.4,-1.2),(0.9,1.6),(-3.2,0.2) \end{cases} . \tag{4.243}$$

The sample-period $T_s = 0.8$ is used in one of the simulations to illustrate that more than two different sample rates may be employed. In that case, the u_s control term in (4.241) is implemented using sample-period T_s. No recalculations are necessary to incorporate the sample-period T_s.

The simulation results in Figure 4.48 and Figure 4.50 illustrate the plant output $y(t)$, the disturbance $w(t)$, and the servo-command $y_c(t)$, and the simulation results in Figure 4.49 and Figure 4.51 show the corresponding servo-tracking error $\varepsilon_y(t) = y_c(t) - y(t)$ for the case of $T_y = 0.04$, $T_c = 0.8$ (Figure 4.48 and Figure 4.49 only), $T_c = 0.1$ (Figure 4.49 and Figure 4.50 only) and parameter-perturbations $\Delta a = (0,0),(0.4,-0.8),(-0.4,0.8)$, and $(0.8,-1.8)$. Although the tracking is slower in Figure 4.48 compared to Figure 4.50 (tracking done at $T_c = 0.8$ versus $T_c = 0.1$), the response is much smoother than that obtained in Figure 4.50. In fact, the effects of the parameter-perturbations $\Delta a = (0,0),(0.4,-0.8),(-0.4,0.8)$, and $(0.8,-1.8)$ are virtually undetectable in the simulation plots in Figure 4.48 and Figure 4.49, but become quite noticeable in the plots in Figure 4.50 and Figure 4.51. Why does the case of $T_y = 0.04$ and $T_c = 0.8$ appear to be more robust than the faster sample-rate case of $T_y = 0.04$ and $T_c = 0.1$? Recall the assumption in (3.80) that the samplers of the system are synchronized, integer multiples. That is,

$$T_c = \eta T_y ,$$

where η is some positive integer. And remember that the control term $u_{a_m}(kT_y)$ actually changes the value of the plant's A_N matrix, thus requiring the control terms running at the sample-rate $1/T_c$ to be recomputed to reflect this change in parameter. If the different sample-rates are not synchronized, integer multiples, the terms running at the lower sample-rate $1/T_c$ will compute the new value of A_N incorrectly and respond with an inappropriate control-action. The sample-periods $T_y = 0.04$ and $T_c = 0.1$ (see Figure 4.50 and Figure 4.51) are not related by an integer, or equivalently,

$$0.1 \stackrel{?}{=} \eta 0.04 \quad \Rightarrow \quad \eta \neq \text{integer},$$

and consequently do not meet the assumptions for implementing the digital servo-tracking controller as a multirate controller when the control term $u_{a_m}(kT_y)$ is included. If the $u_{a_m}(kT_y)$ control term is excluded, and $u(t;kT)$ is implemented as in (4.234), the integer-multiple restriction no longer applies. However, in that case, the response for this particular example will suffer severely (become unstable) due to the natural instability of the plant.

The simulation results in Figure 4.52, Figure 4.54, and Figure 4.56 illustrate the plant output $y(t)$, the disturbance $w(t)$, and the servo-command $y_c(t)$, and the simulation results in Figure 4.53, Figure 4.55, and Figure 4.57 show the corresponding servo-tracking error $\varepsilon_y(t) = y_c(t) - y(t)$ for a variety of sample-periods and parameter-perturbations for Subcase 5b. Those simulation plots illustrate the performance of the example problem for a variety of parameter-perturbations, including perturbations on the order of +/-2000% of the nominal value of the a_{n1} parameter $(a_{n1} = -1)$ and as large as 95% of the nominal value of the a_{n2} parameter $(a_{n2} = 2)$. The perturbations and sample-periods are given in the figure headings and in (4.243).

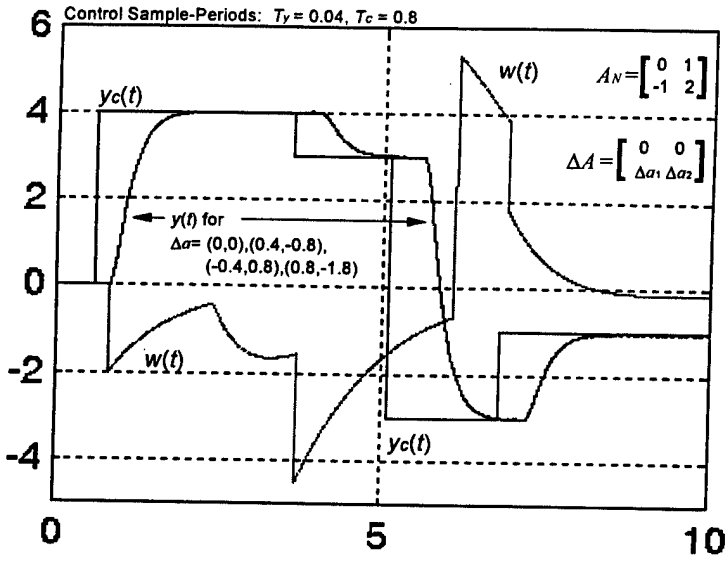

Figure 4.48 Illustration of the Plant Output $y(t)$, Disturbance $w(t)$, and Servo-Command $y_c(t)$ for Subcase 5b With An Unstable Second-Order Plant Subjected to Parameter-Perturbations $\Delta a = (0,0),(0.4,-0.8),(-0.4,0.8)$, and $(0.8,-1.8)$, and Compensated by a Multirate D/C Controller Using Sample-Periods $T_y = 0.04$ and $T_c = 0.8$.

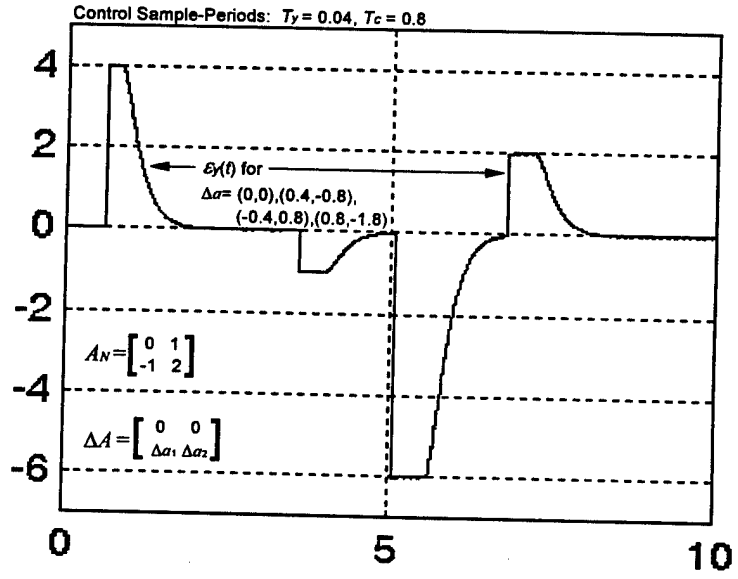

Figure 4.49 Illustration of the Tracking Error $\varepsilon_y(t)$ for Subcase 5b With An Unstable Second-Order Plant Subjected to Parameter-Perturbations $\Delta a = (0,0),(0.4,-0.8),(-0.4,0.8)$, and $(0.8,-1.8)$, and Compensated by a Multirate D/C Controller Using Sample-Periods $T_y = 0.04$ and $T_c = 0.8$.

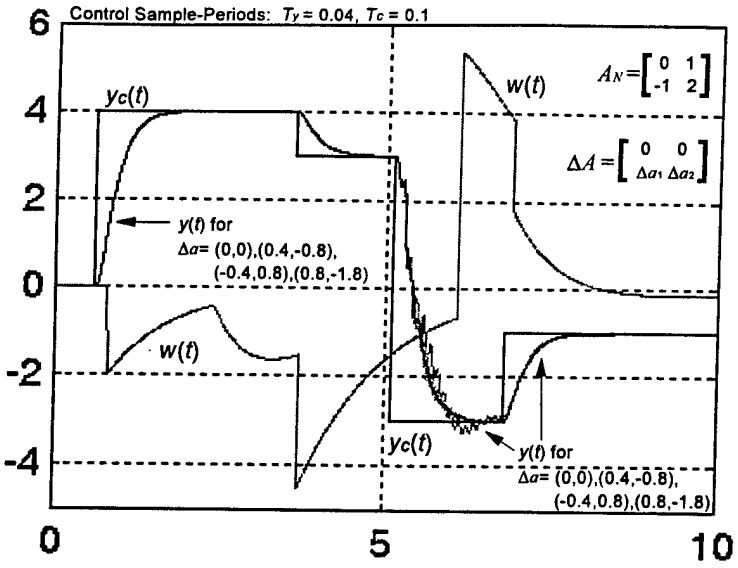

Figure 4.50 Illustration of the Plant Output $y(t)$, Disturbance $w(t)$, and Servo-Command $y_c(t)$ for Subcase 5b With An Unstable Second-Order Plant Subjected to Parameter-Perturbations $\Delta a = (0,0),(0.4,-0.8),(-0.4,0.8)$, and $(0.8,-1.8)$, and Compensated by a Multirate D/C Controller Using Sample-Periods $T_y = 0.04$ and $T_c = 0.1$.

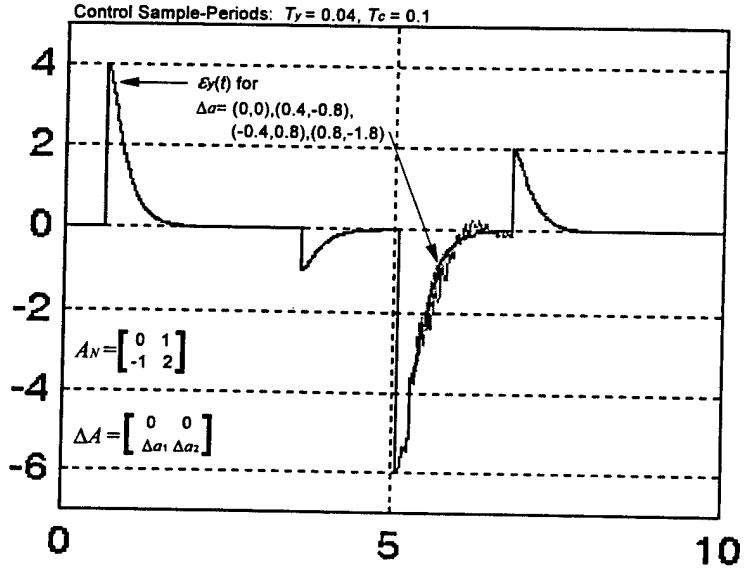

Figure 4.51 Illustration of the Tracking Error $\varepsilon_y(t)$ for Subcase 5b With An Unstable Plant Subjected to Parameter-Perturbations $\Delta a = (0,0),(0.4,-0.8),(-0.4,0.8)$, and $(0.8,-1.8)$ and Compensated by a Multirate D/C Controller Using Sample-Periods $T_y = 0.04$ and $T_c = 0.1$.

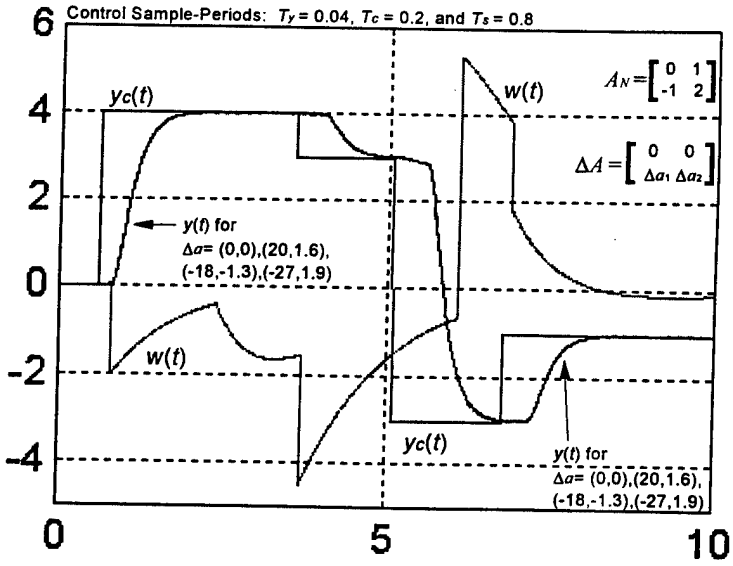

Figure 4.52 Illustration of the Plant Output $y(t)$, Disturbance $w(t)$, and Servo-Command $y_c(t)$ for Subcase 5b With An Unstable Second-Order Plant Subjected to Parameter-Perturbations $\Delta a = (0,0),(20,1.6),(-18,-1.3)$, and $(-27,1.9)$, and Compensated by a Multirate D/C Controller Using Sample-Periods $T_y = 0.04$, $T_c = 0.2$, and $T_s = 0.8$.

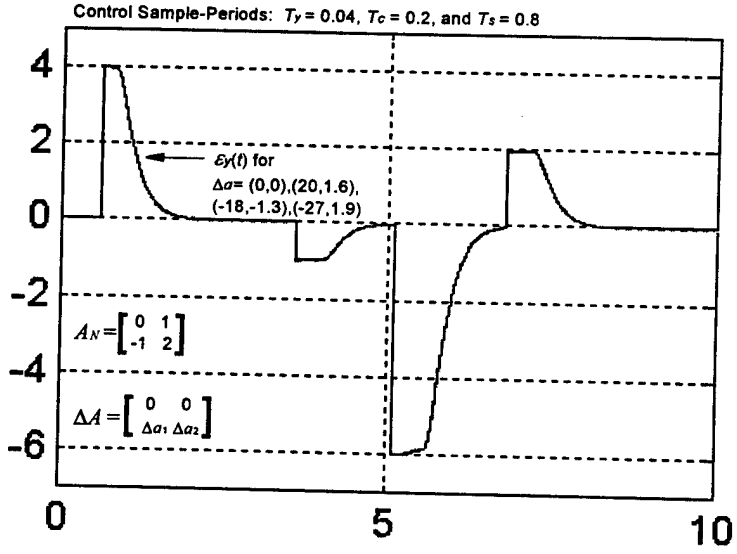

Figure 4.53 Illustration of the Tracking Error $\varepsilon_y(t)$ for Subcase 5b With An Unstable Second-Order Plant Subjected to Parameter-Perturbations $\Delta a = (0,0),(20,1.6),(-18,-1.3)$, and $(-27,1.9)$, and Compensated by a Multirate D/C Controller Using Sample-Periods $T_y = 0.04$, $T_c = 0.2$, and $T_s = 0.8$.

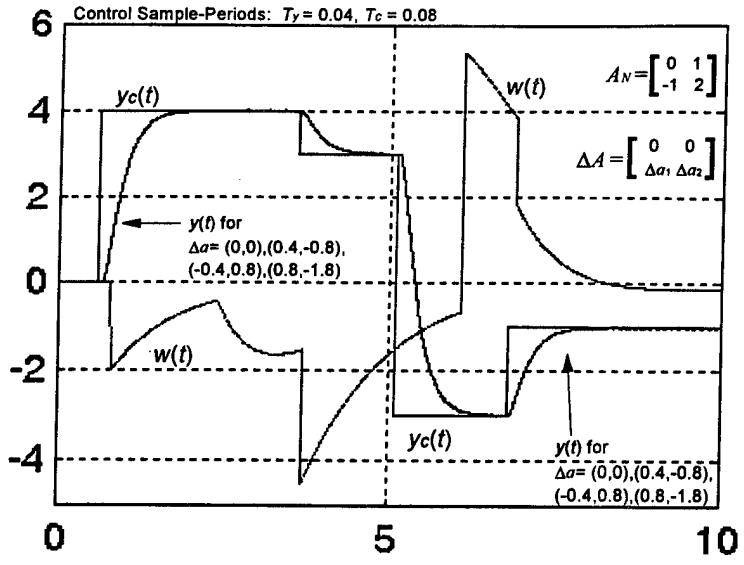

Figure 4.54 Illustration of the Plant Output $y(t)$, Disturbance $w(t)$, and Servo-Command $y_c(t)$ for Subcase 5b With An Unstable Second-Order Plant Subjected to Parameter-Perturbations $\Delta a = (0,0),(0.4,-0.8),(-0.4,0.8)$, and $(0.8,-1.8)$ and Compensated by a Multirate D/C Controller Using Sample-Periods $T_y = 0.04$ and $T_c = 0.08$.

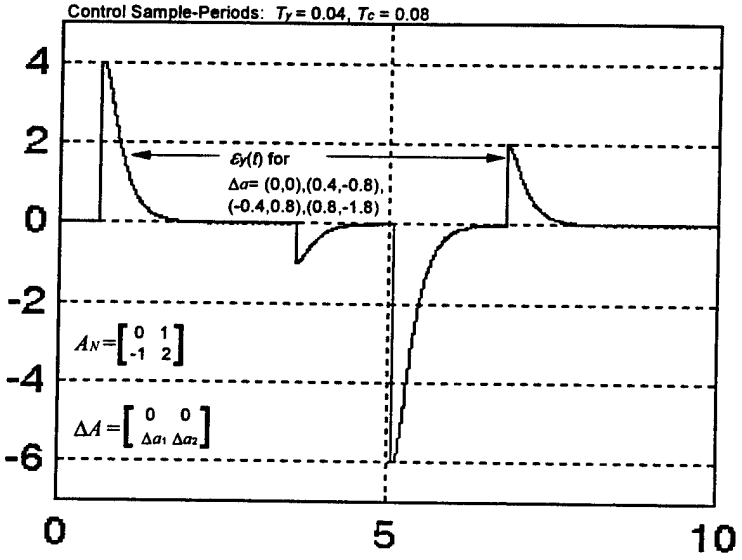

Figure 4.55 Illustration of the Tracking Error $\varepsilon_y(t)$ for Subcase 5b With An Unstable Second-Order Plant Subjected to Parameter-Perturbations $\Delta a = (0,0),(0.4,-0.8),(-0.4,0.8)$, and $(0.8,-1.8)$ and Compensated by a Multirate D/C Controller Using Sample-Periods $T_y = 0.04$ and $T_c = 0.08$.

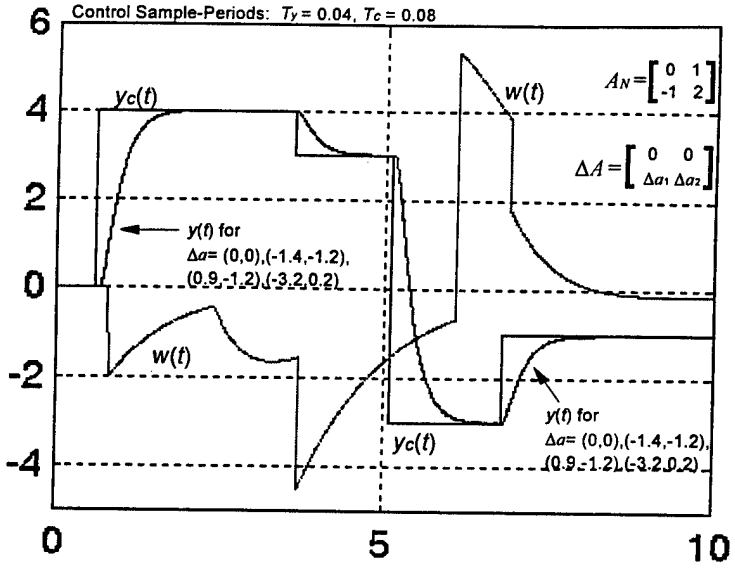

Figure 4.56 Illustration of the Plant Output $y(t)$, Disturbance $w(t)$, and Servo-Command $y_c(t)$ for Subcase 5b With An Unstable Second-Order Plant Subjected to Parameter-Perturbations $\Delta a = (0,0),(-1.4,-1.2),(0.9,1.6)$, and $(-3.2,0.2)$ and Compensated by a Multirate D/C Controller Using Sample-Periods $T_y = 0.04$ and $T_c = 0.08$.

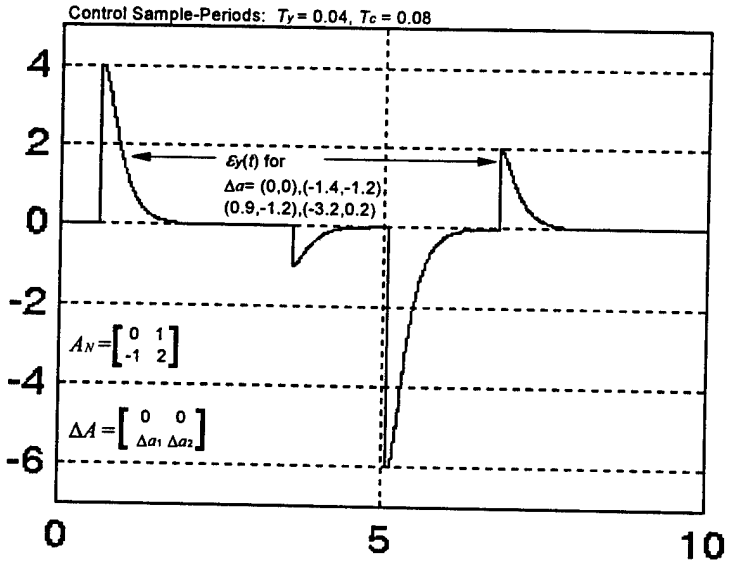

Figure 4.57 Illustration of the Tracking Error $\varepsilon_y(t)$ for Subcase 5b With An Unstable Second-Order Plant Subjected to Parameter-Perturbations $\Delta a = (0,0),(-1.4,-1.2),(0.9,1.6)$, and $(-3.2,0.2)$ and Compensated by a Multirate D/C Controller Using Sample-Periods $T_y = 0.04$ and $T_c = 0.08$.

5. CONCLUSIONS AND RECOMMENDATIONS FOR FURTHER WORK

5.1. Introduction

This report presents and illustrates (through examples) a new and general theory for developing high-performance digital servo-tracking controllers for linear, time-invariant, MIMO systems. Conclusions of this research and recommendations for further work are presented in this chapter.

5.2. Conclusions

The most significant contribution of this work is the development of a new, general linear-algebraic theory for developing digital servo-tracking controllers which will achieve high-performance servo-tracking that is unmatched by currently available digital servo-design methods. Some of the key shortcomings of conventional digital servo-controllers are: 1) failure to exploit useful dynamic information encoded in the uncertain servo-commands, disturbances, and plant states; 2) assume Type 1, 2, and 3 commands; 3) lack of intelligent control-actions between sample times; and, 4) sensitivity of tracking performance to plant parameter-perturbations.

In addition, the technique presented in this paper overcomes common obstacles that are encountered when attempting to achieve high-performance servo-tracking using digital controllers. Some of those obstacles are: 1) the complex time-behavior of the uncertain multivariable servo-commands and disturbances; 2) performance degradation due to uncertain variations in plant parameters; and, 3) intersample misbehavior due to the time-varying nature of the servo-commands and disturbances and also due to the open-loop instability of the plant.

The digital servo-controller theory presented in this report is ideal in the sense that the design procedure encompasses a superset of desirable characteristics. That is, the design procedure:

1) is purely linear-algebraic in nature so that there are no matric Riccati equations or other complex equations that require evaluation;

2) accommodates linear time-invariant systems subjected to generalized, multi-variable, independent disturbances having complex time-behavior;

3) produces a servo-controller that provides high-fidelity servo-tracking of generalized, multi-variable servo-commands having complex time-behavior;

4) is generalized to include any order of system having multiple-inputs and multiple-outputs (MIMO systems);

5) provides performance robustness against uncertain variations in plant-parameter values ΔA;

6) minimizes intersample misbehavior (ripple) to the highest degree possible utilizing a digital controller; and,

7) regulates and maintains the motions of the servo-state vector e_{ss} to a subspace S_v of the null-space of the output matrix $(e_{ss}(kT) \rightarrow S_v \subseteq \mathcal{N}[C])$.

The primary control task of the digital servo-controller, developed by the techniques presented in this report, is to achieve and maintain closed-loop stability for the plant while simultaneously regulating the servo-tracking error $\varepsilon_y(t)$ to zero and achieving certain desired performance-criteria, such as closed-loop settling-time. The methods of DAC theory [40,71,72] are used throughout this report to model the motions of the uncertain servo-commands, disturbances, and parameter-perturbations; to determine cancellation conditions of disturbance effects; and to decompose the total (vector) control-effort into a sum of individual (vector) control terms, each with a unique control task. The decomposition of the servo-control effort, and the subsequent decomposition of the servo-problem into logical subproblems, simplifies the design procedure significantly.

The servo-controller design technique presented in this report uses state-estimators (state-observers) to physically realize the digital servo-control algorithm. A discrete-time, reduced-order observer is used to estimate the servo-command state $c(kT)$and a composite discrete-time full-order or hybrid composite full-order observer is used to estimate the plant state $x(kT)$, disturbance state $z(kT)$, and parameter-perturbation state $z_a(kT)$.

In Chapter 2, a method is presented for stabilizing the discrete-time servo-state vector $e_{ss}(kT)$ to a subspace $S_v \subseteq \mathcal{N}[C]$ of largest dimension, and consequently regulating the servo-tracking $\varepsilon_y(t)$ to zero at each of the sample times, $t = kT$, $k = 0, 1, 2, \ldots$. As illustrated in Example 1 in Chapter 4, it may be difficult, or even impossible, to stabilize the servo-state vector $e_{ss}(kT)$ to the <u>entire</u> $\mathcal{N}[C]$. However, there may exist some subspace $S_v \subseteq \mathcal{N}[C]$, that $e_{ss}(kT)$ may be controlled to and held, and this may be the more desirable, or the only solution for asymptotically stabilizing the tracking-error. A method exists for accomplishing this subspace stabilization task in continuous-time [76]. This report work adapted the method in [76] to the discrete-time case and developed a procedure for formulating all possible candidate subspaces $S_v \subseteq \mathcal{N}[C]$. Example 2 in Chapter 4 illustrates the case of stabilizing $e_{ss}(kT) \rightarrow \mathcal{N}[C]$. The subspace stabilization approach in Chapter 2 utilizes a stepwise-constant control-action (a z.o.h. type action) to regulate the tracking-error $\varepsilon_y(t)$ to zero at each of the sample times, $t = kT$, $k = 0, 1, 2, \ldots$. That approach is all that is necessary in the case of zero, constant, or stepwise-constant disturbances or servo-commands.

Complex, time-varying commands and disturbances require a holding strategy that is smarter than the traditional zero-order, second-order, and exponential hold methods used by conventional digital control algorithms. The time-varying nature of the commands and the disturbances, along with the open-loop instability of the plant, result in misbehavior of the plant output <u>between</u> the sample times, $kT < t < (k+1)T$. Consequently, even though a zero tracking-error is obtained at each of the sample times, the plant output $y(t)$ will deviate from the servo-command $y_c(t)$ between those times. This intersample misbehavior was illustrated in Subcase 3a in Chapter 4. A method for intelligently selecting the control action for the next sample-period was presented in Chapter 3. This method uses the intersample waveform behaviors that both the servo-command and the external disturbance are projected to exhibit to reduce intersample misbehavior to a degree not previously obtained by conventional techniques. Subcase 3b in Chapter 4 illustrates the performance improvements that are attained by incorporating the intelligent holding-strategy into the digital servo-controller design method.

Robustness to uncertain changes in the plant's parameter values is a necessary quality of a high-performance digital servo-tracking controller. A method was presented for modeling those

parameter variations and thus designing a control term $u_a(t;kT)$ to accommodate their effects. The particular design method given incorporates an intelligent intersample holding-strategy to counteract the effects of those unknown parameter-perturbations between the sample times. Examples using this enhancement are given throughout Chapter 4. In particular, Subcase 3c compares a system compensated with and without the robustness control term $u_a(t;kT)$.

The digital servo-controller designed by the techniques presented in this paper may be implemented using a single sample-period or using multiple sample-periods. There are many different ways of implementing the digital servo-tracking control algorithm using multiple sample-periods. Multirate sampling could arise from the physical characteristics of the system, or may be introduced deliberately into the servo-controller. A particular implementation was considered for this research that has practical application. It involves two distinct and synchronized sample-periods associated with the two distinct vector-inputs to the digital servo-controller ($y(kT)$ and $y_c(kT)$). One sample-period is associated with the availability of measurements, or processing, of the plant output $y(t)$, while the second sample-period is associated with the availability of measurements, or processing, of the servo-command $y_c(t)$. In the multirate case, an unstable or highly oscillatory plant may be brought under control by incorporating an additional control term $u_{a_m}(kT)$ into the digital servo-controller that runs at the faster sample-rate. When the $u_{a_m}(kT)$ term is used, the control terms running at the slower rate may need to be recomputed to reflect the plant's new A matrix. Simulation results are given in Subcase 4b in Chapter 4 for a plant compensated by a digital servo-controller with and without the additional $u_{a_m}(kT)$ control term. Also, Subcase 5b in Chapter 4 includes simulation results illustrating performance degradation for the case of sample periods that do not satisfy the integer multiple relationship in (3.80).

5.3. Recommendations for Further Work

Several areas for further study in the field of digital servo-tracking control theory have been uncovered during the course of this research. In particular, the suggested areas for further study are described briefly in the listing below:

1) The focus of this work is on output servo-tracking. That is, the problem of the plant output $y(t)$ tracking a given servo-command $y_c(t)$. The general theory presented here should be extended to cover the case of plant state servo-tracking. That is, $x(t) \rightarrow x_c(t)$ in a sufficiently small amount of time (where $x_c(t)$ represent time-varying commands that the plant states are required to follow). In that way, disturbance cancellation and accommodation of plant parameter-perturbations as they affect individual plant states would also require further analysis;

2) Another subject area for further research involves expanding the digital servo-controller theory developed in this report to linear time-invariant systems having the dynamical model

$$\begin{aligned} \dot{x}(t) &= Ax(t) + Bu(t) + Fw(t) \\ y(t) &= Cx(t) + Eu(t) + Gw(t) \end{aligned} \quad ;$$

3) A high-performance digital servo-control theory that addresses time-varying parameters is an area requiring additional research. Initially, the time-varying system represented by

$$\dot{x}(t) = A(t)x(t) + B(t)u(t) + F(t)w(t)$$
$$y(t) = C(t)x(t) \quad ,$$

might be considered, and then expanded to achieve a general theory for time-varying systems of the form

$$\dot{x}(t) = A(t)x(t) + B(t)u(t) + F(t)w(t)$$
$$y(t) = C(t)x(t) + E(t)u(t) + G(t)w(t) \quad ;$$

4) Variations in the plant's A matrix have been considered in this work, however, the general theory begs for inclusion of the case addressing variations in the nominal values of the B, C, and F matrices. A linear digital control method does exist [34, 35, 39] which accommodates variations in those parameters; however, some investigation will be required to determine if and how this technique can be applied for the case of time-varying servo-commands;

5) The multirate solution given in this paper assumes that all sample-periods are integer multiples of one another. As was seen in Subcase 5b in Chapter 4, a non-integer multiple relationship causes degradation in the tracking performance. The control terms operating at the slower sample-rate rely on this integer multiple relationship for their computations. Further investigation is required to determine how their computation should be altered to include any relationship of control sample-periods;

6) Another area involving multiple sample-rates, related to the recommendation given above, is the case involving samplers that drift slightly from their nominal rate. The method presented in this report assumes the samplers are synchronized and remain synchronized for all time. In practical hardware implementation, the samplers may be subjected to temperature variations, or other disrupting effects, and may tend to drift slightly, leading to a possible decline in tracking performance;

7) Again in the area of multiple sample-rates, is the dilemma of selecting the best combination of sample rates to achieve the desired performance, while staying within certain design boundaries. Some sample-rates may be determined or constrained by the physical characteristics of the system or the hardware on which the controller is implemented. Issues such as availability of data, computing power of the hardware, or time-sensitive deadlines impose limits on the sample-rates that may be used. In addition, a new digital servo-controller must be computed for each change in sample-rates, unless the sample-period is carried as a variable throughout the computations. This becomes quite cumbersome for anything other than very low-order systems. Therefore, a technique for arriving at the optimal combination of sample-rates, given the constraints and design criteria of the system, is an area that would require extensive effort, but with high pay-off;

8) The digital servo-tracking controller design method developed in this report assumes satisfaction of a complete-cancellation condition for the effects of the external

disturbances and disturbance-like effects caused by the servo-commands and parameter perturbations on the servo-tracking error $\varepsilon_y(t)$. If those conditions are not met, then the corresponding control term cannot be designed. The theory of DAC [40,71,72] includes methods of disturbance-minimization and disturbance-utilization. Those DAC methods could be incorporated into the general theory presented in this paper;

9) A method was presented in Subsection 2.11.7 for formulating all possible subspaces $S_v \subseteq \aleph[C]$. Those subspaces are systematically tested for suitability using the linear subspace stabilization technique presented in Chapter 2. Additional research is needed to fully evaluate the possibilities that exist for this method. Upon testing a general representation for v-dimensional subspaces, the designer can then discern a range of acceptable subspaces for regulating $e_{ss}(kT)$. A computer program that automates the procedures in Section 2.11 for enumerating subspaces, performing the subspace testing, and determining appropriate ranges of subspaces, will help to ease the burden on the control system designer; and

10) The application of the digital servo-tracking control theory to realistic problems is desirable in order to further ascertain the benefits of this technique versus conventional methods. In particular, this theory could be applied to the missile guidance problem of tracking a maneuvering target while subjected to a wide variety of atmospheric disturbances, noisy measurements, and parameter uncertainties.

REFERENCES

[1] Hazen, H., Theory of Servomechanisms, *Journal of the Franklin Institute*, Vol. 218, pp. 279-331, September 1934.

[2] Bower, J., and Schultheiss, P., *Introduction to the Design of Servomechanisms*, John Wiley and Sons, 1958.

[3] Vaccaro, R. J., *Digital Control, A State-Space Approach*, McGraw-Hill Book Co., 1995.

[4] James, H., N. Nichols, and R. Phillips, *Theory of Servomechanisms*, McGraw Hill Book Co., N.Y., 1947, reprinted in paperback by Dover Books, N.Y., 1965.

[5] D'Azzo, J., and Houpis, C., *Linear Control Systems Analysis and Design- Conventional and Modern*, McGraw-Hill Book Co., 1975.

[6] Chen, C. T., *Analog and Digital Control Systems Design: Transfer-Function, State-Space, and Algebraic Methods*, Saunders College Publishing, 1993.

[7] Chestnut, Harold, and Mayer, Robert W., *Servomechanisms and Regulating System Design*, John Wiley & Sons, Inc., New York, 1959.

[8] Franklin, G.F., Powell, J.D., and Emami-Naeini, A., *Feedback Control of Dynamic Systems*, Addison-Wesley, Reading, MA, 1991.

[9] Hara, S., Yamamoto, Y., Omata, T., & Nakano, M., Repetitive Control System: A New Type Servo System for Periodic Exogenous Signals, *IEEE Transactions on Automatic Control*, Vol. 33, Issue 7, July 1988, pp. 659-68.

[10] Hostetter, G., Savant, Cl, and Stefani, R., *Design of Feedback Control Systems*, CBS College Publishing, 1982.

[11] Hsia, T. C. S., A New Technique for Robust Control of Servo Systems, *IEEE Transactions on Industrial Electronics*, Vol. 36, Issue 1, February 1989, pp. 1-7.

[12] Kamen, E. W., Tracking in Linear Time-Varying Systems, *Proceedings of ACC Conference in Pittsburgh*, 1989, (TJ212.2 A512), pp. 263-8.

[13] Kucera, Vladimir, A Deadbeat Servo Problem, *International Journal of Control*, 1980, Vol. 32, No. 1, pp. 107-113.

[14] Kuo, B. , *Automatic Control Systems*, Prentice-Hall, N.J., 1991.

[15] Lang, G., and Ham, J.M., Conditional Feedback Systems- A New Approach to Feedback Control, *AIEE Winter General Meeting*, New York, N.Y., January-February 1955. MacColl, L., *Fundamental Theory of Servo-mechanisms*, D. Van Nostrand Co., 1945, reprinted in paperback by Dover Books, NY, 1968.

[16] Ogata, K., *Modern Control Engineering, Second Edition*, Prentice-Hall, NJ, 1990.

REFERENCES (Cont.)

[17] Pernebo, Lars, An Algebraic Theory for the Design of Controllers for Linear Multivariable Systems - Part I: Structure Matrices and Feedforward Design, *IEEE Transactions on Automatic Control*, Vol. AC-26, No. 1, February 1981, pp. 171-82.

[18] Phillip, C.L., and Harbor, R.D., *Feedback Control Systems*, Prentice-Hall, Englewood Cliffs, NJ, 1991.

[19] Phillips, C., and T. Nagle, Jr., *Digital Control System Analysis and Design*, Prentice-Hall, N.J., 1984.

[20] Phillips, C., and T. Nagle, Jr., *Digital Control System Analysis and Design, Second Edition*, Prentice-Hall, N.J., 1990.

[21] Robson, J. M., The Design of Servo Mechanisms Which are Required to Smooth as well as Retransmit Data, Department of Scientific and Industrial Research, SERVOMECHANISMS, Selected Government Research Reports, Vol. 5, Her Majesty's Stationery Office, 1953, pp. 178-215.

[22] Wolovich, W. A., Deadbeat Error Control of Discrete Multivariable Systems, *International Journal of Control*, 1983, Vol. 37, No. 3, pp. 567-582.

[23] Nyquist, H., Regeneration Theory, *Bell System Technical Journal*, 1932.

[24] Black, H.S., Stabilized Feedback Amplifiers, *Bell System Technical Journal*, 1934.

[25] Bode, H.W., *Network Analysis and Feedback Amplifier Design*, Van Nostrand, Princeton, N.J., 1945.

[26] Hall, A.C., Applications of Circuit Theory to the Design of Servomechanisms, *Journal of Franklin Institute*, 1946.

[27] Harris, H., The Analysis and Design of Servomechanisms, OSRD Report 454, Jan. 1942.

[28] Harris, H., The Frequency Response of Automatic Control Systems, *Transactions AIEE*, Vol. 65, pp. 539-546, 1946.

[29] Evans, W.R., Graphical Analysis of Control Systems, *Transactions AIEE*, Vol. 67, pt. II, pp. 547-551,1948.

[30] DiStefano, J.J., Stubberud, A.R., and Williams, I.J., *Theory and Problems of Feedback and Control Systems, Second Edition*, McGraw-Hill Book Co., 1990.

[31] Johnson, C.D., Discrete Time Disturbance-Accommodating Control Theory with Applications to Missile Digital Control, *Journal of Guidance and Control*, Vol. 4, No. 2, pp. 116-125.

REFERENCES (Cont.)

[32] Johnson, C.D., A Discrete-Time Disturbance Accommodating Control Theory, Chapter 6 in the book, *Control and Dynamic Systems: Advances in Theory and Applications*, Vol. 18, Edited by C.T. Leondes, Academic Press, 1982.

[33] Johnson, C.D., A Discrete-Time Version of a New Adaptive Control Theory, UAH Research Report No. 645, Sept. 1987.

[34] Johnson, C.D., A New Approach to Adaptive Control, Chapter 1 in the book *Control and Dynamic Systems- Advances in Theory and Applications*, Vol. 27, Edited by C.T. Leondes, Academic Press, N.Y., 1988.

[35] Johnson, C.D., Accommodation of External Disturbances in Linear Regulator and Servomechanism Problems, *IEEE Transactions on Automatic Control*, vol. AC-16, No. 6, pp. 635-44, December 1971.

[36] Johnson, C.D., Algebraic Solution of the Servomechanism Problem with External Disturbances, *ASME Journal of Dynamic Systems, Measurement, and Control*, Vol. 96, Ser. G, No. 1, pp. 25-35, March 1974; see also ibid, Vol. 97, No. 2, p. 161, 1975.

[37] Johnson, C.D., and N. Kheir, An Optimal Holding Strategy for Discrete-Time MIMO Servo-Tracking Controllers, *Proc. Symposium on Fundamentals of Discrete-Time Systems*, Chicago, IL, June 1992; published in the book, *Fundamentals of Discrete-Time Systems*, TSI Press, Albuquerque, NM, 1993.

[38] Johnson, C.D., Example Applications of the Linear Adaptive Design Technique, *International Journal of Adaptive Control and Signal Processing*, Vol. 3, pp. 111-129, 1989.

[39] Johnson, C.D., Theory of Disturbance-Accommodating Controllers, Chapter 7 in the book: Advances in Control and Dynamic Systems, Vol. 12, Edited by C.T. Leondes, Academic Press, 1976.

[40] Davison, E. J., The Robust Control of a Servomechanism Problem for Linear Time-Invariant Multivariable Systems, *IEEE Transactions on Automatic Control*, Vol. AC-21 (1), 1976, pp. 25-34; addendum, Vol. AC-22, p. 283, 1977.

[41] Desoer, C. A., & Wang, Y. T., Linear Time-Invariant Robust Servomechanism Problem: A Self-Contained Exposition, *Control and Dynamic Systems*, Vol. 16 (C. T. Leondes, Ed.). New York: Academic, pp. 81-129, 1980.

[42] Emani-Naeini, A., & Franklin, G. F., Zero Assignment in the Multivariable Robust Servo Mechanism, *Proceedings of the 21st IEEE Conference on Decision and Control*, pp. 891-893, December 1982.

[43] Franklin, G. F. , and Emami-Naeini, A., A New Formulation of the Multivariable Robust Servomechanism Problem, an internal report, ISL, Stanford University, Stanford, California, July 1983.

REFERENCES (Cont.)

[44] Franklin, G. F., & Emami-Naeini, A., Design of Ripple-Free Multivariable Robust Servomechanisms, *IEEE Transactions on Automatic Control*, Vol. AC-31, No. 7, July 1986, pp. 661-4.

[45] Kuo, B., *Digital Control Systems*, Saunders College Publishing, 1992.

[46] Ogata, K., *Discrete-Time Control Systems*, Prentice-Hall, N.J., 1987.

[47] Young, P. C., & Willems, J. C., An Approach to the Linear Multivariable Servomechanism Problem, *International Journal of Control* 15 (5), 1972, pp. 961-979.

[48] Hostetter, G. H., Controller Design for Exact Signal Model Tracking, *Proceedings of the 18th Asilomar Conference on Circuits, Systems, and Computers*, November 1984, pp. 449-453.

[49] Anderson, B., and Moore, J., *Optimal Control Linear Quadratic Methods*, Prentice-Hall, NJ, 1990.

[50] Bellman, R., *Mathematical Optimization Techniques*, The University of California Press, 1963.

[51] Brogan, W., *Modern Control Theory, Third Edition*, Prentice-Hall, NJ, 1991.

[52] Houpis, Constantine H., and Lamont, Gary B., *Digital Control Systems, Theory, Hardware, Software*, McGraw-Hill, Inc., 1992.

[53] Iftar, Altug, & Ozguner, Umit, An Optimal Control Approach to the Decentralized Robust Servomechanism Problem, *IEEE Transactions on Automatic Control*, Vol. 34, Issue 12, December 1989, pp. 1268-71.

[54] Isermann, R., *Digital Control Systems Volume 1: Fundamentals, Deterministic Control*, Springer-Verlag, 1989.

[55] Jacquot, R.G., *Modern Digital Control Systems, Second Edition*, Marcel Dekker, Inc., 1994.

[56] Franklin, F., J. Powell, and M. Workman, *Digital Control of Dynamic Systems*, Addison-Wesley Publishing, Mass., 1990.

[57] Kuo, B., *Analysis and Synthesis of Sampled-Data Control Systems*, Prentice-Hall, N.J., 1963.

[58] Hughes, W., and C.D. Johnson, Obstacles to Achieving High-Performance Servo-Tracking Using Conventional Digital-Controller Designs, *Proceedings of the 27th Southeastern Symposium on System Theory*, pp. 429-433, March 1995.

[59] Freudenberg, J. S., Middleton, R. H., and Braslavsky, J. H., Inherent Design Limitations for Linear Sampled-Data Feedback Systems, *International Journal of Controls*, Vol. 61, No. 6, 1995, pp. 1387-1421.

[60] Skelton, Robert E., and Iwasaki, Tetsuya, Increased Roles of Linear Algebra in Control Education, *IEEE Control Systems*, Vol. 15, No. 4, August 1995, pp. 76-90.

REFERENCES (Cont.)

[61] Hara, Shinji, & Sung, Hak-Kyung, Ripple-Free Conditions in Sampled-Data Control Systems, *Proceedings of the 30th Conference on Decision and Control*, Brighton England, December 1991.

[62] Jury, E., *Sampled-Data Control Systems*, John Wiley and Sons, N.Y., 1958.

[63] Tou, J., *Digital and Sampled-Data Control Systems*, McGraw-Hill Book Co., N.Y., 1959.

[64] Urikura, Shigeru, & Nagata, Akira, Ripple-Free Deadbeat Control for Sampled Data Systems, *IEEE Transactions on Automatic Control*, Vol. AC-32, No. 6, June 1987, pp. 474-482.

[65] Wu, Yung-Chun, & Yen, Nie-Zen, A Ripple Free Sampled-Data Robust Servomechanism Controller Using Exponential Hold, *IEEE Transactions on Automatic Control*, Vol. 39, No. 6, June 1994, pp. 1287-1291.

[66] Yamamoto, Yukata, A Function Space Approach to Sampled Data Control Systems and Tracking Problems, *IEEE Transactions on Automatic Control*, Vol. 39, No. 4, April 1994, pp. 703-713.

[67] Zak, Stanislaw H., & Blouin, Eric E., Ripple-Free Deadbeat Control, *IEEE Control Systems*, August 1993, pp. 51-56.

[68] Bryson, A.E., Jr. and Ho, Yu-Chi, *Applied Optimal Control*, Hemisphere Publishing Corp., New York, 1975.

[69] Johnson, C.D., Improved Computational Procedures for "Algebraic Solution of the Servomechanism Problem with External Disturbances", *ASME Journal of Dynamic Systems, Measurement, and Control*, pp. 161-163, June 1975.

[70] Dharia, R., and C.D. Johnson, On the Theoretical Sub-Optimality of Optimal Disturbance-Utilizing Control Laws, *Proceedings of the IEEE SouthEastCon Conference*, Vol. 2, Birmingham, AL, April 1992.

[71] Johnson, C.D., Disturbance-Accommodating Control; A History of its Development, *Proceedings of the 15th Annual Meeting of the Society for Engineering/Science*, University of Florida, Gainesville, Florida, pp. 331-336, Dec. 1978.

[72] Johnson, C.D., Disturbance-Accommodating Control; An Overview, *Proceedings of the 1986 American Control Conference*, Vol. 1, p. 526, June 1986.

[73] Johnson, C.D., Invariant Hyperplanes for Linear Dynamical Systems, *IEEE Transactions on Automatic Control*, AC-11, No. 1 Jan. 1966, pp. 113-116.

[74] Penrose, R., A Generalized Inverse for Matrices, *Proceedings of the Cambridge Philosophy Society*, Vol. 51, 1955.

[75] Johnson, C.D., Stabilization of Linear Dynamical Systems with Respect to Arbitrary Linear Subspaces, *Journal of Mathematical Analysis and Applications*, Vol. 44, No. 1, October 1973.

REFERENCES (Cont.)

[76] Zadeh, Lofti A and Desoer, C.A.., *Linear System Theory- The State Space Approach*, McGraw-Hill Book Co., 1963.

[77] Johnson, C.D., A Unified Canonical Form for Controllable and Uncontrollable Linear Dynamical Systems, *International Journal of Control*, Vol. 13, No. 3, pp. 497-517, 1971.

[78] Kranc, G.M., Compensation of an Error-Sampled System by a Multirate Controller, *Transactions of the AIEE*, July 1957, Vol. 77, pp. 149-159.

[79] Kranc, G.M., Input-Output Analysis of Multirate Feedback Systems, *IRE Transactions on Automatic Control*, Nov. 1957, pp. 21-28.

[80] Roberts, Fred S., Applied Combinatorics, Prentice-Hall, NJ, 1984.

[81] Lipschutz, S., *Theory and Problems of Linear Algebra, Second Edition*, McGraw-Hill Publishing Co., 1991.

BIBLIOGRAPHY

1. Baheti, Radhakisan S., Multivariable Frequency Domain Controller for Magnetic Suspension and Balance Systems, *IEEE Transactions on Automatic Control*, Vol. AC-29, No. 8, August 1984, pp. 725-8.

2. Bhattacharyya, S. P., Pearson, J. B., and Wonham, W. M., On Zeroing the Output of a Linear System, *Information and Control* V20 (2), 1972, pp. 135-142.

3. Brockett, R.W., and Mesarovic, M.D., The Reproducibility of Multivariable Systems, *Journal of Mathematical Analysis and Applications 11*, pp. 548-563, 1965.

4. Bronson, R., *Theory and Problems of Matrix Operations*, McGraw-Hill Publishing Co., 1989.

5. Bryrup, B., Blanke, M., Holst, J., and Scholiert, J., Path Prediction for Ships Subject to External Disturbances, *Control and Computers*, Vol. 14, No. 2, 1986, pp. 63-70.

6. Buja, G. S. & Souliaev, Alexander, A Variable-Structure Controller, *IEEE Transactions on Automatic Control*, Vol. 33, Issue 2, Feb. 1988, pp. 206-9.

7. Chalam, V.V., *Adaptive Control Systems, Techniques, and Application*, Marcel Dekker, Inc., New York, 1987.

8. Danielle, P. J., Operational Methods for Servo Systems, Department of Scientific and Industrial Research, SERVOMECHANISMS, Selected Government Research Reports, Vol. 5, Her Majesty's Stationery Office, 1953, pp. 13-33.

9. Das, B. B. & Zachariah, S. K., Optimal Pulse-Position Pulsewidth-Modulated Control of Sampled Data Position Servosystems, *IEEE Proceedings, Control Theory and Applications*, Vol. 137, Issue 5, September 1990, pp. 307-310.

10. DeKeyser, R. M. C., Simple Adaptive Controller for Systems with Fast Parameter Variations, *Control and Computers*, Vol. 13, No. 2, 1985, pp. 72-7.

11. DeWeerth, Stephen P., Mead, Carver A., & Astrom, Karl J., A Simple Neuron Servo, *IEEE Transactions on Neural Networks*, Vol. 2, Issue 2, March 1991, pp. 248-51.

12. Desoer, C. A., & Wang, Y. W., On the Minimum Order of a Robust Servo-Compensator, *IEEE Transactions on Automatic Control*, Vol. AC-23 (1), pp. 70-73, 1978.

13. Desoer, Charles A., & Lin, Ching-An, Tracking and Disturbance Rejection of MIMO Nonlinear Systems with PI Controller, *IEEE Transactions on Automatic Control*, Vol. AC-30, No. 9, September 1985, pp. 861-7.

14. Dorf, R.C., *Modern Control Systems*, Addison-Wesley, Reading, MA, 1992.

BIBLIOGRAPHY (Cont.)

15. Emani-Naeini, A., & Franklin, G. F., Deadbeat Control and Tracking of Discrete-Time Systems, *IEEE Transactions on Automatic Control*, Vol. AC-27, No. 1, February 1982, pp. 176-181.

16. Fahmy, M. M., & O'Reilly, J., Dead-beat Control of Linear Discrete-Time Systems, *International Journal of Control*, 1983, Vol. 37, No. 4, pp. 685-705.

17. Feick, Rodolfo, & Salgado, Mario, Evaluation of Adaptive Control Algorithms in the Presence of Disturbances and Noise, *Control and Computers*, Vol. 15, No. 1, 1987, pp. 34-9.

18. Franklin, F., and J. Powell, *Digital Control of Dynamic Systems*, Addison-Wesley Publishing, Mass., 1980.

19. Franklin, G. F., & Emami-Naeini, A., Robust Servomechanism Design Applied to Control of Reel-to-Reel Digital Tape Transports, *Proceedings of the Asilomar Conference*, pp. 108-113, 1981.

20. Franklin, G. F., Zero Placement and Steady-State Accuracy in the Pole Assignment Design Technique, Internal Memorandum, ISL, Stanford University, Stanford, California, March 1975.

21. Friedberg, S. H., Insel, A. J., and Spence, L. E., *Linear Algebra*, Prentice-Hall , N.J.,1979.

22. Friedland, B., *Control System Design, An Introduction to State-Space Methods*, McGraw-Hill Book Co., 1986

23. Furuta, Katsuhisa, & Komiya, Katsumi, Design of Model-Following Servo Controller, *IEEE Transactions on Automatic Control*, Vol. AC-27, No. 3, June 1982, pp. 725-7.

24. Gabor, Denis, Communication Theory and Cybernetics, *The Fourth Session of "Science Days": Symposium on Electronics and Television*, Milan, Italy, April 1954.

25. Gibson, John E., and Tuteur, Franz B., *Control System Components*, McGraw-Hill Book Company, New York, 1958.

26. Graham, R., Linear Servo Theory, *Bell System Technical Journal*, Vol. XXV, No. 4, pp. 616-651, October 1946.

27. Grasse, Kevin A., Sufficient Conditions For The Functional Reproducibility of Time-Varying Input-Output Systems, *SIAM Journal of Control and Optimization*, Vol. 26, No. 1, January 1988.

28. Grasselli, O. M., Jetto, L., and Longhi, S., Ripple-free Dead-Beat Tracking for Multirate Sampled-data Systems, *International Journal of Controls*, Vol. 61, No. 6, 1995, pp. 1437-1455.

29. Grasselli, O. M., Longhi, S., & Tornambe, A., Robust Ripple-Free Tracking and Regulation Under Uncertainties of Physical Parameters for Ramp-Exponential Signals, *Proceedings of the 32nd Conference on Decision and Control*, San Antonio Texas, December 1993, pp. 783-784.

BIBLIOGRAPHY (Cont.)

30. Grasselli, O. M., Tornambe, A., & Longhi, S., Robust Tracking and Disturbance Rejection Under Physical Parameter Uncertainties for Polynomial-Exponential Signals, *Proceedings of the 31st Conference on Decision and Control*, Tucson Arizona, December 1992, pp. 668-673.

31. Hostetter, G. H., *Digital Control System Design*, Holt, Rinehart and Winston, Inc., 1988.

32. Itkis, Y., Dynamic Switching of Type-I/Type-II Structures in Tracking Servosystems, *IEEE Transactions on Automatic Control*, Vol. AC-28, No. 4, April 1983, pp. 531-4.

33. Jannerup, O., Discrete Time Servomechanisms with Disturbance Rejection, *Control and Computers*, Vol. 17, No. 1, 1989, pp. 26-31.

34. Jetto, Leopoldo, Deadbeat Ripple-Free Tracking with Disturbance Rejection: A Polynomial Approach, *IEEE Transactions on Automatic Control*, Vol. 39, No. 8, August 1994.

35. Johnson, A., On the Sampled-Data Linear Quadratic Tracking Problem, *Dynamics and Control*, Vol. 3, No. 1, January 1993, pp. 91-100.

36. Johnson, C.D., A Family of "Universal Adaptive Controllers" for Linear and Non-Linear Plants, *Proceedings of the 20th Southeastern Symposium on System Theory*, pp. 530-534, March 1988.

37. Johnson, C.D., A New Discrete-Time State Model for Linear Dynamical Systems with Continuously-Varying Control/Disturbance Inputs, reference citation data to be added later.

38. Johnson, C.D., Adaptive Controller Design Using Disturbance-Accommodating Techniques, *International Journal of Controls*, Vol. 42, No. 1, pp. 193-210, 1985.

39. Johnson, C.D., Adaptive Disturbance-Accommodations, *Proceeding of the 23rd Southeastern Symposium on System Theory*, pp. 60-64, March 1991.

40. Johnson, C.D., and Wonham, W.M., Another Note on the Transformation to Canonical (Phase Variable) Form, *IEEE Transactions on Automatic Control*, Vol. AC-11, No. 3, p. 609, January 1966.

41. Johnson, C.D., Applications of a New Approach to Adaptive Control, *International Journal of Adaptive Control and Signal Processing*, Vol. 3, p.111, 1989.

42. Johnson, C.D., Disturbance-utilizing Controllers for Noisy Measurements and Disturbances- The Continuous Time Case, *International Journal of Controls*, Vol. 39, No. 5, pp. 859-868, 1984.

43. Johnson, C.D., Disturbance-utilizing Controllers for Noisy Measurements and Disturbances- The Discrete Time Case, *International Journal of Controls*, Vol. 39, No. 5, pp. 859-868, 1984.

44. Johnson, C.D., Further Study of the Linear Regulator with Disturbances- The Case of Vector Disturbances Satisfying a Linear Differential Equation, *IEEE Transactions on Automatic Control*, Vol. AC-15, No. 2, pp. 222-228, April 1970.

BIBLIOGRAPHY (Cont.)

45. Johnson, C.D., Learning-Adaptive Control Using Disturbance-Accommodation Techniques, *Proceedings of the 21st Southeastern Symposium on System Theory*, pp. 629-635, March 1989.

46. Johnson, C.D., Linear Adaptive Control via Disturbance Accommodation; Some Case Studies, (source unknown)

47. Johnson, C.D., On a Recurrent Misconception in Sampled-Data/Digital Control Textbooks, *Proceedings of the 17th Southeastern Symposium on System Theory*, pp. 188-191, March 1985.

48. Johnson, C.D., On Observers for Systems with Unknown and Inaccessible Outputs, *International Journal of Controls*, Vol. 21, No. 5, pp. 825-831, 1975.

49. Kaczorek, Tadausz, Deadbeat Servoproblem for Multivariable n-D Systems, *IEEE Transactions on Automatic Control*, Vol. AC-31, No. 4, April 1986, pp. 360-2.

50. Kalman, R.E., and Bertram, J.E., General Synthesis Procedure for Computer Control of Single-Loop and Multiloop Linear Systems (An Optimal Sampling System), *Transactions of the AIEE*, Vol. 77, Part II, pp. 602-609, January 1959.

51. Kangsanant, Theorayuth, & Lim, Peng Yew, Design of Digital Controllers for Motion Control Systems Via Model Reduction, *19th Annual IEEE Power Electronics Specialists Conference*, April 1988, Vol. 1, pp. 439-44.

52. Kompass, Edward J., Analog Design, By the Numbers, *Control Engineering*, August 1989, page 155.

53. Lee, Gordon K. F., Dynamic Output Feedback Design for Single-Input, Multi-Output Discrete Regulators, *International Journal of Control and Computers*, Vol. 15, No. 3, 1987, pp. 99-103.

54. Leigh, J.R., *Applied Digital Control, Theory, Design, & Implementation*, Prentice-Hall, 1985.

55. Li, Z., A Discrete-Time Adaptive Controller For Time-Varying Systems, Northeast University of Technology, The Peoples Republic of China.

56. Li, Z., and Unbehauen, H., Adaptive Control of Systems Subject to Deterministic Time-Varying Disturbances Via an Additional Measurement, Ruhr-University Bochum, Federal Republic of Germany.

57. Lipschutz, S., *Theory and Problems of Linear Algebra, Second Edition*, McGraw-Hill Publishing Co., 1991.

58. Luenberger, David G., An Introduction to Observers, *IEEE Transactions on Automatic Control*, Vol. AC-16, No. 6, December 1971, pp. 596-602.

59. Miller, Daniel E., & Davison Edward J., The Self-Tuning Robust Servomechanism Problem, *IEEE Transaction on Automatic Control*, Vol. 34, Issue 5, May 1989, pp. 511-23.

BIBLIOGRAPHY (Cont.)

60. Mita, Tsutomu, & Yoshida, Hiroshi, Undershooting Phenomenon and Its Control in Linear Multivariable Servomechanisms, *IEEE Transactions on Automatic Control*, Vol. AC-26, No. 2, April 1981, pp. 402-7.

61. Pak, H. A., & Li, G. Q., Zero Phase Error Tracking Control for Square Sampled-Data Systems, *Journal of Dynamic Systems, Measurement, and Control*, Vol. 113, September 1991, pp. 506-509.

62. Pak, H. A., & Shieh, Rowman, On Discrete-Time Feedforward Asymptotic Tracking Controllers, *Journal of Dynamic Systems, Measurement, and Control*, Vol. 113, September 1991, pp. 509-514.

63. Pao, L. Y., & Franklin, G. F., Proximate Time-Optimal Control of Third-Order Servomechanisms, *IEEE Transactions on Automatic Control*, Vol. 38, No. 4, April 1993, pp. 568-580.

64. Philbrick, G.A., Unified Symbolism for Regulatory Control, *ASME Annual Meeting*, New York, N.Y., November 1945.

65. Ragazzini, J., and Franklin, G.F., *Sampled-Data Control Systems*, McGraw-Hill Book Co., 1958.

66. Ritow, I., *A Servomechanism Primer*, Dolphin Books, 1963.

67. Ritow, I., *Advanced Servomechanism Design*, Dolphin Books, 1963.

68. Savant, C. J., *Basic Feedback Control System Design*, McGraw-Hill Book Company, New York, 1958.

69. Schumacher, J. M. Hans, Regulator Synthesis Using (C,A,B)-Pairs, *IEEE Transactions on Automatic Control*, Vol. AC-27, No. 6, December 1982, pp. 1211-21.

70. Sira-Ramirez, Hebertt, A Dynamical Variable Structure Control Strategy in Asymptotic Output Tracking Problems, *IEEE Transactions on Automatic Control*, Vol. 38, No. 4, April 1993, pp. 615-620.

71. Strenio, Don, The Application of Servo Control, *IEEE Conference Record of 1988 40th Annual Conference of Electrical Engineering Problems in the Rubber and Plastic Industries*, April 1988, pp. 66-83.

72. Truxal, J.G., *Automatic Feedback Control System Synthesis*, McGraw-Hill Book Co., N.Y., 1955.

73. VanLandingham, H.F., *Introduction to Digital Control Systems*, Macmillan Publishing Co., 1985.

BIBLIOGRAPHY (Cont.)

74. Wang, S. H., & Davison, E. J., Penetrating Transmission Zeros in the Design of Robust Servomechanism Systems, *IEEE Transactions on Automatic Control*, Vol. AC-26, No. 3, June 1981, pp. 784-7.

75. Wiberg, D., *Theory and Problems of State Space and Linear Systems*, McGraw-Hill Publishing Co., 1971.

76. Wonham, W. M., Tracking and Regulation in Linear Multivariable Systems, *SIAM Journal of Control* 11 (3), 1973, pp. 424-437.

77. Yamamoto, Yukata, & Hara, Shinji, Relationships Between Internal and External Stability for Infinite-Dimensional Systems with Applications to a Servo Problem, *IEEE Transactions on Automatic Control*, Vol. 33, No. 11, November 1988, pp. 1044-1052.

78. Young, K. D., Deviation Variables in Linear Multivariable Servomechanisms, *IEEE Transactions on Automatic Control*, Vol. AC-29, No. 6, June 1984, pp. 567-9.

79. Zheng, Li, Discrete-Time Adaptive Control For Time-Varying Systems Subject to Unknown Fast Time-Varying Deterministic Disturbances, *IEEE Proceedings*, Vol. 135, Part D, No. 6, November 1988.

80. Zheng, Li, Discrete-Time Adaptive Control of Deterministic Fast Time-Varying Systems, *IEEE Transactions on Automatic Control*, Vol. AC-32, No. 5, May 1987.

LIST OF SYMBOLS

Symbol	Definition
A	Plant coefficient matrix; dimension n x n.
A_m	Ideal model coefficient matrix; dimension n x n.
A_N	Nominal value of the plant coefficient matrix; dimension n x n.
$\tilde{A}$	Discrete-time counterpart to A; dimension n x n.
$\tilde{A}_m$	Discrete-time counterpart to A_m; dimension n x n.
$\tilde{A}_N$	Discrete-time counterpart to A_N; dimension n x n.
$\tilde{A}_1$	Term representing the quantity $\overline{C}\tilde{A}\overline{C}^{\#}$.
$\tilde{A}_2$	Term representing the quantity $(MR)^{\#}\left(\tilde{A}-\tilde{B}\left(\overline{C}\tilde{B}\right)^{+}\overline{C}\tilde{A}\right)MR$.
α	Decay value on exponential; e.g. $e^{-\alpha t}$.
α	Constant matrix of coefficients in the set of homogeneous equations $\alpha\beta = 0$ where $\alpha = \rho M$.
B	Plant control distribution matrix; dimension n x r.
$\tilde{B}$	Discrete-time counterpart to B; dimension n x r.
$\hat{\tilde{B}}$	Term used to represent the quantity $\tilde{B}\tilde{\Gamma}_c + \tilde{F}H$.
$\tilde{B}_1$	Term representing the quantity $\overline{C}\tilde{B}$.
$\tilde{B}_2$	Term representing the quantity $(MR)^{\#}\tilde{B}\left(\mathrm{I}-\left(\overline{C}\tilde{B}\right)^{+}\overline{C}\tilde{B}\right)$.
c	Servo-command state-vector; dimension v x 1.
$\hat{c}$	Composite state-reconstructor estimate of servo-command state-vector c.
c_j	Set of unknown constants that may "jump" in value from time-to-time.
C	Plant output coefficient matrix; dimension m x n.
ξ	Auxilliary vector using in calculations for a reduced-order observer.

LIST OF SYMBOLS (Cont.)

Symbol	Definition
ξ_{ss}	Linear transformation state of $\bar{e}_{ss}$.
D	Disturbance coefficient matrix; dimension ρ x ρ.
$\tilde{D}$	Discrete-time counterpart to D; dimension ρ x ρ.
D_a	Parameter-perturbation vector coefficient matrix; dimension n^2 x n^2 or less.
$\tilde{D}_a$	Discrete-time counterpart to D_a; dimension same as that of D_a.
$\mathcal{D}$	Term used to denote the quantity $\bar{T}_{12}\tilde{E}T_{12}$.
δa_{ij}	The (i,j) element of the matrix ΔA.
ΔA	Matrix of plant parameter-perturbations; dimension n x n.
$\tilde{\Delta}$	Term used to represent the quantity $\tilde{K}_p MR$.
E	Servo-command coefficient matrix; dimension v x v.
$\tilde{E}$	Discrete-time counterpart to E; dimension v x v.
E^{-1}	One-step delay defined such that $\mathrm{E}^{-1}x(kT) = x\big((k-1)T\big)$
e_{ss}	Servo- state vector.
$\bar{e}_{ss}$	e_{ss} with residual-effects ignored.
ε_x	Full-order observer error between estimate and actual value of the plant state x; $\varepsilon_x = \hat{x} - x$.
ε_y	Servo-tracking error.
$\bar{\varepsilon}_y$	ε_y with residual-effects ignored.
ε_z	Full-order observer error between estimate and actual value of the disturbance state z; $\varepsilon_z = \hat{z} - z$.
ε_{z_a}	Full-order observer error between estimate and actual value of the parameter-perturbation state z_a; $\varepsilon_{z_a} = \hat{z}_a - z_a$.
$f_i(t)$	Natural basis function, the set of which mirror the waveform pattern of an uncertain waveform-structured input.

LIST OF SYMBOLS (Cont.)

Symbol	Definition
F	Disturbance input matrix; dimension n x p.
$\tilde{FH}$	Discrete-time counterpart to FH; dimension n x ρ.
G	Output matrix in dynamic model of servo-commands; dimension m x v.
$G(s)$	Transfer function of uncertain waveform-structured signal.
$\tilde{\gamma}(kT)$	Completely unknown, unpredicatable, and unmeasurable "residual-effect" caused by the $\sigma(t)$ impulses.
$\tilde{\gamma}_a(kT)$	Completely unknown, unpredicatable, and unmeasurable "residual-effect" caused by the $\sigma_a(t)$ impulses.
Γ_a	Gain matrix associated with the digital-continuous control term $u_a(t;kT)$; dimension r x n^2 or less.
Γ_c	Gain matrix associated with the digital-continuous control term $u_c(t;kT)$; dimension r x ρ.
Γ_s	Gain matrix associated with the digital-continuous control term $u_s(t;kT)$; dimension r x v.
$\tilde{\Gamma}_c$	Gain matrix associated with the digital control term $u_c(kT)$; dimension r x ρ.
$\tilde{\Gamma}_s$	Gain matrix associated with the digital control term $u_s(kT)$; dimension r x v.
H	Output matrix in dynamic model of external disturbances; dimension p x ρ.
H_a	Output matrix in dynamic model of parameter-perturbation vector; dimension n x n^2.
$\tilde{H}_a$	Discrete-time counterpart to H_a.
$\mathcal{H}$	Term used to denote the quantity $G\tilde{E}T_{12}$.
kT	Indicates discrete times; $k = 0, 1, 2, \ldots$ with constant spacing T.
$(k+1)T$	Forward discrete time-shift of kT.
$\kappa(t)$	Sparse sequences of impulses associated with the dynamical process model of the uncertain waveform-structured input.
K_m	Gain matrix used in feedback stabilization of plant, e.g. $u_{a_m} = K_m x$; dimension r x n.

LIST OF SYMBOLS (Cont.)

Symbol	Definition
K_p	Gain matrix used in feedback stabilization of servo-state error e_{ss}, e.g. $u_p = -K_p e_{ss}$; dimension r x n.
$\tilde{K}_m$	Discrete-time counterpart to K_m; dimension r x n.
$\tilde{K}_p$	Discrete-time counterpart to K_p; dimension r x n.
$\tilde{K}_0$	Gain matrix used in feedback stabilization of discrete-time full-order observer tracking-error.
$\tilde{\mathbf{K}}$	The set of all $\tilde{K}_p$ satisfying certain criteria.
L	Output matrix in dynamic model of uncertain waveform-structured signal; dimension m x d.
$\tilde{L}$	Gain matrix chosen to stabilize the system $\xi_{ss1}((k+1)T) = \left[\tilde{A}_1 + \tilde{B}_1\tilde{L}\right]\xi_{ss1}(kT)$.
λ_i	A solution to a characteristic equation; e.g., a solution to $p(\lambda)_{desired} = 0$.
m_i	Column vector of the matrix M in definition (2).
M	(1) Uncertain waveform-structured signal coefficient matrix; dimension d x d. (2) Maximal rank matrix satisfying CM=0; dimension n x (n-m).
M_1	Some positive constant $< \infty$.
μ	Sparse sequence of impulses associated with the servo-command $y_c(t)$ dynamical process model.
$\tilde{\mu}$	Completely unknown, unpredictable, and unmeasurable "residual-effect" caused by the $\mu(t)$ impulses.
$\aleph[\bullet]$	Denotes the nullspace of the matrix contained in the brackets.
$\mathfrak{N}$	Any matrix whose columns form a basis for the nullspace of $\left[\tilde{B}_1 \mid \tilde{A}_1\tilde{B}_1 \mid \tilde{A}_1^2\tilde{B}_1 \mid \cdots \mid \tilde{A}_1^{(n-\nu-1)}\tilde{B}_1\right]$.
ω	Impulsive forcing function in the differential equation describing waveform-structured inputs.
Ω	Matrix satisfying $\overline{C}\left(\tilde{A} + \tilde{B}\tilde{K}_p\right) = \Omega\overline{C}$.

LIST OF SYMBOLS (Cont.)

Symbol	Definition
$P(s)$	Numerator of the Laplace transformation of the waveform structured input differential equation.
$P_m(\lambda)$	Characteristic polynomial of the ideal model for the servo-state vector e_{ss}.
$P(\lambda)_{desired}$	Desired characteristic polynomial for full-order observer error dynamics.
$\Phi(t,t_o)$	Plant state transition matrix ($\widetilde{A} = \Phi(t,t_o)$).
$\Phi_D(t,t_o)$	Disturbance state transition matrix ($\widetilde{D} = \Phi_D(t,t_o)$).
$\Phi_{D_a}(t,t_o)$	Parameter-perturbation vector state transition matrix ($\widetilde{D}_a = \Phi_{D_a}(t,t_o)$).
$\mathbf{P}$	Any matrix whose columns form a basis for the nullspace of $\left[\widetilde{B}_2 \mid \widetilde{A}_2\widetilde{B}_2 \mid \widetilde{A}_2^2\widetilde{B}_2 \mid \cdots \mid \widetilde{A}_2^{(v-1)}\widetilde{B}_2\right]$.
$\psi(u_t)$	Discrete representation of the time-varying portion of $u(t,kT)$.
$q(t)$	State vector for the uncertain waveform-structured input $\mathbf{s}(t)$; dimension d x 1.
$Q(s)$	Denominator of the Laplace transformation of the waveform-structured signal differential equation.
r_a	Residual-effect driven by σ_a.
r_c	Residual-effect driven by σ.
r_s	Residual-effect driven by μ.
r_i	(1) Row vector of the matrix R. (2) Solution vectors to $\alpha\beta = 0$.
r_{vh}	Individual elements of r_i as defined in (2).
R	Any $(n\text{-}m)$ x v matrix such that $\mathsf{v} \le (n\text{-}m)$ and rank$[R] = \mathsf{v}$.
$\mathbf{R}$	The set of all $\mathbf{R}_\mathsf{v}$, $\mathsf{v} = 1, 2, ..., (n\text{-}m\text{-}1)$.
$\mathbf{R}_v$	The set of all R that form a basis for a particular subspace having dimension v.
$\Re[\bullet]$	Denotes the column range-space of the matrix contained within the brackets.
S_v	Arbitrary subspace contained within the nullspace of the matrix C.

LIST OF SYMBOLS (Cont.)

Symbol	Definition
$\mathbf{s}$	Vector of uncertain inputs having waveform structure; dimension $m \times 1$.
σ	Sparse sequence of impulses associated with the external disturbance $w(t)$ dynamical process model.
$\tilde{\sigma}$	Completely unknown, unpredicatable, and unmeasurable "residual-effect" caused by the $\sigma(t)$ impulses.
σ_a	Sparse sequence of impulses associated with the parameter-perturbation vector $z_a(t)$ dynamical process model.
$\tilde{\sigma}_a$	Completely unknown, unpredicatable, and unmeasurable "residual-effect" caused by the $\sigma_a(t)$ impulses.
Σ	Gain matrix used in feedback stabilization of discrete-time reduced-order observer tracking-error.
t	Indicates continuous time.
t_o	An inital time, often assumed to be 0.
T	A fixed constant sampling-period.
T_c	Control sample-period associated with measurements, or processing, of the servo-command y_c.
T_y	Control sample-period associated with measurements, or processing, of the plant output y.
T_{12}	Any matrix satisfying $GT_{12}=0$.
$\bar{T}_{12}$	Term used to denote the quantity $(T_{12}^{\mathrm{T}}T_{12})^{-1}T_{12}^{\mathrm{T}}$.
θ	A possibly nonunique matrix satisfying $G = C\theta$.
u	Composite control vector in plant equations; dimension $r \times 1$.
u_a	The control part of u associated with cancelling the effects of the parameter-perturbations ΔA.
u_{a_m}	The control part of a multirate u associated with stabilizing and achieving certain desired characteristics for the plant.
u_c	The control part of u associated with canceling the effects of the external disturbance $w(t)$.

LIST OF SYMBOLS (Cont.)

Symbol	Definition
u_p	The control part of u associated with stabilizing and achieving certain desired characteristics for the servo-tracking error.
u_s	The control part of u associated with canceling the disturbance-like effects of the servo-command $y_c(t)$.
u_t	Portion of $u(t;kT)$ that is time-varying between sample times.
$u_{kT}(kT)$	Poriton of $u(t;kT)$ that is held constant between sample times.
$\tilde{v}((k+1)T$	A term requiring knowledge of the motions of the disturbance over a future sampling interval; $\tilde{v}((k+1)T = \int_0^T e^{A(T-\tau)} F w(\tau) d\tau$.
$\tilde{v}_a((k+1)T$	A term requiring knowledge of the motions of the parameter-perturbation vector over a future sampling interval; $\tilde{v}_a((k+1)T = \int_0^T e^{A_w(T-\tau)} w_a(\tau) d\tau$.
w	External disturbance input vector; dimension p x 1.
w_a	Parameter-perturbation state-vector; dimension n x 1.
$\hat{w}_a$	Observer-generated estimate of w_a.
x_o	Initial value for the plant state-vector; dimension n x 1.
x_T	Desired or final value for the plant state-vector; dimension n x 1.
x	Plant state-vector; dimension n x 1.
$\hat{x}$	State-reconstructor estimate of plant state-vector x.
$\hat{\tilde{\chi}}$	Term used to represent the quantity $\theta\tilde{E} - \tilde{A}\theta - \tilde{B}\tilde{\Gamma}_s$.
Ξ	Matrix satisfying $\left(\tilde{A} + \tilde{B}\tilde{K}_p\right) MR = MR\Xi$.
y	Plant output-vector; dimension m x 1.
y_c	Output servo-command vector; dimension m x 1.
z	External disturbance state-vector; dimension ρ x 1.
$\hat{z}$	Composite state-reconstructor estimate of external disturbance state-vector z.
z_a	Parameter-perturbation disturbance state-vector; dimension n^2 x 1 or less.

LIST OF SYMBOLS (Cont.)

Symbol	Definition
$\hat{z}_a$	Composite state-reconstructor estimate of parameter-perturbation state-vector z_a.
$\tilde{Z}$	Gain matrix chosen to stabilize the system $\xi_{ss2}((k+1)T) = \left[\tilde{A}_2 + \tilde{B}_2\tilde{Z}\right]\xi_{ss2}(kT)$.
$[\bullet]^{-1}$	Denotes matrix inverse of matrix in brackets.
$[\bullet]^k$	Denotes matrix multiplied by itself k times.
$[\bullet]^T$	Denotes matrix transpose of matrix in brackets.
$[\bullet]^+$	Denotes Moore-Penrose pseudo-inverse of matrix in brackets.
$[\bullet]^\#$	Denotes matrix left or right generalized inverse of matrix in brackets; left defined by $([\bullet]^T[\bullet])^{-1}[\bullet]^T$ and right defined by $[\bullet]^T([\bullet][\bullet]^T)^{-1}$.

INITIAL DISTRIBUTION LIST

		Copies
IIT Research Institute ATTN: GACIAC 10 W. 35th Street Chicago, IL 60616		1
AMSMI-RD		1
AMSMI-RD-CS-R		5
AMSMI-RD-CS-T		1
AMSMI-RD-MG		1
AMSMI-RD-MG-GA,	Ed Herbert	1
	Phil Jenkins	1
AMSMI-RD-SS		1
AMSMI-RD-TI,	Wanda M. Hughes	10
AMSMI-GC-IP,	Fred Bush	1